Investigating the role of downy mildew effectors in host resistance and susceptibility

Sophie Jeanne Maria Piquerez

A thesis submitted to the University of East Anglia (Norwich, UK)
in partial fulfilment of the requirements for the degree of

DOCTOR OF PHILOSOPHY

IN BIOLOGY

December 2011

The Sainsbury Laboratory
Norwich Research Park,
Norwich, NR4 7UA
United Kingdom

Table of contents

Abstract

Through specialised structures called haustoria, filamentous eukaryotic plant pathogens such as rusts and mildews can deliver "effector" proteins directly into plant cells in order to manipulate specific defence responses and processes. *Hyaloperonospora arabidopsidis* (*Hpa*) is a haustorium-producing biotrophic oomycete pathogen that causes downy mildew on Arabidopsis. Over 100 candidate effectors (called "HaRxLs"), carrying a characteristic RxLR protein motif, have been predicted from the *Hpa* genome sequence. This PhD work focused on the characterisation of some of these effectors and their interaction with plant defences.

First, the *Pseudomonas syringae* pv. *tomato* (*Pst*) strain DC3000 type III secretion system was used to examine the effect of single oomycete effectors *in planta*. One of these, ATR13 from *Hpa* isolate Emco5 ($ATR13^{Emco5}$) has been shown to be recognised in some Arabidopsis accessions by the RPP13 protein, preventing *Hpa* Emco5 from completing its life cycle on such resistant plants. *Hpa* Emco5 can however complete its life cycle on Ws-0 but paradoxically, $ATR13^{Emco5}$ is also recognised in this accession. Here, I show that $ATR13^{Emco5}$ is weakly recognised in Ws-0 by a single *RPP13*-independent, *EDS1*-independent dominant gene called *RHA13*, shown by rough mapping to position on Arabidopsis chromosome 4.

Second, I contributed to two independent functional screens performed in our laboratory to experimentally characterise the *Hpa* effectorome. The first screen focused on HaRxLs effects on bacteria virulence using the EDV system. The second screen was based on HaRxLs subcellular localisation using *Agrobacterium*-mediated transient expression. As presented in this work, I showed that both screens identified putative interesting effectors which increased plant susceptibility to *Pst* and *Hpa* and localised to various plant subcellular compartments. One particular effector candidate, HaRxL79, localised to microtubules *in planta* and interacted with two microtubule-associated proteins in a yeast-two-hybrid assay. HaRxL79 was also found to interact with Arabidopsis histone chaperones (AtNAP1s) in the plant cytoplasm, which were observed to play a role in plant susceptibility to *Hpa* and partially to the necrotroph *Botrytis cinerea*, but not to the hemibiotrophs *Pst* and *Phytophthora parasitica*. AtNAP1s also interact with HaRxL67, a vacuole-associated *Hpa* effector. From this, I propose that AtNAP1s are susceptibility factors for *Hpa*, specifically targeted by *Hpa* effectors HaRxL67 and HaRxL79 in order to promote susceptibility and maintain biotrophy.

Author's declaration

I hereby certify that the work contained in this thesis is entirely the result of my own work, except where reference is made to other authors. It has not been submitted in any other form to the University of East Anglia or any other University.

Naveed Ishaque (The Sainsbury Laboratory, UK) performed the SHOREmap analysis of *RHA13* mapping presented in Chapter 3.

Dr. Anastasia Gardiner and Naveed Ishaque (The Sainsbury Laboratory, UK) were involved in the description and characterisation of HaRxL79 gene family in *Hpa* and *Phytophthora spp* detailed in Chapter 4.

Dr. Malou Fraiture and Dr. Frédéric Brunner (Tubingen University, Germany) identified AtNAP1s as interactors of HaRxL67 and we are pursuing a collaboration which should result in the publication of results presented in Chapter 5.

Dr. Agnès Attard (INRA Nice-Sophia-Antipolis, France) performed the *Phytophthora parasitica* infection assays on the *Atnap1s* mutants presented in Chapter 5.

Sophie Piquerez

Aknowledgments

I would like to thank Jonathan for offering me this opportunity and giving me the freedom to conduct my research and explore additional directions in this project.
I would like to thank my two examiners, Dr. Jeremy Murray (John Innes Centre, Norwich, UK) and Pr. Jane Parker (Max-Planck Institute, Cologne, Germany) for reading the manuscript and examining this work.

I would like to thank the people who had a direct input in my thesis work: Kee, Eric, Anastasia, and the *Hpa* group members: Marie (best known as MCC), Lennart, Georgina, Naveed, Jorge, and Shuta. Special thanks to Marie and Lennart for editing the first drafts of my thesis chapters and Cécile for correcting the typos.

Thanks to all my friends at The Sainsbury Lab and John Innes Centre, past and present, for the fun and help you have brought me. Especially to my Korean friends Kee and Joo whom I'm surely going to visit in the future in their beautiful country, to Mitch for his unexpectedness, to Chris and his cigars, to Freddy and Carol for the raclette/sushi parties, to Gaelle, and to the others I have forgotten, thanks for being there. Additional special thanks to a few special persons who made the experience as awesome as it has been: Mel, you were the first to be there, sharing the ups and downs, the recipes and you showed me how to find the additional confidence I was missing; Valie, for your smile, everlasting good mood and all your support whatsoever; Marie, for believing in me, supporting me until the end and beyond, and for initiating me to the exciting and beautiful world of cell biology; I thank you all for your friendship.

I dedicate this thesis manuscript to my parents and my sister who supported me through the adventure and understood my work path without wondering if I would ever get a proper job. Je dédie cette thèse à mes parents et à ma petite soeur qui m'ont non seulement soutenue dans cette aventure mais qui ont toujours compris à quel point le jeu en valait la chandelle.

Last but not least, to Guillaume, my love, my partner and my friend no matter what happens, thanks for being here. Without you I would not have made it.

Publications arising from this work

Fabro, G., Steinbrenner, J., Coates, M., Ishaque, N., Baxter, L., Studholme, D.J., Korner, E., Allen, R.L., Piquerez, S.J.M, Rougon-Cardoso, A., Greenshields, D., Lei, R., Badel, J.L., Caillaud, M.C., Sohn, K.H., Van den Ackerveken, G., Parker, J.E., Beynon, J., and Jones, J.D.G. (2011). Multiple Candidate Effectors from the Oomycete Pathogen Hyaloperonospora arabidopsidis Suppress Host Plant Immunity. **PLoS Pathogens 7**(11): e1002348.

Caillaud, M.C., Piquerez, S.J.M, Fabro, G., Steinbrenner, J., Ishaque, N., Beynon, J., and Jones, J.D. (2012). Subcellular localization of the *Hpa* RxLR effector repertoire identifies a tonoplast-associated protein HaRxL17 that confers enhanced plant susceptibility. **The Plant Journal** 69(2):252-265.

Caillaud, M.C., Piquerez, S.J.M, and Jones, J.D.G. (2012). Characterization of the membrane-associated HaRxL17 *Hpa* effector candidate. **Plant Signaling & Behavior** 7(1):145-149.

Badel, J.L., Greenshields, D., Rallapalli, G., Piquerez, S.J.M., Fabro, G., Ishaque, N., Dangl, J.L., Weigel, D., Doebelid, M. and Jones, J.D.G. *In planta* effector competition assays detect *Hyaloperonospora arabidopsidis* effectors that contribute to virulence by targeting different host subcellular compartments. *in preparation*.

Sohn, K.H., Hughes, G.R., Piquerez, S.J.M., Jones, J.D.G. and Banfield, M.J. Crystal structure and natural variation based functional analysis bacterial effector AvrRps4. *in preparation*.

Piquerez, S.J.M., Caillaud, M.C., Fraiture, M., Brunner, F., Attard, A. and Jones, J.D.G. Arabidopsis histone chaperones NAP1s are required for susceptibility to the biotrophic pathogen *Hyaloperonospora arabidopsidis*. *in preparation*.

Major abbreviations

ATR	*Arabidopsis thaliana* recognised
Avr	Avirulence
coIP	Co-immunoprecipitation
CRN	Crinkling and Necrosis
dpi	Days post infection
EER	Glu-Glu-Arg (proteic motif of oomycete effectors)
EHM	Extra-haustorial membrane
EHMx	Extra-haustorial matrix
ETI	Effector-triggered immunity
ETS	Effector-triggered susceptibility
FRAP	Fluorescence recovery after photobleaching
Hpa	*Hyaloperonospora arabidopsidis*
hpi	Hours post infection
HR	Hypersensitive response
KO	Knock-out
Nap1	Nucleosome-assembly protein 1
OE	Over-expression
PAMP	Pathogen-associated molecular patterns
PCR	Polymerase chain reaction
PIP	Phosphatidyl inositol phosphate
PTI	PAMP-triggered immunity
ROS	Reactive oxygen species
RPP	Resistance to *Peronospora parasitica* (ex-*Hpa*)
RT-PCR	Retro-transcription polymerase chain reaction
RxLR	Arg-x-Leu-Arg (proteic motif of oomycete effectors)
T3E	Type III secreted effectors
T3SS	Type III secretion system
Y2H	Yeast-two-hybrid

1. Introduction

The interaction of plants with pathogens has always been a crucial constraint on agriculture. The most cultivated crops (rice, corn, wheat, soybean and potato) are targeted by a number of devastating filamentous eukaryotic pathogens that cost millions of pounds each year to the agriculture industry and are potentially disastrous for many societies (Haverkort et al. 2008; Singh et al. 2011). For instance, the rice blast fungus *Magnaporthe oryzae*, as well as various smuts, rusts, mildews, but also oomycetes from the *Phytophthora* genus are particularly virulent and widespread. Some of the spread of these diseases can be partially controlled by the use of fungicides; however there are major drawbacks to their use as they are costly because of the requirement for repeated applications and because they can be very deleterious for the environment (Wilson and Tisdell 2001).

The burden of plant pathogens is very important in crops, although it is observed that plant disease in wild settings is very rare, and most wild plants are healthy. The major reason is that plants have evolved a complex battery of defence layers to prevent any potential intruder from attacking (Dangl and Jones 2001; Jones and Dangl 2006). The appearance of symptoms can therefore be considered as an exception, dependent on particular settings in which pathogens have co-evolved mechanisms to subvert plant defences effectively.

In this thesis, I will present some of the mechanisms involved in the interaction between an oomycete pathogen, *Hyaloperonospora arabidopsidis*, and its host plant *Arabidopsis thaliana*. This introduction chapter will focus on the advantages of working with this model pathosystem, our current knowledge of the infection process in this pathosystem and the ecological links with other biotrophic or hemi-biotrophic eukaryotic filamentous pathogen-plant interactions. In the light of the interaction between plants and pathogens, I will briefly

discuss how the plant host can sense and react to the presence and invasion of the pathogen, and the mechanisms used to promote virulence and disease.

1.1. Why work with biotrophic oomycete pathogens?

1.1.1. Oomycetes and their wide range of interactions with plants

Oomycetes are filamentous eukaryotic microbes that can reproduce sexually and asexually. Oomycetes are often mistaken for fungi as they share many aspects of their biology and physiology, most notably their filamentous growth. However, oomycetes are phylogenetically closer to diatoms, brown algae and members of the Chromalveolata kingdom such as the malaria parasite *Plasmodium falciparum* (**Figure 1.1.**) (Beakes et al. 2011).

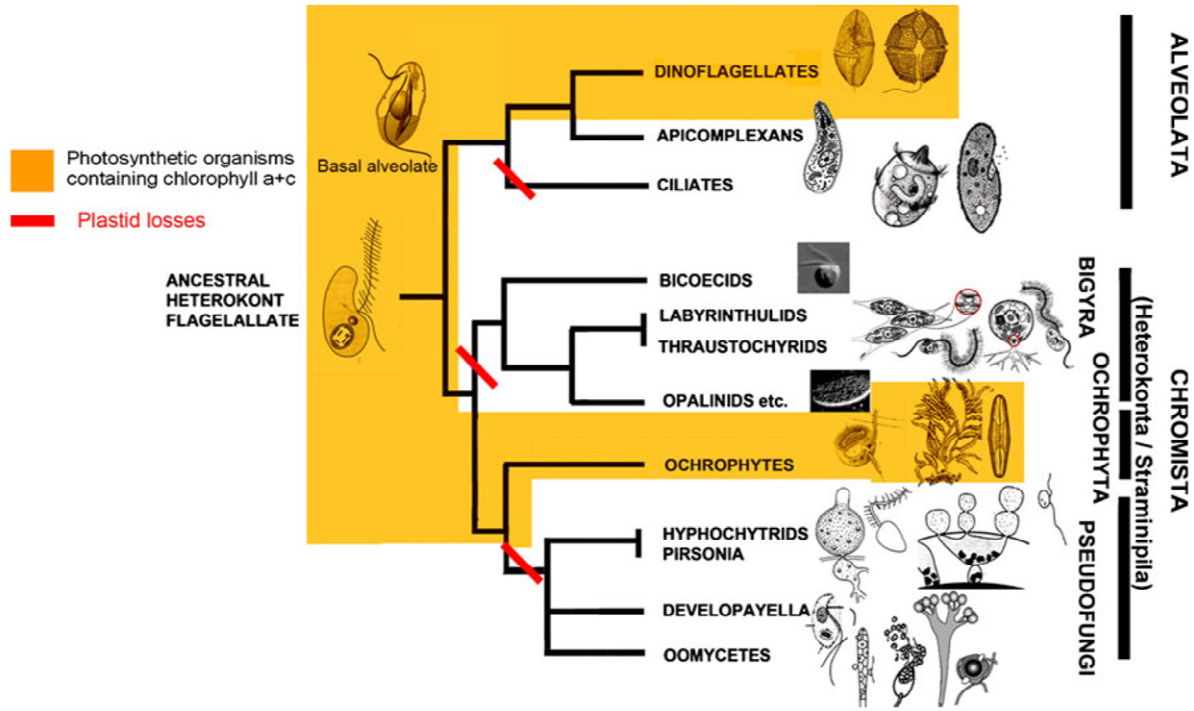

Figure 1.1. Schematic phylogenetic tree summarizing phylogenetic relationships between the diverse members of the Chromalveolate kingdom, comprising the Alveolata and Chromista superphyla (from Beakes et al. 2011). The photosynthetic lines are shaded in orange and postulated plastid loss events are indicated by the red bars.

Oomycetes possess specific features that differentiate them from fungi. They possess a cellulose-based cell wall with very little chitin and coenocytic hyphae, whereas fungi mostly

possess chitin-based cell walls with septated hyphae. Most notably, oomycetes include some of the most destructive plant pathogens. The infamous *Phytophthora infestans* destroyed potato crops in Ireland leading to the Great Famine in the 1840s (Reader 2009). Oomycete pathogens are very diverse in their host range and disease strategy as they are not only plant but also human, fish and algae pathogens (reviewed in Thines and Kamoun 2010) (**Figure 1.2**).

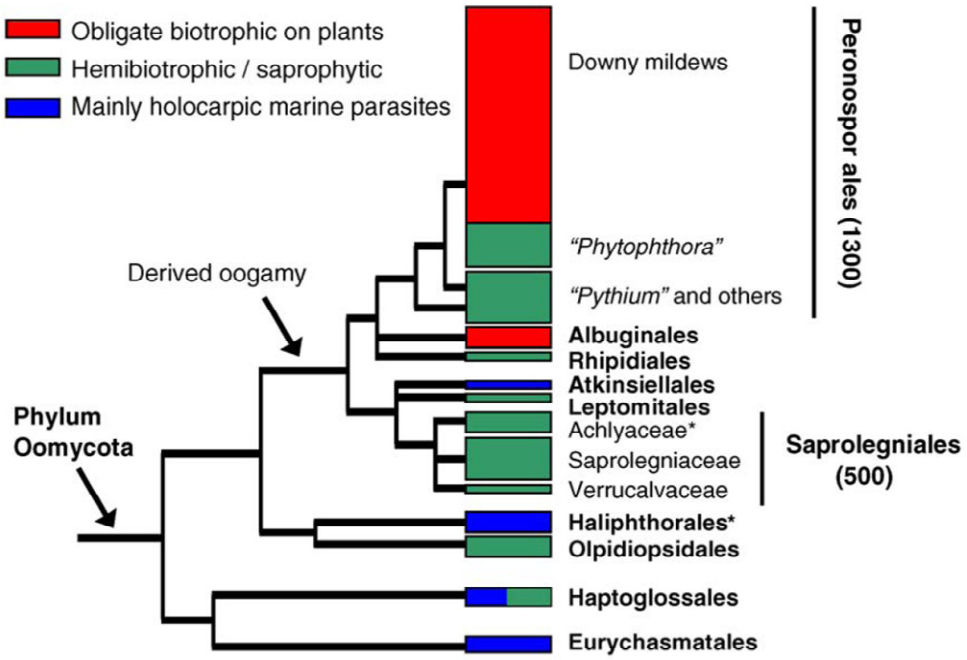

Figure 1.2. Schematic overview of the current model of oomycete evolutionary history (from Thines and Kamoun 2011). Names in inverted commas denote taxa currently in taxonomic revision. Taxa that are not yet formally introduced are marked with an asterisk. Species numbers are indicated for the two largest oomycete orders.

Oomycete plant pathogens exhibit drastically variable ecological strategies in their interaction with their hosts: they can be either biotrophs (i.e., the downy mildew agent *Hyaloperonospora arabidopsidis*, further referred to as *Hpa*, and the white rust agent *Albugo laibachii*), hemi-biotrophs (i.e., *P. infestans*) or necrotrophs (i.e., *Pythium ultimum*). Obligate

biotrophs are totally dependent on their hosts to complete their life cycle and therefore have to constantly attenuate host defence responses and obtain nutrients while keeping their host alive. This infection mode requires a sophisticated manipulation of the host from the pathogen. Obligate biotrophs like mildews are generally highly adapted to their host and have co-evolved with them for a very long time (Holub 2001; Holub 2008). Alternatively, necrotrophic pathogens usually rapidly kill their hosts to obtain nutrients from dead tissues, without any elaborate strategy of maintenance or manipulation (Glazebrook 2005). Another lifestyle is adopted by the hemi-biotrophic pathogens, which usually first develop like biotrophs in order to establish infection, and then switch to a necrotrophic lifestyle. During *P. infestans* infection, these two phases of infection are associated with very distinct sets of genes that are induced either during biotrophy or necrotrophy (van West et al. 1998; Haas et al. 2009; Raffaele et al. 2010; Vleeshouwers et al. 2011).

Because of their exclusive lifestyle and unfortunately for the researcher, obligate biotrophs like *Hpa* have not been successfully cultured *in vitro* and have been so far refractory to molecular genetic engineering (Kemen et al. 2011). Nonetheless, they constitute a very important ecological model to study the molecular basis of obligate biotrophic parasitism. In my thesis, I used the *Hpa*-Arabidopsis pathosystem model in order to shed light on how communication works between both organisms. As knowledge on filamentous eukaryotic pathogens is not restricted to our pathosystem of study but composed of many different pathosystems, I will throughout this chapter refer to many different species of pathogens (summarised for clarity in **Table 1.1**) including other obligate biotrophs forming haustoria (powdery mildew agents), other fungal biotrophs not forming haustoria (*Ustilago maydis*, *Magnaporthe oryzae*), and other oomycetes (*A. laibachii*, *Phytophthora spp.*, *P. ultimum*, *Saprolegnia parasitica*, *Aphanomyces euteiches*).

Class	Symptoms	Species	Lifestyle	Haustorium	Plant host
Oomycetes	downy mildew	*Hyaloperonospora arabidopsidis*	Obligate biotrophy	Yes	Arabidopsis
	downy mildew	*Pseudoperonospora cubensis*	Obligate biotrophy	Yes	Cucurbitaceae
	white blister rust	*Albugo laibachii*	Obligate biotrophy	Yes	Arabidopsis
	late blight	*Phytophthora infestans*	Hemibiotrophy	Yes	Solanaceae
		Phytophthora sojae			Soybean
		Phytophthora capsici			Solanaceae
		Phytophthora parasitica			Arabidopsis
		Pythium ultimum	Necrotrophy	No	Broad host range
Fungi	powdery mildew	*Golovinomyces cichoracearum*	Obligate biotrophy	Yes	Asteraceae, Cucurbitaceae
		Golovinomyces orontii			Brassicaceae, Solanaceae, Cucurbitaceae
		Erysiphe crucifearum			Brassicaceae
	rust	*Uromyces fabae*	Biotrophy	Yes	Bean
	rust	*Melampsora lini*	Obligate biotrophy	Yes	*Linum* species (including flax)
	rust	*Puccinia graminis*	Obligate biotrophy	Yes	Wheat
	smut	*Ustilago maydis*	Biotrophy	No	Maize
	blast	*Magnaporthe grisea*	Hemibiotrophy	No	Rice
		Cladosporium fulvum	Biotrophy	No	Tomato
		Leptospheria maculans	Hemibiotrophy	No	Brassicaceae
		Botrytis cinerea	Necrotrophy	No	Broad host range
		Pyrenophora tritici-repentis	Necrotrophy	No	Wheat

Table 1.1. Summary of all filamentous eukaryotic plant pathogens mentioned in this thesis.

1.1.2. *Hyaloperonospora arabidopsidis* - Arabidopsis as a model pathosystem

Because of the prevalence of Arabidopsis as a very well described plant model organism, the naturally co-evolving *Hpa*-Arabidopsis pathosystem has been considered as a model since the 1990s (Koch and Slusarenko 1990) although the symptoms of Arabidopsis downy mildew were first reported as early as in the 1900s in Germany (reviewed in Holub 2008). During the last decades, many *Hpa* isolates able to grow on different Arabidopsis accessions were collected in various locations, and because of the natural variation observed in terms of resistance, the *Hpa*-Arabidopsis model was described as a promising system to identify new resistance sources and understand plant defence mechanisms (Holub et al. 1994; Holub and Beynon 1997). Recently, the genome sequence and gene models for the *Hpa* Emoy2 isolate has been released, making this pathosystem model even more convenient to work with (Baxter et al. 2010). The infectious life cycle of *Hpa* on Arabidopsis has been described extensively (**Figure 1.3)** (Koch and Slusarenko 1990; Mauch-Mani and Slusarenko 1993; Coates and Beynon 2010).

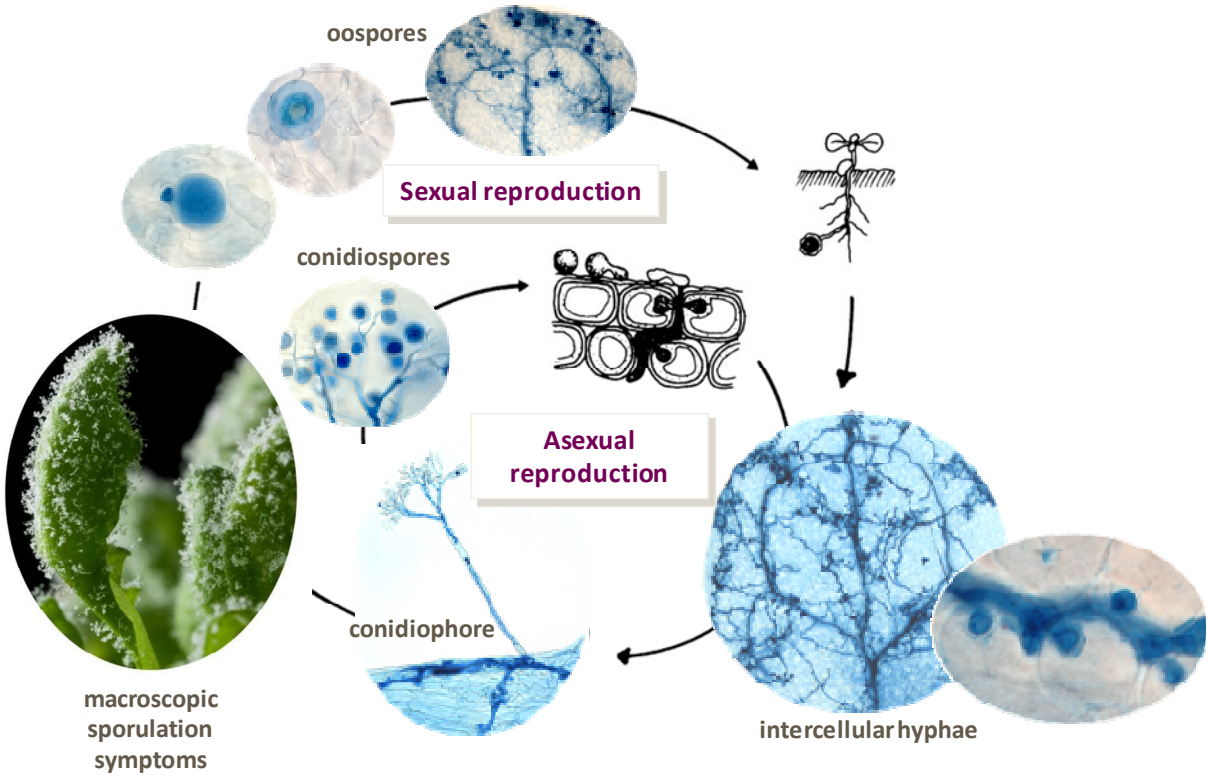

Figure 1.3. Schematic overview of the life cycle of *Hyaloperonospora arabidopsidis* on *Arabidopsis thaliana* (modified from Koch and Slusarenko 1990). Infections arise initially from oospores germinating on a root or conidiospores germinating on a leaf. Plants are colonized by mycelium growing intercellularly. Hyphae project haustoria into host cells. After a variable period of growth, conidiophores bearing conidiospores grow out of stomata. On germination, conidia initiate new rounds of infection. Oospores are formed concurrently with asexual spores. *Hpa*-infected plant tissues were stained with trypan blue to highlight *Hpa* structures throughout its life cycle. The components of this diagram are not drawn to scale. Illustrating photographs in this figure were kindly provided by Dr Marie-Cécile Caillaud (TSL, Norwich).

Infection starts with the germination of a spore which is produced either by sexual or asexual reproduction. The oospores, produced by sexual reproduction within tissues, are believed to represent a resistant form of disseminating spores as they can presumably survive during winter in soil. When environmental conditions are more suitable for germination (generally after winter), oospores can infect roots of Arabidopsis and grow through tissues to reach the aerial parts of the plant. Alternatively, asexual reproduction occurs when hyphae located under stomata start differentiating to form conidiophores, carrying conidiospores that will emerge through stomata. The downy mildew disease caused by *Hpa* is named after the visual description of the symptoms it can cause on Arabidopsis, consisting of a “lawn” of

conidiophores that cover the leaf surfaces. The conidiospores of *Hpa* are hyaline –which gave *Hpa* its genus name– and non-motile and are disseminated in the air.

Upon landing on leaf surfaces, conidiospores can breach into the epidermis (along the anticlinal walls between epidermal cells) and reach the leaf mesophyll. *Hpa* then grows hyphae between plant mesophyll cells and can project highly specialised structures involved in feeding and secretion, called "haustoria", directly into plant cells. Because of the practicality and efficiency of leaf infection, conidiospores are used in the laboratory to propagate *Hpa*, taking one week per asexual reproductive cycle (Parker et al. 1993). The haustorium is a central component of the work presented in this thesis, described further in the sections 1.3.2. and 1.3.3.

As mentioned earlier, disease is rare in the wild, most probably because plants have evolved very efficient immunity mechanisms to cope with pathogens. When infected or threatened by a pathogen, plants activate an arsenal of defence responses to protect themselves. These responses act as different layers of defence and have commonly been categorised into different classes (although the involved mechanisms often overlap): non-host resistance, pre-invasive resistance, PAMP-triggered immunity (PTI) and effector-triggered immunity (ETI) (Dangl and Jones 2001; Jones and Dangl 2006). Non-host resistance and pre-invasive resistance prevent entry of the pathogen, whereas post-invasive resistance prevent pathogen spreading into the plant tissues. In the next sections, I will briefly discuss general aspects of Arabidopsis immunity, with a focus on *Hpa* whenever possible.

1.2. Arabidopsis responses to pathogens

As soon as pathogens try to breach their aerial surfaces, plants can sense their presence and attempt to prevent the invasion using an array of diverse but complementary responses. In this section, I will present general aspects of Arabidopsis response to pathogen infection, with a large focus on the interaction with *Hpa*.

1.2.1. General concepts in Arabidopsis resistance against *Hpa*

Plants like Arabidopsis can perceive and respond to external stimuli by inducing an appropriate response *via* very complex signalling cascades. In response to a pathogen, multiple and diverse defence responses are induced and these include rapid ion fluxes and reactive oxygen species (ROS) and nitric oxide (NO) bursts (Blume et al. 2000; Fellbrich et al. 2002; Slusarenko and Schlaich 2003), phosphorylations and mitogen-activated protein kinases (MAPK) activation, hormone signalling, specific gene induction, and production of toxic secondary metabolites such as phytoalexins, reorganisation of the host cell structure (Takemoto et al. 2003) and occasionally cell death (Hammond-Kosack and Jones 1996). All these various responses are initiated by the plant in order to block the pathogen invasion, but also during the infection process, making timing and intensity of defence responses a very tightly regulated phenomenon. Notably, this defensive array of responses at pathogen penetration sites is not specific, and more or less similar in response to adapted or non-adapted pathogens (Takemoto et al. 2003). Different layers of defence exist, from the initial detection of the pathogen presence sometimes long before infection, to the specific detection of pathogen-synthesised molecules (**Figure 1.4**).

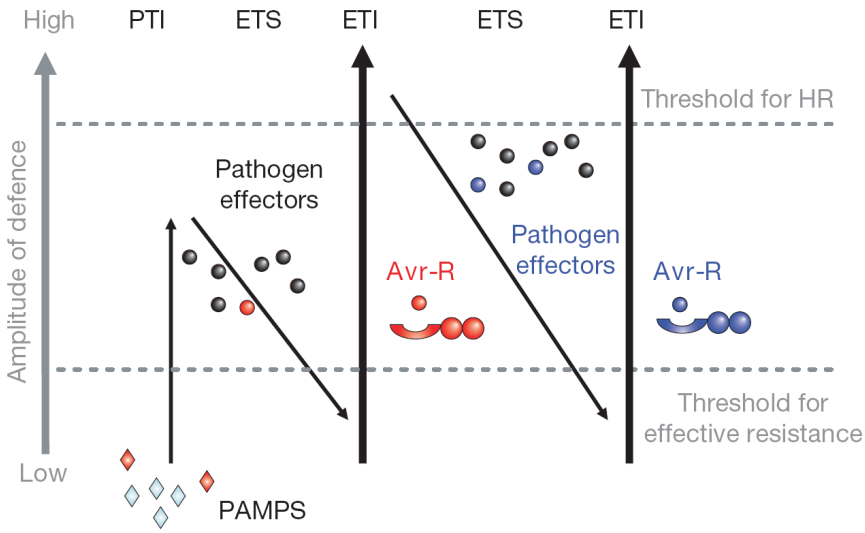

Figure 1.4. The "zig-zag-zig" model illustrates the quantitative output of the plant immune system in a plant-pathogen arms race (from Jones and Dangl 2006). In the first phase of defence, plants can detect pathogen-associated molecular patterns (PAMPs, red diamonds) and trigger PAMP-triggered immunity (PTI). In a second phase, successful pathogens able to overcome the initial PTI will do so by delivering secreted effectors, which can also enable pathogen nutrition and dispersal resulting in effector-triggered susceptibility (ETS). In a third phase, one effector (indicated in red) is recognised by an NB-LRR protein, thus activating effector-triggered immunity (ETI) which is an amplified version of PTI that often passes a threshold for induction of hypersensitive cell death (HR). In a fourth phase, pathogen isolates are selected if they have lost the effector (in red) which is now recognised by the plant and of limited advantage for the pathogen fitness, or perhaps if they have gained new effector variants (in blue). In parallel, selection will favour new plant NB-LRR alleles that can recognize one of the newly acquired effectors, resulting again in ETI.

The first layer of plant defence responses that the pathogen encounters is triggered by host receptor-mediated recognition of pathogen-associated molecular patterns (PAMPs). PAMPs are relatively well conserved molecules which are essential to the pathogen, and therefore upon which diversifying selection cannot easily occur. The bacterial flagellum, often an important fitness factor for plant pathogenic bacteria, is constituted of flagellin monomers, which are recognised as PAMPs and can elicit a range of PAMP-triggered immunity (PTI) responses. Similarly, the chitin present in the fungal cell wall or the most abundant bacterial protein, the elongation factor EF-Tu, are PAMPs recognised by some

plants. In this thesis, I focus my work on the mechanisms involved in the biotrophic manipulation of hosts, mediated by the secretion of effectors by the pathogen. I will not present here many details on the first layer of defences associated with PTI, but invite the interested reader to refer to the available literature on the subject for oomycetes (Brunner et al. 2002; Gaulin et al. 2006; Chaparro-Garcia et al. 2011). PTI can be effectively suppressed by various secreted effectors which can act either directly on the PAMP receptors or alternatively on the signalling components of PTI in order to promote effector-triggered susceptibility (ETS). When a pathogen successfully suppresses PTI, a second layer of plant defence can be provided by resistance (*R*) genes that can specifically detect effectors and trigger effector-triggered immunity (ETI). ETI generally leads to a more intense defensive response, involving localised programmed cell death during the hypersensitive response (HR) in order to constrict the growth of the pathogen (Jones and Dangl 2006). There is an evolutionary arms race between pathogen recognition and defence evasion, the escalation of which is illustrated in plants and their pathogens by the interplay between PTI and ETI. This arms race is classically summarized by the "zig-zag-zig" model (Jones and Dangl 2006, summarised in **Figure 1.4**).

Plants have evolved a battery of R genes able to specifically detect directly or indirectly the presence of single or multiple effectors secreted by pathogens (and encoded by so-called avirulence (*Avr*) genes as their recognition leads to resistance) (Jones and Dangl 2006). During ETI, the recognition of an avirulence gene is typically associated with a localised programmed cell death (HR), which can prevent an invading pathogen to spread further. Most resistance genes identified so far and involved in targeted resistance against various pathogens, are from the NB-LRR-type gene family (Dangl and Jones 2001). These NB-LRR genes encode proteins harbouring a nucleotide-binding site and leucine-rich repeats. In the sequenced Col-0 accession of Arabidopsis, 125 full length NB-LRR genes have been

annotated (Meyers et al. 2003). NB-LRR proteins are predicted to be cytoplasmic (van der Biezen and Jones 1998) and are believed to be able to monitor the plant proteins that can be targeted by effectors within the cell cytoplasm (McHale et al. 2006). Additionally, NB-LRR proteins can be subdivided in two groups, based on their N-terminal structural features: (a) TIR-NB-LRR when their N-terminus has homology to the Toll and interleukin receptors or (b) non-TIR-NB-LRR, including many CC-NB-LRR proteins which contain in their N-terminus putative coiled-coil domains (Dangl and Jones 2001).

The variation in compatibility between *Hpa* races and Arabidopsis accessions reflects the natural ancient co-evolution of both organisms (Holub 2001; Holub 2008) as well as the ongoing nature of the evolutionary arms race between the pathogen and its host. A glimpse of this variation in population ecologies is shown in **Table 1.2.** Compatibility (C) is associated with virulence and disease (*Hpa* growth) on a given Arabidopsis accession, while incompatibility (I) is associated with avirulence and resistance (absence of *Hpa* growth) (**Table 1.2.**).

Genetic analysis of avirulence in *Hpa* most often fits the gene-for-gene model (Flor 1971; Holub et al. 1994) and Arabidopsis resistance genes against *Hpa* are called *RPP* genes (for resistance to *Peronospora parasitica*, the former name of *Hpa*). A total of 27 *RPP* genes have been mapped (reviewed in Slusarenko and Schlaich 2003), but only 6 *RPP* genes have been cloned and/or characterised so far: *RPP1* (Botella et al. 1998), *RPP2* (Sinapidou et al. 2004), *RPP4/5* (Parker et al. 1997), *RPP7* (McDowell et al. 2000), *RPP8* (McDowell et al. 1998) and *RPP13* (Bittner-Eddy et al. 2000) (**Table 1.2**). All 6 of these characterised *RPP* genes are NB-LRR genes: *RPP7*, *RPP8* and *RPP13* are CC-NB-LRR whereas *RPP1*, *RPP2* and *RPP4/5* are TIR-NB-LRR.

Arabidopsis genotype	*Hyaloperonospora arabidopsidis* isolate								
	Cala2	Emco5	Emoy2	Emwa1	Hiks1	Hind2	Maks9	Noks1	Waco1
C24	I	I	I	I	I	I	I	I	I
Col-0	I RPP2	C	I RPP4	I RPP4	I RPP7	I RPP28	C	C	C
Ler-0	C	I RPP8	I RPP5, 8	I RPP5	I RPP7, 27	I	I RPP21	I RPP5	I
Nd-0	C	I RPP13	I RPP1	C	I RPP1	C	I RPP13	C	C
Ws-0	I RPP1	C	I RPP1	C	I RPP1	I	I RPP1	I RPP1	I
Ksk-1	I RPP2	I	I	I	C	?	C	C	?
Oy-0	I RPP2	I	C	C	C	I	C	I	C
Wei-0	I	C	C	C	I RPP9	C	C	I	I
Ws-*eds1*	C	C	C	C	C	C	C	C	C

Table 1.2. Examples of natural variation in the incompatibility of Arabidopsis with *Hpa* (modified from Holub 2007). Several Arabidopsis accessions were tested for susceptibility to various *Hpa* isolates. Arabidopsis – *Hpa* interactions are categorised as incompatible (I) or compatible (C). Incompatibility (also called resistance) is conferred by R genes, which if they were identified are indicated. Compatibility (also called susceptibility) occurs when *Hpa* can grow on a certain plant genotype/accession. The defense mutant Ws-*eds1* is hypersusceptible to all *Hpa* isolates.

As illustrated in **Table 1.2**, in Arabidopsis accession Nd-0, the presence of the *RPP13* gene (designated $RPP13^{Nd}$) confers resistance to *Hpa* isolates Emco5 and Maks9 (Bittner-Eddy et al. 1999; Bittner-Eddy et al. 2000). Characterisation of natural allelic variants of *RPP13* highlighted that it had evolved under strong diversifying selection (Rose et al. 2004) and that this variation is matched by the allelic variation at the corresponding *Avr* gene *ATR13* locus (Allen et al. 2004; Allen et al. 2008). This observation confirms that an R gene and its corresponding effector often undergo a co-evolutionary arms race and, in the case of RPP13-ATR13, may also interact directly. *RPP13* belongs to the CC-NB-LRR class of *R* genes (Bittner-Eddy et al. 2000). Interestingly, $RPP13^{Nd}$-mediated resistance does not require SA-induced defence responses or the classic defence components *eds1, ndr1, rar1, pad4, npr1* (described below), suggesting that *RPP13*-mediated resistance involves novel defence signalling components (Bittner-Eddy and Beynon 2001).

1.2.2. Defence signalling components

ETI triggers a large set of defence responses, including the induction of major defence genes such as *EDS1* or *NDR1*, or the production of the phytohormones (Torres et al. 2002; Eulgem et al. 2004; Glazebrook 2005).

Only a few other major components involved in disease resistance have been described in the literature. Among those, *Enhanced disease susceptibility 1* (*EDS1)* and *Non-race-specific disease resistance 1* (*NDR1)* were the first genes identified as defence components required for *R* gene-mediated resistance (Century et al. 1995; Parker et al. 1996; Century et al. 1997). Interestingly, a dichotomy is observed within most *R* genes: genes requiring *EDS1* do not require *NDR1*, whereas genes requiring *NDR1* do not require *EDS1* and it seems that *EDS1* is preferentially required for TIR-NB-LRR genes function whereas *NDR1* is preferentially required for CC-NB-LRR genes function (Aarts et al. 1998). An exception has been observed for *RPP8* and *RPP13*, two CC-NB-LRR genes which do not require any known defense components (Aarts et al. 1998).

Several *phytoalexin-deficient* mutants have been isolated, among which *pad4*, which was able to trigger a *Hpa*-compatible interaction in a naturally *Hpa*-incompatible background (Glazebrook et al. 1997). PAD4 is involved in the production of the camalexin phytoalexin (Glazebrook et al. 1996; Glazebrook et al. 1997). Additionally, the *senescence-associated gene 101* (SAG101) was identified later as interacting with EDS1 (Feys et al. 2005). Interestingly, EDS1, PAD4 and SAG101 can form different complexes with distinct function in different pathosystems (Feys et al. 2001; Rietz et al. 2011; Zhu et al. 2011). The EDS1/PAD4/SAG101 complex is essential for *RPP1*-, *RPP2*- and *RPP5*-mediated resistance (Parker et al. 1996; Aarts et al. 1998; van der Biezen et al. 2002).

Despite the identification of *eds1* in 1996 as a major defence component in plants, the EDS1 protein function remains unknown. EDS1 and PAD4 proteins share some similarity

with the catalytic site of eukaryotic lipases, suggesting that they may function by hydrolysing a lipid-based substrate (Falk et al. 1999; Jirage et al. 1999). NDR1 was recently shown to maintain the integrity of the cell wall-plasma membrane continuum during pathogen infection (Knepper et al. 2011).

Other proteins involved in *RPP*-mediated resistance, possibly in an EDS1-independent manner include the chaperone proteins Suppressor of the G-two allele of *skp1* (SGT1b), Required for Mla12 resistance 1 (RAR1) and the heat-shock protein 90 (HSP90) (Muskett et al. 2002; Takahashi et al. 2003; Kadota and Shirasu 2011). While SGT1b seems important for *RPP*-mediated resistance, RAR1 and HSP90 are only partially and differentially required (Austin et al. 2002; Muskett et al. 2002; Tor et al. 2002).

As mentioned above, phytohormones are also major components of defence signalling pathways. The salicylic acid (SA) signal transduction pathway plays a key role in defence signalling against biotrophic pathogens (Vlot et al. 2009) such as *Hpa*, but not against necrotrophic pathogens for which both the jasmonic acid (JA) and ethylene-mediated signalling pathways are induced (Glazebrook 2005). Moreover, the loss of SA accumulation or responsiveness in plants has been shown to alter pathogenesis-related (PR) gene induction and leads to an increased susceptibility to pathogen infection (Cao et al. 1997; Ryals et al. 1997; Falk et al. 1999; Jirage et al. 1999; Nawrath and Metraux 1999; Wildermuth et al. 2001).

Very interestingly, BRI1-associated kinase 1 (BAK1), a major co-receptor involved in PTI signalling (Chinchilla et al. 2007; Heese et al. 2007; Roux et al. 2011) is required for *N. benthamiana* resistance to *P. infestans* and for the induction of cell death triggered by the *P. infestans* elicitor INF1 (Chaparro-Garcia et al. 2011).

1.2.3. Susceptibility factors

As biotrophic pathogens are entirely dependent on their hosts to grow, it seems inevitable that some plant-associated genes and functions are essential for the pathogen maintenance. Such genes are called susceptibility genes: contrary to resistance genes they are not involved in cell death or constitutive activation of defences. Rather, susceptibility genes are involved in plant development and growth and are believed to be hijacked by the pathogen for the maintenance of biotrophy and its associated diversion of resources. In contrast with the long list of known plant defence components and resistance genes, only a few plant susceptibility factors have been described so far, as they are experimentally more difficult to pinpoint.

The first susceptibility gene to be required for powdery mildew growth was identified as the *mildew resistance locus O* (*MLO*) gene in barley (Wolter et al. 1993). However, the function of MLO is still unclear (Kim et al. 2002; Consonni et al. 2006). Later, the Arabidopsis *powdery mildew resistance* (*PMR*) genes (Vogel and Somerville 2000) and the *enhanced disease resistance 1* (*EDR1*) gene, required for both powdery mildew and bacteria growth, were identified (Frye and Innes 1998). More precisely, PMR4 is a wound- and pathogen-induced callose synthase required for powdery and downy mildew growth (Vogel and Somerville 2000; Nishimura et al. 2003). PMR6, a pectate lyase, and PMR5 were also reported to be susceptibility factors as they did not involve NPR1, COI1 or ETR defence signalling components and were effective only towards closely related powdery mildews (Vogel et al. 2002; Vogel et al. 2004).

Susceptibility genes required for downy mildew growth have been found in genetic screens for loss of susceptibility in hypersusceptible mutants (van Damme et al. 2005; Stuttmann et al. 2011). Van Damme et al. (2005) subsequently identified 6 *downy mildew*

resistant (*dmr*) loci, among which 2 loci (*dmr1* and *dmr2*) conferred enhanced disease resistance to *Hpa* but did not enhance activation of plant defences (van Damme et al. 2005; van Damme et al. 2008). One of these genes, *DMR1*, was recently shown to encode a homoserine kinase (van Damme et al. 2009). Interestingly, in *dmr1* mutant, the high levels of homoserine accumulated in the chloroplasts trigger resistance independently of any known immune responses (van Damme et al. 2009). Stuttmann et al. (2011) later identified two *reduced susceptibility* (*rsp*) mutants encoding an aspartate kinase (*rsp1*) and a dihydrodipicolinate synthase (*rsp2*), with an apparently perturbed amino-acid homeostasis due to threonine over-accumulation in the cells (Stuttmann et al. 2011). As expected given the biotrophic nature of this pathogen, all susceptibility genes required for *Hpa* growth identified so far are involved in metabolism.

Huibers et al. (2009) identified using microarray a set of compatibility genes induced early during infection but not during incompatible interaction. Interestingly, these 14 genes were also responsive to diverse abiotic stresses, suggesting that the plant responds to the water and nutrient losses caused by the infection (Huibers et al. 2009). Unfortunately knock-out mutants in these genes were not all tested, which may have helped to assess their precise role during infection. In a similar study, Hok et al. (2011) also examined genes differentially regulated upon infection with *Hpa* using microarrays and identified a *malectin-like* gene that is induced both early and late during infection. This malectin-like protein belongs to the LRR-Receptor-Like Kinase (RLK) family, which includes the protein SYMRK, shown to be essential for establishment of symbioses in plants (Stracke et al. 2002; Gherbi et al. 2008). The *malectin-like* mutant was more resistant to *Hpa*, suggesting that this gene is a susceptibility gene.

There is a real interest in studying susceptibility genes in addition to resistance genes. While resistance genes introduced in crops are rapidly overcome in the field due to extensive

monocultures which generates high pressure selection on pathogens to evolve rapidly new effector variants, developing durably resistant plants could involve the use of susceptibility factors as the main targets for engineering.

1.2.4. Defence-induced plant cell modifications upon contact and projection of *Hpa* haustoria

Hpa contacts the aerial surfaces of its plant host *via* conidiospores. As soon as spores germinate upon suitable conditions, plants are able to respond. In *Hpa*-infected cotyledons, epidermal cells undergo drastic subcellular reorganisation at penetration sites which includes aggregation of cytoplasm, focalisation of actin microfilaments, endoplasmic reticulum and Golgi networks, and possibly microtubule depolymerisation (Takemoto et al. 2003; Hardham et al. 2008). This reorganisation is located at the penetration site of the pathogen, in an effort to contain and eliminate infection early. Interestingly, endoplasmic reticulum and Golgi networks were observed to aggregate specifically at the neck of forming haustoria (Takemoto et al. 2003), highlighting the importance of vesicle trafficking at haustoria. Interestingly, these rearrangements in epidermal cells are similar to the rearrangements induced by the mechanical pressure of a micro-needle, suggesting that subcellular rearrangements may only be triggered by the physical penetration of *Hpa* into the cell, and not by chemical sensing (Hardham et al. 2008). However, even if *Hpa* can produce haustoria in leaf epidermal cells, it mainly grows and produces haustoria in mesophyll cells (Koch and Slusarenko 1990) prompting questions on the nature of cellular rearrangements occuring in mesophyll cells upon haustoria formation.

Callose deposition is associated with the development of haustoria, constricted at the neck of young haustoria in a ring shape and completely encasing older ones (located away from the tip of hyphae). The observation and quantification of callose deposition is thus a good way for the researcher to roughly quantify the age of haustoria. It is possible to stain callose with aniline blue and observe it under UV light by confocal microscopy. Encasements are rich in callose, celluloses, pectins, silicon, phenolic compounds but also antimicrobial peptides, toxic secondary metabolites and reactive oxygen species (Fellbrich et al. 2002; Soylu and Soylu 2003). On the molecular level, it seems that phytohormones are directly involved in callose deposition, as *Hpa* haustoria produced in SA-deficient plants are never fully encased (Donofrio and Delaney 2001). It seems very likely that the age of the haustorium matters for its function, as thick encasements can presumably shut down haustoria when they are too old and start to collapse therefore preventing trafficking (effectors and nutrients) at the haustorial interface. It is not well understood why *Hpa* growth is so particularly associated with callose, but in that case, callose deposition is more considered as a hallmark of defence rather than something that suppresses pathogen growth. Interestingly, the Arabidopsis *powdery mildew resistant 4* (*pmr4*) mutant, in which a callose synthase is non-functional, is more resistant to *Hpa* (Vogel and Somerville 2000). This resistance is lost in SA-deficient plants, suggesting that either callose or callose synthase negatively regulates the SA pathway (Nishimura et al. 2003). It is also possible that callose deposition at the neck of haustoria participates in the stability of haustoria within the plant cell (Jacobs et al. 2003).

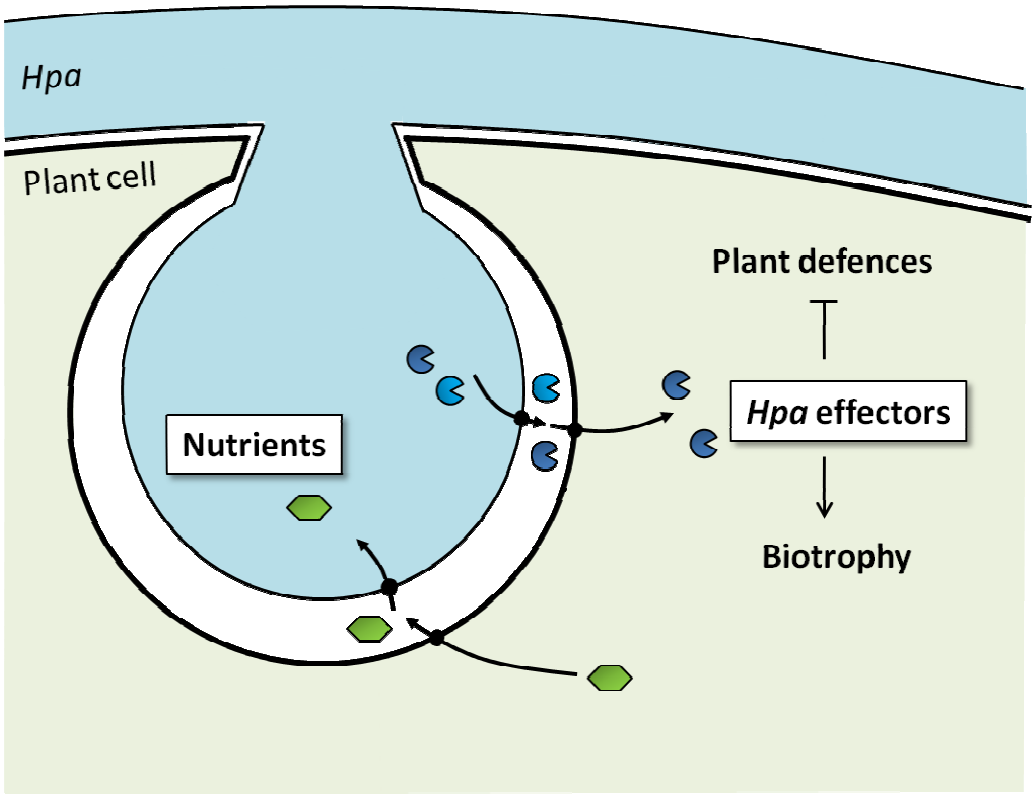

Figure 1.5. Schematic overview of the material exchanges between the plant pathogen haustorium and the plant cell. Effectors and nutrients traffick at the plant-pathogen interface. The plant pathogen structure/material is depicted in blue and the plant cell structure/material is depicted in green.

Haustoria are very specialised structures, assembled directly into plant cells. They are thought to be the sites of effector and nutrient trafficking, making them central components in creating an exchange interface between the biotrophic pathogen and its host (**Figure 1.5**). As it is the focus of parts of the experimental work presented in this thesis, a more detailed description of haustorial development and physiological role can be found in section 1.3.3 of this introduction chapter. In the next section, I focus on how various pathogens generally secrete effector molecules, whether they are able to assemble a haustorium or not.

1.3. Plant pathogens manipulate their hosts by secreting effectors that are translocated into plant cells

To successfully colonise their hosts and promote disease, plant pathogens secrete a large number of effector molecules into host cells, some of which can hamper plant defence responses (Alfano and Collmer 2004; Kamoun 2006). Effectors are produced by all kinds of plant pathogens, eukaryotes and prokaryotes, biotrophs, necrotrophs and symbionts. The main role of effector molecules is thought to be the alteration of host cell structures and functions, resulting in the facilitation of infection in the case of virulence factors or toxins, sometimes triggering defence responses when recognised by the plant (this is the case for so-called avirulence factors or elicitors) (Kamoun 2006). In this section, I will briefly discuss the secretion of effectors by various pathogens, the known classes of oomycete and fungal effectors, and the production of a specific interfacial structure, called the haustorium, by filamentous eukaryotic pathogens to manipulate their hosts. .

1.3.1. Common themes on effector secretion

Plant pathogenic effectors were first identified in bacteria. Specifically, type III effectors (T3E) are secreted by a bacterial pilus-like type III secretion system (T3SS) assembled upon contact with the plant surface, which bridges the bacterium intracellular space to the plant cell cytoplasm (Galan and Wolf-Watz 2006). Type III effectors are major bacterial virulence determinants on some host plants (Espinosa and Alfano 2004). Bacterial T3E possess specific signal sequences in their promoters (termed *hrp* box in *P. syringae*) targeting them to the secretion apparatus for translocation into the plant cell (Innes et al. 1993).

Other plant pathogens have also been shown to secrete effectors and manipulate the host defences and physiology. Similarly to bacterial effectors, oomycete effectors are modular proteins possessing a signal peptide for secretion, an N-terminal delivery motif and a C-terminal domain in which resides the effector function (Kamoun 2006; Morgan and Kamoun 2007). It should be mentioned here that in fungi, no clear particular motif has ever been identified in the sequences of secreted proteins despite the presence of a signal peptide (de Jonge et al. 2011). Consequently, an attempt at *in silico* prediction of effectors using genomic and transcriptomic data in the fungus *U. maydis* yielded 386 genes annotated as potential effectors only on the basis of their specific expression during the biotrophic stage (Kamper et al. 2006), leaving the possibility that these proteins are not actually translocated into the plant host. This point illustrates another notable difference between oomycetes and fungi, and thus presents a clear advantage to working with oomycetes when examining effectors and their interaction with plant cells.

Because of their central role in the promotion of disease, effectors have been extensively studied in many pathosystems and have been classified into different groups. In the next section, I will present a few of these groups relevant to the biology and ecology of filamentous eukaryotic pathogens, with specific reference to oomycetes.

1.3.2. Different classes of effectors can target various plant structures

Many oomycete avirulence factors known to date have been characterised only within the last decade in various species (**Table 1.3**). Among those, only 3 *Avr* genes have been characterised so far in *Hpa* and are termed ATR (for *Arabidopsis thaliana* recognised): *ATR1* (Rehmany et al. 2005), *ATR13* (Allen et al. 2004) and more recently *ATR5* (Bailey et al. 2010). Overall, the largest majority of known oomycete avirulence factors has been identified

in the *Phytophthora* genus and includes Avr3a from *P. infestans* (Armstrong et al. 2005) and Avr1b from *P. sojae* (Shan et al. 2004) (see **Table 1.3** for full description). The description of many effectors from whole genome sequences has allowed the discovery of consensus protein motifs specifically associated with effectors, namely RxLR and crinkler, of which the motifs and structures are described further below.

Species	Effector	Class	Secretion	Translocation	*in planta* localisation	Recognition	Phenotype	Function	Plant target	References
Hpa	ATR1	RxLR	nd	Yes[C]	Nuclear-cytoplasmic*	RPP1	Vir / Avr	Contribution to bacterial virulence	nd	[1][2][3]
	ATR5	RxLR-like	nd	nd	nd	RPP5	Vir / Avr	Contribution to bacterial virulence	nd	[4][5]
	ATR13	RxLR	nd	Yes[C]	Nuclear-cytoplasmic*	RPP13	Vir / Avr	Suppression of callose deposition and ROS	nd	[6][7]
P. infestans	Avr1	RxLR	nd	nd	nd	R1	Avr	nd	nd	[8][9]
	Avr2	RxLR	nd	nd	nd	R2	Avr	nd	nd	[8][10][11]
	Avr3a	RxLR	Yes	Yes	Haustoria*	R3a	Vir / Avr	Suppression of cell death; CMPG1	CMPG1	[12][13][14]
	Avr3b	RxLR	nd	nd	nd	R3b	Avr	nd	nd	[15]
	Avr4	RxLR	Yes	Yes	nd	R4	Avr	Avr4 is not crucial for virulence	nd	[16]
	Avrblb1	RxLR	Yes	nd	nd	Rpi-blb1	Vir / Avr	Disruption of PM-cell wall continuum	LecRK-I.9	[17][18][35][36]
	IPI-O4	RxLR	nd	nd	nd		Vir	Suppression of cell death	nd	[19][20]
	AvrBlb2	RxLR	Yes	nd	Haustoria*	Rpi-blb2	Vir / Avr	interferes with polarized host defenses	C14	[21][22]
	PexRD2	RxLR	Yes	nd	nd		Weak cell death	nd	nd	[17][21]
	PexRD8	RxLR	Yes	nd	nd		Vir	Suppression of cell death	nd	[21]
	PexRD36	RxLR	Yes	nd	nd		Vir	Suppression of cell death	nd	[21]
	CRN1	CRN	Yes	Yes	Nucleus*		Cell Death	nd	nd	[23]
	CRN2	CRN	nd	Yes	Nucleus*		Cell Death	nd	nd	[23][24]
	CRN8	CRN	nd	Yes	Nucleus*		Cell Death	Similarity to RD kinase	nd	[23][24]
	CRN16	CRN	nd	Yes	Nucleus*		Cell Death	nd	nd	[24]
	SNE1	RxLR-like	nd	nd	Nucleus*		nd	Suppression of cell death	nd	[25]
P. sojae	Avr1a	RxLR	nd	nd	nd	Rps1a	Avr	nd	nd	[26]
	Avr1b	RxLR	Yes	Yes[AB]	Nucleus*	Rps1b	Vir / Avr	Supression of cell death	nd	[27][28][29]
	Avr1k	RxLR	nd	nd	nd	Rps1k	Avr	nd	nd	[30]
	Avr3a/5	RxLR	nd	nd	nd	Rps3a, Rps5	Avr	nd	nd	[26][37]
	Avr3b	RxLR	nd	nd	nd	Rps3b	Avr	ADP-ribose/NADH pyrophosphorylase	nd	[31]
	Avr3c	RxLR	nd	nd	nd	Rps3c	Avr	nd	nd	[32][33]
	Avr4/6	RxLR	nd	nd	nd	Rps4/6	Avr	nd	nd	[15]
	CRN63	CRN	nd	nd	nd		Cell death	nd	nd	[15]
	CRN115	CRN	nd	nd	nd		nd	Suppression of cell death	nd	[15]
S. parasitica	HTP1	RxLR	Yes	Yes[D]	Cytoplasm[D]		nd	In host cell cytoplasm	nd	[34]
A. euteiches	CRN5	CRN	Yes	Yes[C]	Nucleus*		Cell death	nd	nd	[24]

← **Table 1.3. Host-translocated effectors of oomycete pathogens with described effects** (modified from Stassen and Van den Ackerveken 2011). Oomycetes: *Hpa*, *P. infestans*, *P. sojae*, *Saprolegnia parasitica* and *Aphanomyces euteiches*. Class: RxLR effector, RxLR-like effector or Crinkler effector (CRN). Secretion tested with yeast invertase secretion assay or tested in association with translocation. Translocation: A internalisation in root cells of purified GFP-tagged effector protein, B effector binding to phosphoinositol phosphates, C *Phytophthora* transformants expressing the N-terminus of the effector tagged to Avr3a are avirulent, D immunolocalisation with specific antibody. Localisation *in planta*: transient expression in *N. benthamiana* (*). Recognition: if the effector is avirulent, name of the corresponding R gene. Phenotype: Virulent (Vir), Avirulent (Avr), Cell death (not associated with R gene). nd: non-determined. References: [1] (Botella et al. 1998), [2] (Rehmany et al. 2005), [3] (Sohn et al. 2007), [4] (Parker et al. 1997), [5] (Bailey et al. 2011), [6] (Bittner-Eddy et al. 2000), [7] (Allen et al. 2004), [8] (Tyler 2002), [9] (Ballvora et al. 2002), [10] (Lokossou et al. 2009), [11] (Gilroy et al. 2011), [12] (Armstrong et al. 2005), [13] (Huang et al. 2005), [14] (Bos et al. 2010), [15] (Liu et al. 2011), [16] (van Poppel et al. 2008), [17] (Vleeshouwers et al. 2008), [18] (Bouwmeester et al. 2011), [19] (Champouret et al. 2009), [20] (Halterman et al. 2010), [21] (Oh et al. 2009), [22] (Bozkurt et al. in press), [23] (Haas et al. 2009), [24] (Schornack et al. 2010), [25] (Kelley et al. 2010), [26] (Qutob et al. 2009), [27] (Shan et al. 2004), [28] (Dou et al. 2008), [29] (Dou et al. 2008), [30] (Gao et al. 2005), [31] (Dong et al. 2011a), [32] (Sandhu et al. 2004), [33] (Dou et al. 2010), [34] (van West et al. 2010), [35] (Senchou et al. 2004), [36] (Gouget et al. 2006), [37] (Dong et al. 2011b).

1.3.2.1. In silico *prediction of RxLR and CRN effectors from genome sequences*

In eukaryotes, secreted proteins usually carry a short N-terminal sequence of 13–30 hydrophobic amino acids, known as the signal peptide which directs the proteins to transfer across the membrane of the endoplasmic reticulum. The signal peptide is often cleaved before completion of the transmembrane transport of the protein (Schatz and Dobberstein 1996; Lee et al. 2004). Proteins are then transported to the Golgi and trans-Golgi network where they undergo further modifications (if required), and sorting into vesicles. Finally the secretory vesicles are delivered to and fuse with the plasma membrane, releasing their contents into the extracellular space (Palade 1975). The software SignalP can predict the cleavage site of the secretion peptide using a combination of several neural networks (http://www.cbs.dtu.dk/services/SignalP/). However, such predictions are not always sensitive. For instance, SignalP identifies secretion peptides of RxLR effectors but is less effective to detect those of CRN effectors (L. Cano and S. Kamoun, personal communication). Additional experimental assays are thus required to test if the secretion

peptide is indeed present or not. As an example, effector secretion can be tested using a yeast invertase secretion assay (Jacobs et al. 1997). The assay, based on the fusion of the sequence to test to a yeast invertase, which needs to be secreted for the yeast to grow on raffinose, was used to show the secretion of RxLR and RxLR-like effectors (Oh et al. 2009; Gu et al. 2011; Tian et al. 2011). The signal peptide of *Hpa* RxLR effectors has been predicted by SignalP, with high probability of secretion, but never validated (Baxter et al. 2010). Interestingly, even though some effectors can be secreted from haustoria, many of them are already expressed in conidiospores (Allen et al. 2004; Rehmany et al. 2005; Bailey et al. 2011) which suggests that they are required for early infection. But because some avirulent effectors can be recognised by the plant before any haustoria is formed, we believe that effectors could be secreted from the hyphae too. Indeed, two effectors of *Puccinia graminis f.sp. tritici* are recognised by the resistance gene *RPG1* before any haustorium is formed (Nirmala et al. 2011).

1.3.2.2. Apoplastic effectors

Additional to intracellular RxLR and CRN effectors, another class of fungal and oomycete effectors has been described, whose functions are primarily located in the plant apoplast, and not within the plant cytoplasm.

The fungal tomato pathogen *Cladosporium fulvum* secretes many apoplastic effectors that tend to block the action of enzymes and defence responses occurring specifically in the plant apoplast. Notably, protease inhibitors such as Avr2 can inhibit various tomato cysteine proteases that are synthesised as part of the defence response, including Rcr3 (Kruger et al. 2002; Rooney et al. 2005). *C. fulvum* additionally secretes two effectors, called Ecp6 and Avr4, that can bind to its own chitin or chitin oligosaccharides to actively prevent elicitation of chitin-triggered immunity (during PTI, as briefly introduced in section 1.2.1) (van den Burg et al. 2006, van Esse et al. 2007, de Jonge et al. 2010). Several apoplastic effectors have

been characterised in *Phytophthora spp.* and include enzyme inhibitors, NEP1-like proteins (NLP) and elicitins (reviewed in Kamoun 2006; Kamoun 2009). Similarly to those of *C. fulvum*, several of these *Phytophthora spp.* effectors can protect the pathogen from host proteases and glucanases that are secreted in the apoplast (Rose et al. 2002; Tian et al. 2004; Tian et al. 2005; Tian et al. 2007).

Not all apoplastic effectors have a protective role against plant defences; the NLPs mentioned above are toxins that can actively cause plant necrosis (Pemberton and Salmond 2004). In *P. sojae* and *P. infestans*, NPP1s (a family of NLPs) are upregulated specifically during the necrotrophic, but not the biotrophic phase of the pathogen growth, indicating that apoplastic effectors can also have an aggressive role during pathogenic infection (Qutob et al. 2002; Kanneganti et al. 2006). Surprisingly for an obligate biotroph, 10 NLPs were annotated in *Hpa* genome but the closest NPP1 homolog (HaNLP3) has not been observed to elicit necrosis in *N. tabacum* (Baxter et al. 2010), possibly suggesting alternative or species-specific functions of NLPs in biotrophs. To support this hypothesis, even some predicted NLPs in *P.infestans* do not seem to cause plant necrosis or are specifically induced during the biotrophic phase (Kanneganti et al. 2006; Haas et al. 2009). In addition, *Hpa* has been shown to secrete small cysteine-rich proteins of the *P. parasitica* (*At*) 12/24 (PPAT)-like family, but whose functions are still unknown (Bittner-Eddy et al. 2003; Baxter et al. 2010).

Expectedly, plants are not defenceless against apoplastic effectors as some of them can be sensed by the plant at its plasma membrane during PTI. This is the case for the *Phytophthora* cell wall transglutaminase GP42, which is perceived at the plant plasma membrane and induces defence responses (Nurnberger et al. 1994; Hahlbrock et al. 1995; Sacks et al. 1995; Brunner et al. 2002). It can be hypothesised that some effectors initially secreted in the apoplast can use plasma membrane receptors to get into the plant cell. This is the case for ToxA, an effector secreted from the fungus *Pyrenophora tritici-repentis,* which

uses its RGD motif to bind an unknown plant receptor to be directly translocated inside the plant cell (Manning and Ciuffetti 2005; Sarma et al. 2005).

Plant pathogens generally secrete cell wall degrading enzymes (CWDE) to make their way inside plant tissues. Expectedly, necrotrophs secrete many CWDE whereas biotrophs secrete very few, or at least just enough to breach through the epidermis or to grow hyphae in between plant cells and project their haustoria. As a result of this, only a very small number of CWDE were found in both the *Hpa* and the *A. laibachii* genomes as compared to *Phytophthora* and *Pythium* genomes (Baxter et al. 2010; Kemen et al. 2011).

1.3.2.3. RxLR effectors

Before genome sequences were available, Rehmany et al. (2005) identified that several oomycete effectors characterised at that time (Avr3a, Avr1b, ATR13 and ATR1) contain a conserved RxLR (Arg-x-Leu-Arg) motif in their N-terminal protein sequences, often followed by an acidic EER (Glu-Glu-Arg) motif (Rehmany et al. 2005) (**Figure 1.6**).

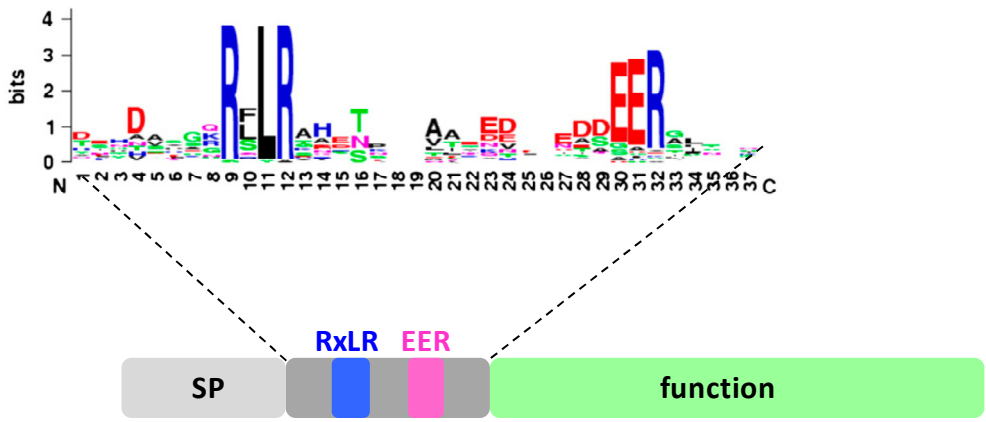

Figure 1.6. RxLR effectors are modular proteins (modified from Win et al. 2007). RxLR effectors are composed of a secretion signal (also termed signal peptide, SP) and an RxLR-EER motif in their N-terminus which is involved in the translocation, and a C-terminus part in which resides the function of the effector.

Using oomycete genomic and transcriptomic data and effector prediction tools, hundreds of RxLR effectors were since predicted, waiting for further molecular confirmation and characterisation (**Table 1.3**). These RxLR effector candidates were defined as small proteins with a signal peptide and an N-terminal RxLR motif that are expressed during infection (Haas et al. 2009; Baxter et al. 2010). Specifically, the *Hpa* reference isolate Emoy2 genome sequence allowed the *in silico* prediction of a set of 134 RxLR motif-containing effector candidates, termed "HaRxLs" (Baxter et al. 2010). In comparison with *P. sojae* and *P. ramorum* genomes, from which about 400 RxLR effector candidates have been predicted (Tyler et al. 2006; Jiang et al. 2008), *Hpa* possess far fewer RxLR effectors (Baxter et al. 2010). An explanation to this observation has been suggested: as *Hpa* only infects *Arabidopsis thaliana* whereas *P. sojae* and *P. ramorum* have much broader host ranges (Tyler et al. 2006; Jiang et al. 2008; Baxter et al. 2010) it is therefore plausible that some RxLR effectors are only functional when the pathogen is infecting particular hosts. In any case, most of the predicted RxLR effectors have no homology to other known proteins, which makes their characterisation a slow and challenging process (Kamoun 2007).

Since RxLR effectors eliciting defences in resistant plants have been shown to be recognised by resistance proteins located inside the host cell, RxLR effectors are believed to be intracellular effectors delivered into the cytoplasm of the host cell (Tyler 2002; Armstrong et al. 2005; Chisholm et al. 2006; Ellis et al. 2006; Jones and Dangl 2006). As a mechanism of immune evasion, effector sequences within pathogen populations are often under positive selection, which means that they usually undergo rapid diversification events leading to the synthesis of new effector variants potentially escaping plant immunity while retaining function (Dodds et al. 2006). Accordingly, rates of polymorphism and positive selection are observed in the C-terminus of oomycete RxLR effectors (Rehmany et al. 2005; Win et al.

2007) and particularly in *ATR13*, which is the best studied *Hpa* RxLR effector gene (Allen et al. 2004; Allen et al. 2008). As an illustration of this point, in 16 *Hpa* isolates, 15 distinct ATR13 protein variants were described (Allen et al. 2008). All these ATR13 variants show a high level of non-synonymous polymorphism and a decline of optimal codon usage, suggesting that a strong positive selection acts on *ATR13* gene (Allen et al. 2004; Allen et al. 2008). ATR13 contains repetitive elements in its C-terminal function domain, a heptad leucine/isoleucine repeat and 11-amino-acid-long repeated sequence (Allen et al. 2004). Intriguingly, while the number of 11-amino-acid-long repeats was extremely variable across *Hpa* isolates, the leucine or isoleucine residues were rather conserved and mutations in these residues alter ATR13 recognition by RPP13 (Allen et al. 2008). Because of this positive selection observed on a number of effectors, it is used as a criterion to identify new effector genes (Liu et al. 2005).

Interestingly, *ATR1*, *ATR5* and *ATR13* are already expressed in spores, before any infectious event (Allen et al. 2004; Rehmany et al. 2005; Bailey et al. 2011) which can suggest two things: (a) in resistant genotypes these effectors are recognised extremely rapidly and (b) in susceptible genotypes these effectors may be required from the very early stages of infection. In *P. infestans*, RxLR effectors are not expressed in mycelium growing *in vitro* but are expressed in zoospores and show a peak of expression at 2 days post infection on potato (van West et al. 1998; Whisson et al. 2007; Haas et al. 2009; Vleeshouwers et al. 2011) which interestingly coincides with the *P. infestans* biotrophic phase, when haustoria are formed.

Aside from *Phytophthora spp.* and *Hpa*, RxLR effectors have been searched for in other oomycete genomes. Interestingly, no RxLR effectors were predicted in the necrotroph *P. ultimum* genome (Levesque et al. 2010) and so far only one RxLR effector with homology to *Phytophthora* elicitins was identified in the fish pathogen *Saprolegnia parasitica* (van West

et al. 2010). In the cucurbit pathogen *Pseudoperonospora cubensis*, RxLR but also QxLR effectors have been predicted from its draft genome (Tian et al. 2011), suggesting that RxLR effectors may nevertheless be a rather common feature in pathogenic oomycetes.

Additionally, a number of RxLR effectors carry in their C-terminus conserved sequence motifs termed W, Y and/or L motifs that are often repeated (Jiang et al. 2008; Boutemy et al. 2011). This large family of RxLR effectors carrying the WY domain includes about 44% RxLRs in *Phytophthora* and 26% in *Hpa* (Boutemy et al. 2011). Very recently, Boutemy et al. (2011) elegantly showed that the WY domain constitutes a conserved α-helical fold of the effectors, and that this central fold is also present in *P. infestans* Avr3a11, Avr3a4 and PexRD2 and *Hpa* ATR1 effectors (Boutemy et al. 2011; Chou et al. 2011; Yaeno et al. 2011). This result suggests that structural similarities may account for similar functions shared by all the effectors carrying a WY domain. However, *Hpa* ATR13 was shown to have a different α-helical-based structure (Leonelli et al. in press) and may not conform to this model.

Interestingly, a biological role during translocation of effectors into plant cells has been suggested for RxLR, based on comparisons and studies with the malarial agent *Plasmodium falciparum*. This aspect is further discussed in section 1.3.3.2.

1.3.2.4. Crinklers and CHxCs effectors

CRN effectors were first identified from *P. infestans*; they can cause crinkling and necrosis in *N. benthamiana* leaves (Torto et al. 2003) (**Table 1.3.**). Around 200 *CRN* genes have been recently described in the *P. infestans* genome (Haas et al. 2009), suggesting their importance for this pathogen and possibly others. Interestingly, CRN proteins are modular effectors as they carry a signal peptide in their N-termini followed by an LxLFLAK (Leu-x-Leu-Phe-Leu-Ala-Lys) domain and an adjacent DWL (Asp-Trp-Leu) domain (Haas et al. 2009). These domains are required for effective translocation into the host cell (Schornack et

al. 2010). Interestingly, all 5 tested CRN effectors were observed to target the plant nucleus (Schornack et al. 2010). The C-terminus of CRN proteins is usually very variable and most probably reflects the extensive recombination of different modules in between different *Phytophthora* clades (Haas et al. 2009), which is reminiscent of the terminal domain reassortment reported for some bacterial effectors (Stavrinides et al. 2006). One CRN effector, CRN8 looks like an interesting effector to work with as it has homology with RD kinases (Kamoun 2009).

Few CRN and RxLR/Q effectors were identified in the genome of the biotroph *A. laibachii*, but Kemen et al. (2011) recently identified a promising additional class of effector candidates carrying in their N-termius a CHxC (Cys-His-x-Cys) motif. *A. laibachii* contains 29 CHxC effector candidates whereas *A. candida* contains 40 of them (Kemen et al. 2011; Links et al. 2011)

In this section, I briefly described different classes of effector molecules synthesised by oomycete pathogens that can manipulate the plant host according to their various ecological strategies of infection. However, the molecular mechanisms of effector trafficking and translocation from the pathogen to the plant cell are of extreme importance. Although their physiological role is still discussed, oomycete effectors seem to possess N-terminal motifs possibly allowing their translocation into plant cells. In the next section, I provide a further focus on the process of oomycete effector delivery into plant cells, and a brief overview of the research progress on the subject.

1.3.3. The haustorium as an exchange interface between the plant and filamentous eukaryotic pathogens

The diversity of function and localisation of effectors highlights the tremendous diversity of these secreted molecules and their central role in the manipulation of the host during infection. In addition to their role in effector secretion, haustoria have a role in nutrient uptake from plant cells which results from millions of years of co-evolution. Dissecting the function of effectors is therefore crucial to better understand the plant-pathogen interface.

1.3.3.1. Haustoria mediate the acquisition of nutrients

The word "haustorium" comes from the latin *haustus*, which means "drinking". Ever since their first description (de Bary 1863), haustoria have been mainly considered as feeding structures, and thus as a way for the pathogen to acquire water and nutrients from its host. Morphologically, haustoria are pathogen-produced structures surrounded by an extra-haustorial membrane (further referred as EHM) which is probably continuous with the plant plasma membrane, and an extra-haustorial matrix (further referred as EHMx) that effectively excludes *Hpa* from the plant cell cytoplasm. Haustoria are connected to intercellular hyphae by a very short haustorial "neck" (Soylu and Soylu 2003). The development of *Hpa* haustoria is associated with callose deposition in an age-dependent manner. Ring-shaped callose deposits are usually observed at sites of penetration around the proximal region of the haustorial neck, but also sometimes completely encase the haustoria (Parker et al. 1993; Donofrio and Delaney 2001; Soylu and Soylu 2003; Mims et al. 2004) (**Figure 1.7**), as observed in powdery mildew-infected cells (Skou et al. 1984).

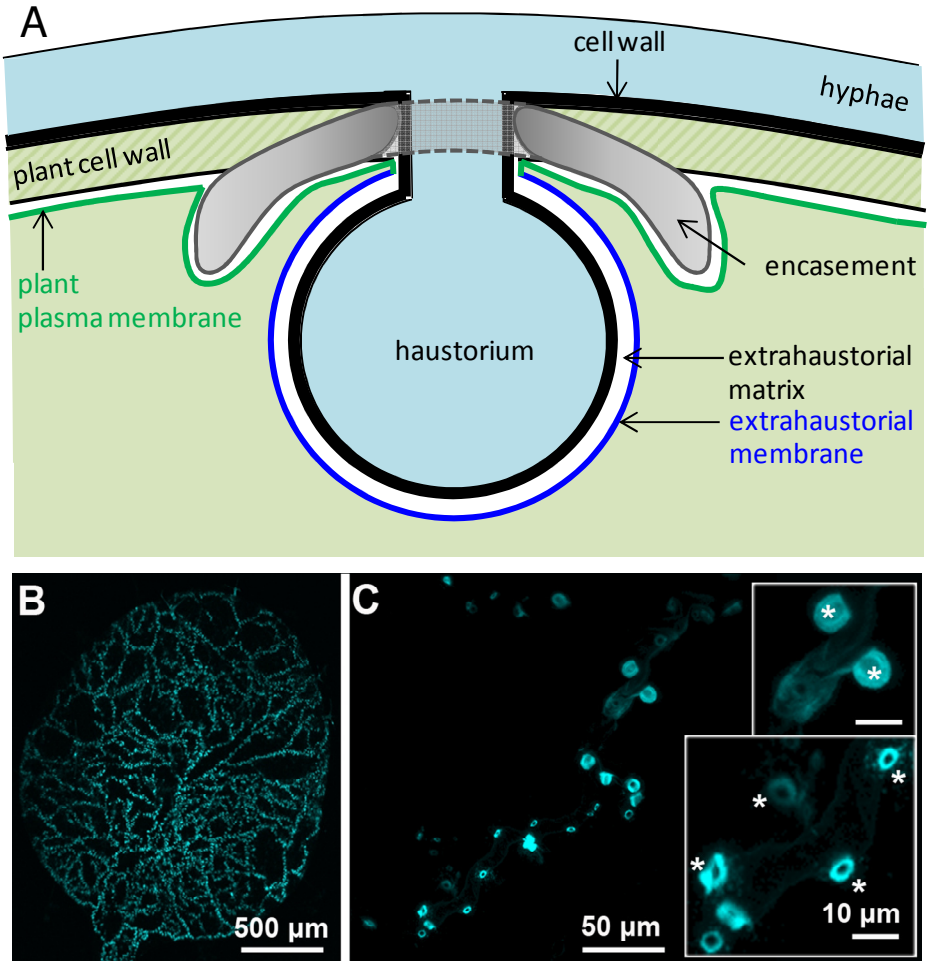

Figure 1.7. Callose deposition is associated with the development of *Hpa* haustoria.
A. Schematic overview of a *Hpa* haustorium projection (blue) into a plant cell (green).The haustorium is excluded from the plant cell cytoplasm by the extra-haustorial membrane. The extra-haustorial matrix is at the interface between the pathogen and the plant. B, C. Callose staining of *Hpa*-infected Arabidopsis cotyledons. B. Image of a full cotyledon. C. Close-up image of a *Hpa* hyphae in mesophyll cells. Callose is present in ring shape deposition at the neck of young haustoria, and in full encasements in mature haustoria. Callose was stained with aniline blue and observed under UV light with a Leica SP5 confocal microscope. Haustoria are labelled with asterisks (*).

There is little proof that *Hpa* haustoria take up nutrients, mainly because of the lack of tools. Most of the work to understand the pathogen nutrition has been done in haustoria from rust pathogens, thanks to the development of protocols to specifically isolate haustoria from this species (Hahn and Mendgen 1992). Regarding this point, I will emphasise the very important foundation work done by the Mendgen laboratory on haustoria from the bean rust *Uromyces fabae* (recently reviewed in Voegele and Mendgen 2011) and summarised in

Figure 1.8. Initially, Hahn et al. identified 31 genes specifically expressed in haustoria, among which a third could be annotated based on homology to known genes (Hahn et al. 1997). In 2001, Voegele et al. (2001) identified a functional monosaccharide transporter associated with haustoria, HXT1p, bringing the first direct evidence that haustoria can take up nutrients. HXT1p was shown to specifically transport D-glucose in a proton-symport mechanism in yeast and *Xenopus*. Even if the origin of the proton gradient required for HXT1p-mediated glucose transport is still unknown, an H^+-ATPase, PMA1p, was identified to have an increased activity in haustoria, hence generating a possible source of protons in the EHMx (Struck et al. 1996; Struck et al. 1998). The discovery of this glucose transporter suggested that sucrose, the most abundant transport sugar form in plants, was likely to be catabolised before uptake by the pathogen (Voegele et al. 2001). A few years later, Voegele et al. (2006) identified an invertase, INV1p, localised at the haustorium periphery, that could catabolise sucrose into D-fructose and D-glucose *in vitro*. This observation suggests that the pathogen itself is able to break down sucrose and take up the resulting sugars (Voegele et al. 2006). Once taken up by haustoria, D-fructose and D-glucose concentrations are probably tightly regulated. Voegele and Mendgen suggest in a recent review (2011) that D-fructose is likely to be converted into mannitol by MAD1p whereas D-glucose is likely to be converted into glucose-6-phosphate by GLK1. Haustoria can also take up amino-acids. Three *U. fabae* amino-acid permeases are up-regulated specifically in haustoria (Hahn and Mendgen 1992), with different amino-acid specificities (Struck et al. 2002; Struck et al. 2004). Additionally, rust haustoria were shown to participate in the biosynthesis of metabolites such as thiamine (Hahn et al. 1997; Sohn et al. 2000), indicating that haustoria can also initiate the production, and not only the consumption, of metabolic compounds.

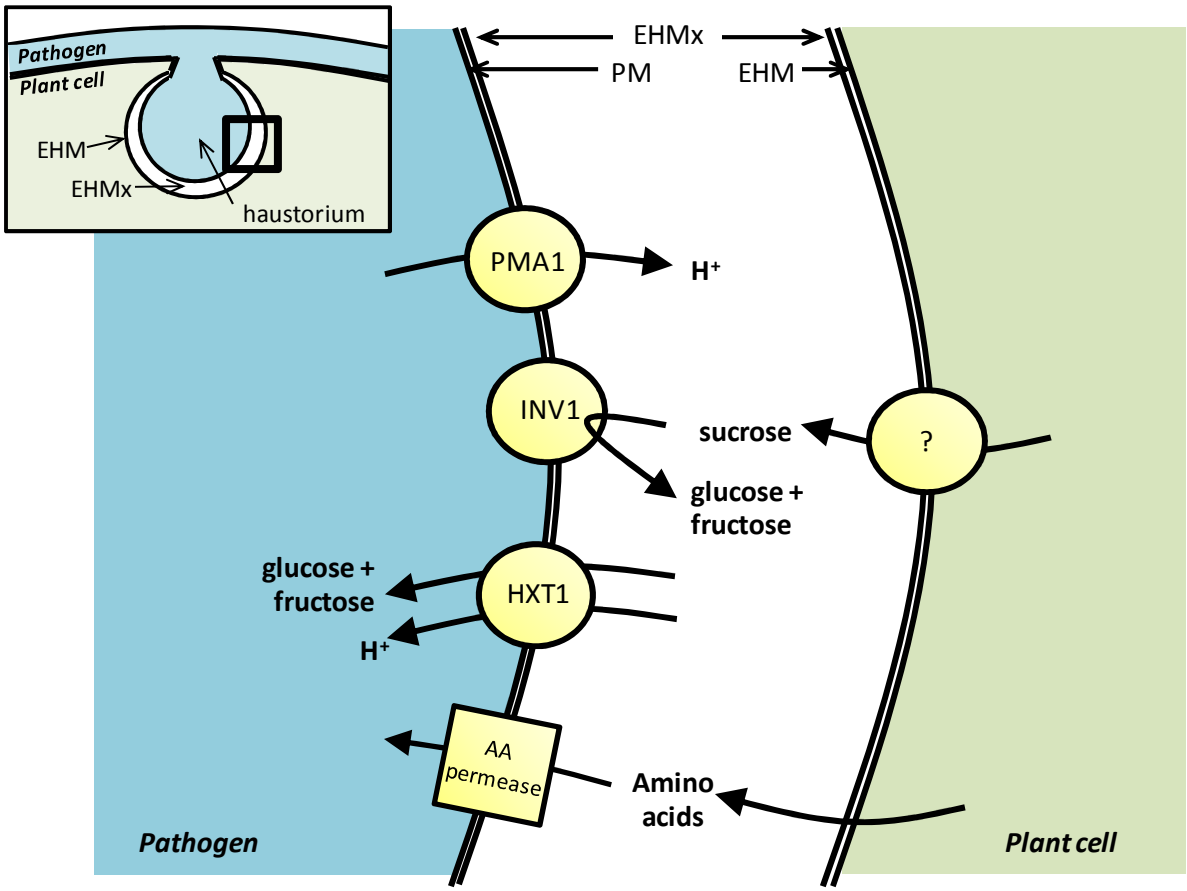

Figure 1.8. Schematic representation of the current knowledge about the rust haustorium metabolism (modified from Voegele and Mendgen, 2011). The fungal structure is depicted in blue, and the plant cell in green. The extra-haustorial matrix (EHMx) is shown in white and separates the extra-haustorial membrane (EHM) from the fungal plasma membrane.

Despite the central role of haustoria and the importance of the interface between the pathogen and its host, the biogenesis of the haustorium including the assembly of the EHM and the EHMx is poorly understood. To our knowledge, no work has been reported to focus on the EHM in *Hpa*-infected Arabidopsis cells, although even if specificities to each pathosystem are expected, it is likely that there are some common features for EHMs in various filamentous pathogens. The EHM appears to be structurally different from the plant plasma membrane, with an altered composition. For instance, the EHM in rust-infected tissues shows a composition greatly reduced in sterols (Harder and Mendgen 1982) and the EHM in powdery mildew-infected tissues shows a significant depletion in arabinogalactan

(Micali et al. 2011) compared to the plant plasma membrane. In addition, among 12 plant plasma membrane proteins tested in Arabidopsis, none was found to localise specifically to the EHM in various powdery mildew-infected tissues, but rather at the haustoria neck or encasement (Koh et al. 2005; Meyer et al. 2009) highlighting that the EHM is of different composition than the plasma membrane. Only two proteins have been reported to localise specifically at the EHM, and interestingly, neither of them localises to the plant plasma membrane in uninfected conditions: the Arabidopsis powdery mildew resistance protein RPW8.2, which localises to the EHM of mature haustoria in cells infected with various mildews (Wang et al. 2009; Micali et al. 2011) and an uncharacterised glycoprotein from pea (Roberts et al. 1993).

Between the haustorial membrane and the EHM is the EHMx, which is a gel-like structure rich in polysaccharides originating from both plant and pathogen material (Harder and Chong 1991). It seems likely that this interface is of prime importance for the biotrophic lifestyle, as hemi-biotrophic pathogens were also found to produce this interface during their biotrophic phase (reviewed in Perfect and Green 2001). Not much is known about the EHMx, but it is thought that nutrients and water can cross it (Mendgen and Hahn 2002), as well as pathogen-produced effector molecules, that are involved in the suppression of plant defence responses *in planta* (Kamoun 2006; Sohn et al. 2007), in the accommodation of pathogen structures into the host, the maintenance of biotrophy and the feeding of the pathogen.

Effectors are produced by all kinds of plant pathogens, prokaryotes or eukaryotes. Like bacteria, nematodes and aphids also secrete effectors, through the stylet they use for feeding on plant tissues (Davis and Mitchum 2005; Will and van Bel 2006). Fungi and oomycetes project haustoria into plant cell, through which effectors are secreted (Kamoun 2006). Interestingly several fungal biotrophic pathogens, like *U. maydis* or *M. oryzae*, do not

produce haustoria but are still able to secrete effectors and get nutrients from their hosts (Vollmeister et al. 2011, Kankanala et al. 2007). They develop other structures fulfilling the role of haustoria. The rice blast fungus *M. oryzae* develops invasive hyphae in rice cells. When looking at *M. oryzae* effector localisation in infected tissues, Khang et al. (2010) elegantly showed that several effectors were translocated into rice cells through the biotrophic interfacial complex (BIC), a structure localised at the tip of invasive hyphae. AvrPiz-t, an effector conferring avirulence, has also been shown to localise at the BIC (Khang et al. 2010), which has thus been described as a route for rice blast effectors secretion from the hyphae into the plant cells. This example illustrates once more that although the need for effector translocation is similar across various plant pathogens, they have evolved a tremendous diversity of effector delivery systems. In the next section, I will briefly present how filamentous eukaryotic pathogens use haustoria to actively secrete effector molecules directly into their plant host cells.

1.3.3.2. Haustoria mediate the secretion of effectors into plant cells

After the identification of the RxLR motif in oomycete effectors and the following identification of a great number of other effector candidates, the function of this motif was investigated. Because it was such a conserved motif, it was hypothesised that the RxLR motif of oomycete effectors could play an important role in effector translocation into plant cells. A visual summary of the different methods used to show effector translocation into plant cells is presented in **Figure 1.9**. In 2007, Whisson et al. showed that the RxLR-EER motif of *P. infestans* Avr3a is essential for its translocation into *N. benthamiana* cells and sufficient to translocate the reporter β-glucuronidase (Whisson et al. 2007) (**Figure 1.9**). Most strikingly, the Avr3a RxLR-EER domain was sufficient to even export a reporter green fluorescent protein from the malarial agent *Plasmodium falciparum* into erythrocytes (Bhattacharjee et al.

2006), suggesting that plant and animal eukaryotic pathogens share conserved mechanisms to deliver effectors into host cells (Haldar et al. 2006). It is usually very difficult to experimentally show that effectors are directly translocated into plant cells. The way to do so is typically to perform immunolocalisation experiments with specific antibodies in infected tissues, as it was done for the rust *Uf*RTP1 shown to localise sequentially in the EHMx and in the plant nucleus (Kemen et al. 2005; Kemen et al. 2011) (**Figure 1.9**). So far, the only RxLR effector ever shown to be translocated into host cells is *Sp*HTP1 from the fish pathogen *S. parasitica,* which was immunolocalised *in situ* in fish cells (van West et al. 2010). Most generally, indirect methods have been developed to follow effector translocation. One of these methods employs the avirulence property of some effectors, recognised by plant cytoplasmic resistance genes (**Table 1.1**). Grouffaud et al. (2008) used *P. infestans* to deliver various N-termini regions of effector candidates fused to the C-terminus region of the known avirulent Avr3a effector. They observed that if the fusion protein is indeed translocated into the plant cytoplasm, the Avr3a C-terminus is recognised and triggers resistance to *P. infestans*, thus indicating that the N-terminal part of the tested effector candidate is able to promote translocation (Armstrong et al. 2005; Huang et al. 2005). Using this system, they additionally showed that *P. falciparum* HRPII and *Hpa* ATR1 and ATR13 N-terminal sequences containing the RxLR motif could successfully translocate Avr3a into plant cells (Grouffaud et al. 2008). A similar system based on *Phytophthora capsici* was developed to deliver effector candidates N-termini tagged with the C-terminus of Avr3a (Huitema et al. 2011). This method was used to show that *P. infestans* CRN N-termini mediates the translocation of Avr3a into plant cells, but also that the LxLFLAK motif was required for translocation (Schornack et al. 2010). Additionally, this technique was recently used to show that *A. laibachii* effectors are effectively translocated into the plant cytoplasm (Kemen et al. 2011). In this last study, it was shown that the N-termini of several RxLR, CHxC and CRN

effectors (including the motif and extra flanking sequences) were able to translocate Avr3a and that the CHxC motif, when replaced by a non-functional AAAA protein motif, was unable to translocate Avr3a (Kemen et al. 2011). Finally, by testing *P. sojae* Avr1b mutants in resistant soybean plants, Dou et al. (2008) showed that the RxLR and EER motifs are required for Avr1b avirulence function.

The translocation of effectors based solely on the presence of a protein motif in their sequences is somewhat surprising and would indicate that the effector proteins are able to translocate independently of any other process. To test if the effector translocation from the EHMx to the plant cell is dependent on factors specific to either the pathogen or the host, a few attempts were made to express effectors in heterologous systems. Dou et al. (2008) reported that *E. coli*-expressed and purified *P. sojae* Avr1b N-terminus fused to GFP can enter soybean cells and reach the plant cell nucleus without the presence of any pathogen, suggesting that the translocation of RxLR effectors into plant cells is solely dependent on plant-mediated processes (Dou et al. 2008) (**Figure 1.9**). This finding was later contrasted by the suggestion of a pathogen-only process of *P. falciparum* effector translocation (de Koning-Ward et al. 2009). However more recently, the CFP-tagged AvrM and AvrL567 effectors of the flax rust *Melampsora lini* (which are neither RxLR nor CRN effectors) expressed transiently and secreted from tobacco cells, appear to be taken up in plant cells (Rafiqi et al. 2010), bringing evidence that effector uptake is indeed a pathogen-free mechanism (**Figure 1.9**). It seems likely that effector translocation relies on the effector ability to bind plant surface receptors or pores.

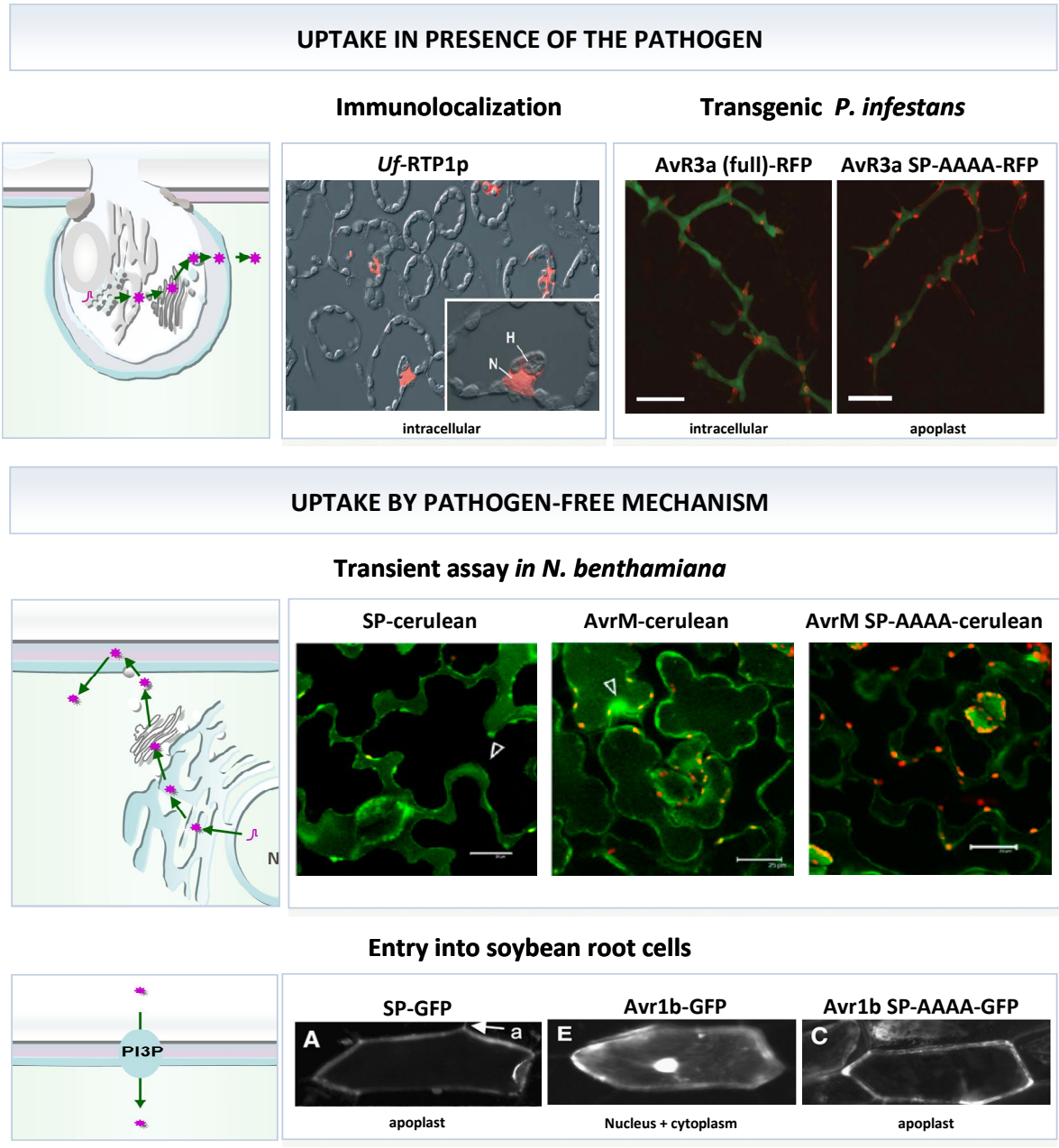

Figure 1.9. Cartoon summarizing the different methods used to show that pathogen effectors are translocated into plant cells (microscopy pictures were taken from Kemen et al. 2005; Whisson et al. 2007; Dou et al. 2008; Rafiqi et al. 2010).

The mechanisms of this motif-mediated translocation process are still largely elusive, but recently, Kale et al. (2010) reported that several RxLR effectors, including Avr1b, could bind *via* their RxLR motif to phosphatidylinositol phosphates (PIPs) present at the extracellular side of the plant plasma membrane, which could mediate their endocytosis in plant cells (Kale et al. 2010). Such a report has since been contrasted by the observation that a positively

charged patch in the C-terminus part of Avr1b was required for PIPs binding (Yaeno et al. 2011). Similarly, AvrM was shown to bind PIPs but surprisingly the portion of AvrM required for host translocation did not bind PIPs (Gan et al. 2010). In addition, AvrL567 binding to PIPs through its RxLR-like motif as shown by Kale et al. (2010) could not be reproduced by Gan et al. (2010). Other "RxLR-like motifs" identified in fungal effectors (from *Leptospheria maculans*, *Laccaria bicolor*, *Puccinia striiformis*) have been shown to bind PIPs and translocate the effector into plant cells (Kale et al. 2010; Gu et al. 2011; Plett et al. 2011), but given that some laboratories cannot reproduce these data, one has to be cautious about this interpretation. Such discrepancies, possibly caused by differences in methods and experimental conditions illustrates that although lipid binding to host membranes may be a common feature of oomycetes and fungal effectors, it may not be required for translocation.

1.3.4. Functions and targets of pathogen effectors inside the host plant cell

One of the driving questions when working with plant pathogenic effectors is about the functions and targets of the plant pathogenic effectors inside the plant. From as early as when Flor first described the gene-for-gene relationship model to when the actual effectors were first characterised in bacteria, the only phenotype indicating the presence of putative effectors was their recognition by the plant host, causing avirulence. The concept of avirulence can be confusing when addressing the question of effector functionality as it is merely a visible consequence of the ongoing evolutionary arms race between pathogens and their hosts. Consequently, the active avoidance of avirulence is a highly selected trait as, aside from the hijacking of host development to favour the biotrophic pathogen growth, the other main role of most effectors appears to precisely be the suppression of plant defences. There are a few

important and common instances in necrotrophic pathogens for which effectors are secreted to kill the host, upon the action of toxins. However, in the case of biotrophic or hemi-biotrophic pathogens, it appears essential that effectors are used as a way to maintain biotrophy, instead of actively damaging the plant. The function of such effectors then logically includes the active impairing of plant defence reactions either by overcoming them or by avoiding triggering them. The fact that hemi-biotrophic pathogens express very distinct sets of effectors during biotrophic and necrotrophic stages would suggest that these functions are quite compartmentalised in time. Time and space regulation of effectors secretion or production have indeed been shown for *U. maydis* effectors produced in maize (Skibbe et al. 2010).

Surprisingly, the precise biochemical activities and functions of only a few plant pathogen effectors are known to date compared to the number of known effectors that have been observed to elicit defence responses in plants. Knowledge on bacterial effectors is more advanced, mainly because they were identified earlier. A few *Pseudomonas syringae* effectors have been observed to target the same plant protein, RIN4 (RPM1-INTERACTING PROTEIN 4), but by different mechanisms. This is the case for AvrRpm1, AvrRpt2 and AvrB which can trigger resistance by modifying the plant protein RIN4: AvrB and AvrRpm1 both target the plant plasma membrane upon delivery by the T3SS, where they are able to phosphorylate RIN4, then recognised by RPM1 in resistant plants; AvrRpt2, is a cysteine-rich protease, which by degrading RIN4 triggers RPS2-mediated resistance in resistant plants (Mackey et al. 2002; Axtell et al. 2003; Axtell and Staskawicz 2003; Mackey et al. 2003; Kim et al. 2005). In the absence of the resistance proteins RPS2 and RPM1, AvrRpt2 or AvrRpm1 can potentially manipulate plant proteins including RIN4 in order to promote susceptibility (Lim and Kunkel 2004). An additional effector HopF2 was shown to interact with RIN4 to promote virulence and prevent AvrRpt2-mediated ETI (Wilton et al. 2010).

Despite the lack of known biochemical function, HopF2 suppresses PTI (Wang et al. 2010; Wu et al. 2011). This example shows that one effector does not necessarily have only one given function, and that in different settings, plants and interaction conditions, overlapping functions can be observed.

Interestingly, another group of bacterial effectors, the Transcription activation-like (TAL) effectors from *Xanthomonas spp.*, can bind to particular plant promoter sequences in order to modulate the expression of target genes, notably some that contribute to the development of symptoms (reviewed in Kay and Bonas 2009). This example once more indicates that the interaction between plants and pathogens is complex, with sophisticated and diverse mechanisms for the effector-mediated manipulation of the host cell.

There is only scarce literature on how effectors can precisely hijack plant resources, but it was nonetheless recently shown that *U. maydis* secretes a chorismate mutase enzyme into plant host cells which actively diverts plant metabolism towards the production of phenylalanine and tyrosine-derived compounds that can be used by the pathogen, instead of their role in salicylic acid production, which is required for maize defense (Djamei et al. 2011).

Comparatively, much less is known about precise and detailed oomycete effector functions, particularly in *Hpa* mainly because of the difficulty of working with biotrophic pathogens. This difficulty drove researchers to develop heterologous systems to indirectly assess *Hpa* effector functions (Sohn et al. 2007; Rentel et al. 2008). The Effector Detector Vector (EDV) system, developed in our laboratory, is based on the delivery by the bacterial T3SS of *Pst* of an effector of interest fused to the N-terminal part of the bacterial effector AvrRPS4 (Sohn et al. 2007). Using this EDV system, Sohn et al. (2007) have shown that the *Hpa* effectors ATR1 and ATR13 confer enhanced virulence to the bacterial pathogen *Pst* DC3000 (Sohn et al. 2007). In addition, ATR13 can actively suppress plant defences, notably

PAMP-induced ROS burst and callose deposition, which are typical indicators of plant immune response activation (Sohn et al. 2007). As mentioned above when describing apoplastic effectors, it is not surprising to identify effectors that can suppress PTI responses. *Hpa* indeed grows in very close contact with Arabidopsis, the plant cells surrounding *Hpa* structures, and it appears logical that *Hpa* has evolved ways to mask its PAMPs and/or to inhibit PTI.

A promising way to investigate the function of effectors comes from structural biology. A few studies so far have presented successful attempts to solve the three-dimensional structure of effectors. Getting the structure of effector proteins could potentially indicate any match to structural folds reported in other organisms present in protein databases, and possibly lead to the identification of their targets in the plant cell. Structures are also useful in the sense that they can reveal if two proteins are structurally related despite weak sequence homology. This present year has been successful in resolving the structure of 5 different RxLR effectors from oomycetes: two from *Hpa* and three from *Phytophthora* (Boutemy et al. 2011; Chou et al. 2011; Yaeno et al. 2011; Leonelli et al. in press). Recently, the structure of the transglutaminase GP42 from *P. sojae*, which is secreted in the plant apoplast and triggers defence responses, was also resolved and indicates that GP42 has similarity to other cysteine proteases (Reiss et al. 2011).

Understanding the virulence functions of RxLR effectors can be achieved by identifying their targets *in planta*. Using a yeast-two-hybrid (Y2H) assay, *P. infestans* AVR3a was shown to interact with the plant E3 ligase CMPG1. *In planta*, Avr3a can stabilize CMPG1, potentially preventing host cell death during the biotrophic phase of infection (Bos et al. 2010). The function of a second oomycete RxLR effector is known: *P. infestans* Avrblb1 can interact with the plant lectin LecRKI.9 *via* its RGD motif, therefore causing a disruption of the plant plasma membrane-cell wall continuum and an increase in susceptibility (Senchou et

al. 2004; Gouget et al. 2006; Bouwmeester et al. 2011). A large-scale identification attempt of *Hpa* and *Pseudomonas* effectors plant targets has been conducted through the development of an automated Y2H system to test ~8000 Arabidopsis proteins (AtORFeome2.0) against 83 different effectors (Mukhtar et al. 2011). This allowed the identification of 165 putative effector targets, some of which are considered as hubs, as summarised in the plant-pathogen immune network, version 1 (PPIN1) database (Mukhtar et al. 2011). Such large scale experiments can prove extremely useful to guide the quest for knowledge of effector functions.

1.4. Context of this work

As shown in this introduction chapter, successful plant pathogens can deliver effector proteins into their hosts. These effectors are active in the plant cells and can interfere with different plant functions, in particular by suppressing plant immunity. However, how the effectors function within the plant cell, whether effectors are virulent or avirulent, is poorly understood. I believe that the understanding of pathogen effectors function will allow us to better understand how pathogens successfully colonise their hosts. Additionally, there is an important need for understanding how various ecological strategies of interaction between pathogens and hosts can take place, and what are the molecular mechanisms involved. Biotrophy in oomycetes probably requires secreted effectors, that precisely and specifically manipulate host functions. In this work, I used the *Hpa*–Arabidopsis model pathosystem to address the question of the manipulation of Arabidopsis responses by *Hpa* effectors to promote susceptibility (including the maintenance of biotrophy), and try to understand how this manipulation can sometimes fail and thereby trigger resistance.

During this PhD project, I was mainly involved in two lines of research:

- **Characterisation of a novel additional resistance source to the avirulent effector protein ATR13**

This research started with the identification of an additional resistance source in the Arabidopsis ecotype Ws-0 recognising the effector ATR13 from the *Hpa* isolate Emco5. Dr Kee Hoon Sohn observed that despite the fact that *Hpa* Emco5 could complete its life cycle on Ws-0, the single ATR13^{Emco5} effector protein was recognised in this accession (Sohn et al. 2007). I therefore started to characterise the resistance to ATR13^{Emco5} in Ws-0 by genetic mapping. The results I obtained in this work are presented in **Chapter 3** of this thesis.

- **Identification and early characterisation of candidate effectors of *Hpa*.**

The release of the *Hpa* genome sequence allowed the bio-informatic prediction of 134 RxLR effector candidates (Baxter et al. 2010). Dr Georgina Fabro initiated the cloning of a subset of these effector candidates in order to test their function *in planta* using different heterologous systems (Fabro et al. 2011). My colleagues and I followed up the characterisation work (presented in **Chapter 4** of this thesis). In parallel, collaborators identified putative plant targets of these effector candidates (Mukhtar et al. 2011), which allowed me to identify and further characterise an Arabidopsis gene family required for susceptibility to *Hpa* (presented in **Chapter 5** of this thesis).

During this PhD work, I participated in the preparation of different scientific publications that arose from excerpts of my personal work presented here and from collaboration with colleagues from my laboratory and beyond. Three of these accepted peer-reviewed manuscripts are presented in the Appendix, at the end of this thesis.

2. Material and methods

2.1. Plants used in this study

2.1.1. Plant material and growth conditions

Arabidopsis seeds were surface sterilized, sown and stratified for two to seven days at 4°C. Seedlings were grown for 10-14 days in compost under 10 hours light / 14 hours dark at 22°C (light levels were approximately 170-190 mmols, HQI lighting) and 75% humidity. After pricking out in Arabidopsis mix (F2 compost, grit, Intercept), plants were grown under 10 hours light / 14 hours dark at 22°C (light levels were approximately 90-110 mmols).

Turnip plants (*Brassica rapa* cv. Just Right) were grown in the same conditions as Arabidopsis (with no stratification step).

Tomato (*Solanum lycopersicon* cv. Moneymaker) and tobacco (*Nicotiana benthamiana*) plants were grown for 3 weeks on F2 compost under 16 hours light / 8 hours dark at 22°C and 55% humidity.

2.1.2. Arabidopsis mutant lines

All Arabidopsis mutant lines used in this study are presented in **Table 2.1**.

Seeds of the different T-DNA insertion lines in Col-0 and Ws-4 backgrounds were obtained from the Arabidopsis Biological Resource Centre (http://arabidopsis.org.uk/) and INRA (http://www-ijpb.versailles.inra.fr/en/cra/fichiers/T-DNA_information.htm) respectively. The lines were analysed after kanamycin selection of seeds grown *in vitro*. T-DNA insertions were verified by PCR genotyping using primers for the T-DNA left border and gene-specific primers designed (**Appendix 2.1**) using the Salk Institute Genomic Analysis Laboratory (SIGnAL) (http://signal.salk.edu/tdnaprimers.2.html) using default conditions. Homozygote lines were identified.

Transgenic Arabidopsis plants were generated using the floral dip method (Clough and Bent 1998). Briefly, flowering Arabidopsis plants were dipped with *A. tumefaciens* carrying a plasmid of interest and the seeds were harvested to select the T1 transformants on selective GM media. T1 plants were checked for expression of the protein of interest either by fluorescence microscopy and/or by western-blot analysis. T2 seeds were sown on selective GM media and the proportion of resistant *versus* susceptible plants was counted in order to identify lines with a single T-DNA insertion.

Arabidopsis thaliana mutants		AGI number		reference	used in
Col-0	35S:YFP-Nap1;1	*At4g26110*	SALK_013610	Liu et al. 2009	Chap. 5
	35S:YFP-Nap1;2	*At5g56950*	SALK_131746	Liu et al. 2009	Chap. 5
	35S:YFP-Nap1;3	*At2g19480*	SAIL_373_H11	Liu et al. 2009	Chap. 5
	nap1;1 nap1;2 nap1;3-1 (m123-1)			Liu et al. 2009	Chap. 5
	nap1;1 nap1;2 nap1;3-2 (m123-2)			Liu et al. 2009	Chap. 5
	klc	*At3g27960*	SALK_148216	NASC	Chap. 4
Ws-0	*eds1-1*	*At3g48090*		Parker et al. 1996	
Ws-4	*rpp13*	*At3g46530*	FLAG_522B05	INRA Versailles, France	Chap. 3

Table 2.1. List of Arabidopsis mutants used in this study.

2.2. Plant pathogen material

2.2.1. Oomycete material and growth conditions

Several *Hyaloperonospora arabidopsidis* (*Hpa*) isolates, called Emoy2, Emco5, Noco2, Waco9, were propagated in the laboratory. For other isolates (like Cala2, Emwa1, Hiks1, Hind2 and Maks9), only genomic DNA preparations were used.

- Emoy2, Emwa1 and Emco5 isolates originated from East Malling, Kent, UK.
- Hiks1 and Hind2 isolates originated from Hiller Arboretum, Hampshire, UK.
- Noco2 isolates originated from Norwich, Norfolk, UK.
- Cala2 isolates originated from Canterbury, Kent, UK.

- Maks9 isolates originated from Maidstone, Kent, UK.
- Waco9 isolates originated from Wageningen, The Netherlands.

Hpa propagation was performed as described previously (Holub et al. 1994). Basically, frozen *Hpa*-infected tissues were kept in the -80°C freezer as lab stock. For conidiospores propagation, frozen stocks were thawed on ice, resuspended in sterile water and filtered through Miracloth (Merck Chemicals Ltd). Two-week-old plants were sprayed with the spore solution. Infected plants were covered with a lid for 100 % humidity and were kept in a growth cabinet at 16°C for seven days with a 10 hours light / 14 hours dark cycle. High humidity conditions favor *Hpa* sporulation, whereas low humidity conditions favour hyphal growth. After one week, fresh spores are harvested for another round of infection on new plants, and thus the maintenance of a live pathogen stock.

2.2.2. Fungal material and growth

Spores from the necrotrophic fungus *Botrytis cinerea* strain B05.10 were obtained from Dr. Henk-Jan Schoonbeek (John Innes Centre, Norwich, UK). Inoculation of Arabidopsis with *Botrytis* spores was performed as described previously (Stefanato et al. 2009). Briefly, 5-week-old plants were inoculated with a suspension of 2.5×10^5 spores / mL in quarter-strength potato dextrose broth (6 g / L). Five microliters droplets of spore suspension were deposited on six leaves per plant, with eight to twelve plants per experiment and lesion diameters were measured at three days post-infection.

2.2.3. Bacteria material and growth

The bacteria used in this study are listed in **Table 2.2**. Bacterial frozen stocks were conserved in 20% glycerol in cryovials at −80°C. *Escherichia coli* strain DH10b was used for

subcloning and was grown at 37°C in Luria Bertani (LB) medium. Prior to infection experiments using *Pseudomonas* or *Agrobacterium* strains, bacteria were streaked from glycerol stocks on L-agar selective media and grown for two days at 28°C. Single fresh colonies were used to inoculate 5 to 10 mL liquid cultures. Bacteria on plates were grown in temperature-controlled incubators, whereas liquid cultures were put in orbital shakers at 200 rpm.

Bacterium	strain	used for	used in
Pseudomonas syringae pv. *tomato*	DC3000	deliver HaRxLs in plants	Chap. 5
	DC3000 LUX	deliver HaRxLs in plants	Chap. 4
	DC3000 ΔCEL	test if HaRxLs can suppress callose deposition	Chap. 4
Pseudomonas fluorescens	*Pfo-1*	HR and callose assay	Chap. 3 & 4
Escherichia coli	DH10b	subcloning	
Agrobacterium tumefaciens	GV3101, GV3103	transient expression in *N. benthamiana*, Arabidopsis transformation	Chap. 4 & 5

Table 2.2. List of bacteria used in this study.

2.3. Plant pathology assays

2.3.1. Bacterial infection

2.3.1.1. Infiltration

- Infiltration of *Pseudomonas spp.*

Single freshly grown bacterial colonies were used to inoculate 5 mL cultures. *P. syringae* or *P. fluorescens* overnight cultures were washed and resuspended in 10 mM $MgCl_2$. Cells were diluted serially to 5×10^4 to 10^6 cfu / mL (optical density at 600nm (OD_{600})= 0.0001 to 0.002, respectively) in 10 mM $MgCl_2$. Within one hour after the preparation of bacteria, four to five-week-old Arabidopsis plants were inoculated by infiltrating bacterial suspensions using a 1 mL syringe. Leaf samples were collected from zero to four days post inoculation to quantify bacterial population sizes in infected leaves.

For HR assays, 5×10^7 to 1×10^8 cfu / mL of bacteria suspensions were used for infiltration. HR was scored between 12 and 30 hours post inoculation.

For experiments on turnip, small scratches on leaves were made prior to infiltration using a needle to minimize the pressure caused by infiltration, as turnip leaves are harder to infiltrate.

For experiments on tomato, plants were vacuum infiltrated twice for 5 min with bacteria at a concentration of 10^5 cfu / mL (OD_{600}= 0.0002).

- Infiltration of *Agrobacterium tumefaciens*

Single freshly grown bacterial colonies were used to inoculate 10 mL cultures. *A. tumefaciens* cells were harvested by a centrifugation at 3500 rpm and resuspended in a buffer containing 10 mM MES (pH 5.6), 10 mM $MgCl_2$ and 200 µM acetosyringone to a final OD_{600} of 0.2. For co-infiltration assays, OD_{600} were adjusted to 0.4 so when mixed, each agrobacteria solution was at a final OD_{600} of 0.2. The cultures were shaken at room temperature for 2 to 3 hours and then hand-infiltrated in *N. benthamiana* leaves using a 1 mL syringe.

2.3.1.2. Spraying

Single freshly grown bacterial colonies were used to inoculate 10 mL pre-cultures. These overnight cultures were used to inoculate 25 mL cultures (1/1000 inoculum). Cultures were washed and resuspended in 10 mM $MgCl_2$ and the inoculum density was adjusted to 2.5×10^8 cfu / mL (OD_{600} = 0.5). Four to five-week-old plants were sprayed with the bacterial suspensions (containing 0.02% of the surfactant Silwet-77) and kept around 90% humidity by covering the trays with transparent plastic lids for 24 hours. Subsequently, the lids were removed and infected plants were kept at 70% humidity. Leaf bacterial population sizes were measured from 0 to 4 days post inoculation.

2.3.1.3. Quantification of bacterial population sizes in infected leaves

Infected leaf samples were taken with a №4 cork borer (2 leaf disks equal 1 cm^2). Two leaf punctures were pooled in one 1.5 mL tube. The content of six tubes (12 leaf punctures) were ground per each type of infection in 200 µL 10 mM $MgCl_2$ immediately followed by the addition of 800 µL 10 mM $MgCl_2$ to make a total volume of 1 mL. The tubes containing ground samples were vortexed briefly, 100 µL were transferred to a 96-well plate containing 100 µL of sterile water in each well and this was considered as 10^{-1} dilution. Subsequently, 20 µL of 10^{-1} diluted samples were transferred to the next well containing 180 µL to make a 10^{-2} dilution. This procedure was continued up to 10^{-6} when needed. 20µL of each of the serial dilutions were spotted on L medium containing appropriate antibiotics and incubated in 28°C incubator until the colonies appeared at which point colony counts were performed.

2.3.1.4. Ion leakage measurement

HR is concomitant with the leakage of ions from the dying cells (Goodman and Novacky 1994), therefore by measuring ion leakage we can quantify the cell death response. Leaves of five to six-week-old Arabidopsis plants were infected as described above (HR assay protocol). Within 30 min after infection, 12 to 24 leaf discs were taken (with a №4 cork borer) and pooled in a 50 mL conical tube containing 40 mL sterile water. The tubes were gently shaken for 1 hour and the leaf discs were transferred to 24-well plates containing 2 mL sterile water in each well (two leaf discs in each well). In the case of Col-5 Dex:ATR13^{Emco5} plants, leaf disks were floated on 40 µM dexamethasone. Conductivity was measured over time using a conductivity meter (B-173, Horiba).

2.3.2. *Hyaloperonopsora arabidopsidis* infection

For *Hpa* infection, 2-week-old plants were sprayed with a conidiospore suspension at a concentration of 5×10^4 spores/ml. Plants were covered with a plastic lid for 100% humidity and were kept in a growth cabinet at 16°C for 6 to 7 days with a 10 hours light / 14 hours dark cycle.

2.3.2.1. Hpa quantification

To quantify *Hpa* sporulation on Arabidopsis mutants, 3 to 4-week-old infected plants were harvested in Falcon tubes. Pools of 3 plants were resuspended in 0.5 mL to 1 mL of water (depending on the infection rate) in order to get the conidiospores in solution. Ten microliters of spore suspensions were deposited on a Neubauer-improved haemacytometer slide (Superior Marienfeld) and the number of spores was counted using a light microscope (Zeiss Axiophot or Leica DMR).

2.3.2.2. Trypan blue staining

Trypan blue staining was used for two purposes (van Wees 2008): to stain *Hpa* structures within plant tissues, and to stain dead plant cells that underwent hypersensitive response (HR). Arabidopsis leaves were boiled in trypan blue solution (0.015 % w/v in 1:1 lactophenol : ethanol) for 1 min, cooled down for 30 min and subsequently destained with chloral hydrate (see Appendix). Leaves were mounted in 60% v/v glycerol and examined macroscopically or with light microscopy (Zeiss Axiophot or Leica DMR).

2.3.2.3. Aniline blue staining

Aniline blue staining was used to stain callose structures in plant tissues (Thistlethwaite et al. 1986) which appear after infection, like ring or encasements of *Hpa*

haustoria, or like dots after *Pseudomonas* infection or PAMP treatment. Samples (either *Hpa*-infected seedlings or leaf disks punctured from PAMP/*Pseudomonas*-infiltrated leaves) were cleared in 100% methanol, washed in water and then stained with aniline blue (0.05% w/v in 50 mM phosphate buffer pH 8) overnight. Samples were observed with a Leica DM6000B / TCS SP5 confocal microscope (Leica Microsystems). Using this technique, I generated the pictures presented in **Figure 1.7B, C** in the introduction.

2.3.3. PAMPs assays

2.3.3.1. Reactive oxygen species measurement

Reactive oxygen species (ROS) are produced by the plant in response to pathogen attack (Lamb and Dixon 1997). We triggered ROS bursts, either in Arabidopsis mutants or after transient expression in *N. benthamiana* in order to see if the ROS response was impaired. Detection of ROS production was monitored by a luminol-based assay on leaf disc samples (Keppler et al. 1989). Twelve to twenty-four leaf disks from five-week-old Arabidopsis plants were distributed on a 96-well plate and incubated overnight in water. Before measurement, the water was removed and 100 µL of assay solution (17 mM luminol [Sigma], 1 mM horseradish peroxidise [Sigma], and 100 nM flg22 [Peptron] or 100 µg / mL chitin [Nacosy]) was added to the wells. Luminescence was measured using a Photek camera system and acquired over time (up to 60 min after elicitation) (Photek Ltd., St Leonards-on-sea, UK).

2.3.3.2. Visualization and quantification of callose

For the monitoring of callose deposition triggered by PAMPs or bacteria carrying a construct of interest, the leaves of 4 to 5 week-old Arabidopsis plants were hand-infiltrated

with 100 nM flg22 or 1×10^8 cfu / ml of bacterial suspension. A total of 12 leaf disks were taken from 12 leaves, 12 to 15 hours after infiltration, for subsequent callose staining. Samples were treated like in section 2.3.2.3. For quantification, the images were analyzed using PDQuest software program (Bio-Rad).

2.4. Molecular biology techniques

2.4.1. DNA methods

2.4.1.1. Genomic DNA extraction

- Arabidopsis genomic DNA extraction

Frozen plant leaf tissues (0.5 – 1 g) were ground in liquid nitrogen. The resulting powder was transferred to 50 mL SS-34 centrifugation tube with 15mL extraction buffer [100 mM Tris pH8, 500 mM NaCl, 50 mM EDTA pH8, 10 mM β-mercaptoethanol]. Two millilitres of 10% SDS were added to the tube. Samples were incubated at 65°C for 10 min and mixed occasionally by inversion. Five millilitres of freshly prepared 5 M potassium acetate were added to the samples and kept on ice for 10 - 20 min. Samples were centrifuged for 20 min at 25000 g. The supernatant was filtered with miracloth into 50mL tube containing 10mL isopropanol. Samples were mixed and incubated for 30 min at -20˚C. Samples were centrifuged for 15 min at 20000 g. Pellets were air-dried and then dissolved in 700 µL TE buffer. Samples were transferred into Eppendorf tubes and purified by phenol/chloroform purification. Samples were finally resuspended in 100 µL TE buffer and kept in the fridge or at -20˚C.

- Arabidopsis genomic DNA extraction for genotyping Arabidopsis mutants

Two leaf disks (cork borer №1) were pooled in PCR tubes for each plant for genotyping. Tissues were homogenised in 100 µL 5% Chelex 100 resin (Bio-rad; HwangBo et al. 2010),

vortexed and incubated at 100˚C for 5 min. Samples were vortexed again and centrifuged briefly. One microliter of the supernatant was used for PCR.

- *Hpa* genomic DNA extraction

Asexual conidiospores were collected by gently shaking sporulating leaves in water. Spores were then collected by centrifugation and DNA was isolated as described previously (Rehmany et al. 2000).

2.4.1.2. Polymerase chain reaction (PCR)

PCRs were carried out using 5 to 20 ng genomic DNA preparations as templates. Each 20 µL reaction contained: 1 X Phusion HF buffer, 0.2 mM dNTPs, 0.002 U Phusion polymerase (Finnzymes), and 0.5 µM of each primer. PCR cycles were optimised for different primers and length of amplicons. An extension of 30 sec per kb was used. PCR was performed in a DNA thermal cycler (Peltier Thermal Cycler 225, MJ Research). PCR for mapping purposes, colony PCR and genotyping were done with homemade Taq polymerase instead of a commercial polymerase. Colony PCR was used to identify positive colonies containing recombinant plasmids during cloning. The PCR was performed as above except that the DNA template was substituted with bacterial cells diluted in sterile water.

RPP13 genotyping was performed using a CAPS marker (primers KS 349 and KS 350 amplify 529 bp of *RPP13* LRR region, **Appendix 2.1**). $RPP13^{Ws}$ PCR products incubated with the restriction enzyme HaeIII (for 2 - 3h at 37°C) are cleaved whereas $RPP13^{Col}$ are not (as illustrated in **Figure 2.1**).

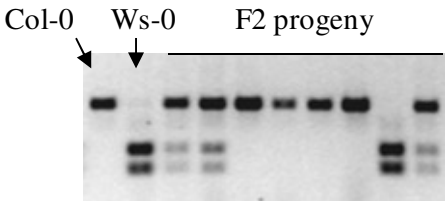

Figure 2.1. *RPP13* CAPS marker allows to differentiate between *RPP13* alleles.

2.4.1.3. Purification of DNA from agarose gels

When PCR gave several amplicons, the amplicons were run and separated on agarose gel. DNA was visualised on a long wavelength UV transilluminator (TM40, UVP) and the desired fragment was carefully excised using a razor blade. Fragments of less than 10 kb were purified using QIAquick spin columns (Qiagen) following the manufacturer instructions.

2.4.1.4. Cloning

EpiGreenK3 vector was used to express ATR13^{Emco5} in Arabidopsis and *N. benthamiana*. *ATR13^{Emco5}* was amplified from the signal peptide cleavage site to the stop codon from *Hpa* Emco5 genomic DNA with gene specific primers using standard PCR conditions and cloned in the pGEM-T-Easy vector (Promega) for sequencing. The sequence verified clones were double digested with restriction enzymes, ClaI and BamHI, and then ligated with ClaI and BamHI treated EpiGreenK3 using T4 DNA ligase (Roche) for two hours in room temperature. The ligated product was used to transform electrocompetent *E. coli* cells and plasmids were isolated from the overnight cultures from the positive colonies. The plasmids were again verified by digesting with ClaI and BamHI and run on 1% agarose gel. Electrocompetent *A. tumefaciens* GV3101 cells were transformed with the confirmed plasmid for expression of ATR13^{Emco5} in plant cells.

All HaRxLs mentioned in this thesis can be found in NCBI database, in the **Appendix 4.1** and/or in Fabro et al. (2011). To produce the HaRxLs collection, primers for amplification were designed from the *Hpa* Emoy2 genome version 8.3 (Baxter et al. 2011). Selected HaRxLs were amplified from the signal peptide cleavage site to the stop codon using genomic DNA extracted from *Hpa* Emoy2 conidiospores and PCR conditions described in 2.4.1.2. Arabidopsis genes *AtNap1;1*, *AtNap1;2* and *AtNap1;3* were amplified from the start codon to the stop codon from non infected Col-0 cDNAs. The Arabidopsis gene *MKRP2* was amplified from the RAFL clone (pda08485) (RIKEN institute, Japan). Using Gateway technology following the manufacturer instructions (Invitrogen), the PCR fragments were inserted into the pENTR-TOPO vectors and then into plant expression vectors pK7WGF2, pK7FWG2, pH7WGR2 or pH7WGY2 for transient expression in *N. benthamiana* and stable expression in Arabidopsis (Karimi et al. 2002), into the split-YFP vectors for bi-fluorescence complementation (Caillaud et al. 2009), or into pEDV6 for expression in *Pseudomonas spp.* (Fabro et al. 2011).

The constructs were sequenced at each cloning step as described in 2.4.1.6. All PCR primers can be found in the **Appendix 2.1**.

2.4.1.5. Transformation of electrocompetent competent E. coli or A. tumefaciens

E. coli or *A. tumefaciens* strains electrocompetent cells were thawed on ice for 5 min. One to two microliters of plasmid were added to 20 µl of electrocompetent cells. Cells were transformed in an electroporation cuvette with a gap width of 1 mm in a Bio-Rad electroporator (Gene Pulser Xcell). The electroporation settings were: 1800V with a capacity

of 25 μF and 200 Ω resistance for *E. coli*, and 2400V with a capacity of 25 μF and 200 Ω resistance for *A. tumefaciens*. Five hundred microliters of liquid L medium were added to the cells without antibiotics and incubated in a shaker at the right temperature for 1 to 2 hours. Transformed cells were selected on L medium supplemented with the appropriate antibiotics.

2.4.1.6. DNA sequencing

After cloning and multiplication, the sequences of the inserted DNA fragments were verified by sequencing. For constructs in pENTR, M13F and M13R universal primers were used, for other vectors, see in **Appendix 2.1**.

DNA sequencing reactions were carried out in a final volume of 10 μl containing 150 ng template plasmid DNA, 0.5 μl of 3.2 μM, 1.5 μl 5x buffer and 1 μl ABI Big Dye Terminator Ready Reaction Mix (Big Dye 3.1 by Perkin Elmer). The PCR cycle conditions were: initial denaturation step at 96°C for 1 min, denaturation at 96°C for 10 sec, annealing at 50°C for 5 sec and elongation at 60°C for 4 min (25 cycles total). Sanger sequencing was carried out at The Genome Analysis Centre (TGAC, Norwich). Sequencing data were analysed, edited, and aligned using Vector NTI (Invitrogen).

2.4.1.7. Phenol/chloroform purification

An equal volume of phenol : chloroform : isoamyl alcohol (25 : 24 : 1) (Sigma) was added to the DNA / RNA solution and the mixture was inverted several times. The aqueous and organic phases were separated by centrifugation for 5 min in a micro-centrifuge at 15,000 × g. The upper, aqueous phase was transferred to a clean Eppendorf tube, taking extra care to avoid the interface.

2.4.1.8. Ethanol precipitation

Two volumes of 100 % ethanol and 0.1 volume of 3 M sodium acetate were added to the DNA/RNA solution. The mixture was briefly mixed by hand inversion and placed at −20°C overnight. DNA/RNA was recovered by centrifugation for 10 min in a micro-centrifuge at 15,000 × g. The pellet was washed with 70% ethanol and air-dried 10 min at room temperature. The RNA pellet was then resuspended in DEPC water and the DNA pellet was resuspended in TE buffer. If necessary, the concentration of DNA was estimated by comparison to DNA standards of known concentration after gel electrophoresis and ethidium bromide staining or by Micro-Volume UV-Vis Spectrophotometer for Nucleic Acid Quantitation (Nanodrop, Thermo scientific).

2.4.1.9. Triparental mating to transfer plasmids from **E. coli** *to* **Pseudomonas** *strains*

One millilitre of a 2 : 1 : 1 volume ratio of recipient (*Pseudomonas* strain), donor (*E. coli* strain DH10β carrying a broad host range vector construct), and helper strains (*E. coli* strain HB101 carrying pRK2013, Ditta et al., 1980) from cultures grown overnight was briefly centrifuged, resuspended in 200 µL of sterile water, and spotted on King's B agar media for conjugation overnight at 28°C. After incubation overnight, bacteria were streaked onto King's B media selective for the desired transconjugants. Successful conjugation was confirmed by colony PCR.

2.4.2. RNA methods

2.4.2.1. Total RNA isolation

Frozen plant tissues were ground to a fine powder in liquid nitrogen using a pre-cooled pestle and mortar. The powder was immediately transferred to 1.5 mL tube and rapidly frozen in liquid nitrogen. Batches of 12 samples were thawed on ice, and 1 mL Tri-Reagent (Sigma) was added to the tubes and incubated at room temperature for 10 min. The solution was centrifuged for 20 min at 12,000 × g and the supernatant was transferred to a clean tube containing an equal volume of isopropanol. The tube was incubated overnight at −20°C and centrifuged for 10 min at 12,000 × g, 4°C. Pellets were washed with 70 % ethanol, air dried, and resuspended in RNase-free water. The yield and integrity of the RNAs were assessed by measuring the optical density at 260 nm and 280 nm Micro-Volume UV-Vis Spectrophotometer for Nucleic Acid and Protein Quantitation (Nanodrop, Thermo scientific, UK) and agarose gel.

2.4.2.2. RT-PCR

Three micrograms of total RNAs were used for generating cDNAs in a 20 µL volume reaction according to Life technologies protocol for M-MLV reverse transcription. RNA samples, oligodT and dNTPs were incubated at 65°C for 5 min and then cooled on ice. Then First Strand buffer, DTT and RNaseOUT (Invitrogen, Life technologies) were added to the tube and incubated for 2 min at 37°C. Finally M-MLV retro-transcriptase was added. The reaction mixtures were then incubated for 50 min at 37°C. The enzyme was inactivated by 70°C for 15 min. The obtained cDNAs were diluted ten times and 5 µL were used for 10 µL qPCR reaction and 10 µL were used for 20 µL PCR reaction.

2.4.2.3. Quantitative RT-PCR (qPCR)

qPCR was performed in 20 µL final volume using 10 µL SYBR Green mix (Sigma), 10 µL diluted cDNAs, and primers. qPCR was run on the CFX96 Real-Time System C1000 thermal cycler (Biorad) using the following program: (1) 95 °C, 4 min, (2) [95 °C, 10 sec then 62 °C, 15 sec, then 72 °C, 30 sec] × 40, (Mackey et al.) 72 °C, 10 min followed by a temperature gradient from 65 °C to 95 °C, and then 72 °C, 10 min. The relative expression values were determined using EF1α (At5g60390) as a reference gene and the comparative cycle threshold method ($2^{-\Delta\Delta Ct}$). Primers were designed using Primer3 with the default settings. Primer sequences used for qPCR are described in **Appendix 2.1**.

2.4.2.4. 3' RACE PCR

Rapid Amplification of cDNA Ends (RACE) was performed with the GeneRacer kit following mostly the manufacturer instructions (Invitrogen, Life technologies). First-strand cDNA synthesis was performed using the GeneRacer oligodT provided with the Superscript III RT module (5′-GCTGTCAACGATACGCTACGTAACGGCATGACAGTG(T)24-3′). Nested 3′ PCR was carried out with two gene specific primers, GSP1 (5′-ATGACCAAGTGCTCCCTACTTCTCGTGCCCTTCC-3′) and GSP2 (5′-AAAGAAAGACACGAAGGGTGCGGCTGATGAAGAAAG-3′) against the GeneRacer 3′ (5-GCTGTCAACGATACGCTACGTAACG-3') and the GeneRacer 3′ nested (5'-CGCTACGTAACGGCATGACAGTG-3') primers, respectively. A gradient PCR was performed: [95 °C for 30 s, 72 °C for 3 min] × 5, [95 °C for 30 s, 70 °C for 30 s, 72 °C for 3 min] × 5 and [95 °C for 30 s, 68 °C for 30 s, 72 °C for 3 min] × 25, followed by 10 min at 72 °C, using Phusion polymerase (Finnzymes). The PCR products were analysed by gel electrophoresis and were cloned into pGEM-T-Easy (Promega).

2.4.3. Protein methods

2.4.3.1. Protein expression in plant cell

For transient expression in *N. benthamiana*, *A. tumefaciens* cells were prepared as mentioned in 2.3.1.1. Samples were collected 1 to 3 days post infiltration for subsequent protein extraction. For checking HaRxLs expression in Arabidopsis transgenic lines, leaf samples were collected from 5-week-old plants for protein extraction.

2.4.3.2. Total protein extraction from plant tissue and Western blot

Frozen plant tissues were ground and mixed with an equal volume of cold protein isolation buffer [20 mM Tris-HCl (pH 7.5), 1 mM EDTA (pH 8.0), 5 mM DTT, 150 mM NaCl, 0.1% SDS, 10% glycerol, 1x Protease Inhibitor Cocktail (Sigma)]. The mixture was spun down and the supernatant was transferred to a new tube and 5X SDS loading buffer [300 mm Tris-HCl (pH 6.8), 8.7% SDS, 5 % β-mercaptoethanol, 30 % glycerol, 0.12 mg / ml bromophenol blue] was added. Proteins were separated by SDS-PAGE, electroblotted onto PVDF membrane (Biorad), and probed with horseradish peroxidase-conjugated anti-RFP (Abcam) or anti-GFP (Roche) antibody. Bands were visualized using Pico/Femto (Thermo Scientific).

2.4.3.3. Co-immunoprecipitation

Frozen leaf samples were ground in liquid nitrogen. The resulting powder was transferred into pre-chilled SM-24 20 mL centrifuge tubes containing chilled extraction buffer (4-10 mL) [1M Tris HCl pH 7.5, 5M NaCl, 0.5M EDTA, 60 % glycerol, 10 mM DTT, 1X Protease inhibitor (Sigma), 20 % Triton X-100, 2 % PVPP]. Tubes were vortexed and equilibrated before centrifugation 20 min at 20000 rpm at 5 °C. After centrifugation, supernatants were filtered to get rid of plant debris (Biorad Poly-Prep Chromatography colums). Proteins were

quantified with Bradford assay. Three micrograms of total proteins extracts were used for co-immunoprecipitation in protein low-bind safe-lock tubes (Eppendorf) in which 25µL of slurry solution of GFP beads (Kromotek) were added. Tubes were incubated on a rolling wheel for 2 to 4 h at 5°C. After incubation beads were washed with extraction buffer without PVPP by repeated low speed centrifugations (up to 4 washes). Washed beads were resuspended in 5X SDS loading buffer (see recipe in 2.4.3.2) prior to flash-freezing in liquid nitrogen.

2.5. Cell biology assays – Confocal microscopy

For transient expression in *N. benthamiana* using agro-infiltration, samples were taken 1 to 3 days post-infiltration, mounted in water and observed by confocal microscopy (Leica DM6000B/TCS SP5, Leica Microsystems). The fluorescence of GFP-tagged constructs was observed after excitation of the samples at 488 nm, YFP was observed after excitation at 514 nm and RFP was observed after excitation at 561 nm.

To image plant microtubules, z-stacks were made and maximal projections were presented in this thesis. When indicated, taxol (100 µM) was used to stabilise microtubules. A stock solution of 100 mM taxol (Sigma) was prepared in DMSO, and diluted to 100 µM in water immediately prior to the experiment. For co-expression of two constructs, when two FP-tagged proteins were co-expressed, scanning was performed in sequential mode. For split-YFP (BiFC) experiments, the first true leaves of *N. benthamiana* were infiltrated.

The same conditions applied for imaging fluorescent proteins stably expressed in Arabidopsis transgenic lines. For the observation of callose induced in *Hpa*-infected tissues, aniline blue was excited at 350 nm. All images were generated using the Leica analysis software LAS AF Lite 2.2.1.

2.6. Statistical analyses

Statistical analyses of experimental data were performed using GraphPad Prism v7.01, following the test conditions as detailed in the Prism help files. Basically, the comparison of experimental replications of measurements was performed using t-tests or two-way ANOVA (for 2 conditions) and ANOVA (for more than 2 conditions). Comparison of frequencies or scores was performed using contingency tests.

3. Characterisation of the recognition of the *Hpa* ATR13^{Emco5} effector in Arabidopsis accession Ws-0

3.1. Context of this project

As mentioned in chapter 1, *Hpa* cannot currently be genetically manipulated. Therefore, to study the function of single *Hpa* effectors, we rely on the use of heterologous systems to express the effector proteins in other organisms and study their phenotypes in plants. Examples include transient *Agrobacterium*-mediated expression of effectors in *N. benthamiana* (Chou 1970), effector delivery in plants using the *Pst* T3SS (Sohn et al. 2007; Rentel et al. 2008), or expression of effectors as transgenes in Arabidopsis (Hauck et al. 2003; Fabro et al. 2011).

3.1.1. Previous research

ATR13 was the first avirulent oomycete effector to be identified (Allen et al. 2004). The ATR13 protein became a well-studied *Hpa* effector and is an RxLR effector recognised in Arabidopsis by the resistance protein RPP13 (Allen et al. 2004). The *ATR13* gene shows extreme allelic diversity within *Hpa* isolates which is matched by a high allelic diversity in *RPP13*, consistent with the gene-for-gene hypothesis (presented in section 1.2.1) which suggests that ATR13 and RPP13 proteins might be interacting directly (Allen et al. 2004; Allen et al. 2008; Hall et al. 2009).

It was shown that RPP13 from the Arabidopsis accession Niederzenz (RPP13Nd) can recognise ATR13 from the *Hpa* isolate Emco5 (ATR13^{Emco5}) (Allen et al. 2004). The HR triggered by this recognition is able to prevent *Hpa* isolate Emco5 from growing on accession

Nd. RPP13Nd can additionally recognise other alleles of ATR13, such as ATR13^{Maks9}, but does not recognise ATR13^{Emoy2} (Allen et al. 2004). Therefore, *Hpa* Emoy2 can complete its life cycle on Nd. The Arabidopsis accession Col-0 is susceptible to *Hpa* Emco5, as is a glabrous derivative of Col-0, called Col-5. However, transformation with a cosmid clone containing RPP13Nd (Col-5 *RPP13*Nd) renders Col-5 resistant to *Hpa* Emco5 (Bittner-Eddy et al. 2000). As *Hpa* Emco5 is virulent on Ws-0, the RPP13^{Ws} gene is supposedly non-functional.

To test the hypothesis that ATR13 is a virulence/avirulence determinant during *Hpa* infection in Arabidopsis, Sohn et al. (2007) developed the "effector detector vector" (EDV) system. They showed that *Pst* DC3000 could deliver *Hpa* ATR13^{Emco5} effector into plant cells *via* the EDV system and that delivering ATR13^{Emco5} triggers ETI in Col-5 *RPP13*Nd leaves. They also showed that several alleles of ATR13 (namely ATR13^{Emoy2}, ATR13^{Emco5} and ATR13^{Maks9}) delivered by *Pst* could contribute to enhanced bacterial virulence in the susceptible Arabidopsis accession Col-0. Interestingly, this result suggests that the *Hpa* ATR13 effector can interfere with host mechanisms involved in resistance to both bacterial and oomycete pathogens. In addition, Sohn et al. (2007) showed that even though *Hpa* Emco5 is virulent on accession Ws-0, suggesting that none of its effectors are strongly recognised, delivery of ATR13^{Emco5} on its own does trigger immunity in Ws-0 (**Figure 3.1**).

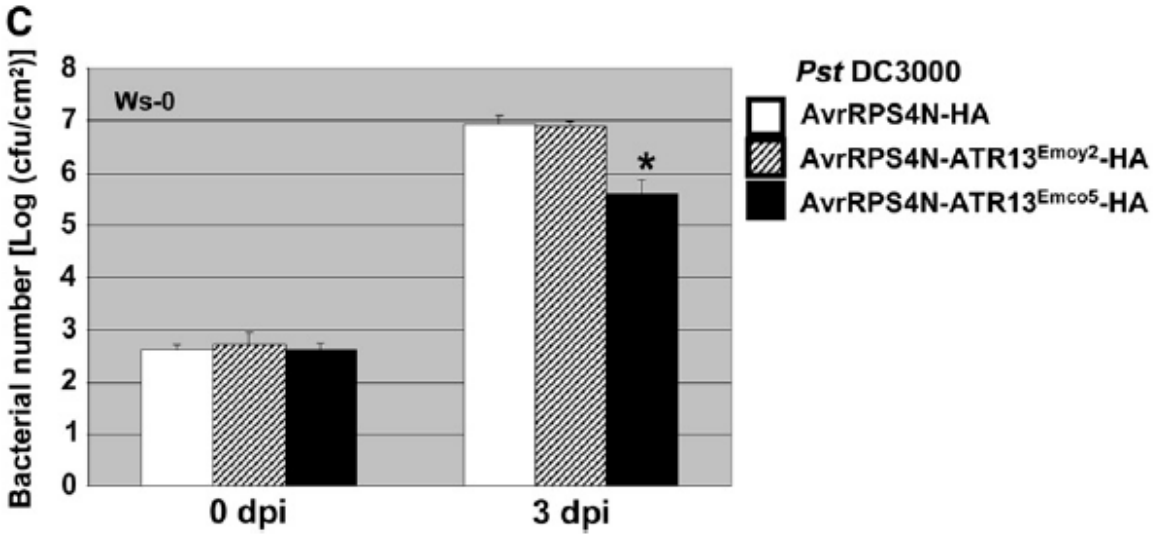

Figure 3.1. ATR13^{Emco5} triggers immunity in Ws-0 (taken from Sohn et al. 2007).

Bacterial populations of Ws-0 leaves were hand-infiltrated with 5×10^5 cfu/mL *Pst* DC3000 wild-type carrying pEDV3 (AvrRPS4N), pEDV3 (AvrRPS4N-ATR13^{Emoy2}), or pEDV3 (AvrRPS4N-ATR13^{Emco5}). Bacterial populations were measured at 0 and 3 days after inoculation. Each bar represents the mean number of bacterial colonies recovered on selective agar medium containing appropriate antibiotics from four independent replicates. This experiment was repeated twice with similar results. The asterisk ($P < 0.01$) represents a significant difference (t-test) compared with *Pst* DC3000 (AvrRPS4N-HA).

This latter observation could be explained by two different scenarios: either *Hpa* Emco5 might be able to suppress the ATR13^{Emco5}-triggered HR in Ws-0, possibly through the action of additional effectors jointly secreted with ATR13^{Emco5}, or the recognition of ATR13^{Emco5} in Ws-0 could be too weak to result in full resistance to *Hpa* Emco5, allowing the pathogen to overcome this weaker form of resistance.

3.1.2. This work

In this work, I followed up on these observations obtained in our laboratory in the past (Sohn et al. 2007) and sought to understand why the ATR13^{Emco5} effector triggers resistance in Ws-0 when delivered by EDV even if *Hpa* Emco5 (presumably secreting ATR13 and

additional effectors) is able to complete its life cycle on Ws-0. I took a genetic approach to identify the source of resistance in Ws-0 to ATR13^{Emco5}. It was understood that using a mapping approach on a presumably weak phenotype may be risky, as a clear phenotype is usually recommended to be able to accurately score the segregating plants, but I considered that the novelty of this observation was worth investigating. In the next section, I present results on the characterisation of the interaction between ATR13^{Emco5} and Arabidopsis accession Ws-0.

3.2. Results

3.2.1. ATR13^{Emco5} recognition in Ws-0 is due to a single dominant gene, independent of *RPP13* and *EDS1*

3.2.1.1. ATR13^{Emco5} recognition in Ws-0 is due to a single dominant gene other than RPP13

ATR13^{Emco5} is recognised by RPP13Nd in Arabidopsis accession Nd. Therefore I first tested if recognition of ATR13^{Emco5} in Ws-0 requires *RPP13^{Ws}*. To this end Arabidopsis homozygous *rpp13* knock-out mutants in Ws-4 background were isolated (T-DNA insertion line in *RPP13* gene, FLAG_522B05). We used the Ws-0 derivative Ws-4 for this experiment for practical reasons, as the T-DNA insertion lines were only available in this background. *Hpa* isolate Emco5 grows as well on Ws-4 as on Ws-0, suggesting that the use of Ws-4 should be a good surrogate for this study. The T-DNA insertion was located where predicted, in the middle of *RPP13* single exon (**Figure 3.2**) and no full length *RPP13* transcript could be detected by RT-PCR, indicating that the insertion of the T-DNA indeed disrupted *RPP13* coding sequence in Ws-4. The development of *rpp13* mutant did not seem altered when compared to Ws-4.

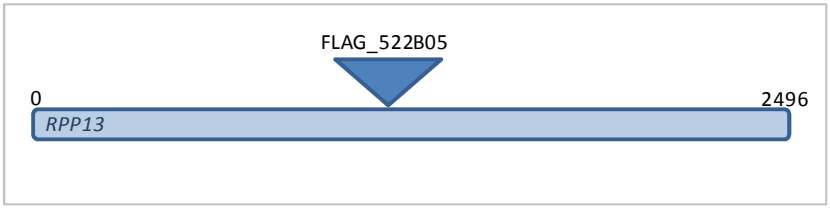

Figure 3.2. Ws-4 *rpp13* T-DNA insertion line used in the study.
The T-DNA is inserted in the middle of the *RPP13* gene constituted of a single exon of 2496 bp in Ws-0.

The Ws-4 *rpp13* mutant was tested for susceptibility to *Pst* DC3000 delivering ATR13^{Emco5}. Arabidopsis leaves of the Ws-4 *rpp13* mutant and control plants (Col-5 *RPP13*Nd resistant plants and Ws-4 wild type plants) were infiltrated with *Pst* DC3000 ATR13^{Emco5}, or with the empty vector with no effector delivered (*Pst* DC3000 pEDV3) as negative control. Bacterial growth was measured 3 days post infection (dpi) (**Figure 3.3**).

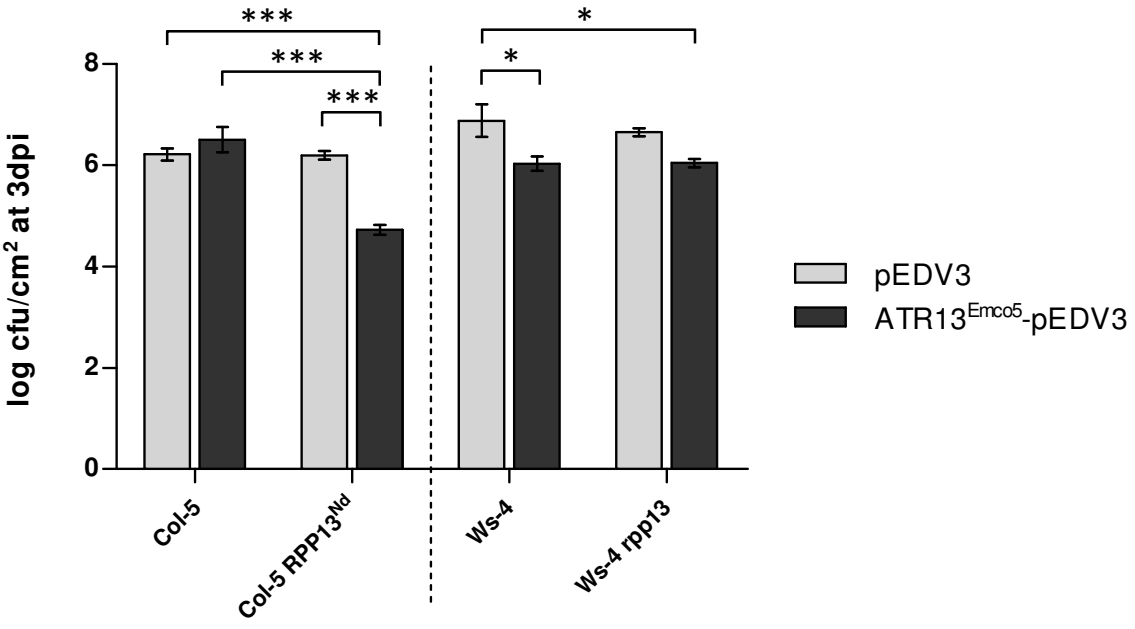

Figure 3.3. ATR13^{Emco5} is recognised in Ws-4 *rpp13* plants.
Bacterial titres of *Pst* DC3000 carrying pEDV3 (grey) or ATR13^{Emco5}-pEDV3 (black) in infected leaves 3 days post infection. Six-week old Arabidopsis Col-5, Col-5 RPP13Nd, Ws-4 and Ws-4 *rpp13* leaves were infiltrated with 10^6 cfu/mL *Pst* DC3000 carrying empty vector (pEDV3) or ATR13^{Emco5} (ATR13^{Emco5}-pEDV3). Asterisks denote statistically significant differences (with * for $p<0.05$ and *** for $p<0.0001$) between columns based on a Bonferroni post-hoc comparison after one-way ANOVA test on data from either the Col-5 or Ws-4 experiments. The error bars represent the standard error of the mean (sem). The dotted line separates experiments performed in the two genetic backgrounds.

As expected, *Pst* DC3000 ATR13^{Emco5} was recognised by RPP13Nd, which led to a reduced bacterial growth in Col-5 RPP13Nd plants ($p<0.0001$). As expected from the work of Sohn et al. (2007), Ws-4 conferred resistance to *Pst* DC3000 ATR13^{Emco5}, as *Pst* DC3000 ATR13^{Emco5} growth was reduced significantly ($p<0.05$). In the Ws-4 *rpp13* mutant, *Pst*

DC3000 ATR13^{Emco5} also grew less than the empty vector control. This trend was observed reproducibly in three independent experiments. The difference in growth was statistically significant according to a two-sided t-test but not significant when tested by an ANOVA followed by Bonferroni post-hoc comparison. Whereas two-sided t-tests are an accepted way to test for significant differences in pathogen proliferation (Garcia et al. 2010; Zeng et al. 2012), the use of multiple comparison tests such as Bonferroni after an ANOVA provides a statistical significance level applied to the entire dataset rather than a pairwise comparison. This approach is more stringent and reduces the chance of including differences entirely caused by random sampling, which makes this test more appropriate for comparing more than two conditions of the same experimental setting (from the GraphPad Prism v7.01 manual). However, as the reduced bacterial titres on Ws-4 *rpp13* were observed in 3 independent experiments, I concluded that there was a significant reduction of bacterial growth when ATR13 was delivered in both Ws-4 and Ws-4 *rpp13* genotypes compared to controls (empty vector), indicating that RPP13^{Ws} is most probably not involved in ATR13^{Emco5} recognition.

To confirm this observation and identify the additional source of resistance to ATR13^{Emco5} recognition in Ws-0 (Sohn et al. 2007), I took a map-based cloning approach based on a cross between Arabidopsis accessions Col-0 (susceptible parent) and Ws-0 (resistant parent). Here I assumed that ATR13^{Emco5} recognition is the same in Ws-0 and Ws-4 given that Sohn et al. (2007) published HR and resistance phenotypes in Ws-0 and my results demonstrating ATR13^{Emco5} recognition in Ws-4. Although the hypersensitive response (HR) induced by ATR13^{Emco5} was weaker when compared to *Pst* AvrRPM1-triggered HR (data not shown), scoring for HR (identified by leaf collapse) allowed me to discriminate between susceptible and resistant F2 progenies. I screened a set of 96 F2 [Col-0 × Ws-0] plants for the occurrence of HR upon delivery of ATR13^{Emco5}. ATR13^{Emco5} recognition resulted in a

segregation of 68 resistant to 28 susceptible plants. This result was consistent with a 3:1 ratio (χ^2=0.89, p=0.34) which would be expected if a single dominant resistance gene in Ws-0 were responsible for ATR13^{Emco5} recognition.

To test if ATR13^{Emco5} recognition in the F2 population was linked to the *RPP13* locus I used a molecular marker in the *RPP13* gene: using the sequence variation between *RPP13^{Col}* and *RPP13^{Ws}*, a CAPS marker (for "cleaved amplified polymorphism sequence") was designed, which generates a 568 bp amplificon in the *RPP13* LRR region. The marker was designed in such a way that when the PCR amplicons are incubated with the restriction enzyme *Hae*III, only the Ws-0-originating PCR product will be digested, allowing me to conveniently distinguish the allelic variants by agarose gel electrophoresis. Using this CAPS marker, I observed that in F2 plants the *RPP13* gene segregated independently from the *Pst* DC3000 ATR13^{Emco5} recognition phenotype (data not shown). This result is not expected if RPP13 were responsible for ATR13^{Emco5} recognition. This demonstrates that a single dominant gene other than *RPP13* is responsible for ATR13^{Emco5} recognition, and that *RPP13* may not be functional in terms of ATR13^{Emco5} recognition in Ws-0.

Following this result, I decided to map the genetic locus that mediates recognition of ATR13^{Emco5} in Ws-0. As the macroscopic HR phenotype was difficult to score I adopted a different screening strategy based on disease symptoms. For this purpose, a second set of [Col-0 × Ws-0] F2 plants was screened for bacterial disease symptoms characterised by spots of chlorosis and necrosis (**Figure 3.4**).

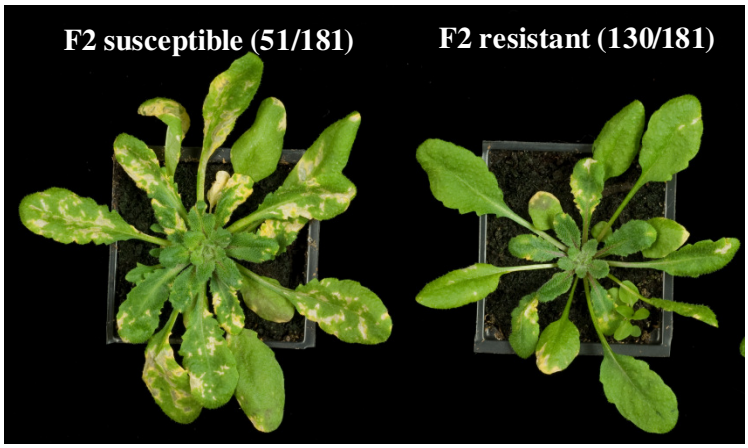

Figure 3.4. Disease symptoms observed on [Col-0 × Ws-0] F2 plants infected with *Pst* DC3000 ATR13^{Emco5}.
Five-week old F2 plants were sprayed with 10^8 cfu/mL *Pst* DC3000 ATR13^{Emco5}. Photographs were taken 5 days after infection. 51 F2 out of 181 tested showed heavy disease symptoms. 130 plants out of 181 showed minor disease symptoms.

As a consequence of ATR13^{Emco5} recognition in Ws-0, this parental accession showed few disease symptoms when sprayed with *Pst* DC3000 ATR13^{Emco5}. In contrast, the susceptible parental accession Col-0 showed much stronger disease symptoms when sprayed with *Pst* DC3000 ATR13^{Emco5}. Among 181 F2 individuals 130 recognised ATR13^{Emco5} and 51 were susceptible. This segregation was consistent with a 3:1 ratio (χ^2=0.97, p=0.32) of segregants and therefore substantiated my findings from phenotyping based on HR.

In order to further substantiate the accuracy of the screening method based on disease symptoms, I sought to confirm that the 51 F2 plants were correctly scored by testing the progeny of each individual (F3 plants arising from individual self-crosses of each susceptible F2 individual) for HR symptoms. The aim of using a F3 progeny was to check whether the disease scoring results performed in F2 could be reproduced in the F3, thus eliminating any potentially mis-scored individuals from the F2 generation. Out of the 51 selected F2, 45 lines still exhibited a loss of ATR13^{Emco5} recognition upon delivery by *Pst*, indicating that the large majority of the F2 plants were correctly scored.

Similarly to what was observed when plants were screened for leaf collapse, the CAPS molecular marker within the *RPP13* gene (which amplified 43/45 of susceptible plants) segregated independently from the screened ATR13^{Emco5} recognition phenotype (**Table 3.1**), corroborating the presence of a single dominant resistance gene to ATR13^{Emco5} other than *RPP13* in Arabidopsis accession Ws-0.

RPP13 **allelism**	**Number of susceptible F2 individuals (confirmed in F3 generation)**
RPP13 ^{Col}	7
RPP13 ^{Ws}	13
RPP13 $^{Col/Ws}$	23
Total	43

Table 3.1. *RPP13*^{Ws} does not segregate with loss of ATR13^{Emco5} recognition.
Forty five F2 from a Col-0 x Ws-0 cross were selected as being non responsive to ATR13^{Emco5} and tested with a CAPS marker in *RPP13* (sequences were amplified for 43/45 F2 individuals). F2 were equally heterozygous *RPP13*$^{Col/Ws}$ as homozygous *RPP13*^{Col} or *RPP13*^{Ws}.

3.2.1.2. ATR13^{Emco5} recognition in Ws-0 is EDS1- independent

Work described in the previous section established that the recognition of ATR13^{Emco5} is dependent on a single dominant gene. Assuming that this gene is a resistance gene, I wanted to test if ATR13^{Emco5} recognition required EDS1, a key component for TIR-NB-LRR-mediated resistance (Wiermer et al. 2005). In order to test if ATR13^{Emco5}-triggered HR in Ws-0 is dependent on EDS1, HR assays were performed on Ws-0 and Ws-*eds1-1* plants by infiltration with *Pst* DC3000 ATR13^{Emco5}. Twenty-two hours after infiltration no visual differences were observed between the HR produced on Ws *eds1-1* and Ws-0 (**Figure 3.5**). Although more quantification and molecular characterisation is required to be assertive, this observation strongly suggests that ATR13^{Emco5} recognition in Ws-0 is independent of EDS1.

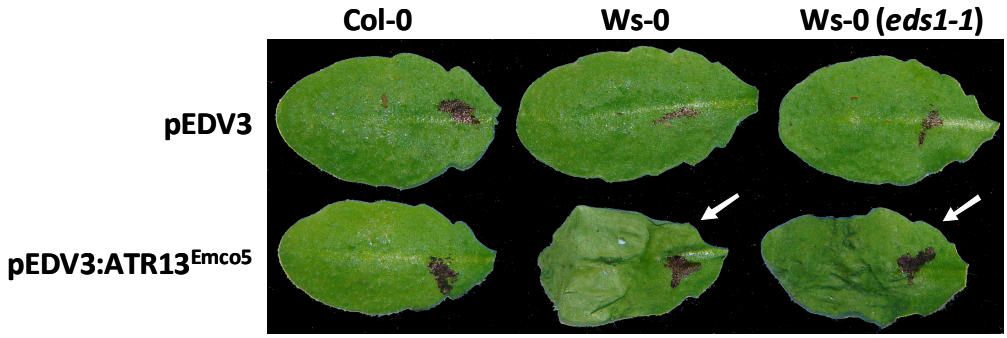

Figure 3.5. ATR13^{Emco5} recognition in Ws-0 does not require EDS1.
HR assay was performed on six-week old Col-0, Ws-0 and Ws *eds1-1* plants by infiltration with 10^8 cfu/mL *Pst* DC3000 carrying empty vector (pEDV3) or ATR13^{Emco5} (pEDV3:ATR13^{Emco5}). Photographs were taken 22 hours post infiltration. White arrows indicate HR.

Taken together, the results presented in this section suggest that despite the ability of *Hpa* Emco5 to complete its life cycle on Ws-0, Ws-0 can recognise the ATR13^{Emco5} effector when delivered as a single effector (Sohn et al. 2007) and that this recognition is dependent on a single dominant gene, which is neither RPP13- nor EDS1-dependent. For clarity in the next sections addressing the physical mapping of this gene, I propose to call it *RHA13* for "Recognition of *Hyaloperonospora arabidopsidis* ATR13".

3.2.2. Rough mapping of *RHA13* using a Col-0 × Ws-0 mapping population

In order to determine the physical position of *RHA13* on the Arabidopsis genome, mapping of this single dominant gene using the 28 F2 plants selected as susceptible using the HR assay (*i.e.* presumably lacking *RHA13*) was conducted (see section 3.2.1.1). Twenty PCR markers spread over the five Arabidopsis chromosomes were tested. Unfortunately using this method, I could not link *rha13* to any of the markers tested.

To overcome this, a bulk segregant analysis was performed on the 45 F3 lines that were susceptible to *Pst* DC3000 ATR13^{Emco5} (see section 3.2.1.1) using 34 markers over the five Arabidopsis chromosomes (including the 20 markers tested previously, all indicated in **Figure 3.6**, see Material & Methods for details). This analysis revealed approximate linkage of *rha13* to three chromosomal regions (underlined in red, **Figure 3.6**), to distal chromosome 1, distal chromosome 2 and distal chromosome 4.

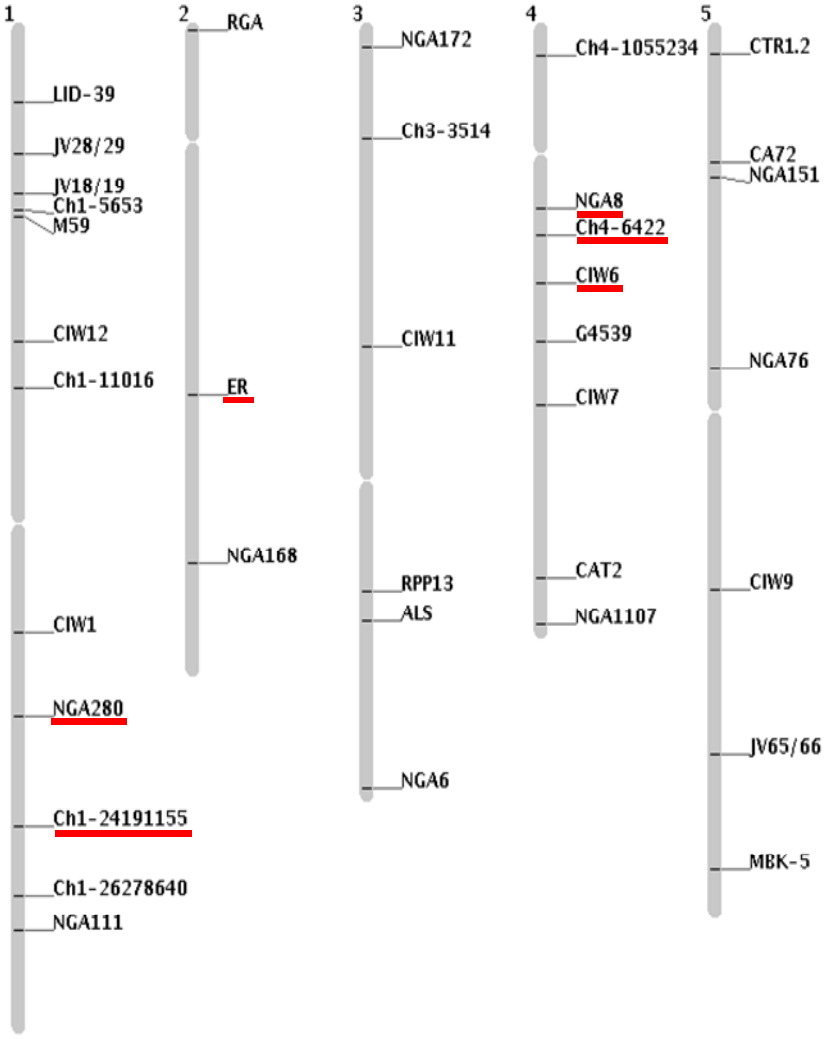

Figure 3.6. Rough mapping of *rha13* locus by bulk segregant analysis.

Forty five plants showing loss of ATR13^{Emco5} recognition were used to map the *rha13* locus. The five Arabidopsis chromosomes are represented in grey vertical bars and numbered 1 to 5 on top of each chromosome. The 34 markers tested are indicated in black, the markers showing linkage to *rha13* are underlined in red.

As no linkage to a single locus was observed with the bulk segregant analysis, the markers spanning the three regions were tested on the 45 individual F3 plants. The genotyping results are shown in **Table 3.2**. As Col-0 was used as susceptible parent in this population, I expected an enrichment of Col-0 DNA at the *rha13* locus. Interestingly, more F3 individuals were found to be homozygous Col-0 for the two markers tested on chromosome 4 (χ^2; p_{NGA8}=0.1586; $p_{Ch4\text{-}6422}$=0.1879), but not for the markers on chromosome 1 or 2 (χ^2; p_{NGA280}=0.9825, $p_{Ch1\text{-}24191155}$=0.8206; p_{ER}=0.6791) (**Table 3.2, Figure 3.6**). Although the χ^2 contingency tests against an expected 1:2:1 segregation presented above did not highlight a significant ($p<0.05$) difference for markers on chromosome 4 (possibly because of the low number of plants tested), the p-values, much lower for these markers, suggests that *rha13* might be located on chromosome 4. Focusing on this region for fine mapping, I found another marker, G4539 (van der Biezen et al. 2002), also linked to the *rha13* locus (χ^2; p_{G4539}=0.1971, **Figure 3.6**, **Table 3.2**). This result suggests that *rha13* might be in between the two markers G4539 and NGA8. However, the genotyping with the CIW6 marker (located in between the two aforementioned markers) failed on the F3 individuals, so I cannot conclude further. Using the TAIR website marker database (http://www.arabidopsis.org/) as well as the AtPRIMER database (Nemri et al. 2007), no more markers could be identified in this region of chromosome 4.

To conclude, this classical mapping approach could not pinpoint the physical location of *rha13* to a single locus. It is likely that this result could have been due to the difficulty in phenotyping (as explained in this chapter introduction, $ATR13^{Emco5}$ recognition in Ws-0 is weaker compared to its recognition in Nd-0), but it is possible to envisage that $ATR13^{Emco5}$ recognition is conditioned by other quantitative trait loci (QTLs). Therefore another approach was adopted (presented in the next section) in which I tried to identify *RHA13* using Arabidopsis transgenic lines expressing the *Hpa* effector $ATR13^{Emco5}$.

	Chromosome 1		Chromosome 2	Chromosome 4		
F3 individuals	NGA280	Ch1-24191155	ER	NGA8	Ch4-6422	G4539
1	cw	cw	cw	cc	cc	cc
2	cc	cc	cc	cw	cw	cw
3	cw	cw	cw	cc	cc	cc
4	cw	cw	cw	ww	ww	ww
5	cw	cw	cw	ww	cw	cw
6	ww	ww	cw	cc	cc	cc
7	cw	cw	cw	cw	cw	cw
8	cw	cw	cc	cw?	cw	ww
9	cw	cw	ww	cc	cc	cc
10	cw	cw	cc	cc	cc	cc
11	cw	cw	cw	cw	cw	cw
12	ww	ww	ww	cc	cc	cc
13	cw	cw	cc	cw	cw	cw
14	ww	ww	cw	cc	cc	cc
15	ww	ww	cw	cw	cw	cw
16	cw	cw	cc	cw	cw	cc
17	cc	cc	ww	ww	ww	ww
18	?	ww?	?	cc?	cc	?
19	cc	cc	cw	cc	cc	cc
20	cw	cc	cw	cc	cc	cc
21	cw	cw	cw	cc	cc	cc
22	ww	ww	cc	cc	cc	cc
23	ww	ww	cw	cw	cw	cw
24	cc	cc	cw	cc	cc	cc
25	cw	cw?	cw	cw	cw	cw
26	cc	cc	cw	cw	cw	cw
27	cw	ww	cc	cc	cc	cc
28	cc	cc	cc	cc	cc	cc
29	cc	cw	ww	ww	ww	ww
30	cw	cw	cc	cc	cc	cc
31	cw	cw	ww	ww?	ww	ww
32	cw	cw	cw	cw	cw	cw
33	ww	ww	cw	cc	cw	cw
34	ww	ww	cw	cw	cw	cw
35	ww	ww	cw	ww	ww	ww
36	ww	ww	cw	cw	cw	cw
37	cw	cw	cw	cc	cc	cc
38	cc	ww	cw	cc	cc	cc
39	cc	cw	cc	ww	ww	ww
40	cc	cc	ww	cw	cw	cw
41	ww	cw	cc	ww	cw	cw
42	cw	cc	ww	cw	cw	cw
Col	10	9	11	19	18	18
Col/Ws	20	20	23	15	18	16
Ws	11	13	7	8	6	7
χ^2 p value	0.9825	0.8206	0.6791	0.1586	0.1879	0.1971

Table 3.2. Rough mapping of *rha13* locus by individual segregant analysis.
PCR were performed individually on the 45 F3 selected as susceptible to *Pst* DC3000 ATR13^{Emco5}. Genotyping for forty two individuals are presented in this table as for three F3 individuals, genomic DNA was poorly extracted. For each marker on the different chromosomes, the individuals are homozygous Col-0 (cc), homozygous Ws-0 (ww), heterozygous (Haas et al.) or unclear genotypes (?). At the bottom of the table are shown the total number of individuals homozygous Col-0, homozygous Ws-0 and heterozygous (Col/Ws). The last row indicates the p values given by a χ^2 contingency test against an expected 1:2:1 segregation.

3.2.3. Fine mapping of *RHA13* requires to improve the phenotyping

3.2.3.1. Constructing Arabidopsis transgenic lines expressing the Hpa *effector ATR13^{Emco5}*

One possible reason why the classical map-based cloning approach was not successful for identifying *RHA13* could be the rather weak HR phenotype that might have led to some scoring errors in the initial screen. One factor to consider when examining this weak phenotyping problem could be the potential interference of other secreted *Pst* effectors with ATR13^{Emco5} (*Pst* DC3000 secretes about 30 T3E when infecting Arabidopsis (Cunnac et al. 2009). To rule out this possibility, I used two approaches. First, I used *Pseudomonas fluorescens* which does not secrete any T3E but was engineered to carry a functional T3SS (*Pf0-1*) (Thomas et al. 2009) to deliver ATR13^{Emco5}. But in Ws-0, *Pf0-1* ATR13^{Emco5}-triggered HR was not stronger compared to *Pst* ATR13^{Emco5}-triggered HR (data not shown). Second, I generated transgenic plants constitutively expressing ATR13^{Emco5} in the Col-0 background. In previous studies, transgenic lines have been proven useful to identify R genes; for instance, the mapping of Target of AvrB operation 1 (*TAO1*) was achieved by generating transgenic plants with an inducible AvrB expression system (Eitas et al. 2008). The idea behind generating Col-0 transgenic plants expressing ATR13^{Emco5} was to subsequently cross them with a [Col-0 × Ws-0] F1. In the resulting progeny, half of the progeny is expected to die as a result of ATR13 recognition by RHA13, and the other half of the progeny is expected to survive. The surviving half of the progeny would not carry *RHA13* but only ATR13^{Emco5} and could be effectively used to map *rha13*.

In order to generate these transgenic lines ATR13^{Emco5} was amplified from the signal peptide cleavage site to the stop codon from an *Hpa* Emco5 purified genomic DNA preparation. The resulting 408 bp fragment was cloned in the binary vector EpiGreenK3. This vector allows for constitutive expression (under the 35S promoter) of the cloned effector fused to a 3x hemagglutinin (HA) C-terminal tag (EpiGreenK3 was modified in our laboratory from pGreen0029, a common vector used for Arabidopsis transformation). ATR13^{Emco5} expression was verified in *Nicotiana benthamiana* two days after infiltration with *Agrobacterium tumefaciens* strain GV3101, and was subsequently used to transform Col-0 plants using the flower-dipping method (Clough and Bent 1998). As a control for the functionality of the ATR13^{Emco5}::3xHA fusion construct, Ws-0 plants were transformed with *A. tumefaciens* carrying ATR13^{Emco5} but no T1 transformants were obtained, suggesting that ATR13^{Emco5} recognition in Ws-0 is lethal to seedlings. In the Col-0 background I obtained 11 primary transformants (T1), from which four independent homozygous T3 lines were selected based on segregation of the kanamycin resistance gene carried by the inserted T-DNA. These four T3 lines were tested for ATR13^{Emco5} expression by performing a western-blot with anti-HA antibodies. Unfortunately, none of the four lines showed expression of the ATR13^{Emco5}::3xHA fusion construct, possibly due to gene silencing.

Previous reports have shown that the over-expression of microbial effector proteins *in planta* could affect plant development and sometimes lead to lethality (Sugio et al. 2011). In order to avoid a constitutive and deleterious over-expression of ATR13^{Emco5}, dexamethasone (Dex)-inducible ATR13^{Emco5} transgenic lines were obtained from from L. Leonelli (Laboratory of Brian J. Staskawicz, UC Berkeley, USA). The idea of this approach was that the Col-5 Dex:ATR13^{Emco5} lines could be used as described above to map *rha13*. I could not check myself whether ATR13^{Emco5} was indeed produced upon induction by the Dex treatment

in this lines, as the T7 tag to ATR13^{Emco5} could not be detected by western-blotting (although ATR13^{Emco5} expression was reportedly confirmed beforehand with a specific ATR13 antibody by the seeds provider). Nevertheless, this line was crossed to Ws-0 to test the prediction that all F1 individuals would die because of the simultaneous presence of *ATR13* and *RHA13*. I tested 17 F1s for the HR phenotype after Dex treatment using ion leakage measurements. Ion leakage is a phenomenon that is concomitant with HR in dying plant cells, as during HR, the cells plasma membranes become porous and release ions that can easily be quantifiable by measuring conductivity in solutions (**Table 3.3**).

	Col-0	Col-0 Dex:RPS4^{TIR+80}	Col-5 Dex:ATR13^{Emco5} x Ws-0
HR ratio expected	0%	100%	100%
HR ratio observed	0%	100%	53%

Table 3.3. Col-5 Dex:ATR13^{Emco5} x Ws-0 progenies are not lethal.

Col-0, Col-0 Dex:TIR+80 and [Col-5 Dex:ATR13^{Emco5} x Ws-0] F1 leaf disks were floated on 40 µM dexamethasone for up to 3 days. Ion leakage was measured by the conductivity.

As expected, control plants expressing Dex:RPS4^{TIR+80} plants underwent HR (Swiderski et al. 2009) whereas Col-0 wild type plants did not. Preliminary results showed that only 9 of the 17 F1 individuals that were supposed to express Dex:ATR13^{Emco5} underwent HR. This unexpected HR ration indicated that progenies from the Col-5 Dex:ATR13^{Emco5} line were probably prone to silencing of ATR13^{Emco5} expression too and could not be used for *rha13* mapping. But it is also possible that more than one dominant locus is involved which would explain the unexpected HR ratio observed. However we still attempted another approach to map *rha13*.

3.2.3.2. Mapping by Illumina sequencing (in collaboration with Naveed Ishaque)

The recent development of next-generation sequencing methods had a huge impact on speeding up gene mapping (Ossowski et al. 2008; Sarin et al. 2008; Schneeberger et al. 2009). Therefore to improve the efficiency of the previous mapping attempts, in a last attempt to map *rha13*, we decided to sequence bulked DNA from 45 individuals, all susceptible to *Pst* DC3000 ATR13^{Emco5}, using next-generation sequencing technology (one lane of Illumina GA2 paired-end reads). The idea is to map *rha13* by looking at whole-genome polymorphisms in the susceptible bulk. We expect that the bulk sequences will exhibit polymorphisms compared to Col-0 reference genome sequence, but that in ideally only one region, this polymorphism will drop until it reaches the point where it is completely similar to Col-0 at *rha13* locus. Benefiting from whole-genome sequence variation data for Ws-0, we could identify *RHA13*^{Ws}. Naveed Ishaque, PhD student in the lab used SHOREmap (Schneeberger et al. 2009) to identify the *RHA13*^{Ws} locus.

The SHOREmap 'interval' method was used as we had Ws-0 Illumina sequenced reads. This method requires a minimum of three input files: (1) a consensus file – a file with all the catalogued variation in the sequenced bulk, (2) a marker file – a file of all SNP positions between the Col-0 and Ws-0, a chromosome size file – a file of the sizes of the chromosomes.

To generate the 'consensus file', the bulk sequenced reads were aligned to the Arabidopsis Col-0 TAIR 8 genome assembly using MAQ (Li et al. 2008) with mapping parameters n=2, e=100, a=500. The PCR duplicates were removed. A MAQ 'consensus' file was created with parameters q=10, Q=100, m=7. From this a set of SNPs were predicted using MAQ. These SNPs were filtered using the MAQ.pl script and were filtered for potential INDELs, a minimum depth of 10x, a minimum PHRED scaled SNP and mapping quality of

20 (which hypothetically is equal to a 1% error rate). A total of 26,548 SNP positions were identified from the single lane of data.

To generate the 'marker file' four "lanes" of Ws-0 were sequenced for Pr. Richard Mott and the 1001 genomes project at The Sainsbury Laboratory (Cao et al. 2011; Schneeberger et al. 2011). The reads were aligned to the Arabidopsis Col-0 TAIR 8 genome assembly using MAQ. The PCR duplicates were removed. A MAQ 'consensus' file was created. From this a set of SNPs were predicted using MAQ and then filtered to a minimum depth of 6 and a minimum PHRED scaled SNP quality of 20. A total of 156,151 SNPs were predicted. The SNPs were formatted to work directly with the SHOREmap pipeline.

The 'chromosome size' file was created based on the size of the chromosomes of the TAIR8 assembly.

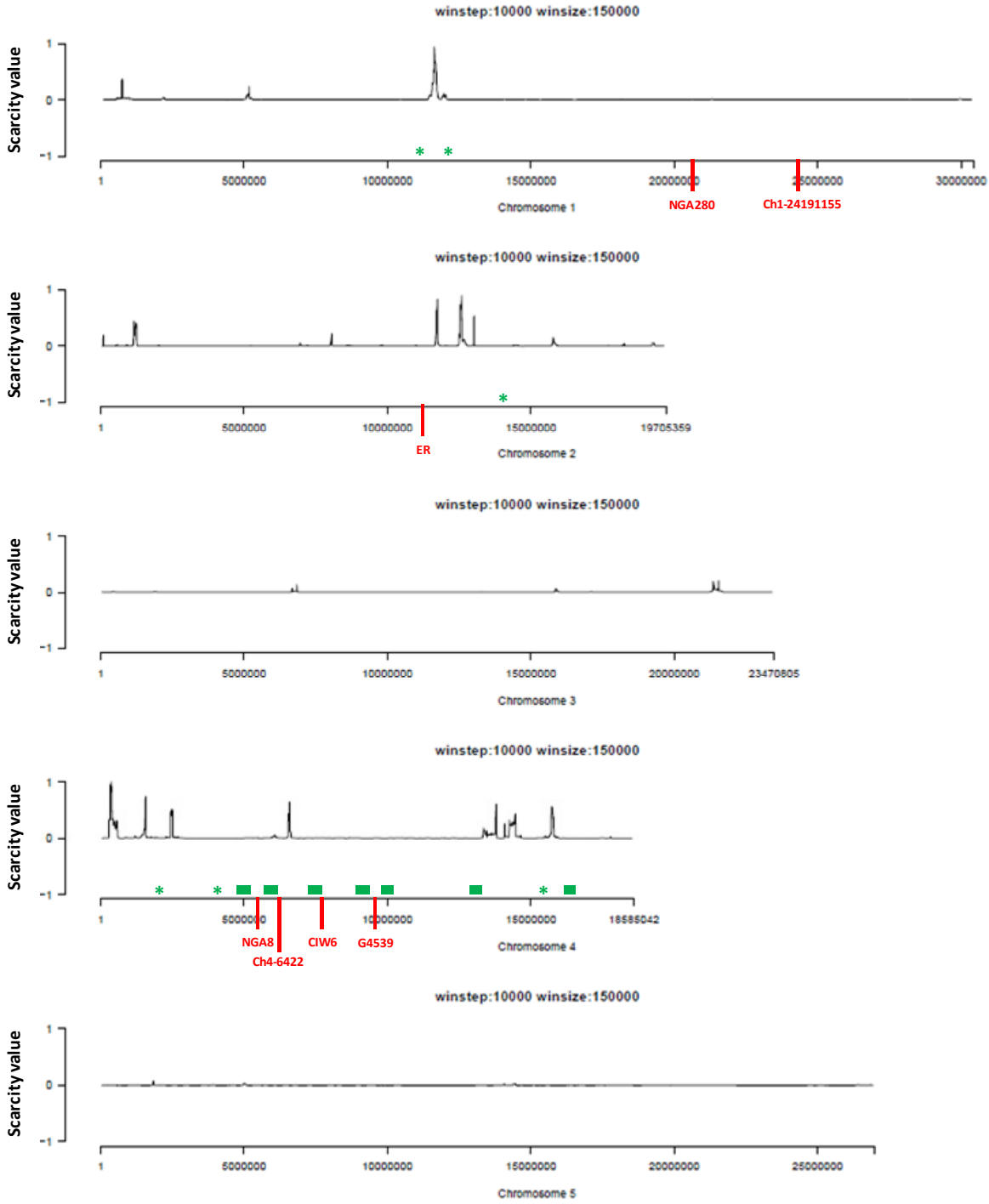

Figure 3.7. Mapping positions identified by SHOREmap for *RHA13*^{Ws}.

SHOREmap output data of *rha13* locus mapping using the sensitive bulk. The five Arabidopsis chromosomes are represented (scale in bp). The scarcity value is calculated as the (normalised) average of the sum of position-wise distance to the nearest marker multiplied with the inverse sum of frequencies of the Ws-0 allele at the predicted marker positions (of Ws). In simpler words, the peaks correspond to regions enriched in Col-0. A single locus was identified on chromosome 1, and multiple loci were identified on chromosomes 2 and 4. The rough/classic mapping markers are indicated in red. Known *R* genes / *R* gene clusters are highlighted in green in proximity to the peak positions (* for single gene, thick line for clusters). *R* genes loci, including CC-NB-LRR, TIR-NB-LRR, CC-NB, TIR-NB and TIR-X genes, were retrieved from http://niblrrs.ucdavis.edu/ website.

Using SHOREmap, we identified several loci (represented as peaks) spread over chromosomes 1, 2 and 4 as putative *rha13* loci (**Figure 3.7**). Again, with this method we could not identify a single locus. In addition, the loci identified by SHOREmap and the loci identified by classic mapping (**Figure 3.6**) only partially overlap (**Figure 3.7**): they do not overlap on chromosome 1, they overlap on chromosome 2 and on chromosome 4. Out of the three positions identified, one position predicted by SHOREmap lies within the region spanned by the markers NGA8 and CIW6. Interestingly, this region of chromosome 4 is rich in *R* genes (as indicated in green in **Figure 3.7**).

To conclude, the classic and sequencing mapping approaches highlighted several loci for *RHA13*, scattered on three chromosomes. Even though one position was common to both approaches, it appears that multiple loci were involved in determining susceptibility. Given that ATR13^{Emco5} recognition in Ws-0 was weak and could potentially be explained by QTLs, we decided to stop the *rha13* mapping project.

3.3. Discussion / Conclusion

In Arabidopsis accession Nd-1, the *R* gene RPP13Nd has been shown to recognise *Hpa* effectors ATR13^{Emco5} and ATR13^{Maks9} (Bittner-Eddy et al. 2000; Allen et al. 2004). Additionally, Sohn et al. (2007) established that ATR13^{Emco5}, when delivered alone, is recognised in the Arabidopsis accession Ws-0. This recognition event triggers a weak HR and is sufficient to restrict bacterial growth. I have shown in this chapter that in accession Ws-0, RPP13^{Ws} is not involved in ATR13^{Emco5} recognition (**Figure 3.3**, **Table 3.1**) and presented several attempts to map the source of resistance.

None of the mapping strategies allowed me to unambiguously narrow down the *RHA13* locus to a precise genomic location. While the segregation ratios of the phenotyping were consistent with a single dominant resistance locus, the genotyping of the F2 mapping populations suggests that this trait may be conditioned by multiple QTLs. The discrepancy observed between the phenotypes and the genotypes highlights the importance of the phenotype scoring method. Indeed, the *Pst* DC3000 ATR13^{Emco5}-triggered HR in Ws-0 is weak, as is the resistance triggered by this strain in Ws-0. In this respect, in a recently published large-scale screening experiment, Fabro et al. (2011) could not rate this recognition as significant, substantiating my finding that ATR13^{Emco5} recognition in Ws-0, although leading Sohn et al. (2007) to hypothesise the existence of *RHA13*, is rather subtle. Another explanation for these ambiguous results may be that the tested mapping populations were not large enough to map the gene responsible for this subtle phenotype, even though I tested 180 F2 individuals. Typically, increasing the number of recombinants reduces the effect of mis-scored individuals. However, in this case, the phenotyping method may still be a major impediment to getting a large enough population. Unfortunately and to our disappointment,

the impracticability of the ATR13^{Emco5} transgenic lines in Arabidopsis (either 35S or Dex-inducible lines), possibly due to silencing occurring in the plants, did not provide the expected solution to this problem.

Although not very informative, the mapping attempts of *rha13* locus revealed a region on chromosome 4 (spanned between the markers NGA8 and G4539) which could likely explain most of the Ws-0 resistance to ATR13^{Emco5}, as it is the strongest lead, but needs further investigation by developing more markers and using a bigger mapping population. In order to develop new markers for fine mapping, using SHOREmap we identified SNPs between Ws-0 and Col-0 which can easily be translated to design dCAPS markers. Interestingly, two *R* genes in close proximity to the CIW6 marker are predicted in accession Col-0, including one TIR-NBS-LRR gene (At4g14370) and one CC-NBS-LRR gene (At4g14610) (Meyers et al. 2003). As RHA13 probably functions independently of EDS1, as I have shown in **Figure 3.5**, one possible good candidate for *RHA13* could be the CC-NB-LRR gene in this region, as this class of *R* genes has been observed to function in an EDS1-independent manner (Aarts et al. 1998). However, no T-DNA insertion mutants in this particular are yet available in Ws-4 to test for loss of recognition.

The discovery of (an) additional source(s) of resistance, able to recognise ATR13^{Emco5} is exciting. This implies that there is a higher degree of complexity in the classical gene-for-gene model of interaction, as verified in numerous instances in the literature, than previously expected. However, this observation is not unprecedented. For instance, the bacterial effector AvrB has been shown to be recognised by the two *R* genes RPM1 and TAO1 (Bisgrove et al. 1994; Eitas et al. 2008). In oomycetes, Hall et al. (2009) showed similar results for the *Hpa* ATR13 effector. Indeed, several ATR13 alleles of different *Hpa* isolates can be recognised independently of RPP13. Two cases were observed: (a) the accession UKID8 is resistant to *Hpa* Hind2 and ATR13^{Hind2} was recognised in this accession by a single dominant gene other

than RPP13^{UKID8}; (b) similarly to what I observed here for ATR13^{Emco5} recognition in Ws-0, the accessions UKID44 and UKID71 were susceptible to *Hpa* Maks9, but ATR13^{Maks9} was recognised in these accessions by a single dominant gene other than RPP13^{UKID44} or RPP13^{UKID71} (Hall et al. 2009). Interestingly, Hall et al. (2009) mapped the *R* gene recognising ATR13^{Maks9} to chromosome 1 in UKID44 and UKID71 (and not chromosome 4 as in my study), suggesting that Arabidopsis may have evolved various receptors and systems to recognise this particular effector. It is worth noting that RPP13 can also recognise other effector(s) than ATR13 (Hall et al. 2009) and that RPM1 can also recognise another bacterial effector than AvrB called AvrRPM1 (Bisgrove et al. 1994). In this study, we bring new evidence of this phenomenon.

So far according to the literature and this study, at least three genes are potentially involved in ATR13 recognition. Because *RPP13* itself is such a diversified gene, this would suggest that the recognition of ATR13 by Arabidopsis is evolutionary and ecologically very important. Conversely, because *ATR13* is present in all *Hpa* isolates tested so far and also extremely diversified, it could suggest that ATR13 has also a very important function for establishing compatibility between *Hpa* and Arabidopsis. In that context, it becomes interesting to know more about these diverging receptors recognising different alleles of *ATR13*.

It is also of interest to understand why Ws is only eliciting a weak HR in response to ATR13^{Emco5}. We can imagine several scenarios: one possibility could be that RPP13 originally recognised ATR13 but to maintain the observed recognition efficiency in parallel with high ATR13 diversification rates, RPP13 also evolved and diversified, as presented by the "zig-zag-zig" model (Jones and Dangl 2006). However, differences in the evolution rates between the pathogen and its host might have led to the fixation of *RHA13*, which functionally complemented *RPP13* to recognise a fast-evolving ATR13. Another possibility

could be the other effectors secreted with ATR13 into Arabidopsis cells, either by *Hpa* Emco5 or *Pst* DC3000 (used here for the delivery of ATR13) can impair ATR13 recognition, by interfering with its cognate *R* gene function for instance. To address the question of a possible suppression by additional secreted molecules in the effector set, I tried to pre-infect plants with *Hpa* Emco5 and 3 days after infection infiltrate *Pst* DC3000 ATR13^{Emco5} (data not shown). Presumably, this strategy would have allowed for the delivery of the whole set of Emco5 effectors in a first time, before *Pst* DC3000 ATR13^{Emco5} can elicit any HR. Unfortunately, I could not find suitable conditions to perform such an experimental assay, which was probably due to the complexity of controlling two successive infections with two different pathogens. Recently, another member of our laboratory, Jorge Badel, developed a mixed infection assay to identify effectors out-competing others *in planta* (Badel et al., in preparation). Potentially, this assay should prove useful to identify any putative suppressor of ATR13^{Emco5}-triggered immunity.

Because of the high allelic variation observed in *ATR13* as well as in *RPP13*, it could be hypothesised that ATR13 and RPP13 interact directly as it was shown in the flax/*M. lini* interaction (Dodds et al. 2006). However, such a direct interaction between ATR13 and RPP13 was never experimentally proven, despite considerable efforts (Jim Beynon and Brian Staskawicz, personal communication). Alternatively, more clues on the virulence or avirulence functions of ATR13 could help us understand why ATR13 exhibits such diversity. Recently, an NMR structure of ATR13 has been obtained (Leonelli et al. 2011). In this study, it was shown that ATR13 contains two surface-exposed patches of polymorphism, with only one of these patches being involved in RPP13-mediated recognition (Leonelli et al. 2011). It is conceivable that the other patch may be important for either *RHA13*-mediated recognition or for possible interactions with other plant proteins important for its virulence function. Interestingly ATR13 subcellular localisation *in planta* was shown to be allele-specific

ATR13^{Emoy2} and ATR13^{Maks9} are nucleolar, while ATR13^{Emco5} is nuclear-cytoplasmic (Leonelli et al. 2011; Caillaud et al. 2012). Surprisingly, subcellular localisation and avirulence property were uncoupled, suggesting that maybe subcellular localisation and virulence properties are linked.

ATR13 contributes to *Hpa* virulence on Arabidopsis (as shown by Sohn et al. 2007 and Rentel et al. 2008) and converging evidence, including those presented in this chapter, seem to pinpoint that this particular effector is of unusual importance for the pathogen and consequently for the plant immune system. Although the precise virulence function of ATR13 is unknown, a recently published large-scale Y2H assay (Mukhtar et al. 2011) revealed Arabidopsis proteins that interact with ATR13 and that are therefore putative virulence targets, which may provide good starting points for future characterisation studies.

4. Initial characterisation of selected downy mildew effector candidates

4.1. Introduction to the project

Plant-associated organisms secrete proteins and other molecules to modulate defence and enable colonization of plant tissue. Understanding the molecular function of these effector molecules is essential for a mechanistic understanding of the processes underlying plant colonization. In contrast to bacterial plant pathogens, only a few fungal or oomycete effector proteins have been characterized (**Table 1.1** in Chapter 1). Emerging findings indicate that several oomycete RxLR effectors suppress host immunity (Sohn et al. 2007; Bouwmeester et al. 2011; Bozkurt et al. 2011). However, the mechanisms through which RxLR effectors interfere with plant defences remain to be elucidated. With ever-accelerating advances in DNA sequencing and other genomics methods, potentially devastating crop pathogens such as rusts, powdery mildews and downy mildews are now "within range" for genomics-based approaches. From the analysis of the *Hpa* Emoy2 reference genome, 134 HaRxLs (RxLR effector candidates) are predicted (Baxter et al. 2010). These HaRxLs constitute a potentially interesting source of effector candidates given that several RxLR effectors have been experimentally shown to be important virulence factors (Sohn et al. 2007; Bouwmeester et al. 2011; Bozkurt et al. 2011).

Prior to the publication of the *Hpa* Emoy2 genome, our laboratory participated in an "Effectoromics" project (ERA-PG project coordinated by Jim Beynon 2007-2010). The goal of this project was to understand host plant susceptibility and resistance by indexing and

deploying obligate pathogen effectors. In this project, the *Hpa* Emoy2 genome and expressed sequence tags (EST) data were mined for potential effector candidates **(Figure 4.1).** Based on *in silico* predictions we selected candidate genes that contained a signal peptide for secretion and an RxLR motif for delivery **(Figure 4.1)**. Allele sequencing in at least five *Hpa* isolates revealed candidates that are under diversifying selection, suggesting probable interaction with co-evolving Arabidopsis *R* genes.

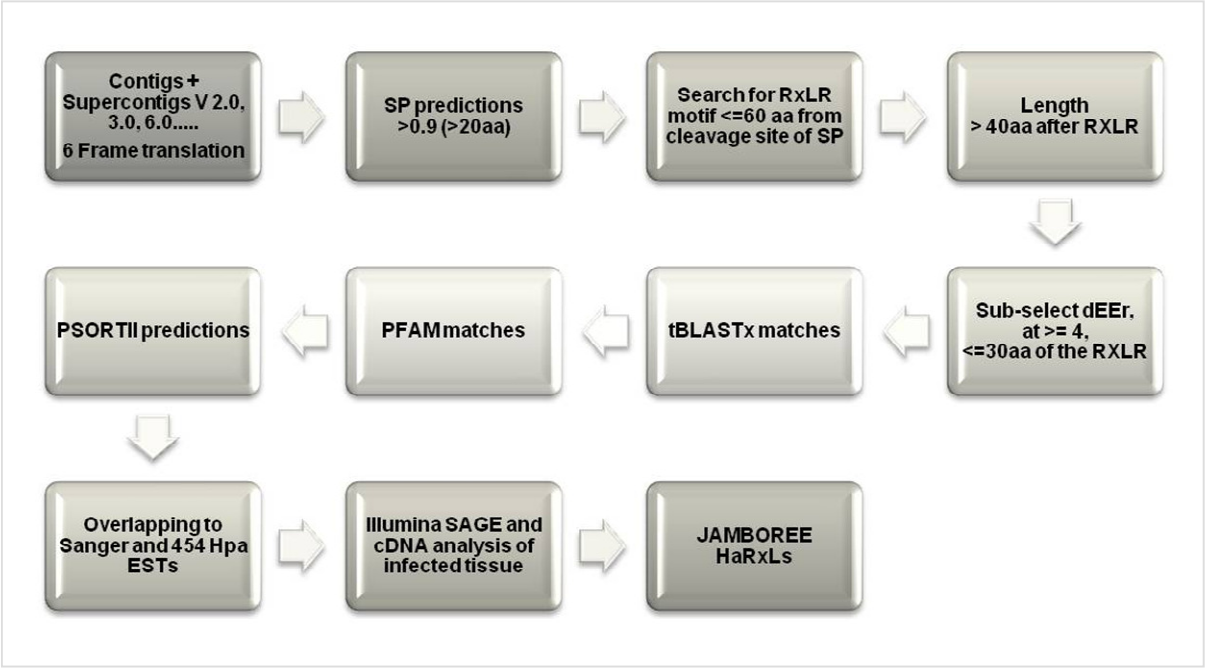

Figure 4.1. Bioinformatic pipeline used for the identification of HaRxLs
(modified from Fabro et al. 2011).

Hundred and forty predicted RxLR effector (*HaRxLs*) genes were annotated in the *Hpa* Emoy2 genome (Fabro et al. 2011). In this project, I participated to the cloning of intronless *HaRxLs* from *Hpa* Emoy2 genomic DNA into the pENTR-TOPO vector. This collection of *HaRxLs* cloned in a Gateway compatible system constitutes a basic resource for use in high throughput screening systems allowing the identification of interesting HaRxLs candidates (Fabro et al. 2011; Caillaud et al. 2012; Badel et al. *in preparation*).

Using an initial set of 88 cloned *HaRxLs* expressed during *Hpa* infection, screening methods were developed to narrow down the effector candidates list to interesting HaRxLs whose function could be later identified (**Figure 4.1, Table 4.1, Appendix 4.1**). I will describe below the two screens in which I took part and from which three publications arose (Fabro et al. 2011; Caillaud et al. 2012; Badel et al. *in preparation*). This initial characterisation of HaRxLs was performed in our laboratory using the "effector tool box" (**Figure 4.2**), which encompasses a set of assays used to identify promising effector candidates, in an effort to prioritise them for further and deeper characterisation.

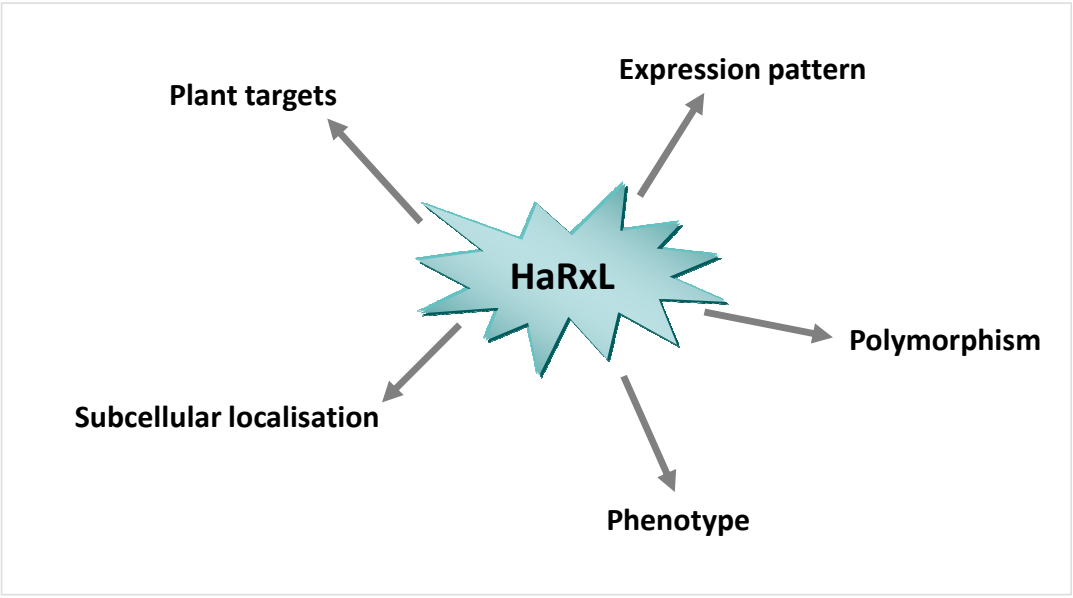

Figure 4.2. The "effector toolbox" to characterise HaRxLs.
To characterise the function of HaRxLs, we look at their expression pattern in infected tissues, their polymorphism among *Hpa* isolates, their phenotype *in planta*, their subcellular localisation *in planta* and their plant targets.

This approach already was used to identify the functions of effectors from another oomycete *P. infestans* (Schornack et al. 2009). This set of assays includes the analysis of: (1) *HaRxLs* expression pattern in infected tissues, (2) *HaRxLs* sequence polymorphisms, HaRxLs

phenotypes when delivered or expressed *in planta*, (4) HaRxLs subcellular localisation *in planta*, and (5) the identification of plant targets.

Using this "effector toolbox" pipeline, members of our laboratory including myself identified properties of several effector candidates (**Table 4.1**) and the reader of this thesis is encouraged to refer to the resulting publications for more details on the general procedure and results (Fabro et al. 2011; Caillaud et al. 2012; Badel et al. *in preparation*). As this work was done in a joint manner between members of our laboratory and external collaborators, I will focus in this chapter on results that I specifically obtained, which were or will be included in the aforementioned publications.

4.2. Results

4.2.1. *Pst* DC3000 HaRxLs-EDV virulence screening

4.2.1.1. *Fabro et al. (2011) identified several HaRxLs that suppress plant immunity*

The collection of 64 HaRxLs cloned as translational fusions in EDV vector (HaRxLs-EDV) was generated in our laboratory (Fabro et al. 2011, **Table 4.1**) to allow their expression in *Pst* and subsequent delivery into Arabidopsis cells (Sohn et al. 2007). This "HaRxL-EDV collection" was screened for bacterial virulence on several Arabidopsis accessions, selected to maximize variability (Bay-0, Br-0, Col-0, Ksk-1, Ler-0, Nd-0, Oy-0, Sha, Ts-1, Tsu-0, Wei-0, Ws-0). The screening method, summarised in **Figure 4.3**, was based on measuring the luminescence emitted by *Pst* DC3000 expressing a luciferase reporter gene (*Pst*-LUX). The luminescence produced by *Pst*-LUX that carried the given HaRxL-EDV (*Pst*-LUX HaRxL-EDV) was compared to the luminescence produced by a control strain that expressed a mutated form of AvrRPS4 inactive *in planta* (*Pst*-LUX AvrRPS4-AAAA-EDV) (Sohn et al. 2009). The impact on the growth of *Pst*-LUX *in planta* of each HaRxL-EDV compared to the control was evaluated and expressed as a ratio. This assay allowed us to establish whether a given candidate effector was able to enhance or decrease *Pst*-LUX virulence, manifested as quantitative differences in bioluminescence, on various host ecotypes (Fabro et al. 2011).

In the Fabro et al. (2011) paper, we next screened the HaRxL-EDV collection for suppression of PAMP-triggered immunity by assaying callose deposition triggered by *Pst*-ΔCEL. *Pst*-ΔCEL is unable to fully suppress callose deposition due to the lack of the bacterial effectors HopM1 and AvrE (DebRoy et al. 2004). In addition, we addressed whether supposed recognition events leading to HR could occur when HaRxL-EDV were delivered

via Pst-ΔCEL or a modified non-host bacteria species (*Pseudomonas fluorescens Pf0-1*) that carry a functional T3SS (Thomas et al. 2009).

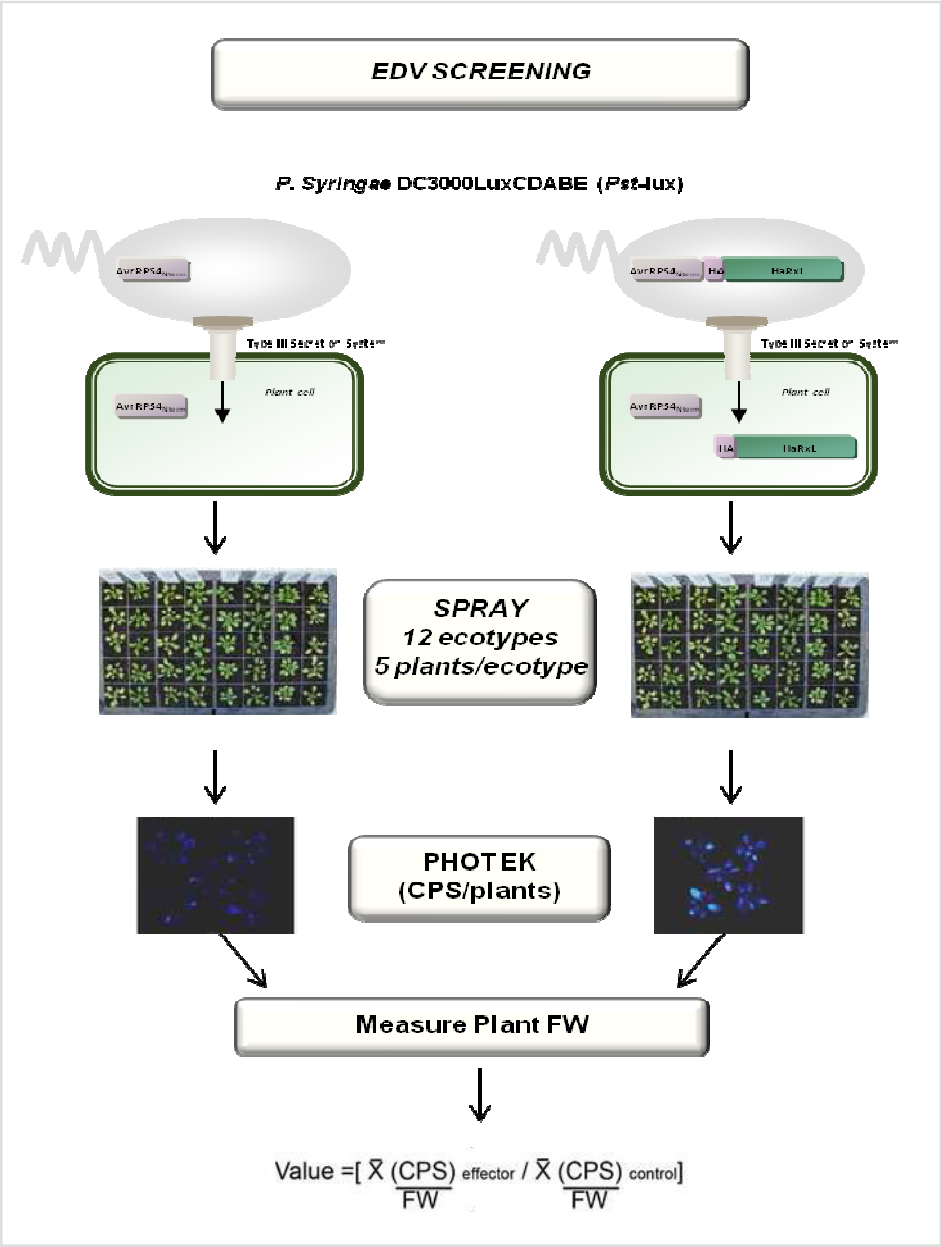

Figure 4.3. HaRxLs-EDV screening method (modified from Fabro et al. 2011).
Pst-LUX strains carrying single *Hpa* effector candidate (HaRxL) were sprayed on 12 Arabidopsis accessions. Levels of bacterial growth were measured quantifying bioluminescence (photon counts) emitted by the bacteria present on whole plants. The ratio of the average photon counts per second (CPS) per gram of fresh weight (FW) emitted by the bacteria delivering a given HaRxL versus the bacteria delivering control proteins was determined per accession.

Using this approach, we identified that most of the 64 selected HaRxLs could confer enhanced bacterial virulence on at least one Arabidopsis accession tested in the study and could also suppress PTI responses (**Table 4.1**). Surprisingly, we observed that strong incompatibility caused by *Hpa* effectors is rare, since only a very few of these HaRxLs could cause a reduction in bacterial growth (**Table 4.1**). None of the HaRxLs tested was able to trigger macroscopic ETI when delivered *in planta* at high titre, as ATR13^{Emco5} did in Nd-0.

To compare the results obtained from the HaRxL-EDV screen with the expression of the pathogen proteins directly in the plant, in the Fabro et al. (2011) paper we cloned a subset of HaRxLs under the control of a constitutive (CaMV 35S) promoter and transformed them into Arabidopsis Col-0. We next assessed the consequences of *in planta* HaRxL expression for pathogen development, PTI and ETI. Seven independent HaRxLs stably expressed in Arabidopsis Col-0 were found to cause an increased susceptibility to *Hpa* and *Pst*-LUX, that correlated well with a decrease in PTI response to PAMP treatments (Fabro et al. 2011). The results of this screen and the analyses presented in this thesis are presented in **Table 4.1** below.

↓ Table 4.1. Expression pattern, polymorphism, phenotype and subcellular localisation *in planta* of HaRxL candidates, conducted by various members of our laboratory.
(table last updated in December 2011). Expression data come from: A, Sanger ESTs generated from *Hpa* Emoy2 conidiospores, B, 454 ESTs generated from *Hpa*-infected tissue (3dpi), C, Illumina GA2 reads from *Hpa*-infected tissue (3 and 7 dpi), D, RT-PCR done on *Hpa*-infected tissues. Polymorphism: number of polymorphic amino-acid positions indicated in brackets. Subcellular localisation of GFP/RFP-tagged HaRxLs. EDV: *Pst*-LUX HaRxLs-EDV tested in 12 Arabidopsis accessions, (+) indicates enhanced bacterial growth, (-) indicates decreased bacterial growth, (=) indicates same bacterial growth as control. Callose suppression: *Pst* DC3000 ΔCEL pEDV-HaRxLs tested for suppression of callose triggered by ΔCEL mutation in plants, "yes+" indicates high suppression, yes indicates suppression, and "no" indicates no suppression. Turnip assay: *Pst* DC3000 LUX pEDV-HaRxLs tested for enhanced growth (+), decreased growth (-) or same growth as control (=) in *Brassica rapa* cv. Just Right. Arabidopsis stable lines expressing single HaRxLs: tested for PTI suppression phenotype (either ROS, callose or HR) and differential pathogen growth (*Pst* or *Hpa*). ---: not determined. References: [1] Fabro et al. (2011), [2] Caillaud et al. (2012), [3] Badel et al. *in preparation*, [4] Rehmany et al. (2005). In purple are highlighted HaRxLs which I will describe in detail in this chapter.

Name	Expression	Polymorphism	Subcellular localisation	EDV			Callose suppresion	Turnip assay	Arabidopsis stable lines expressing single HaRxL		References
				(+)	(=)	(-)			PTI suppression	Pathogen assays	
ATR1	D	HIGH	nucleus, cytoplasm	---	---	---	---	---	yes (ROS); yes (callose)	enhances *Hpa* + *Pst* growth	[1] [2] [4]
ATR13	B, D	HIGH (28)	nucleolus	8	1	3	yes+	(=)	yes (ROS); yes (callose)	enhances *Hpa* + *Pst* growth	[1] [2]
HaRxL1	---	---	cytoplasm	---	---	---	---	---	---	---	[2]
HaRxL2	---	---	nucleolus	---	---	---	---	---	---	---	[2]
HaRxL4	B,C	MEDIUM (10)	---	7	4	1	yes	(+)	---	---	[1] [2]
HaRxL9	B	MEDIUM (12)	plasma membrane	8	4	0	yes	(=)	---	---	[1] [2]
HaRxL10	A,B,C	MEDIUM (14)	nucleus, cytoplasm	---	---	---	---	---	---	---	[2]
HaRxL11	---	---	golgi	1	9	2	no	(=)	---	---	[1] [2]
HaRxL13	B	LOW (4)	---	3	8	1	yes	(+)	---	---	[1]
HaRxL14	B,C	MEDIUM (11)	nucleus, cytoplasm	6	6	0	yes+	(+)	no (ROS); yes (callose)	enhances *Hpa* + *Pst* growth	[1] [2]
HaRxL15	A,B	LOW (3)	cytoplasm	---	---	---	---	---	---	---	[2]
HaRxL16	B,C	LOW (4)	nucleus, cytoplasm	7	5	0	yes	(=)	---	---	[1] [2]
HaRxL17	A,B,C,D	LOW (3)*	tonoplast	8	4	0	yes	(-)	---	enhances *Hpa* growth	[1] [2]
HaRxL18	A,B,C	LOW (2)	nucleus	0	7	5	no	(=)	---	---	[1] [2]
HaRxL21	A,B,C	HIGH (19)	nucleus, nucleolus, cytoplasm	8	4	0	yes+	(-)	yes (ROS); yes (callose)	enhances *Hpa* + *Pst* growth	[1] [2]
HaRxL22	B,C,D	MEDIUM (7)	nucleus, cytoplasm	5	7	0	no	(=)	yes (Pf0-1); yes (callose)	---	[1] [3]
HaRxL23	A,B	LOW (4)	---	---	---	---	---	---	---	---	[2]
HaRxL24	---	---	nucleolus	---	---	---	---	---	---	---	[2]
HaRxL26	---	---	nucleus, cytoplasm	---	---	---	---	---	---	---	[2]
HaRxL27	---	---	NE	---	---	---	---	---	---	---	[2]
HaRxL29	---	---	nucleus, cytoplasm	---	---	---	---	---	---	---	[2]
HaRxL30	D	multigene family	---	---	---	---	---	---	---	---	This thesis
HaRxL32	---	---	cytoplasm	---	---	---	---	---	---	---	[2]
HaRxL36	A,C	LOW (4)	nucleus, nucleolus	0	8	4	no	(=)	---	---	[1] [2]
HaRxL39	---	multigene family	---	---	---	---	---	---	---	---	This thesis
HaRxL40	---	multigene family	---	---	---	---	---	---	---	---	This thesis
HaRxL41	---	multigene family	---	---	---	---	---	---	---	---	This thesis
HaRxL42	---	---	nuclear envelope	---	---	---	---	---	---	---	This thesis
HaRxL44	B,C,D	LOW (2)*	nucleolus	6	4	2	yes+	(=)	yes (ROS); yes (callose)	---	[1] [2]
HaRxL45a	A,B,C	MEDIUM (11)	nucleus	6	3	3	yes	(+)	---	---	[1] [2]
HaRxL45b	B,C	MEDIUM (11)	nucleus, cytoplasm	10	2	0	yes+	(+)	---	---	[1] [2]
HaRxL47	A,B,C,D	multigene family	plasma membrane	6	6	0	yes	(-)	---	---	[1] [2]
HaRxL56	A,B,C	HIGH (17)	---	3	9	0	yes	(=)	---	---	[1]
HaRxL57	A,C	NO (0)	nucleus, cytoplasm	9	2	1	yes+	(=)	yes (ROS); yes (callose)	enhances *Hpa* + *Pst* growth	[1] [2]
HaRxL59	A,B	HIGH (18)	---	4	8	0	no	(=)	---	---	[1]
HaRxL60	B,C	HIGH (17)	---	4	8	0	no	(=)	---	---	[1]
HaRxL62	A,B,C	MEDIUM (6)	nucleus, cytoplasm	12	0	0	yes+	(+)	---	---	[1] [2]
HaRxL63	A,B,C	MEDIUM (7)	---	11	1	0	yes+	(-)	---	---	[1]
HaRxL64	A,B,C	MEDIUM (13)	---	6	6	0	yes	(=)	---	---	[1]
HaRxL65	A,B,C	MEDIUM (6)	---	5	7	0	no	(=)	---	---	[1]
HaRxL67	**B,C**	**LOW (2)**	**vacuole**	**3**	**4**	**5**	**no**	**(=)**	**---**	**---**	**[1] [2] this thesis**
HaRxL68	C	LOW (2)	nucleus, nucleolus, cytoplasm	4	8	0	yes	(+)	---	---	[1] [2]
HaRxL70	A	LOW (4)	cytoplasm	3	8	1	yes+	(+)	yes (ROS); yes (callose)	enhances *Hpa* + *Pst* growth	[1] [2]
HaRxL72	A,B,C	MEDIUM (11)	---	6	6	0	yes+	(=)	---	---	[1]
HaRxL73	A,B,C	HIGH (34)	---	9	3	0	yes	(=)	---	---	[1]
HaRxL74	A	LOW (4)	---	0	4	8	no	(=)	---	---	[1]
HaRxL75	B,C,D	MEDIUM (6)	plasma membrane	8	4	0	yes	(=)	yes (Pf0-1); yes (callose)	---	[1] [3]
HaRxL77	A,B,C	LOW (1)*	plasma membrane	0	7	5	no	(=)	---	enhances *Hpa* growth	[1] [2]
HaRxL78	---	---	nucleus, cytoplasm	---	---	---	---	---	---	---	[2]
HaRxL79	**A,B,C,D**	**multigene family**	**microtubules, nucleus, cytoplasm**	**2**	**3**	**7**	**no**	**(-)**	**---**	**---**	**[1] this thesis**
HaRxL80	A,B	MEDIUM (7)	---	1	3	8	---	(=)	---	---	[1]
HaRxL89	A,B,C	LOW (5)	nucleus, nucleolus	3	7	2	no	(-)	yes (Pf0-1); yes (callose)	---	[1] [3]
HaRxL106	B,C	HIGH (23)	nucleus	9	1	2	yes	(+)	yes (ROS); yes (callose)	enhances *Hpa* + *Pst* growth	[1]
HaRxL120	A,B	LOW (4)	---	7	5	0	yes	(+)	---	---	[1]
HaRxL142	A,B,C	NO (0)	---	7	5	0	yes+	(=)	---	---	[1]
HaRxL144	A,C	LOW (2)	---	3	9	0	no	(=)	---	---	[1]
HaRxL145	A,B,C	NO (0)	---	3	9	0	yes	(=)	---	---	[1]
HaRxL146	A,B,C	NO (0)	plasma membrane	9	3	0	yes	(=)	---	---	[1] [2]
HaRxL147	A,B,C	MEDIUM (15)	---	3	8	1	no	(=)	---	---	[1] [2]
HaRxLL3a	---	multigene family	nucleolus	4	8	0	no	(=)	---	---	[2]
HaRxLL3b	---	multigene family	nucleolus	---	---	---	---	---	---	---	[1] [2]
HaRxLL60	A,B,C	LOW (5)	nucleus, nucleolus, cytoplasm	5	7	0	no	(=)	yes (ROS); no (callose)	enhances *Pst* + decreases *Hpa* growth	[1] [2]
HaRxLL90	---	---	---	3	6	3	no	(=)	---	---	[1] [2]
HaRxLL73	---	multigene family	---	---	---	---	---	---	---	---	This thesis
HaRxLL108	B,C	LOW (3)	nucleus	6	4	2	yes+	(+)	---	---	[1] [2]
HaRxLL143	B,C	MEDIUM (11)	nucleus	---	---	---	---	---	---	---	[2]
HaRxLL148	C	MEDIUM (6)	nucleus, cytoplasm	6	6	0	yes+	(=)	---	---	[1] [2]
HaRxLL169b	A,B,C	LOW (5)	---	5	7	0	yes+	(=)	---	---	[1]
HaRxLL437	A,C	HIGH (19)	---	3	6	3	yes	(=)	---	---	[1] [2]
HaRxLL441	A,D	MEDIUM (15)	endoplasmic reticulum	3	6	3	no	(+)	yes (Pf0-1); yes (callose)	---	[1] [3]
HaRxLL445	A,B,C	MEDIUM (9)	nucleus, cytoplasm	5	6	1	yes	(=)	---	---	[1]
HaRxLL455	A,C	LOW (1)	---	5	7	0	no	(=)	---	---	[1]
HaRxLL464	A,B,C,D	NO (0)	nucleus, cytoplasm	9	3	0	yes	(=)	yes (ROS); yes (callose)	enhances *Hpa* + *Pst* growth	[1] [3]
HaRxL467	B,C	LOW (2)	---	6	6	0	yes+	(=)	---	---	[1]
HaRxL468	A,B,C	HIGH (15)	---	3	9	0	no	(=)	---	---	[1]
HaRxLL470b	A,C	LOW (2)	nucleolus	1	5	6	no	(-)	---	---	[1] [2]
HaRxLL480	A,B,C	LOW (4)	cytoplasm	5	7	0	no	(=)	---	---	[1] [2]
HaRxLL483	B,C	LOW (3)	nucleus, cytoplasm	5	3	4	yes	(=)	---	---	[1] [2]
HaRxLL492	A,B	LOW (2)	endoplasmic reticulum	6	6	0	no	(=)	yes (ROS); yes (callose)	enhances *Pst* + decreases *Hpa* growth	[1] [2]
HaRxLL493J	---	multigene family	endoplasmic reticulum	---	---	---	---	---	---	---	[2]
HaRxLL493b	---	multigene family	endoplasmic reticulum	---	---	---	---	---	---	---	[2]
HaRxLL493e	---	multigene family	---	6	6	0	no	(=)	---	---	[1] [2]
HaRxLL494	A,B,C	LOW (3)	endoplasmic reticulum	---	---	---	no	---	---	---	[2]
HaRxLL495a	A,B,C	multigene family	endoplasmic reticulum	4	6	2	yes+	(+)	---	same *Hpa* growth as WT	[1] [2]
HaRxLL495b	---	multigene family	endoplasmic reticulum	---	---	---	no	---	---	same *Hpa* growth as WT	[1] [2]
HaRxLL495c	---	multigene family	endoplasmic reticulum	---	---	---	no	---	---	same *Hpa* growth as WT	[2]
HaRxLCRN4b	A,B,C	MEDIUM(14)	nucleus, cytoplasm	5	7	0	no	(=)	---	---	[1] [2]

4.2.1.2. Characterisation of HaRxL65, an effector from the HaRxL-EDV screen

- **HaRxL65 phenotype in EDV screen**

From the HaRxLs-EDV screen published in Fabro et al. (2011) (**Table 4.1**) I chose an *Hpa* effector candidate called HaRxL65, which showed increased *Pst* virulence, for further characterisation. In the HaRxL-EDV screen, HaRxL65 caused an enhanced *Pst*-LUX growth in five Arabidopsis accessions (Ksk-1, Nd-0, Sha, Wei-0, Ws-0) but did not affect the bacterial growth in seven other Arabidopsis accessions (Bay-0, Br-0, Col-0, Ler-0, Oy-0, Ts-1, Tsu-1) and on turnip (**Table 4.2**). On tomato, *Pst*-LUX HaRxL65-EDV caused normal disease symptoms, suggesting that HaRxL65 did not block the *Pst* T3SS (Fabro et al. 2011, **Table 4.2**).

Arabidopsis													
Bay-0	Br-0	Col-0	Ksk-1	Ler-0	Nd-0	Oy-0	Sha	Ts-1	Tsu-1	Wei-0	Ws-0	Turnip	Tomato
(=)	(=)	(=)	(+)	(=)	(+)	(=)	(+)	(=)	(=)	(+)	(+)	(=)	disease

Table 4.2. *Pst*-LUX HaRxL65-EDV growth *in planta* (from Fabro et al. 2011).
HaRxL65 conferred either enhanced bacterial growth (+) highlighted in yellow or no differential bacterial growth (=) highlighted in grey. *Pst*-LUX HaRxL65-EDV growth was measured on 12 Arabidopsis accessions, on turnip (*Brassica rapa* cv. Just Right), and on tomato (cv. Moneymaker).

- **HaRxL65 polymorphism**

Many oomycete effectors are found to be highly polymorphic and under positive selection (Allen et al. 2004; Win et al. 2007; Allen et al. 2008; Schornack et al. 2009). Assuming that sequence polymorphism is a common feature of secreted effectors, I compared the sequences of *HaRxL65* in nine different *Hpa* isolates (Cala2, Emco5, Emoy2, Emwa1, Hiks1, Hind2, Maks9, Noco2, Waco9). I first PCR amplified *HaRxL65* from *Hpa* Emoy2

genomic DNA in order to determine if *HaRxL65* was polymorphic in Emoy2. This analysis showed that *Hpa* Emoy2 is heterozygous at *HaRxL65* locus, as two distinct alleles were identified **(Figure 4.4).** These two Emoy2 alleles named *HaRxL65*^{Emoy2A} and *HaRxL65*^{Emoy2G} differ by one nucleotide at position 335 (A or G) which results in a single amino-acid change in the two protein variants **(Figure 4.4)**. However, these amino-acids have similar properties (Serine or Asparagine) since both contain a polar uncharged side chains.

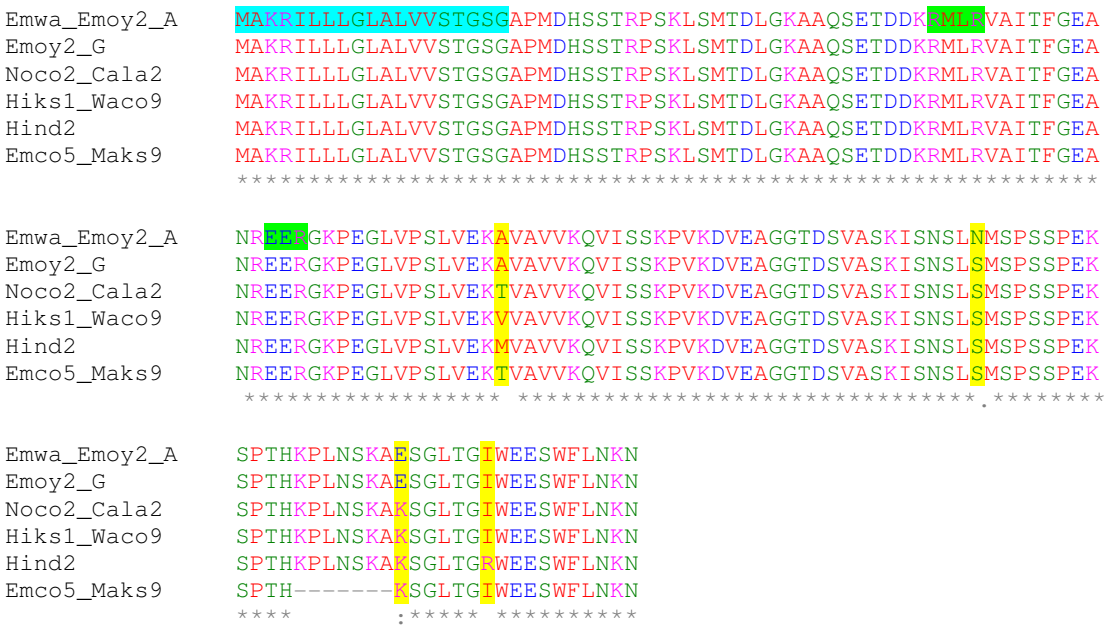

Figure 4.4. Protein sequences alignment of HaRxL65 in different *Hpa* isolates.
HaRxL65 protein sequences were aligned using MAFFT G-INS-I (v6.850b) and displayed in ClustalW format. The signal peptide is highlighted in blue, the RxLR and EER motifs in green. Positions under positive selection (identified as described in Win et al. 2007) are highlighted in yellow.

I then used the primer set designed to amplify *HaRxL65* in *Hpa* Emoy2 to PCR amplify *HaRxL65* from other *Hpa* isolates. At both DNA and protein level, HaRxL65 is polymorphic as shown by the amino-acid alignment presented in **Figure 4.4**. Interestingly in both *Hpa* isolates Emco5 and Maks9, HaRxL65 showed a seven amino-acid-long deletion in the C-terminal region (**Figure 4.4**). This result suggests a possibly variable phenotype for HaRxL65

in these two *Hpa* isolates. In total, six HaRxL65 protein variants were identified, in which four amino-acid positions (highlighted in yellow in **Figure 4.4**) were under positive selection (in collaboration with Joe Win, TSL), including the polymorphic position 335 in *Hpa* Emoy2. Effector sequences within pathogen populations are often under positive selection, potentially to escape plant immunity (**Chapter 1** section 1.3.2.3) (Dodds et al. 2006; Win et al. 2007). Therefore HaRxL65 can be considered as a good effector candidate.

In order to address if the HaRxL65 polymorphism observed in *Hpa* Emoy2 led to a difference in its function, I tested whether HaRxL65^{Emoy2A} and HaRxL65^{Emoy2G} protein variants could differentially affect *Pst* growth in Arabidopsis. HaRxL65^{Emoy2A}-EDV increased *Pst* LUX virulence in Nd-1 in comparison with the control AvrRPS4-AAAA-EDV (**Figure 4.5**). HaRxL65^{Emoy2G}-EDV decreased virulence of *Pst*-LUX in Ws-0 and Oy-0 in comparison with AvrRPS4-AAAA-EDV. However, no bacterial growth difference was observed in Ler and Wei-0 between *Pst*-LUX HaRxL65^{Emoy2A}-EDV, *Pst*-LUX HaRxL65^{Emoy2G}-EDV and the control *Pst*-LUX AvrRPS4-AAAA-EDV (**Figure 4.5**).

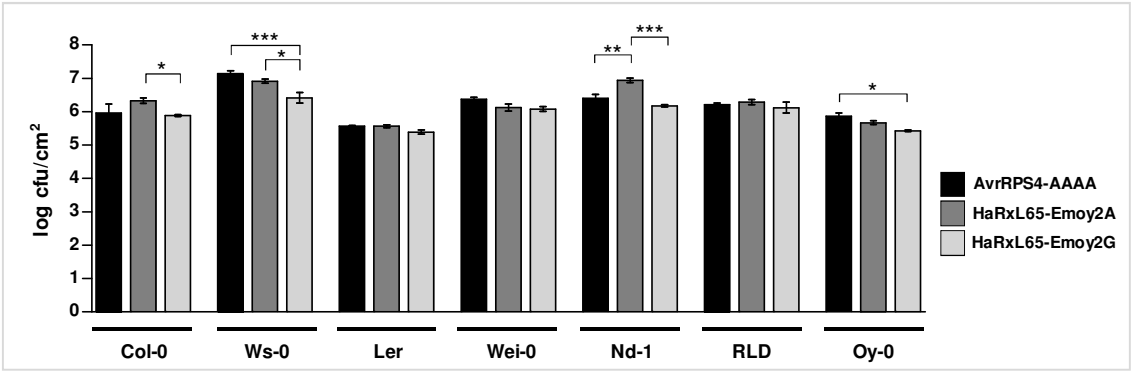

Figure 4.5. *Pst*-LUX HaRxL65-EDV growth on different Arabidopsis accessions.
Bacterial populations were hand-inoculated with 5×10^5 cfu/mL *Pst*-LUX AvrRPS4-AAAA-EDV, *Pst*-LUX HaRxL65-Emoy2A-EDV, or *Pst*-LUX HaRxL65-Emoy2G-EDV. Bacterial populations were measured at 3 days after inoculation. Each bar represents the mean number of bacterial colonies recovered on selective agar medium containing appropriate antibiotics from five independent replicates; error bars represent the standard error of the mean. This experiment was repeated twice with similar results. Asterisks indicate significant differences indicated by a Bonferroni post-hoc comparison test performed after a one-way ANOVA on the whole dataset.

- **HaRxL65 effect on non-host resistance**

Fabro et al. (2011) showed that HaRxLs that did affect *Pst* virulence in Arabidopsis were not always affecting *Pst* virulence in turnip. Therefore, the inability of *Hpa* to grow in turnip might result from inadequate effector complement effectiveness or from the recognition of a subset of effectors that are not recognised in most Arabidopsis accessions. I next wanted to test HaRxL65 effects on a non-host plant, to determine if HaRxL65 has a role in non-host resistance. Various HaRxLs identified in the HaRxLs-EDV screen were tested on turnip, another plant of the *Brassicaceae* family and non-host for *Hpa* (Fabro et al. 2011). In Fabro et al. (2011), only *Pst*-LUX HaRxL65^{Emoy2A}-EDV was tested. I then wanted to determine the effect of HaRxL65^{Emoy2A} and HaRxL65^{Emoy2G} bacterial delivery on turnip **(Figure 4.6).**

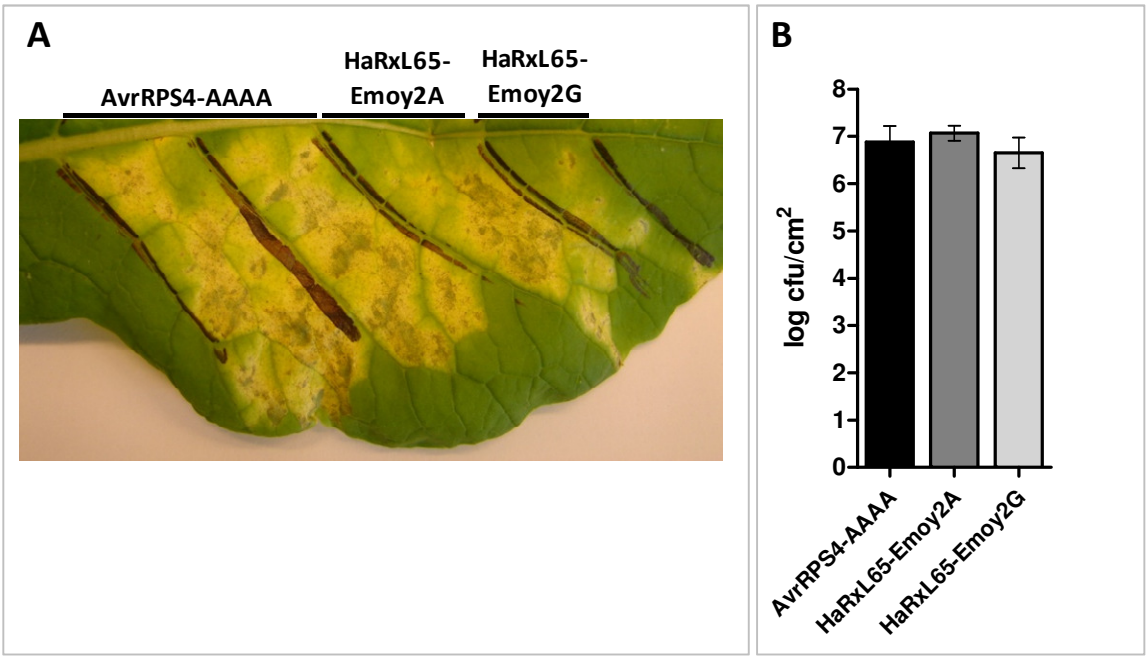

Figure 4.6. HaRxL65 effect on *Pst*-LUX virulence in turnip.
Bacterial populations were hand-inoculated with 5 × 10^5 cfu/mL *Pst*-LUX AvrRPS4-AAAA-EDV, *Pst*-LUX HaRxL65-Emoy2A-EDV, or *Pst*-LUX HaRxL65-Emoy2G-EDV. **A**, Disease symptoms were observed at 5 days after inoculation. **B**, Bacterial populations were measured at 5 days after inoculation. Each bar represents the mean number of bacterial colonies recovered on selective agar medium containing appropriate antibiotics from five independent replicates; error bars represent the standard error of the mean. This experiment was repeated three times with similar results. No significant differences were found by a Bonferroni post-hoc comparison test performed after a one-way ANOVA on the whole dataset.

Pst-LUX HaRxL65^{Emoy2G}-EDV appeared to induce less disease symptoms in turnip compared to *Pst*-LUX HaRxL65^{Emoy2G}-EDV and *Pst*-LUX AvrRPS4-AAAA-EDV (**Figure 4.6A**). However these different disease symptoms were not correlated with a differential bacterial growth as measured by bacterial titres (**Figure 4.6B**).

- **Testing for HaRxL65 avirulence properties**

Because HaRxL65^{Emoy2A} did not show any particular virulence effect on *Pst* growth, I next investigated whether HaRxL65^{Emoy2A} could have an avirulence phenotype. In order to decouple the effects caused by HaRxL65^{Emoy2A} itself from the possible effect of the other effectors of *Pst*, I used *Pfo-1* to deliver HaRxL65. Using this system, only HaRxL65^{Emoy2A}-EDV was then secreted by *Pfo-1* into Arabidopsis cells without any other T3E. Around 60 Arabidopsis accessions from the 96 Nordborg collection were screened for the appearance of HR after *Pfo-1* HaRxL65^{Emoy2A}-EDV infiltration but no HR symptoms could be observed (data not shown), suggesting that HaRxL65^{Emoy2A} recognition in Arabidopsis is probably rare and weak. In the HaRxLs-EDV screen performed by Fabro et al. (2011), none of the HaRxLs tested were able to trigger macroscopic HR when delivered *in planta*. Instead, several were identified that can reduce *Pst*-LUX growth in specific Arabidopsis accessions and triggered micro lesions. The Fabro et al. (2011) survey was not exhaustive since they tested only a subset of HaRxLs from only one *Hpa* isolate (Emoy2), on 12 Arabidopsis accessions. Alternatively, the EDV assay may not be sensitive enough to detect new *Hpa* ATRs because these ATR-RPP recognitions are weaker than those already described with this system. In addition, some ATRs might not carry an RxLR motif and therefore may have been missed as candidate effectors in this study, as with the recently cloned RxLR-like ATR5 (Bailey et al. 2011).

- **HaRxL65 plant interactors (Mukhtar et al. 2011)**

As shown above, despite being a polymorphic effector with amino-acids under positive selection and being identified as an interesting candidate in the HaRxL-EDV screen, HaRxL65^{Emoy2A} did not exhibit a virulence or avirulence phenotype on Arabidopsis with the EDV system, leaving few possibilities to experimentally pursue its characterisation. However, very recently, surprising information was highlighted by Mukhtar et al. (2011) in a large-scale yeast two hybrid (Y2H) screen, in which one putative plant target of HaRxL65^{Emoy2A} identified was a TIR-NB protein encoded by At4g09420 (shown in orange, **Figure 4.7**).

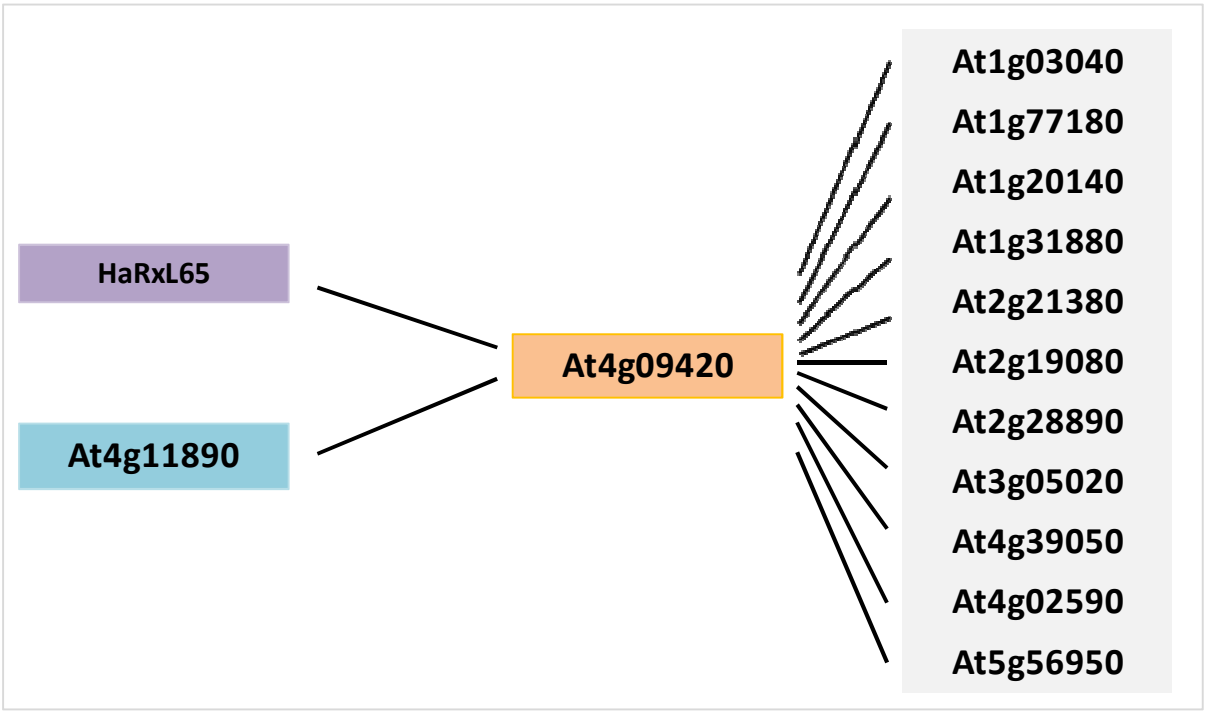

Figure 4.7. Cartoon representing of HaRxL65 and At4g09420 interactors found in the Y2H interactomic projects (Mukhtar et al. 2011, Arabidopsis Interactome Mapping, 2011). In purple, HaRxL65, in orange, the TIR-NB At4g09420, in blue, a defence-associated protein kinase. In grey, other plant interactors.

Resistance genes include TIR-NB-LRR genes but the role of TIR-NB genes lacking the LRR domain is less clear. In addition, according to Y2H data, At4g09420 interacts with one protein kinase (At4g11890) which itself interacts with two uncharacterised receptor like kinases (At3g28040 and At1g34420) (Arabidopsis Interactome Mapping 2011; Mukhtar et al. 2011). This information, in addition to our experimental analyses, could constitute an interesting lead to unravel the functional properties of HaRxL65.

Initially believed to be a promising effector, HaRxL65 did not show any virulence enhancing or decreasing phenotype after a more in depth characterisation, highlighting once more the crucial necessity of experimental characterisation of promising candidates from any large-scale screen. The analysis of HaRxL65 presented here was just one of many, as the functional analyses of several other promising effector candidates that were identified from the initial EDV screen (**Table 4.1**) such as HaRxL106, HaRxL62, HaRxLL464, are currently being followed up by different members of our laboratory.

In the next section, I will present another approach to unravel HaRxLs functions. We focused on the subcellular localisation of HaRxLs *in planta* in a more refined sub-screening of the initial findings presented in **Table 4.1** and published in Fabro et al. (2011).We used microscopy techniques to determine the *in planta* cellular targets of HaRxLs that conferred enhanced/decreased bacterial virulence in the first HaRxLs-EDV screen (**Table 4.1**).

4.2.2. HaRxLs effectors from the HaRxLs-EDV screen can target all the major plant subcellular compartments

Increasing evidence indicates that pathogen effectors can target a wide range of cell compartments, from the plant plasma membrane to the nucleus, in order to suppress host immunity, promote disease and in some instances, modulate plant gene expression (Gurlebeck et al. 2006; Poueymiro and Genin 2009; Block and Alfano 2011). Therefore, we screened for the subcellular localisation of HaRxLs to discover clues as to their mode of action, by determining in which plant cell compartment they are located. Parts of the work described below were initiated and conducted by Dr. Marie-Cécile Caillaud from our laboratory. Therefore, I will only refer in this section to results which I generated myself.

This microscopy-based screen relied on the transient expression of GFP- or RFP-tagged HaRxLs in *N. benthamiana* delivered by *A. tumefaciens* (**Figure 4.8**).

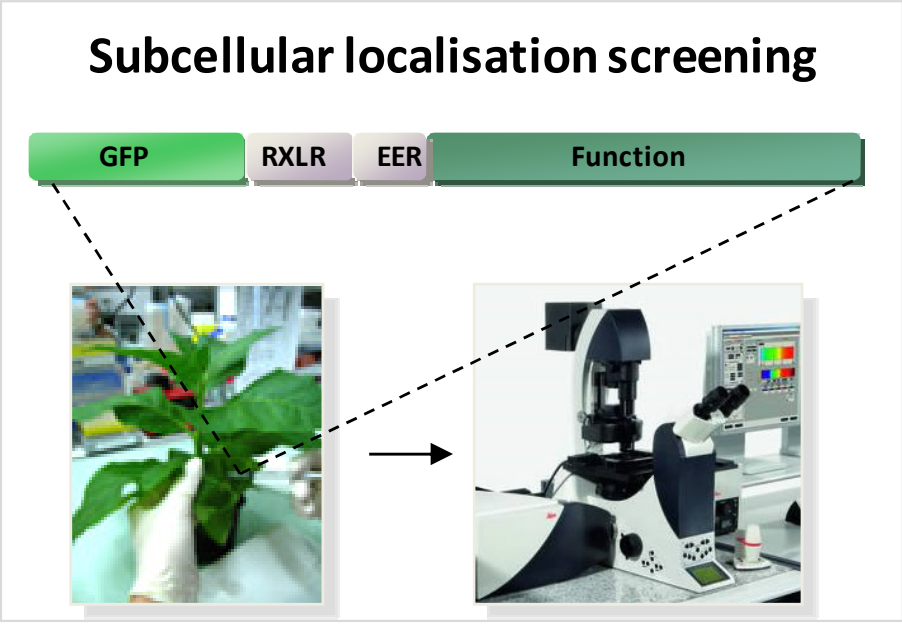

Figure 4.8. Schematic overview of the subcellular localisation screening of HaRxLs.
GFP- or RFP-tagged HaRxLs were agro-infiltrated in *N. benthamiana* leaves. Fluorescence was analysed by confocal microscopy.

In this work, 49 HaRxLs were screened for their subcellular localisation *in planta* by *in vivo* confocal microscopy. This screen, even if not saturated, highlighted that most plant subcellular compartments are targeted by HaRxLs with a predominance of the nucleus (**Figure 4.9, Table 4.1**).

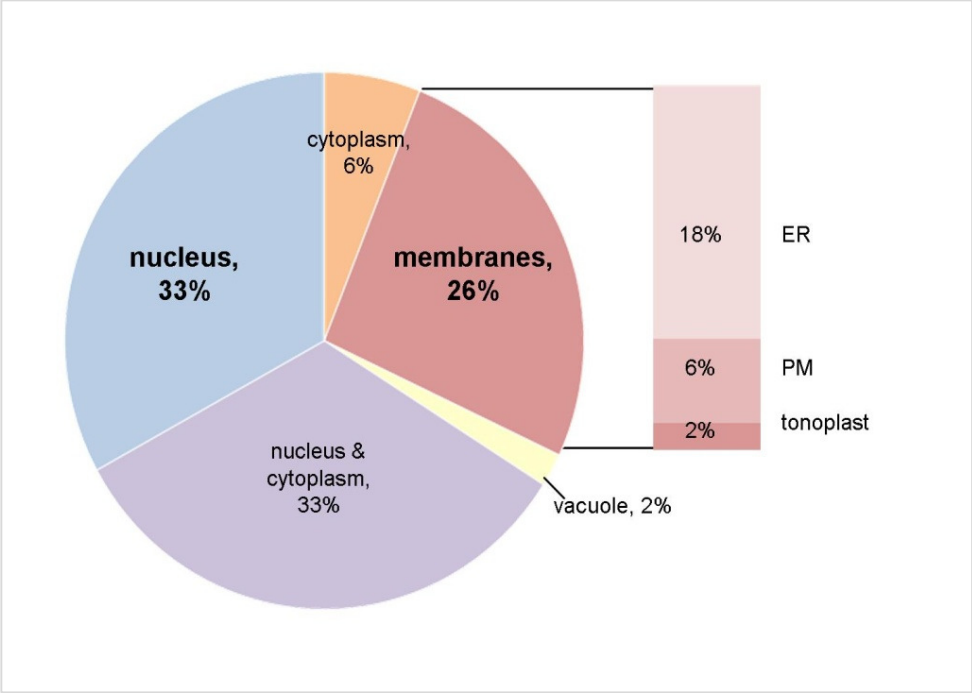

Figure 4.9. Chart pie showing the plant subcellular compartments targeted by HaRxLs (from Caillaud et al. 2011).
Forty nine GFP- or RFP-tagged HaRxLs were transiently expressed in *N. benthamiana* and their subcellular localisation was analysed by *in vivo* confocal microscopy. Percentages indicate the proportion of HaRxL targeting each plant cell compartment.

Indeed, out of these 49 HaRxLs tested, 32 (66%) were observed to target the plant nucleus, among which half (16) were also observed in the plant cytoplasm. Twenty six percent (13) were observed to be associated with plant membranes, including the endoplasmic reticulum, the plasma membrane and the tonoplast. Only very few HaRxLs (Mackey et al.) were observed to be exclusively cytoplasmic, and only one effector, HaRxL67, was located in the vacuole (**Table 4.1**, see Chapter 5). This result demonstrates

that HaRxLs (less than half of the ones predicted in *Hpa* Emoy2 genome (Baxter et al. 2010), target different plant subcellular compartments.

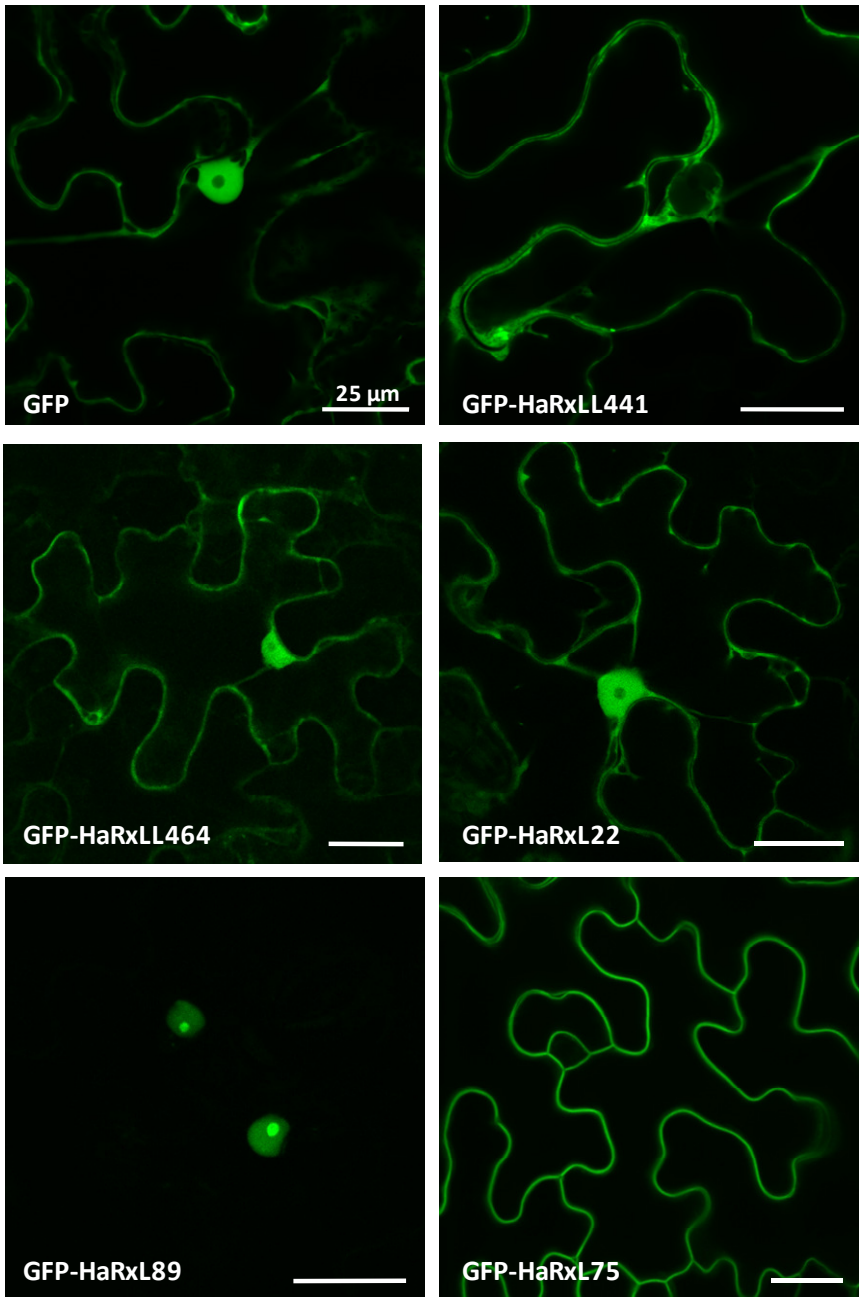

Figure 4.10. Representive subcellular localisation of HaRxLs *in planta*.
GFP-tagged HaRxLs were transiently expressed in *N. benthamiana* and their localisation was analysed by *in vivo* confocal microscopy: GFP-HaRxLL441 is cytoplasmic, HaRxL89 is nuclear/nucleolar, HaRxL22 and HaRxL464 are nuclear-cytoplasmic and HaRxL75 is plasma-membrane associated.

In a recent parallel screen to identify HaRxLs outcompeting each other *in planta* (IPECA), Badel et al. (*in preparation*) delivered multiple candidates as bacterial mixed infections in Arabidopsis and quantified the contribution to virulence of individual effectors. Badel et al. (*in preparation*) identified five HaRxLs that enhance bacterial multiplication in some Arabidopsis accessions but not in others. These HaRxLs exhibited different subcellular localisations representative of what we observed in the subcellular localisation screening: HaRxLL441 was cytoplasmic, HaRxL89 was nuclear/nucleolar, HaRxL22 and HaRxL464 were nuclear-cytoplasmic and HaRxL75 was plasma-membrane associated (**Figure 4.10, Table 4.1**).

The screen I undertook in collaboration with Dr. Marie-Cécile Caillaud was performed in *N. benthamiana* plants in which the effectors are delivered using *A. tumefaciens* and yielded very interesting results. However *Hpa* effectors may show a different localisation in a non-host plant compared to the host plant. In order to localise effectors in the plant cell *in vivo* during oomycete infection, we generated Arabidopsis Col-0 transgenic lines expressing GFP-tagged HaRxL (CaMV 35S promoter). Subcellular localisations were confirmed in Arabidopsis transgenic lines for all the HaRxLs tested (which corresponds to half of the HaRxLs screened in *N.benthamiana*), confirming that either method is useful for examining the localisation of *Hpa* effectors (Caillaud et al. 2012). This subcellular localisation screen led to the identification of one very interesting HaRxL called HaRxL17, which is a plant membrane-associated effector associating with the EHM in *Hpa*- and *A. laibachii*-infected tissues (Caillaud et al. 2012; Caillaud et al. in press) (**Table 4.1**). Because HaRxL17 is tonoplast-associated, the observation that HaRxL17 is in close proximity to the EHM can imply that either the EHM is a tonoplast-derived membrane or the vacuole is entrapped during the encasement of the haustorium. The subcellular localisation screen also led to the

further characterisation of HaRxL79, which has a peculiar localisation to the cytoskeleton. In the next section, I will present results that I personally obtained while characterising further the function of this effector and that were not included in the collaborative work of Caillaud et al. (2011).

4.2.3. One interesting effector candidate, HaRxL79, associates with the plant microtubules

4.2.3.1. HaRxL79 co-localises with microtubules

In this section, I will present results on the characterisation of the plant cellular localisation of another HaRxL arising from the HaRxLs-EDV screen, called HaRxL79 (**Table 4.1**). In order to examine the subcellular localisation of HaRxL79, potentially giving clues on its function, *HaRxL79* was fused to a GFP reporter gene to create either N-terminal or C-terminal fusions. GFP-tagged HaRxL79 constructs were transiently expressed in *N. benthamiana* and analysed by confocal microscopy. Both N-terminal and C-terminal fusions showed the same particular pattern of, labelling dots on lines in the cells like it was filament-associated (**Figure 4.11**).

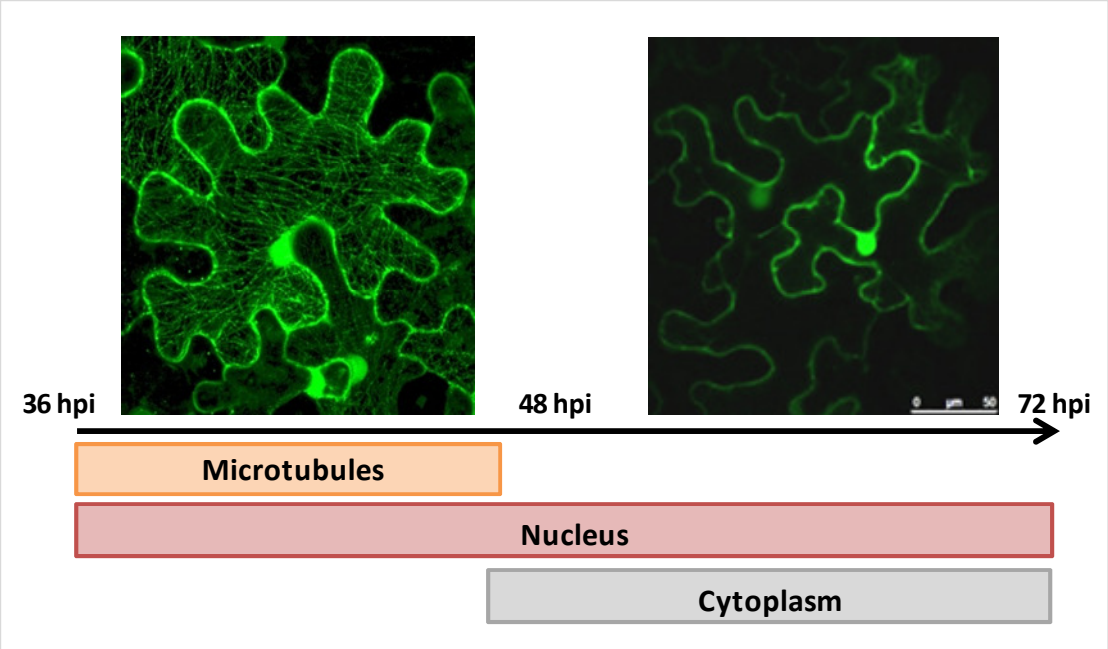

Figure 4.11. Spatio-temporal localisation of transiently expressed HaRxL79 *in planta*.
HaRxL79-GFP was transiently expressed in *N. benthamiana* and analysed by confocal microscopy. At 38 hours post infiltration, HaRxL79-GFP was observed in the nucleus and associated with dots on lines in the cells like it was filament-associated. After 42 hours post infiltration, HaRxL79-GFP no longer associated with the filaments (microtubules), but was nuclear-cytoplasmic. The left image is a maximum projection.

This putative association with intracellular filaments, which is very distinctive of components of the plant cytoskeleton, was transient, as it was only observed between 36 hours post inoculation (hpi) and 42 hpi (**Figure 4.11**). After 42 hpi, for both C- and N-terminal GFP tagged HaRxL79, the GFP signal was nuclear-cytoplasmic.

To examine further whether the subcellular localisation of GFP-tagged HaRxL79 was indeed linked to the plant microtubules, agro-infected *N. benthamiana* leaves were infiltrated with taxol, a drug affecting the dynamics of microtubules by blocking their polymerisation and depolymerisation processes (Caillaud et al. 2009). By using taxol known to directly target the microtubules, I aimed to visualise if the localisation or signal intensity of GFP-tagged HaRxL79 is affected too. If the association is real, we expect that the blocking of

microtubules dynamics after addition of taxol will cause the GFP signal of HaRxL79 to be clearer.

As seen on **Figure 4.12**, in the presence of 100 µM of taxol and within 15 minutes, GFP-tagged HaRxL79 seemed to stably localise to microtubules. This pattern looked very similar whether taxol was added or not, with the exception that the GFP signal was much more enhanced with the drug (**Figure 4.12**). This observation suggests that HaRxL79 can very likely and directly associate with microtubules (**Figure 4.12**). Notably, taxol allowed a brighter visualisation of GFP-HaRxL79 while associated with microtubules, which suggests that in normal conditions, the observed intensity of the association of HaRxL79 with microtubules is affected by the natural dynamics of assembly and stability of these filaments. It is worth mentioning that GFP-HaRxL79 showed aggregates in the cell while HaRxL79-GFP did not (**Figure 4.12**), suggesting that the N-terminal region of HaRxL79 could be important for folding and function, and that the addition of a GFP in this region potentially and to some extent disturbed the function of HaRxL79.

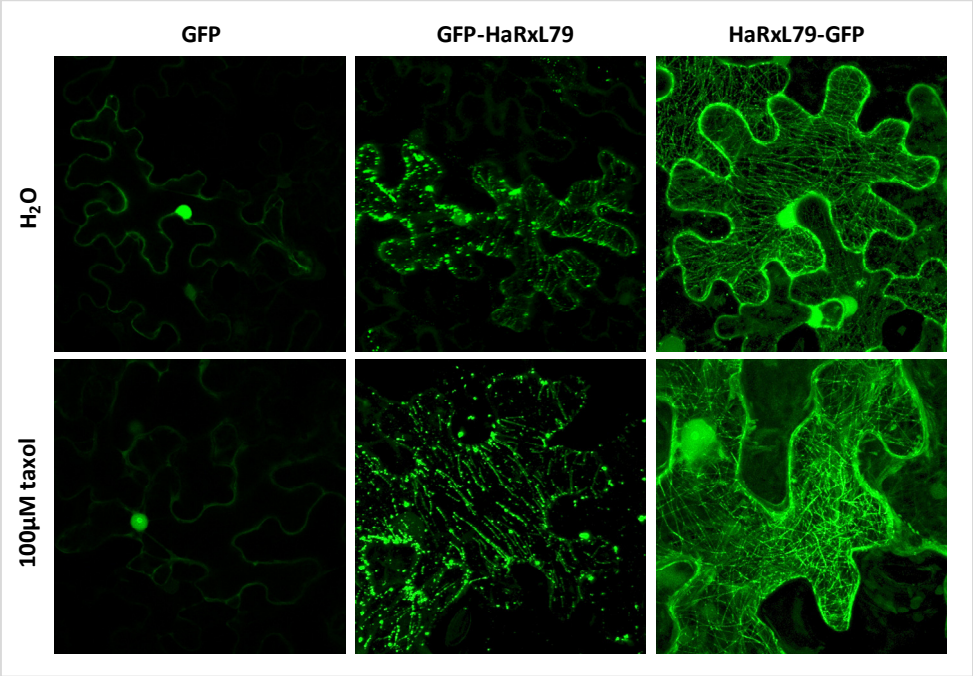

Figure 4.12. HaRxL79 associates to plant microtubules.
GFP-tagged HaRxL79 or GFP were transiently expressed in *N. benthamiana* and analysed by confocal microscopy. At 38 hours post infiltration, water or 100 µM taxol were infiltrated in the previously agro-infiltrated leaves. Images are maximal projections acquired 20 min after the taxol treatment.

In addition to being associated with microtubules, GFP-tagged HaRxL79 also localised to the nucleus in an infection time-dependent manner. To examine whether this localisation was biologically relevant and not a technical artefact, I extracted the total proteins from agro-infected *N. benthamiana* tissues and performed a western-blot analysis using anti-GFP antibodies, to detect the transiently expressed GFP-tagged HaRxL79 (**Figure 4.13**). For both constructs (GFP-HaRxL79 and HaRxL79-GFP), a larger band corresponding to the full length protein fusion was detected at 49 KDa, as well as smaller bands of 36 KDa for the N-terminal fusion, and 22 KDa for the C-terminal fusion (**Figure 4.13**). This observation interestingly suggests that GFP-tagged HaRxL79 is partially degraded *in planta* and that some of the nuclear-cytoplasmic GFP signal may result from the free diffusion of GFP-tagged degradation products.

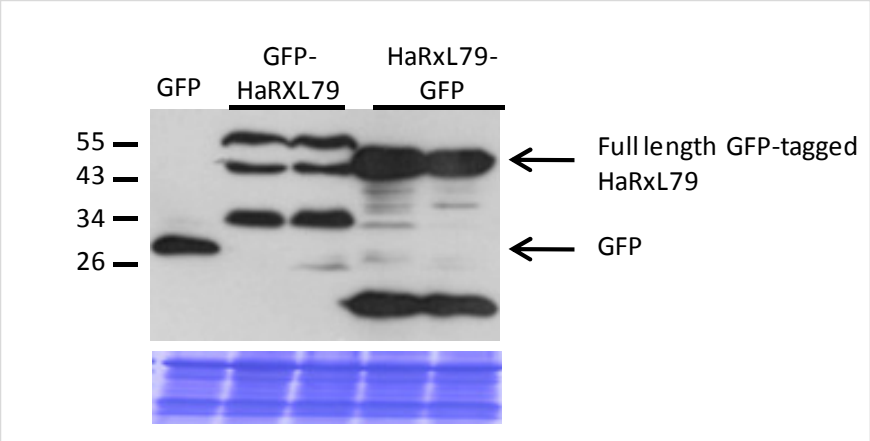

Figure 4.13. GFP-tagged HaRxL79 proteins are degraded *in planta*.
GFP-tagged HaRxL79 were expressed transiently in *N. benthamiana*. At 2 days post infiltration, leaf samples were taken and total proteins were extracted. The proteins were run by SDS-PAGE, transferred to a membrane which was immuno-blotted with anti-GFP antibody. The protein load is shown by Coomassie blue staining of the membrane in the bottom panel.

As an additional confirmation that the targets of HaRxL79 are indeed the plant microtubules, I performed co-localisation assays using a specific microtubule marker. I used the Microtubule-associated protein 4 (MAP4), a protein which was observed to have a structural role by associating with microtubules in various eukaryotes including humans and plants (Mathur and Chua 2000; Van Damme et al. 2004). By simultaneously expressing a RFP-MAP4 fusion and the previously used GFP-HaRxL79 fusion in *N.benthamiana* and stabilising microtubules with taxol, I observed clear co-localisation of GFP-HARxL79 and RFP-MAP4 (**Figure 4.14**), demonstrating convincingly that the *Hpa* RxLR effector candidate HaRxL79 is actively associating with plant microtubules when delivered into plant cells.

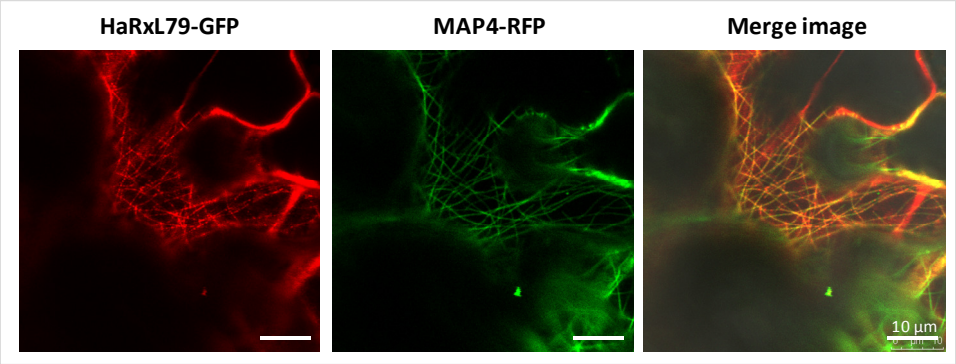

Figure 4.14. HaRxL79-GFP co-localises with the microtubule marker MAP4-RFP.
HaRxL79-GFP and MAP4-RFP were transiently co-expressed in *N. benthamiana* and analysed by confocal microscopy. At 38 hours post infiltration, 100 µM taxol were infiltrated in the previously agro-infiltrated leaves. Images are maximal projections acquired 20 min after the taxol treatment. HaRxL79-GFP and MAP4-RFP signal are shown in red and green respectively for practicality. The merge images were acquired using sequential mode.

Microtubules are key elements of plant development and architecture. Microtubules comprise filaments of tubulin which are believed to be extremely dynamic, as one microtubule end is polymerising while the other end is depolymerising. Cortical microtubules are responsible for the shape of the plant cells. Several plant proteins associate with cortical microtubules (including MAPs such as MAP4 used above) and control their dynamics and associative properties (Lloyd and Chan 2004). Additionally, kinesins are motor proteins moving along microtubule filaments, powered by the hydrolysis of ATP. Kinesins vary in shape but usually have a motor domain constituted of two heavy chains that dimerise and bind two light chains. In most cases transported cargos bind to the kinesin light chains, but in some cases cargo binds to the heavy chains for transport of molecules/vesicles along microtubules.

Later in this chapter, I will present results of further characterisation efforts on the interaction of HaRxL79 with microtubule-associated proteins. Before this, I will present in the next section, some results (that I obtained with Naveed Ishaque, a PhD student in our laboratory) which focussed on the discovery that this promising cytoskeleton-interacting

effector candidate is a member of a multigene family, of which the subcellular localisation is investigated.

4.2.3.2. HaRxL79 *belongs to a gene family specific to* Hpa (*in collaboration with Naveed Ishaque and Dr. Anastasia Gardiner*)

- **Identification of the *HaRxL79* gene family in *Hpa* Emoy2**

HaRxL79 is not present in the published version of the *Hpa* Emoy2 genome assembly (Baxter et al. 2010), but was predicted in earlier versions for which a different assembly method was used. This technical issue can be explained by the fact that *HaRxL79* belongs to a multigene family.

Paralogs and orthologs of genes are related by evolutionary divergence (duplication) from a common ancestral gene. Paralogs are defined within the same species, whereas orthologs are defined in between species. Generally, orthologs genes perform the same (or very similar) functions in different species, whereas paralogs perform the same or different functions within one species.

As *HaRxL79* paralogs carry a well conserved N-terminal sequence consisting of the first 200 base pairs (corresponding to ~30% of *HaRxL79* full length sequence), the current (and published) assembly method merged some of the paralogs together, resulting in a mis-assembly of *HaRxL79* and its paralogs. However, as shown in **Figure 4.15** (for the amino-acid sequences) or in **Appendix 4.2** (for the nucleotide sequences alignments), the C-terminal regions of the different paralogs seems to have functionally diverged as they are quite variable.

Seven paralogs were predicted in earlier versions of the *Hpa* Emoy2 genome and identified to be in a family: *HaRxL30*, *HaRxL39*, *HaRxL40*, *HaRxL41*, *HaRxL42*, *HaRxL47*, *HaRxL79* and *HaRxLL73* (highlighted in purple in **Table 4.1**).

The members of the *HaRxL79* gene family were identified using the Markov cluster (MCL) algorithm implemented with the TribeMCL program (Enright et al. 2002). MCL clustering was performed for all predicted effectors of *Hpa* (list from Jamboree 2010 presented in **Appendix 4.1**), consequently allowing us to distinguish the *HaRxL79* gene family with eight members.

As a complement to the bioinformatics analyses and in order to check whether all *Hpa* Emoy2 *HaRxL79* paralogs were indeed expressed during infection, I performed a 3' RACE PCR experiment using cDNA generated from *Hpa*-infected tissues over a time course of infection. After analysing the clones obtained from the 3' RACE PCR, I confirmed that five paralogs (*HaRxL39, HaRxL41, HaRxL42, HaRxL47* and *HaRxL79*) are expressed during infection. The other paralogs (*HaRxL30, HaRxL40, HaRxL47, HaRxLL73*) were not found to be expressed during infection in this experiment, which may be explained by the fact that only cDNAs from a single time course of infection (i.e., one single "replicate") were used in this preliminary experiment, and that only 60 clones were sequenced. It may be that because of the expression levels, these paralogs were missed using these experimental conditions.

A

```
HaRxL30         MTKCSLLLVPFLVAIAVSDALPARAAGTLPQSATSVQDKATESTVSGKRALQSKEDTKGA
HaRxL79         MTKCSLLLVPFLVAIAVSDALPARVAGTLPQSATSVQDKATESTVSGKRALRSKKDTKGA
HaRxL39         MTKCSLLLVPFLVAIAVSDALPARAAGTLPQSATSVQDKATESTVSGKRALQSKEDTKGA
HaRxL47         MTKCSLLLVPFLVAIAVSDALPARAAGTLPQSATSVQDKATESTVSGKRALQSKEDTKGA
HaRxL40         MTKCSLLLVPFLVAIAVSDALPARAAGTLPQSATSVQDKATESTVSGKRALQSKEDTKGA
HaRxL41         MTKCSLLLVPFLVAIAVSDALPARAAGTLPQSATSVQDKATESTVSGKRALQSKEGTKGA
HaRxL42         MTKCSLLLVPFLVAIAVSDALPARAAGTLPQSATSVQDKATESTVSGKRALQSKEDTKGA
HaRxLL73        MTKCSLLLVPFLVAIAVSDALPARAAGTLPQSATSVQDKATESTVSGKRALQSKEDTKGA
                ************************.**************************:**:.****

HaRxL30         ADEERAL-ISPSRLEPLSTKMKSSTDWMAQTRKGASFGVSRMRQKELVESKDAVVRLE--
HaRxL79         ADEERAL-LSPSILEPLSTKMKSSTDWMAQTRKGASFSVSGVSQKELGESKDVVVRLE--
HaRxL39         ADEERAPNWLQSVPEWLSTMMKKTTNWTARTWKGTAFSMSRVPPKDMVEAKAVLTEMEIV
HaRxL47         ADEERALNRLQSVPEWLSTMTKSITNWTARTWS----------------------------
HaRxL40         ADEERALNWLQSVPERLSTMIKSITNWTARTWS----------------------------
HaRxL41         ADEERALKWLQSVPEWLSTMIKSITNWTTRTWS----------------------------
HaRxL42         ADEERALNRLQSVPEWLSTMTKSITNWTARTWS----------------------------
HaRxLL73        ADEERALNWLQSVPEWLSTMMKKTTDWMARTWKGASFSVSGVSQKEASFSASGVSQKEAS
                ******     *  * ***  *. *:* ::* .

HaRxL30         --------------------------------NLQRNFQKSTERMIIEMARDLTFSGATRK
HaRxL79         --------------------------------NLQRDFQKSTEQMTIDMARDLTFSGATRK
HaRxL39         RHHRSMGYRFLLFLKAAWEAAWEAAWKAA-----SKAS----ELTSVLRRRQSH---RPN
HaRxL47         ----------------------------KAA-----SKAS----ELTRVLLRHQSQ---RRH
HaRxL40         ----------------------------KAA---------LKKKIILAALRTPTPKARRKDK
HaRxL41         ----------------------------KAA-----SKAALKKNNFLMALYKPDPD---REE
HaRxL42         ----------------------------KAA-----SKVALIKKNFFMELE--------RRE
HaRxLL73        VSASGVSQKEASVSASGVSQEDLEDAKAVVVNLQSKLEKANERLTTATRDRQYW---KEN
                                                           :               .

HaRxL30         -------VGRREITWLPL---NRVLQNRKDRELLETMSKRDAYAA-----------KLEE
HaRxL79         -------VG-RGITWLPL---NRVLQDRKYREWLETMSKRDAYAA-----------KLEE
HaRxL39         ----------------------LRKLHEEIYQIW-LAAFESAFTVKELKKEVDKLHKKVMD
HaRxL47         ----------------------LRKMREEFDQAWPVLTFETSVELKVLKKSIGEINEKLMD
HaRxL40         ---------------------MQKLHE------------RKVEDH-RKREES----ELAK
HaRxL41         ---------------------MRMWFK------------KKVEAHDRKQEES----ELVK
HaRxL42         ---------------------ERKLDK-----------------------------RRFED
HaRxLL73        DQNMNWKAAGWGIYRLHLQLKWRLMQKEMYRELRKDMREAKATAAKLAKPIAEAKKKVDD
                                    :   .                                .. .

HaRxL30         LIAAAKKKV----DDITAAI
HaRxL79         LIAAAKKRV----DGINPAI
HaRxL39         FSAAIEAKKVAPSDFVRPSE
HaRxL47         LIAVIEAKKVAPRDFVRPSE
HaRxL40         LVAEVEKR------------
HaRxL41         LVAEVEKR------------
HaRxL42         YLA-VNGKKL---------K
HaRxLL73        INAAIQARRNT------LSI
                  *  : :
```

B

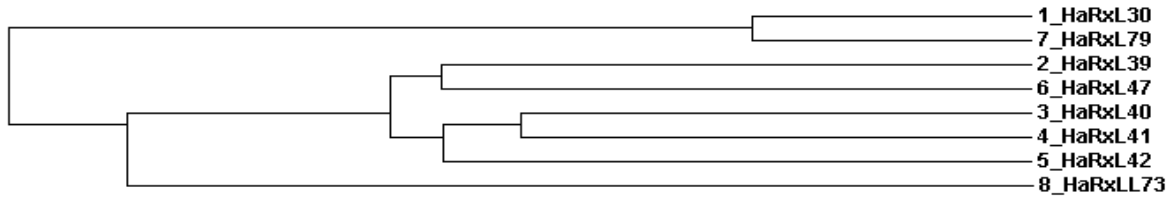

Figure 4.15. *HaRxL79* gene family in *Hpa* Emoy2
A, CLUSTAL format alignment by MAFFT G-INS-i (v6.850b) of *HaRxL79* paralogs in Emoy2. **B**, Cladogram built with the Neighbor Joining method based on the MAFFT sequence alignment described in A.

To determine whether the predicted *HaRxL79* paralogs confirmed by molecular biology also conserved the functional property of microtubules association, I picked two paralogs named, *HaRxL42* and *HaRxL47*, that were observed to cluster in different sub-groups after the MCL clustering, and checked their subcellular localisation *in planta* (**Figure 4.16**).

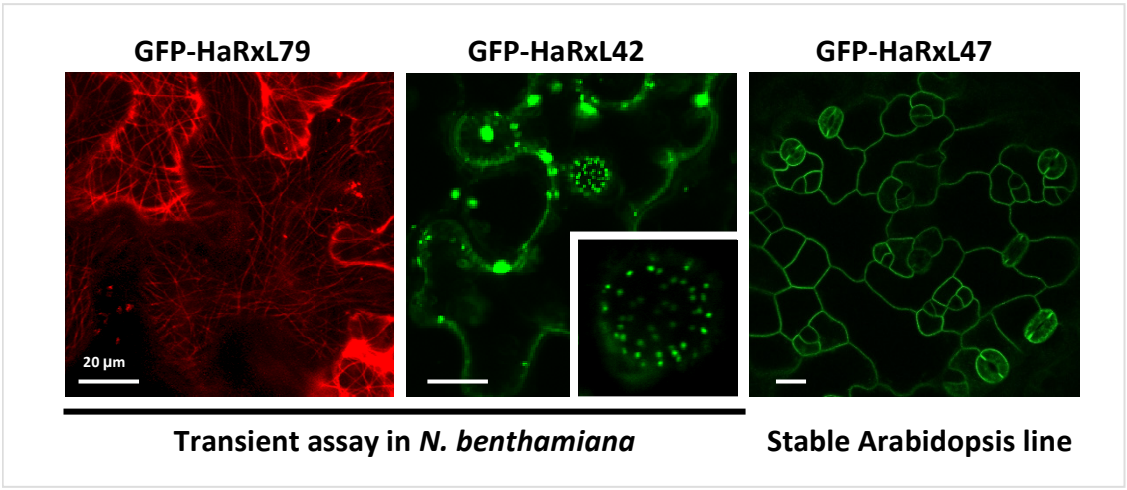

Figure 4.16. Two *Hpa* Emoy2 HaRxL79 paralogs, HaRxL42 and HaRxL47, localise to different plant subcellular compartments.
Transient expression in *N. benthamiana* or stable expression in Arabidopsis (as stated below the photographs) of GFP-HaRxL79, GFP-HaRxL42 and HaRxL47. GFP-HaRxL79 associates with microtubules. GFP-HaRxL42 localises to the nuclear periphery in addition to aggregates in the cytoplasm. GFP-HARxL47 localises to the plasma membrane.

Transient expression of GFP-HaRxL42 in *N. benthamiana* showed that GFP-HaRxL42 localised very specifically at the nuclear periphery (**Figure 4.16**), but also in apparent GFP aggregates. Additionally, the stable expression of GFP-HaRxL47 in Arabidopsis indicated that HaRxL47 localised at the plant plasma membrane (**Figure 4.16**). Thus, three paralogs, HaRxL42, HaRxL45 and HaRxL79 of the same gene family target very different subcellular compartments. This result demonstrated that the N-terminal region of the paralogs (which is more conserved among them than the rest of the protein) is probably not influencing their subcellular localisation specificities. In addition, it seems likely that these three paralogs,

although evolutionarily related, have evolved different functions as indicated by their different association to various plant subcellular compartments.

- ***HaRxL79* gene family is *Hpa*-specific**

In order to determine whether *HaRxL79* gene family is specific to *Hpa*, we searched genomes of other oomycete species for potential out-paralogs or paralogs of *HaRxL79* family genes. Searches were done using BlastP (e-value cut-off of 1×10^{-1}) and the protein sequences of *HaRxL79* family genes were used as queries against *P. infestans*, *P. ramorum* and *P. sojae* genomes. We obtained respectively 12, 6 and 20 hits. The hits encompassing the closest matches were from *P. sojae*; only one hit from *P. ramorum* had an e-value below the set cut-off, while all hits from *P. infestans* had e-values above the threshold of 1×10^{-1}.

We aligned protein sequences of the *HaRxL79* family genes including those found in *Phytophthora* genomes using the MAFFT software and constructed a Maximum Likelihood cladogram showing relationships between the sequences (**Figure 4.17**). The phylogenetic tree was built from an alignment of proteins sequences, but we conduct the interpretation at the gene level.

HaRxL79 family genes in *Hpa* Emoy2 clustered together and were observed to be distinct from *Phytophthora* proteins. Phylogenetic support, as indicated by the support numbers on the branches, was shown only for *Hpa HaRxL79* gene family and few isolated *Phytophthora* genes. If they were orthologs or out-paralogs of *HaRxL79* gene family in *Phytophthora*, they would have clustered with *Hpa HaRxL79* family genes. From this phylogeny analysis, we can conclude that *HaRxL79* gene family is *Hpa*-specific, and most likely evolved after *Hpa* and *Phytophthora* split (**Figure 4.17**).

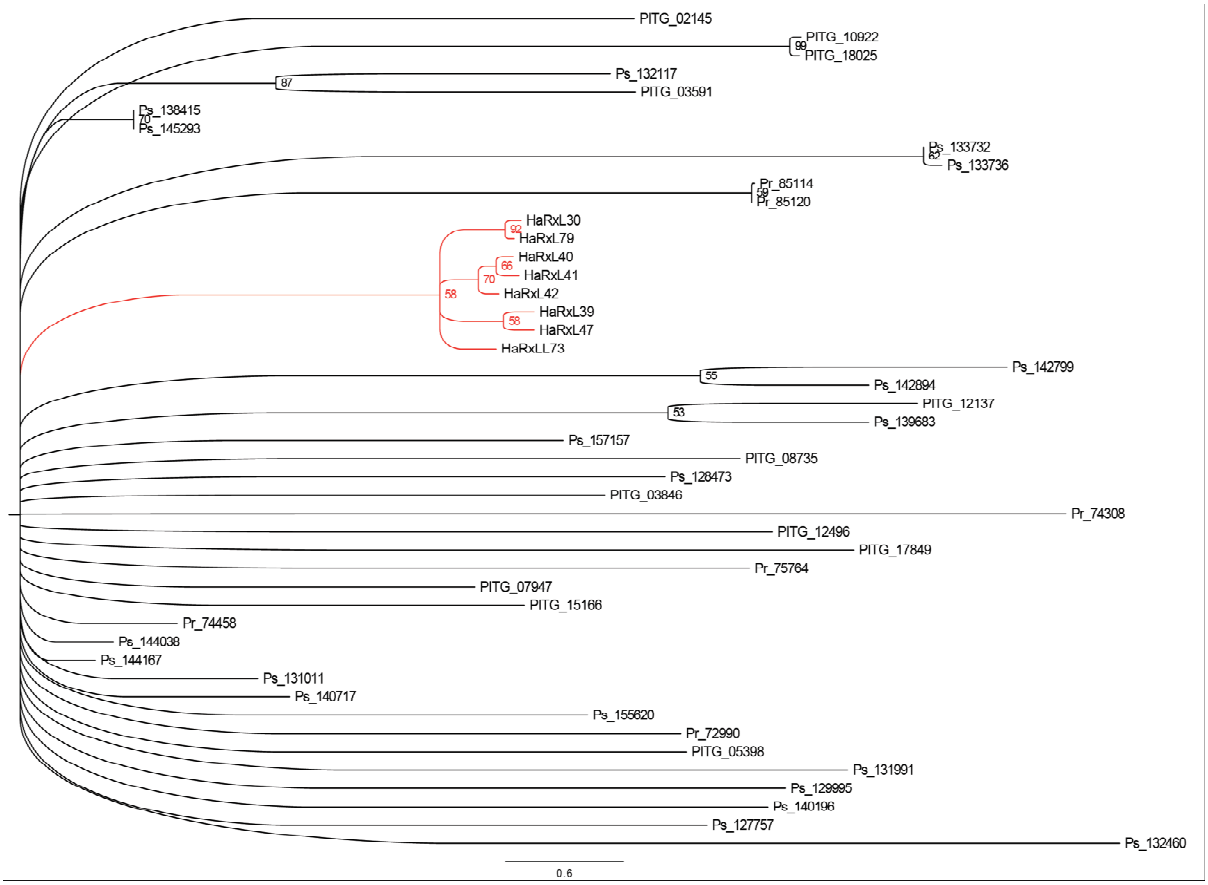

Figure 4.17. *HaRxL79* gene family is specific to *Hpa*.
Cladogram built with the Maximum Likelihood method based on a MAFFT protein sequence alignment done with *Hpa* Emoy2 HaRxL79 paralogs and *P. sojae*, *P. ramorum* and *P. infestans* BlastP hits. The MAFFT sequence alignment was performed using the default parameters. Ps: *P. sojae* genes. Pr: *P. ramorum* genes. PITG: *P. infestans* genes. HaRxL79 paralogs are highlighted in red. Numbers on the branches (>50) indicated phylogenetic support.

- **HaRxL79 multigene family in other *Hpa* isolates**

In order to know how diversified is the *HaRxL79* gene family across *Hpa* isolates, we performed comparative genomics in seven *Hpa* isolates (Cala2, Emco5, Emoy2, Hind2, Maks9, Noco2, Waco9).

In order to characterise the presence or absence of polymorphisms within the *HaRxL79* gene family, a new assembly had to be made, as there was no *Hpa* genome assembly with the sequences of all members of the family present. We chose to use the Mira software (v3.0.3) to do so (Chevreux et al. 1999) as it provides the interesting feature of preventing the merging of duplicated genomic regions by analysing coverage, hypothetically making it ideal for assembling complex gene families such as the *HaRxL79* gene family. The assembly protocol was followed using the default parameters (with the addition of the 'highly repetitive' flag to prevent merging of duplicate regions), using the Sanger sequencing reads and BAC sequences available for *Hpa* Emoy2 (Baxter et al. 2010).

The previously identified sequences for the *HaRxL79* gene family sequences (presented above in this section) were aligned to the resulting genome assembly and the co-ordinates of the genes were recorded. We then aligned the sequencing reads for each *Hpa* isolate (**Appendix 4.4**) using MAQ (v0.7.1; Li et al. 2008) (and mapping parameters allowing for 3 mismatches in the 24 bp seed, and a maximum sum of qualities of mismatching bases to 100). The homologous regions corresponding to each member of the *HaRxL79* gene family were defined. For each gene, the percentage of the gene length covered by sequencing reads of the different *Hpa* isolates was calculated (**Table 4.3**). As a basis for result interpretation, we assumed that a gene with 100% of its nucleotides covered by sequencing reads was indeed

present in the corresponding *Hpa* isolate. If a gene was covered between 90% and 100% of its total sequence, we postulated that the gene may be present with minor differences. Finally, any gene with less than 90% of its sequence covered by reads was conservatively assumed too divergent to make any interpretation, as such a low coverage makes it difficult to say whether the gene is being lost (i.e., in an evolutionary process of "pseudogenisation") or if it present but has significantly mutated.

	Emoy2	Noco2	Waco9	Emco5	Hind2	Maks9	Cala2
HaRxL79	100	82.5	73.5	78.3	95.3	69.2	100
HaRxL30	100	100	64.5	100	96	59.2	59.5
HaRxL42	100	100	100	100	100	100	100
HaRxL39	100	100	100	100	100	100	100
HaRxL47	100	100	100	100	100	100	56.3
HaRxL40	100	100	100	81.5	85.8	70.5	100
HaRxL41	100	100	100	87.6	87.1	87.6	84

Table 4.3. Percentage of coverage for each paralogs in *HaRxL79* gene family in each *Hpa* isolate (compared to Emoy2).
Mira (v3.0.3) assemblies were generated for Emoy2 *HaRxL79* family genes in the different *Hpa* isolates. MAQ was used to align the reads to Emoy2 assembly. Percentage of coverage was calculated for each paralogs in comparison to Emoy2. A colour gradient was used to highlight high coverage percentage (green) to low coverage percentage (yellow).

Only two paralogs, *HaRxL39* and *HaRxL42*, were observed to be conserved in all *Hpa* isolates tested (**Table 4.3**). Interestingly, *HaRxL79* appeared the most divergent gene of the family. *HaRxL79* was conserved in Emoy2 and Cala2 only, appeared slightly divergent in Hind2 but appeared very divergent in the four other *Hpa* isolates (**Table 4.3**). *HaRxL30*, the closest homolog of *HaRxL79* in the gene family, was also quite divergent, conserved in only three out of seven *Hpa* isolates. From this analysis we can conclude that HaRxL79 gene family is a rapidly evolving gene family, on which it would be quite interesting to understand the different ecological and selective pressures involved.

It is currently not possible to fully assemble the genes in the *HaRxL79* family for any of the *Hpa* isolates using Illumina sequencing because the read length is too short and even current short read assemblers are unable to assemble gene families with high nucleotide homology well. Therefore, in order to determine the diversity of the *HaRxL79* gene family across *Hpa* isolates, I amplified *HaRxL79* family genes form six *Hpa* isolates (Emoy2, Emwa1, Emco5, Hind2, Maks9 and Waco9) by PCR using primer sets designed to amplify *HaRxL79* family genes in Emoy2. The PCR profiles are shown in **Figure 4.18**. These PCR profiles cannot inform on the sequence similarity of the different *HaRxL79* family genes, but it shows at least size differences.

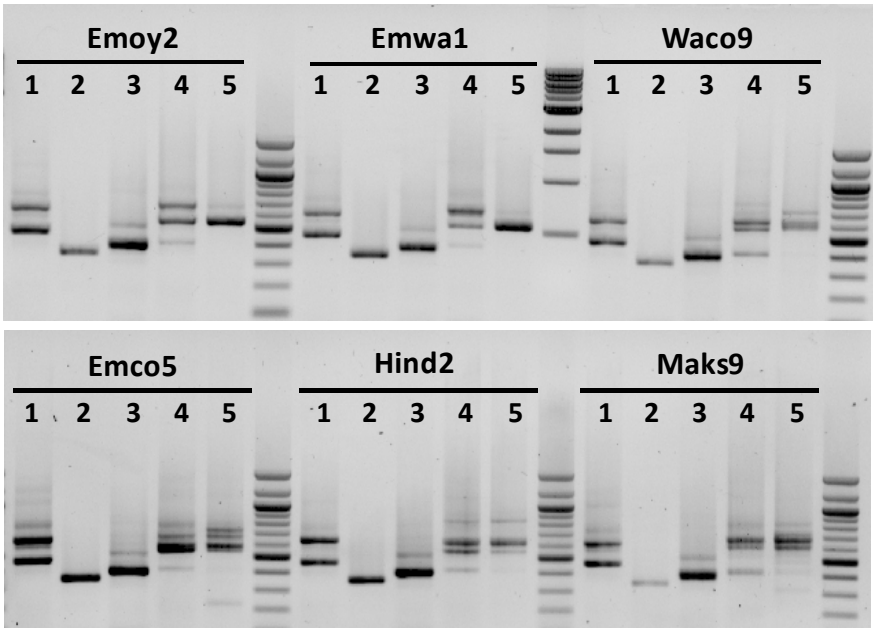

Figure 4.18. Agarose gels showing the PCR profiles obtained for HaRxL79 gene family in *Hpa* isolates.
Hpa isolates are indicated on top of the agarose gel pictures. Molecular weight markers separated PCR profiles of different *Hpa* isolates. Primer sets are different for each lane and were used to amplify different HaRxL79 family genes from genomic DNA as indicated: lane1 for *HaRxL39* and *HaRxL47*, lane 2 for *HaRxL42*, lane 3 for *HaRxL40* and *HaRxL41*, lane 4 for *HaRxL30* and *HaRxLL73*, lane 5 for *HaRxL79*.

Despite that not exactly the same *Hpa* isolates were tested in **Table 4.3** as in **Figure 4.18**, *HaRxL39* and *HaRxL42* and *HaRxL47* still showed a single-band PCR product, correlating well with the sequence coverage data. *HaRxL40* and *HaRxL41* are predicted to be really divergent between *Hpa* isolates (**Table 4.3**), but this is not visible by different PCR product sizes (**Figure 4.18**). Expectedly, *HaRxL30* and *HaRxL79* PCR profiles showed a lot of different size PCR products (**Figure 4.18**) as they were predicted to be quite divergent (**Table 4.3**)

PCR profiles were presented in this section instead of the actual sequences of all the paralogs, because at the time of the thesis submission, not all the sequences were obtained. These sequences need to be obtained to build a solid evolutionary history for the HaRxL79 gene family.

As presented above, we identified an effector family in *Hpa* (*HaRxL79* gene family), comprising at least eight members, which is very interestingly specific to *Hpa*, as it could not be identified in three *Phytophthora* species. This gene family seems to contain members with different functions, as illustrated by the different subcellular localisations observed for three members. The analysis of the *HaRxL79* effector gene family is an exciting opportunity to study the evolution of *Hpa* effectors that may be involved in the biotrophy.

4.2.3.3. HaRxL79 phenotype in Arabidopsis

- **HaRxL79 does not affect bacterial growth when delivered by EDV system**

HaRxL79 was defined as a promising effector candidate because of its unique subcellular localisation and its phenotype *in planta*. Fabro et al. (2011) showed that HaRxL79-EDV conferred decreased susceptibility to *Pst*-LUX in seven Arabidopsis accessions, increased susceptibility in two accessions and no differential bacterial growth in three accessions (**Table 4.4**). Interestingly in turnip and tomato also, HaRxL79-EDV conferred reduced bacterial growth to *Pst*-LUX (**Table 4.4**).

Bay-0	Br-0	Col-0	Ksk-1	Ler-0	Nd-0	Oy-0	Sha	Ts-1	Tsu-1	Wei-0	Ws-0	turnip	tomato
(-)	(-)	(-)	(=)	(-)	(=)	(-)	(-)	(=)	(-)	(+)	(+)	(-)	(-)

Table 4.4. *Pst*-LUX HaRxL79-EDV virulence *in planta* (modified from Fabro et al. 2011).
HaRxL79-EDV conferred either enhanced bacterial growth (+) highlighted in yellow, no differential bacterial growth (=) highlighted in grey or decreased bacterial growth (-) highlighted in red. *Pst*-LUX HaRxL79-EDV growth was measured on 12 Arabidopsis accessions, on turnip (*Brassica rapa* cv. Just Right), and on tomato (cv. Moneymaker).

By measuring bacterial titres, I confirmed that HaRxL79-EDV impairs *Pst*-LUX growth in turnip and in tomato (**Figure 4.19, Figure 4.20**). Interestingly, I observed that *Pst*-LUX HaRxL79-EDV growth was delayed compared to the control *Pst*-LUX AvrRPS4-AAAA-EDV. However, at 3 dpi *Pst*-LUX HaRxL79-EDV reached *Pst*-LUX control titres (**Figure 4.20**). Despite almost the same bacterial counts reached at 3 dpi, disease symptoms were much weaker in *Pst*-LUX HaRxL79-EDV infiltrated areas compared to *Pst*-LUX AvrRPS4-AAAA-EDV. In turnip it was even not possible to measure the *Pst*-LUX HaRxL79-EDV bacterial growth at 4 dpi because the samples were too diseased (**Figure 4.19**). This observation suggests that HaRxL79 impairs the early growth of *Pst*, as if HaRxL79 prevented the establishment of the infection.

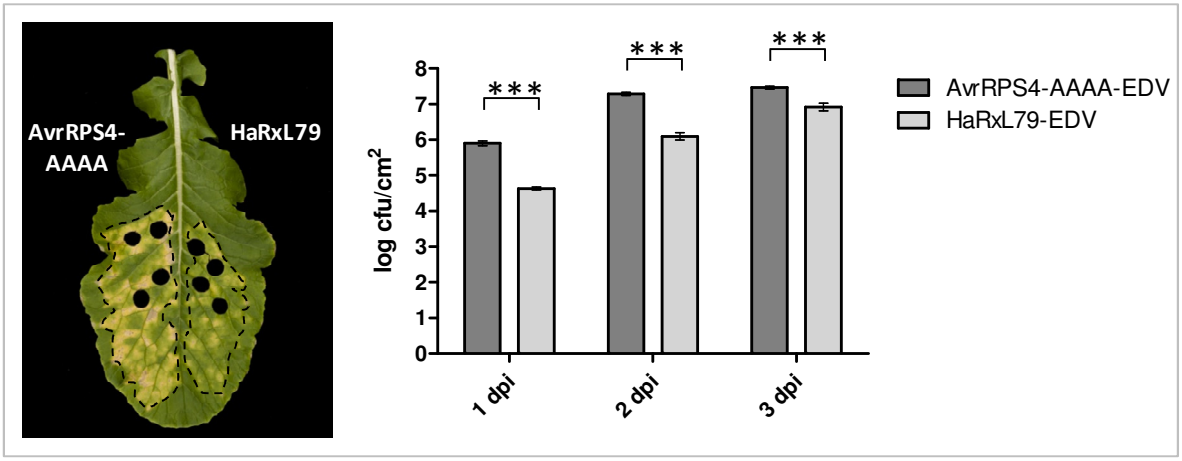

Figure 4.19. *Pst*-LUX HaRxL79-EDV growth in turnip.
Three-week old turnip (cv. Just Right) half leaves were hand-inoculated with 5×10^5 cfu/mL *Pst*-LUX AvrRPS4-AAAA-EDV (control) or *Pst*-LUX HaRxL79-EDV. Disease symptoms were scored at 4 days post infiltration. Bacterial titres were measured between 1 and 3 days post infiltration (dpi). Each bar represents the mean number of bacterial colonies recovered on selective agar medium containing appropriate antibiotics from six independent replicates; error bars represent the standard error of the mean. This experiment was repeated twice with similar results. Asterisks indicate significant differences as indicated by a Bonferroni post-hoc comparison test performed after a two-way ANOVA on the whole dataset, with three asterisks: $p<0.0001$.

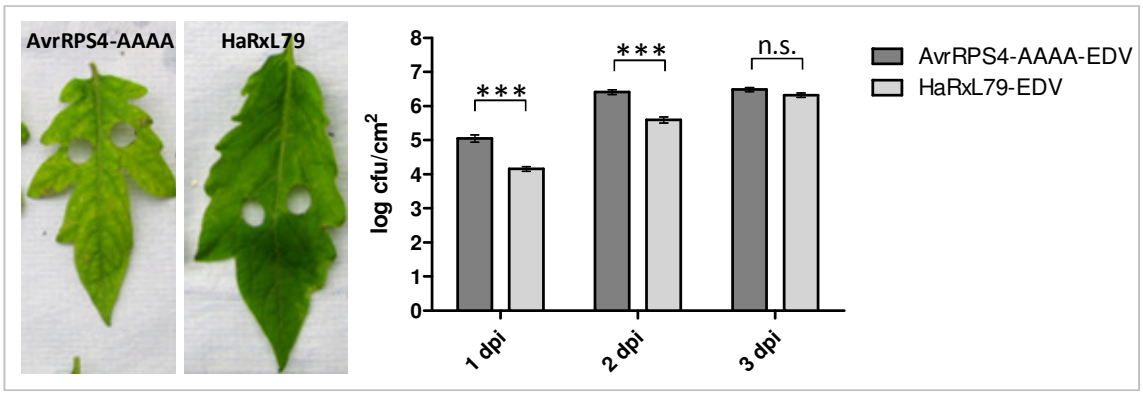

Figure 4.20. *Pst*-LUX HaRxL79-EDV growth in tomato.
Three-week old tomato (cv. Moneymaker) plants were vaccuum-infiltrated with 5×10^4 cfu/mL *Pst*-LUX AvrRPS4-AAAA-EDV (control) or *Pst*-LUX HaRxL79-EDV. Disease symptoms were scored at 3 days post infiltration. Bacterial titres were measured between 1 and 3 days post infiltration (dpi). Each bar represents the mean number of bacterial colonies recovered on selective agar medium containing appropriate antibiotics from six independent replicates; error bars represent the standard error of the mean. This experiment was repeated twice with similar results. Asterisks indicate significant differences as indicated by a Bonferroni post-hoc comparison test performed after a two-way ANOVA on the whole dataset, with three asterisks: $p<0.0001$, n.s. non significant.

It would be necessary to test whether HaRxL79 impairs *Pst* growth in liquid culture in order to discriminate if the early growth impairment is caused by the plant or if it is caused by a toxicity effect of HaRxL79. However in Arabidopsis, HaRxL79-EDV did not impair *Pst*-LUX growth compared to the growth of the control strain (data not shown) when bacteria were infiltrated. Because Fabro et al. (2011) did the screen by spraying *Pst*-LUX HaRxL-EDV, and it is known that a Col-0 *fls2* mutant is more susceptible to *Pst* DC3000 if the bacteria solution is sprayed but not if it is infiltrated (Zipfel et al. 2004), Arabidopsis accessions Col-0, Ws-0, Ler-0 and Ws-eds1-1 were tested for susceptibility to sprayed *Pst*-LUX HaRxL79-EDV (**Figure 4.21**). Basically, in Col-0, Ws-0 and in the hyper-susceptible mutant Ws-*eds1-1*, *Pst*-LUX HaRxL79-EDV growth was not different from the growth of the control *Pst*-LUX AvrRPS4-AAAA-EDV (**Figure 4.21**). But from Fabro et al. (2011), I expected HaRxL79-EDV to enhance *Pst*-LUX growth in Ws-0 and to reduce *Pst*-LUX growth in Col-0 compared to the control. In Ler-0, results were not conclusive given that in one replicate HaRxL79-EDV conferred significant reduced *Pst*-LUX growth in comparison with the control (as shown in **Figure 4.21**). But, in a second replicate, this difference was not significant.

Overall, I could not confirm that HaRxL79-EDV had a particular effect on *Pst*-LUX growth in Col-0, Ws-0 and Ler-0. This results points out that it is crucial to validate large-scale screens in normal scale experiments.

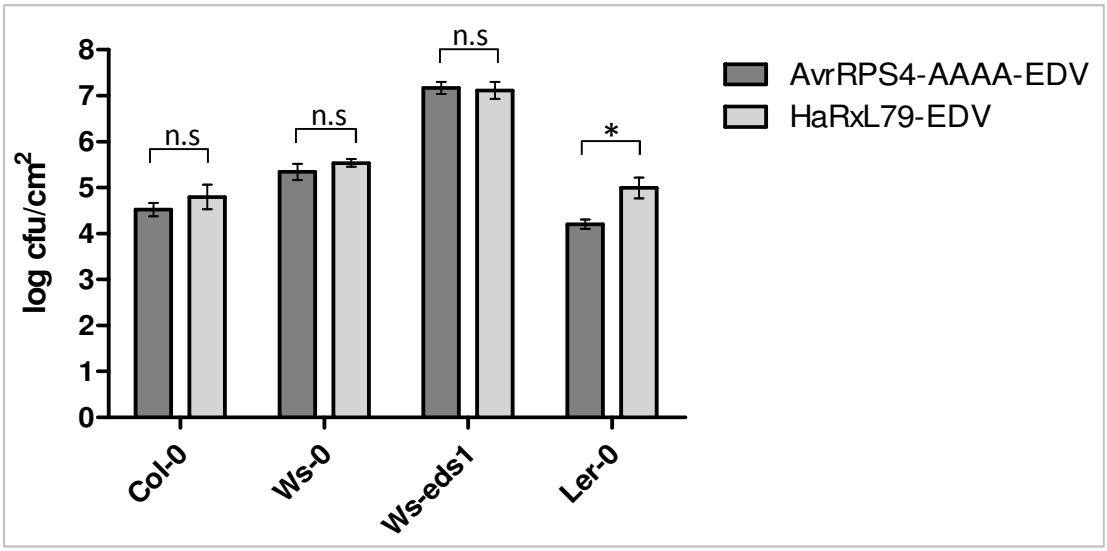

Figure 4.21. *Pst*-LUX HaRxL79-EDV growth in Arabidopsis.
Five-week old Arabidopsis plants (Col-0, Ler-0, Ws-0 and Ws-eds1-1) were sprayed with 5×10^7 cfu/mL *Pst*-LUX AvrRPS4-AAAA-EDV (control) or *Pst*-LUX HaRxL79-EDV. Bacterial titres were measured at 3 days post infiltration. Each bar represents the mean number of bacterial colonies recovered on selective agar medium containing appropriate antibiotics from six independent replicates. This experiment was repeated twice with similar results. Asterisks indicate significant differences as indicated by a Bonferroni post-hoc comparison test performed after a two-way ANOVA on the whole dataset, with one asterisk: $p<0.05$. n.s. non significant.

- **HaRxL79 is able to suppress PTI when transiently expressed *in planta***

Several pathogenic effectors target specific defense components to promote susceptibility. For instance, the *Hpa* effector ATR13 has been shown to suppress the ROS burst and the callose deposition induced in response to the perception of flagellin (Sohn et al. 2007). To understand the role of HaRxL79 during *Hpa* infection, and particularly to test whether HaRxL79 has a role in defence suppression, I tested if HaRxL79 could suppress PTI responses. To induce PTI responses, I used two PAMPs, the flg22 peptide and chitin, known to induce quantifiable ROS and calcium bursts (Segonzac et al. 2011). GFP-tagged HaRxL79 constructs were transiently expressed in *N. benthamiana* for 24 to 32 hours, samples were taken for the assays, floated on water for 8 to 12 hours, and subsequently treated with PAMPs. GFP-tagged HaRxL79 dampened flg22 and chitin-triggered ROS burst compared to

GFP alone (**Figure 4.22A, B**). In addition, GFP-tagged HaRxL79 also seemed to slightly dampen flg22 and chitin-triggered calcium burst (**Figure 4.22C, D**).

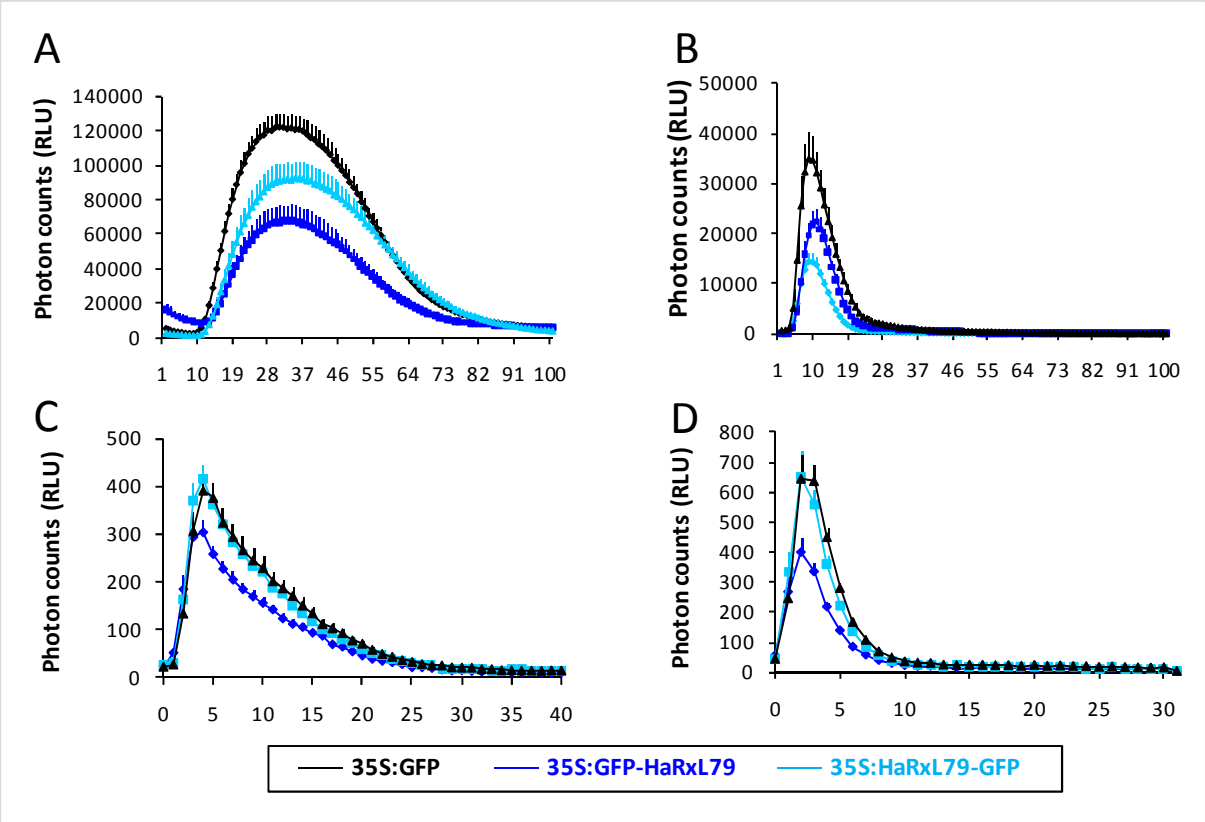

Figure 4.22. Transiently expressed HaRxL79 supresses PTI responses in *N. benthamiana*.
GFP-tagged HaRxL79 and GFP constructs were transiently expressed in *N. benthamiana* leaves and subsequently treated with PAMPs to measure the induced ROS and calcium bursts over time. ROS burst triggered by 100nM flg22 (**A**) or 1mg/mL chitin (**B**). Calcium burst triggered by 100nM flg22 (**C**) or 1mg/mL chitin (**D**). All measurements are in relative light units (RLU). Each bar represents the mean number of photon counts measured from 24 samples. The ROS experiments were repeated three times with similar results. The calcium experiments were repeated twice with similar results.

In order to avoid the use of heterologous systems, like *A. tumefaciens* or *Pst* delivery, I generated Arabidopsis Col-0 transgenic plants expressing constitutively (35S promoter) GFP-HaRxL79. As shown in **Figure 4.23A**, GFP-HaRxL79 lines produced the full length fusion protein (~50 KDa), but showed several degradation products, as previously observed in *N.*

benthamiana. Unfortunately, in GFP-HaRxL79 lines, the flg22-induced ROS burst suppression was not reproduced (**Figure 4.23B**). This suggest that either HaRxL79 cannot dampen the flg22-induced ROS burst in Arabidopsis because it is degraded, but as it is also degraded in *N. benthamiana*, it is more likely that the constitutive expression of HaRxL79 has a negative effect. Therefore, stable transgenic lines expressing HaRxL79 upon induction would be a better choice for experimentation.

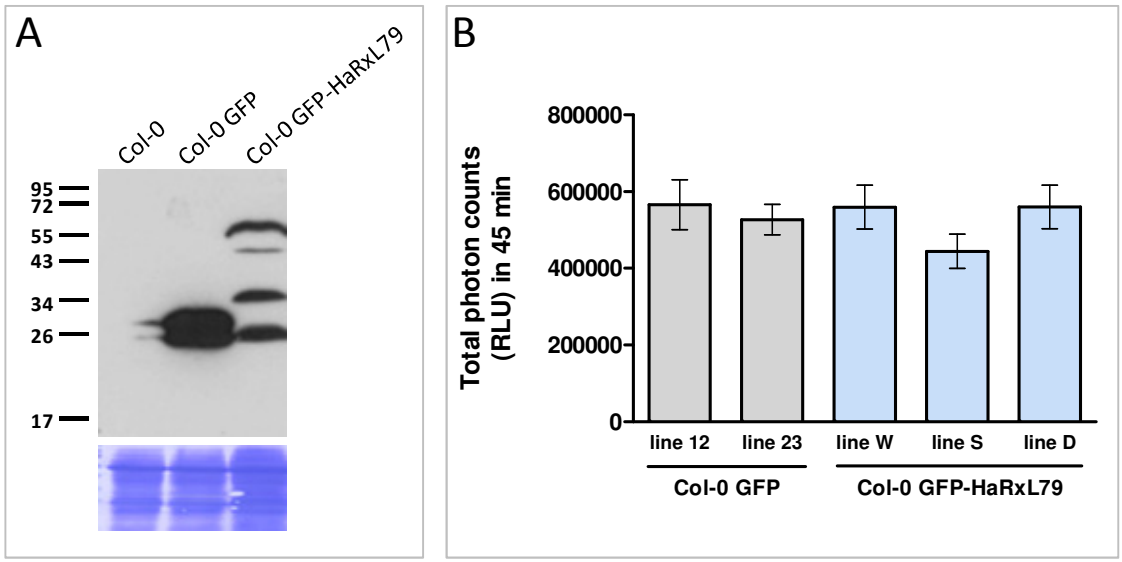

Figure 4.23. Col-0 GFP-HaRxL79 transgenic lines
A, Protein extracts from Col-0, Col-0 GFP and Col-0 GFP-HaRxL79 were immunoblotted against anti-GFP antibody. No GFP detected in wild-type Col-0 as expected. GFP is detected at 27KDa (according to protein marker on the left side). GFP-HaRxL79 and its degradation products are detected. Coomassie blue stained membrane in the bottom panel. **B**, Total photon counts generated by a flg22-induced ROS burst in Col-0 GFP and Col-0 GFP-HaRxL79 lines. All measurements are in relative light units (RLU). Each bar represents the mean number of total photon counts measured from 12 samples. The experiment was repeated twice with similar results. Statistical analysis: Bonferroni post-hoc comparison test performed after a one-way ANOVA on the whole dataset.

HaRxL79 subcellular localisation was checked in Col-0 GFP-HaRXL79 lines using confocal microscopy. GFP-HaRxL79 was nuclear-cytoplasmic, and no microtubule-association pattern was observed like in *N. benthamiana* (**Figure 4.24**). This result was partially expected because of the constitutive overexpression of GFP-HaRxL79 which would

not allow observation of a transient association with the microtubules. An inducible system would be better for such localisation assays, even though it would not stop the protein degradation when its expression is induced, but like in *N. benthamiana*, it might permit observation of a transient microtubule-association if it occurs after induction. In Col-0 GFP-HaRxL79 lines infected with *Hpa*, no relocalisation of HaRxL79 was observed. As in the control line expressing GFP, the nuclear-cytoplasmic signal was surrounding haustoria (**Figure 4.24**).

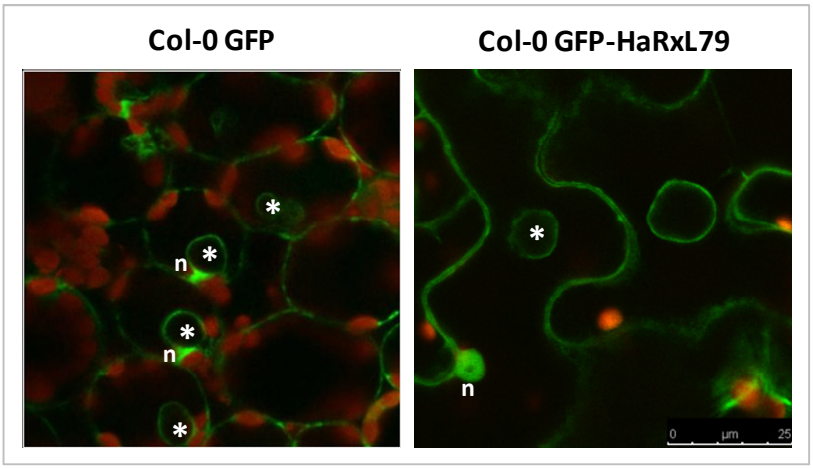

Figure 4.24. GFP-HaRxL79 is nuclear cytoplasmic in *Hpa*-infected Col-0 transgenic lines.
Col-0 GFP or Col-0 GFP-HaRxL79 lines were infected with *Hpa* Waco9. Five days after infection, GFP or GFP-HaRxL79 fluorescence was analysed by confocal microscopy. Asterisks highlight haustoria. n, plant nucleus.

Despite the partial degradation of GFP-HaRxL79 protein in the stable lines, these lines were used to test susceptibility to *Hpa* as little full length protein fusion may still have an effect on *Hpa* growth. Unfortunately, *Hpa* infection assays were not reproducible from one experiment to another, so no conclusion could be drawn. But it is worth mentioning that no strong effect was observed on *Hpa* sporulation.

Despite being a promising effector to study as it seemed to be recognised in several Arabidopsis accessions, HaRxL79 did not show any strong phenotype that confirms that it is a key effector in Arabidopsis defence suppression. One of the phenotypes observed in *N. benthamiana* was the ROS burst suppression, but was not reproduced in Arabidopsis. The strongest phenotype observed was the reduced early bacterial growth in tomato and turnip, two non host plants for *Hpa*. To be in a position to decipher HaRxL79 role in manipulation of the host defence responses, other tools need to be generated. For instance, inducible HaRxL79 lines should help assess HaRxL79 function, assuming that either HaRxL79 degradation or toxicity is problematic. It may also be useful to generate transgenic HaRxL79 lines in other accessions, in case HaRxL79 has a particular negative effect, for instance in the Ws-0 background. Another option to keep in mind is that there is maybe no phenotype to identify with our set of laboratory assays. Therefore another approach considered to understand HaRxL79 function *in planta*, was to look for its plant targets, which will be described in the next section.

4.2.3.4. Identification of putative plant targets from a large-scale yeast-two-hybrid assay done by collaborators (Mukhtar et al. 2011)

The identification of HaRxLs plant targets could help us understand the mode of action of these effectors by narrowing-down the plant processes they are involved in. As referred to several times in this thesis already, Mukhtar et al. (2011) tested by a large-scale Y2H experiment HaRxLs against a library of ~8000 full length Arabidopsis cDNA clones that were also used in the Arabidopsis "Interactome" project (Arabidopsis Interactome Mapping 2011). This approach had the great advantage that any interactors identified in the library (PPIN1, http://signal.salk.edu/interactome/) will also have been tested for their interactions with other plant proteins (AI-1) in the library.

Plant interactor		Function
At4g39050	MKRP2	predicted microtubule association
At3g27960	kinesin light chain-related (KLC)	predicted microtubule association
At4g26110	Nap1;1	histone chaperone
At5g56950	Nap1;2	histone chaperone

Table 4.5. List of HaRxL79 plant interactors as identified in Mukhtar et al. (2011).

Four plant interactors were identified for HaRxL79, two predicted microtubule-associated proteins, MKRP2 and a kinesin light chain-related, and two histone chaperones, Nap1;1 and Nap1;2. The corresponding AGI numbers are indicated.

HaRxL79 was tested in this Y2H assay, and four Arabidopsis targets were identified for HaRxL79 (**Table 4.5**) (Mukhtar et al. 2011): two microtubule-associated proteins, MKRP2 (mitochondria-targeted kinesin-related protein - At4g39050) and KLC (kinesin light chain-related - At3g27960), and two nucleosome-assembly proteins, AtNap1;1 (At4g26110) and AtNap1;2 (At5g56950).

In order to focus on the best HaRxL79 plant interactors, I first analysed several criteria to rank the putative plants target to help me prioritise them (**Table 4.6**). I first checked if any function was reported for the plant targets using TAIR database and then if the plant target was interacting with one or more effector candidates, in order to remove putative sticky proteins that might interact with all the effectors of the screen. I then looked if (1) the plant target was expressed in response to different stresses (pathogen, PAMPs or hormones) using Genevestigator Expression Data (Hruz et al. 2008), (2) Knock-out mutants were available using T-DNA Express website, (Mackey et al.) the candidate was a part of a multigene family, using Phytozome Plant Gene Families, (4) the plant target was predicted to be localised in the same subcellular compartment as the HaRxL79, (5) the plant target was known to have interactors using IntAct (Protein Interaction *Data*base at EBI).

AGI	At4g39050	At3g27960	At4g26110	At5g56950
Name	MKRP2	KLC	Nap1;1	Nap1;2
Function	unknown	unknown	histone chaperone	histone chaperone
Differential expression	no	no	ABA	no
Knock-out mutants	NO	yes	triple KO	triple KO
Multigene family	2 paralogs	nd	4 paralogs	4 paralogs
Localisation	mitochondria	nd	nuclear-cytoplasmic	nuclear-cytoplasmic
Plant Interactors (Y2H)	HopG1, HopZ1	CC-NB-LRR	HaRxL79 paralogs	HaRxL79 paralogs
Validation of the interaction with HaRxL79	NO interaction CoIP	nd	CoIP + BiFC	CoIP + BiFC

Table 4.6. Summary of the state of art on HaRxL79 plant targets identified in Y2H screen.

Data were compiled from TAIR, Genevestigator, T-DNA Express and Phytozome websites. ABA: abscisic acid, KO, knock-out, CoIP: co-immunoprecipitation, BiFC: bi-molecular fluorescence complementation, nd: non determined.

In this section I will present results I obtained about the validation of the interaction between HaRxL79 and the microtubules-associated putative plant targets, MKRP2 and KLC. The interaction between the nucleosome-assembly proteins 1 (NAP1s) and HaRxL79 as well as the characterization of the NAP1s during *Hpa* infection are going to be described in details in **Chapter 5**.

- **HaRxL79 interacts with MKRP2 in Y2H**

MKRP2 (At4g39050) is described as a kinesin-related protein targeting mitochondria (Kim and Endow 2000; Itoh et al. 2001). MKRP2 N-terminus, predicted to target mitochondria, localises in mitochondria when transiently expressed in fusion with GFP in BY-2 tobacco cells (Itoh et al. 2001). MKRP2 is closely related to the KRP85/95, subfamily of kinesins, as it contains in its N-terminus two conserved domains sharing homology to ATP/GTP binding and motor domains (Kim and Endow 2000) (**Figure 4.25A**). However, the kinesin activity of MKRP2 was never tested.

In order to analyse MKRP2 *in planta*, I first cloned the full length genomic DNA into GW compatible vector. I then transiently expressed the fusion protein RFP-MKRP2 (full length) in *N. benthamiana* using *Agrobacterium*-mediated transformation. I found that in contrast with what has been reported for the MKRP2 N-terminus, the RFP-MKRP2 (full length) chimeric protein localised to the cytoplasm of the plant cell (**Figure 4.25C**). We can exclude that RFP-MKRP2 (full length) subcellular localisation is due to degradation as only full length protein was detected by western-blot (**Figure 4.25B**). However, it is possible that the mitochondria-targeting sequence is hidden by the RFP positioned at the N-terminus of MKRP2.

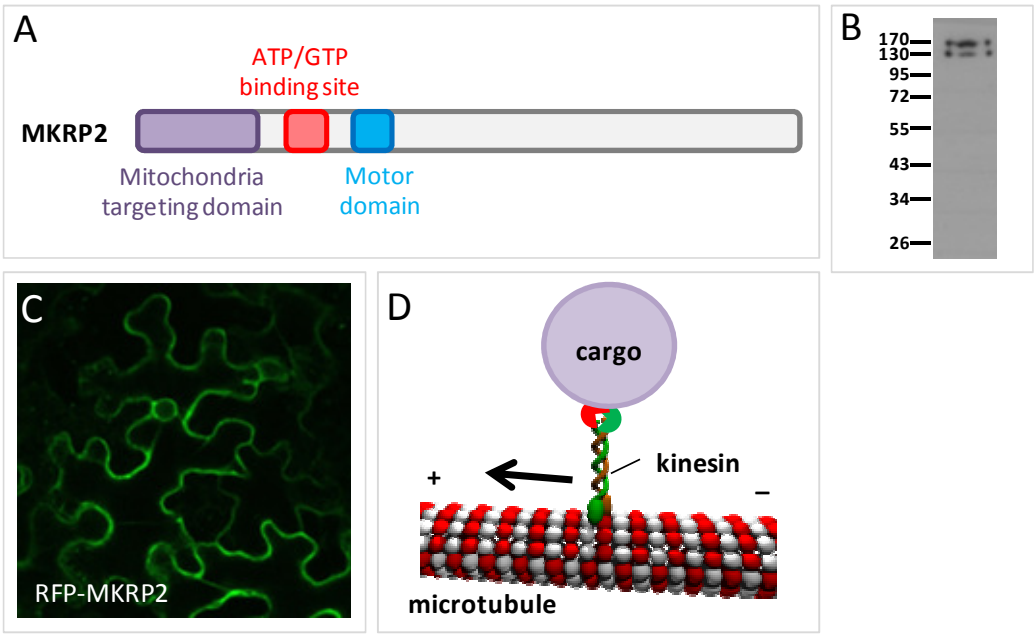

Figure 4.25. MKRP2 is a putative plant target of HaRxL79.
A, MKRP2 domains predicted and identified (Kim and Endow 2000, Itoh et al. 2001). **B**, Western-blot anti-RFP of *N. benthamiana* samples expressing RFP-MKRP2. **C**, transient expression in *N. benthamiana* of RFP-MKRP2 indicates a cytoplasmic localisation. **D**, Cartoon illustrating the role of kinesins in microtubule-associated transport of cargos.

To test whether MKRP2 interacts *in planta* with HaRxL79, I next performed co-immunoprecipitation (co-IP). RFP-MKRP2 and HaRxL79–GFP were transiently co-expressed in *N. benthamiana*. Two days post infiltration, total proteins were extracted and immunoprecipitated with anti-GFP beads (which can pull down GFP-tagged constructs). Preliminary results indicate that RFP-MKRP2 and HaRxL79-GFP do not co-IP (data not shown).

To investigate the role of MKRP2 during *Hpa* infection, I next intended to test the susceptibility of Col-0 *mkrp2* T-DNA insertion mutants towards *Hpa*. Unfortunately, no T-DNA insertion mutants in this gene were recovered (**Table 4.6**). However, Mukhtar et al. (2011) reported that the SALK_026411 line, which carries a T-DNA insertion in *Mkrp2*

3'end, was slightly more resistant to *Hpa* Noco2 than Col-0. This would suggest that MKRP2 has a role in promoting disease.

According to the PPIN1 interactomic database (Mukhtar et al. 2011), MKRP2 interacts with several bacterial effectors (from different *Pseudomonas spp*), including HopG1 that targets mitochondria (Block and Alfano 2011) and HopZ1 that targets microtubules (Dr. David Guttman, personal communication). In addition, in the AI1 interactomic database, MKRP2 interacts mostly with several plastid-associated plant proteins (Arabidopsis Interactome Mapping 2011). Overall these Y2H data tend to confirm that MKRP2 is a mitochondrial kinesin-related protein. Since I could not validate the interaction between HaRxL79 and MKRP2 in planta and that *mkrp2* knock-out mutants were not available, I next analysed the interaction between HaRxL79 and an other putative microtubule-associated protein, KLC.

- **HaRxL79 interacts with KLC in Y2H**

In TAIR website, At3g27960 (KLC) is a described as a Tetratricopeptide repeat (TPR)-like protein with unknown function, but shown to be differentially regulated during pollen tube growth (**Table 4.6**). In order to analyse the KLC interaction with HaRxL79, I wanted to clone the full length genomic DNA into a GW compatible vector. Using genomic DNA of Col-0, cDNA or BAC clone, I have been unable to clone the full length gene, restricting the analysis of the putative plant target. As a KLC knock-out mutant was available, I next tested the effect of the loss of function of KLC during *Hpa* infection. Col-0 *klc* showed increased resistance to *Hpa* Waco9 and *Hpa* Noco2 (**Figure 4.26**). Interestingly, Mukhtar et al. (2011) tested the *klc* mutant for impaired resistance. By testing incompatible *Hpa* isolates (Emwa1

and Emoy2), they showed that *klc* knock-out partially impairs RPP4-mediated resistance as increased sporulation is observed on this mutant.

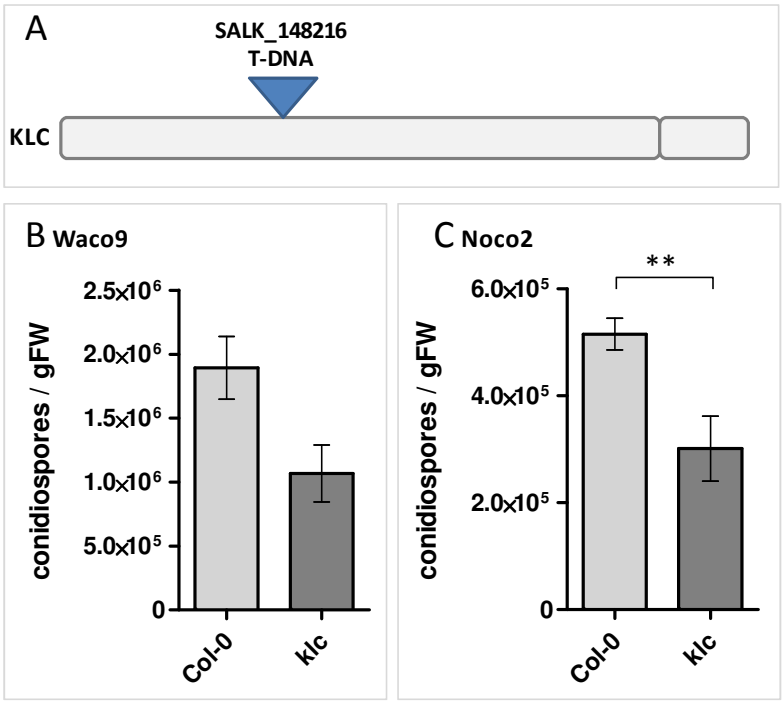

Figure 4.27. Col-0 *klc* mutant is more resistant to *Hpa*.
A, Schematic representation of KLC (At3g27960) gene composed of 2 exons. The T-DNA insertion in Col-0 *klc* mutant (SALK_148216 line) is indicated by a blue arrow. B, C, Col-0 and Col-0 *klc* 3-week old plants were sprayed with a *Hpa* spore solution (5×10^4 conidiospores / mL of Noco2 or Waco9 as indicated) and sporulation was measured 7 days after infection by counting freshly produced conidiospores per gram of plant fresh weight (gFW). Asterisks indicate significant differences as indicated by a Bonferroni post-hoc comparison test performed after a two-way ANOVA on the whole dataset, with two asterisks: $p<0.001$.

According to the PPIN1 interactomic database, KLC interacts with several oomycete effectors and one bacterial effector on the pathogen side, and with one CC-NB-LRR and one receptor-like kinase on the plant side (Mukhtar et al. 2011). Like MKRP2, KLC also interacts with many plastid associated proteins (16/36 interactors identified).

Overall I could not link the microtubule association of HaRxL79 to the two microtubules-associated proteins, identified in a Y2H screen to interact with HaRxL79, but it is worth pursuing, in particular given that several defence-related interactors of MKRP2 and KLC were recently revealed to us. In addition, the other plant interactors found for HaRxL79 in the Y2H screen showed really interesting phenotype which I prioritised.

4.3. Discussion / Conclusion

In this **chapter 4**, I described the result of two screens that were conducted in our laboratory which provided a list of promising effector candidates (HaRxLs) from the *Hpa* Emoy2 reference isolate.

The first screen (HaRxL-EDV screen) conducted by Dr. Georgina Fabro, tested 64 HaRxLs for their effect on *Pst* virulence in Arabidopsis (Fabro et al. 2011). This screen identified several HaRxLs that were mostly increasing bacterial virulence on a set of Arabidopsis accessions, other HaRxLs that were mostly reducing bacterial virulence and others that did not seem to have an effect on bacterial virulence. It is interesting to identify HaRxLs that confer bacterial resistance as it could suggest that these particular HaRxLs may be avirulent factors. But it is even more interesting to identify HaRxLs that increase bacterial virulence, as these HaRxLs may well be promoting *Hpa* growth in Arabidopsis too. Indeed, this "effectoromics" project was meant to identify key virulent factors and study their function in an effort to understand how *Hpa* colonises its host.

The second screen was based on the subcellular localisation of 49 HaRxLs, transiently expressed in *N. benthamiana* (Caillaud et al. 2012). This screen identified that HaRxLs target most plant cell compartments with a predominance of the nucleus and membranes. Notably, this screen identified one particular effector, HaRxL17 which was tonoplast-associated and conferred increased virulence to compatible and incompatible *Hpa* isolates. In addition HaRxL17 was shown to localise most likely at the EHM (Caillaud et al. 2012; Caillaud et al. in press). I described in **Chapter 1** how little we know about the *Hpa* / Arabidopsis interface constituted of the EHMx and the EHM and how important this interface is to understand

effector functions, particularly these of effectors that promote susceptibility. From this second screen, I identified one effector candidate with a peculiar localisation which was not included in the Caillaud et al. (2012) publication.

In the still early step of defining *Hpa* effectorome, other screens were conducted. In our laboratory, Badel et al. (*in preparation*) screened HaRxLs for their competitive properties in mixed infections in order to identify HaRxLs with high competitive index. They identified five HaRxLs to have such properties, and interestingly, all five HaRxLs had different subcellular localisations (Badel et al. *in preparation*). Another laboratory screened ESTs from Waco9-infected tissues and identified 42 effector candidates among which few were Waco9-specific (Cabral et al. 2011). Waco9 HaRxLs were tested for their effect on bacteria virulence, like in Fabro et al. (2011). Notably they identified one effector candidate RXLR29, present in full length only in Waco9 and not in other *Hpa* isolates, and which conferred increased virulence to *Pst*-LUX and was able to suppress *Pst*-ΔCEL-triggered callose deposition (Cabral et al. 2011).

Overall the three screens conducted in our laboratory to identify interesting effector candidates were rather successful, even if few HaRxLs such as HaRxL65 or HaRxL79 seemed to be false positives, but several effectors conferring virulence to *Hpa* and/or *Pst* that target specific plant compartments were identified. Notably the combination of the initial HaRxLs-EDV screen with the subcellular localisation screening highlighted that HaRxLs that had an effect on *Pst* virulence also had variable subcellular localisations thereby likely various functions in *planta* (**Table 4.1**).

It seemed relevant to mention the context of the "Effectoromics" project because the data presented in this chapter may seem "scattered" from time to time. But to me, this is reflecting how the whole laboratory progressed in four years of "scratching our heads" to design and set up the experimental procedures to address the question of the functional characterisation of *Hpa* effectors. If the reader compares the **Table 1.2** presented in **Chapter 1** summarising what we know about oomycete effectors translocated into the host cells, with the **Table 4.1** presented in this chapter, summarising the data we generated in our laboratory for these last four years, it becomes clear that the approaches undertaken were mostly fruitful and constitute the basis for a new area which will focus on effector biology itself.

In this chapter, I showed that HaRxL79 localises to the plant microtubules. Contrary to the smooth localisation of the structural microtubule-associated proteins bundling microtubules like MAP4, HaRxL79-GFP showed a dotty pattern on the microtubules, suggesting that HaRxL79 might be associated with a motor microtubule-associated protein, such as a kinesin. The fact that GFP-HaRxL79 was easier to image in the presence of taxol (blocking the microtubules dynamics) supports the hypothesis that HaRxL79 might be associated with a kinesin. However, given HaRxL79 degradation *in planta* no further experiments could be done on this part of the project. In addition, because we could not express HaRxL79 solubly (in collaboration with Dr. Lennart Wirthmüller), we could not perform microtubule co-sedimentation *in vitro* assays. But Arabidopsis oestradiol-inducible HaRxL79 lines should help for co-localisation with microtubules in Arabidopsis. Why would HaRxL79 localise to microtubules or associate with a kinesin? We can hypothetise that HaRxL79 either competes with traffic on microtubules or hijacks microtubules to target a specific subcellular compartment. But as long as we do not have a phenotype for HaRxL79, we cannot test whether this microtubule–association is crucial to HaRxL79 function.

Interestingly, only one plant pathogen effector has been reported so far to target microtubules, HopZ1a from *Pseudomonas syringae*, but HopZ1a seems to have a different mode of action than HaRxL79 as it acetylates tubulin and degrades microtubules (Dr. David Guttman, Toronto, oral conference communication).

Cytoskeleton rearrangements have been observed during plant-pathogen interactions, at different levels: from the response to the penetration of pathogens in the plant cell plant to the microtubule subversion by viruses to spread from cell to cell and HR (Schmelzer 2002; Caillaud et al. 2008; Harries et al. 2010; Smertenko and Franklin-Tong 2011). *Hpa* penetration in epidermal cells is associated with rearrangements of the actin microfilaments and the microtubules (Takemoto et al. 2003). Recently Caillaud et al. (2011) showed that a nest of actin microfilaments surround *Hpa* haustoria during infection. Collaborators showed that microtubules also create a nest around *Hpa* haustoria during infection (Dr. Mickael Quentin, INRA Nice-Sophia-Antipolis). Because of these various stress-induced microtubule rearrangements, microtubules constitute good targets for some pathogen effectors to manipulate.

Interestingly in yeast, HaRxL79 was shown to interact with two putative microtubule-associated proteins. Despite the fact that neither MKRP2 nor KLC have been shown to be functional kinesins or even to be microtubule-associated, both seem required during *Hpa* infection (this chapter and Mukhtar et al. 2011). Surprisingly, HopZ1a which is a *bona fide* effector associated with microtubules, interacts with MKRP2 in yeast (Mukhtar et al. 2011). So if MKRP2 is a kinesin, why does it localise to mitochondria? And if it does localise to mitochondria, what is the link with HaRxL79 and HopZ1a being associated with microtubules? Given that both MKRP2 and KLC interact with many plastid proteins in yeast,

it raises the question of the reliability of the Y2H data. There are several possibilities one can think of to explain what is going on. It is possible that either MKRP2, KLC or both are false positives identified in the Y2H screen. Y2H screens proteins for interaction in the yeast nucleus, proteins which would never interact with each other in a compartimentalised living plant cell, particularly as MKRP2 and HaRxL79 seem to have different subcellular localisation. Or it is possible that MKRP2 and/or KLC localisation changes during *Hpa* infection. For instance one can imagine that during infection MKRP2 is no longer associated with mitochondria but with HaRxL79. To answer these questions, the interaction *in planta* between HaRxL79 and MKRP2 or KLC need to be proven and the localisation of the N-terminus of MKRP2 during *Hpa* infection has to be investigated. One important thing to consider with these Y2H data is that it is possible that HaRxL79 interacts with the conserved homologs of MKRP2 or KLC in *Hpa* and not *in planta*.

HaRxL79 belongs to a gene family in *Hpa* Emoy2 including at least eight paralogs sharing a conserved N-terminus but exhibiting very divergent C-termini. I showed that three HaRxL79 paralogs localised to three different plant subcellular compartments, suggesting that the C-terminal part of HaRxL79 paralogs address them to specific subcellular compartments. The function of the HaRxL79 resides likely in their C-termini. Interestingly, two paralogs proteins when tagged at the N-terminus showed aggregates in the plant cells. So even if we do not know the function of the N-terminus conserved sequence, we assume that it is important for the folding of the paralog proteins. The *HaRxL79* gene family is present in all *Hpa* isolates but is extremely diversified and absent from the closely related *Phytophthora spp*., suggesting that conceivably this gene family is under high selection pressure and has a crucial role during *Hpa* infection possibly in the biotrophic side of the interaction.

Despite the exciting idea that we identified an *Hpa* effector that targets the plant microtubules and potentially interacts with two proteins, predicted to be associated with microtubules and which play a role during *Hpa* infection, because of technical difficulties I accumulated little evidence to address the role of HaRxL79 at microtubules. Therefore I focused on the other plant interactors identified in the Y2H screen, the NAP1s, for which I found an interesting phenotype as they seem to be susceptibility factors. It will be the topic of **Chapter 5**.

5. Histone chaperones NAP1s act as susceptibility factors during *Hpa* infection

5.1. Introduction to the project

Nucleosomes are the basic structural components of chromatin, allowing DNA to be optimally compacted in cell nuclei. Nucleosomes are constituted of different variants of histone proteins (called H2A, H2B, H3, and H4), organised in octamers each consisting of two copies of the four variants (Bentley et al. 1984; Richmond et al. 1984; Luger et al. 1997). Chromatin structure regulates essential cellular processes including DNA replication, transcription and repair (Clapier and Cairns 2009). Indeed, depending on where the nucleosomes are positioned on the DNA, proteins including transcription factors can access or not their DNA binding sites which determines whether or not they can activate transcription. The assembly of histones in nucleosomes is a very tightly regulated process orchestrated by histone chaperones and chromatin remodelling proteins. Histone chaperones are able to load or unload histones into and from nucleosomes, whereas chromatin remodelling proteins can modify histone-DNA interactions to allow for and regulate transcription at specific DNA loci. For instance, chromatin remodelers include histone-modifying enzymes that target the N-terminal tail of histones by acetylation, methylation or ubiquitination, and thus modify the chromatin structure, with consequences for gene expression (Fuchs et al. 2006). Chromatin remodelling is an important mechanism of transcriptional regulation and several chromatin remodelers are the targets of plant pathogens that subvert plant processes in order to promote disease (Ma et al. 2011).

Arabidopsis encodes several histone chaperones, that tend to be chaperones either of H3/H4 or of H2A/H2B. Anti-silencing function 1 (Asf1), chromatin assembly factor 1 (CAF-1) or FK506 binding ptrotein 53 (FKBP53) are specific chaperones of H3/H4 (Kaya et al. 2001; Daganzo et al. 2003; Li and Luan 2010), whereas nucleosome assembly protein 1 (NAP1), NAP1-related protein (NRP), nucleolin and nucleoplasmin are specific chaperones of H2A/H2B (Angelov et al. 2006; Zhu et al. 2006; Liu et al. 2009; Taneva et al. 2009). Notably the H2A/H2B chaperones *AtNAP1s* gene family comprises four members called *AtNap1;1* to *AtNap1;4* (At4g26110, At5g56950, At2g19480, At3g13782). *AtNap1;1*, *AtNap1;2* and *AtNap1;3* are expressed ubiquitously in plant tissues whereas *AtNap1;4* expression is restricted to roots and pollen (Zhu et al. 2006; Liu et al. 2009). Interestingly, the function of NAP1s seems well conserved across eukaryotes as *AtNap1;1* successfully complements a *nap1* knock-out (KO) mutant in yeast (Galichet and Gruissem 2006). AtNAP1s proteins can homo- and hetero-dimerise and interact with histones H2A and H2B, as part of its chaperone function (Liu et al. 2009, **Figure 5.1**).

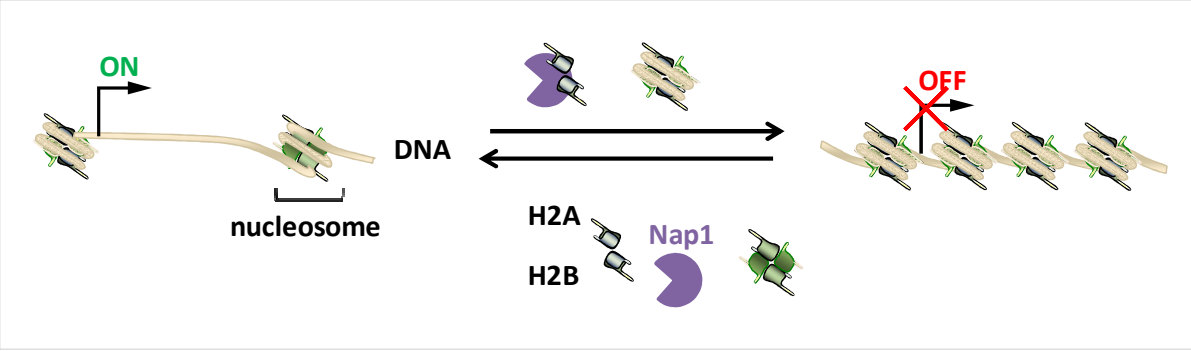

Figure 5.1. Schematic representation of AtNAP1s-mediated nucleosome assembly/disassembly and their role in transcription regulation.

AtNAP1s are represented in purple, DNA is shown in beige, histones in grey and green. AtNAP1s can load and unload histones H2A and H2B into nucleosomes. The function of histone chaperones-mediated assembly and disassembly of nucleosomes at a particular site is to allow for or restrict transcription regulation and DNA replication at this location.

AtNAP1s family members are involved in the repair response induced by ultra-violet-induced stress and the presence of abscisic acid (ABA) (Liu et al. 2009; Liu et al. 2009). AtNAP1;1 is also a stage-specific regulator of cell proliferation and expansion (Galichet and Gruissem 2006), indicating that AtNAP1s have a rather central role during development and in response to stresses. Interestingly, microscopy of fluorescent-tagged AtNAP1s showed that AtNAP1s are mostly cytoplasmic (Galichet and Gruissem 2006, Liu et al. 2009). However, using biochemical approach, Liu et al. (2009) showed that a small amount of AtNAP1s is present in the plant cell nucleus.

In a Y2H assay conducted by collaborators (Mukhtar et al. 2011), AtNAP1s (AtNAP1;1 and AtNAP1;2) were identified to interact with HaRxL79 (**Table 4.5**). In addition to these Y2H data, collaborators in Germany identified by mass spectrometry that another *Hpa* effector candidate, HaRxL67, could pull down all three NAP1s in Arabidopsis protoplasts (Fraiture and Brunner, personnal communication). Thus, AtNAP1s seem to be targeted by *Hpa* effectors. Interestingly, no T3E from various *Pseudomonas syringae* species tested in the Y2H screening were found to interact with AtNAP1s, highlighting the specificity of the interaction. In this chapter, I followed up the role of the histone chaperones AtNAP1s during *Hpa* infection.

5.2. Results

5.2.1. AtNAP1s interact *in planta* with HaRxL79 and HaRxL67

From the work performed by collaborators, two *Hpa* RxLR effector candidates, HaRxL79 and HaRxL67 (presented in **Chapter 4** of this thesis) were shown to interact with the Arabidopsis NAP1s. First, HaRxL79 was shown to interact with AtNAP1;1 and AtNAP1;2 in yeast by Y2H assay (Mukhtar et al. 2011). In addition, HaRxL67 was shown to interact with AtNAP1;1, AtNAP1;2 and AtNAP1;3 in Arabidopsis protoplasts by immunoprecipitation assay (Fraiture and Brunner, personnal communication).

In order to confirm the interaction of HaRxL79 with AtNAP1s *in vivo*, I co-expressed GFP-tagged AtNAP1s with RFP-tagged HaRxL79 transiently in *N. benthamiana* and performed GFP-tagged AtNAP1s pull down on total leaf protein extracts two days post-infiltration. While GFP alone did not pull down HaRxL79, all three AtNAP1s tested (AtNAP1;1, AtNAP1;2 and AtNAP1;3) co-immunoprecipitated with HaRxL79 (**Figure 5.2**), demonstrating that HaRxL79 interacts *in planta* with AtNAP1s. Using the same approach, I validated the interaction *in planta* between HaRxL67 and AtNAP1;1, AtNAP1;2 and AtNAP1;3 (**Figure 5.2**).

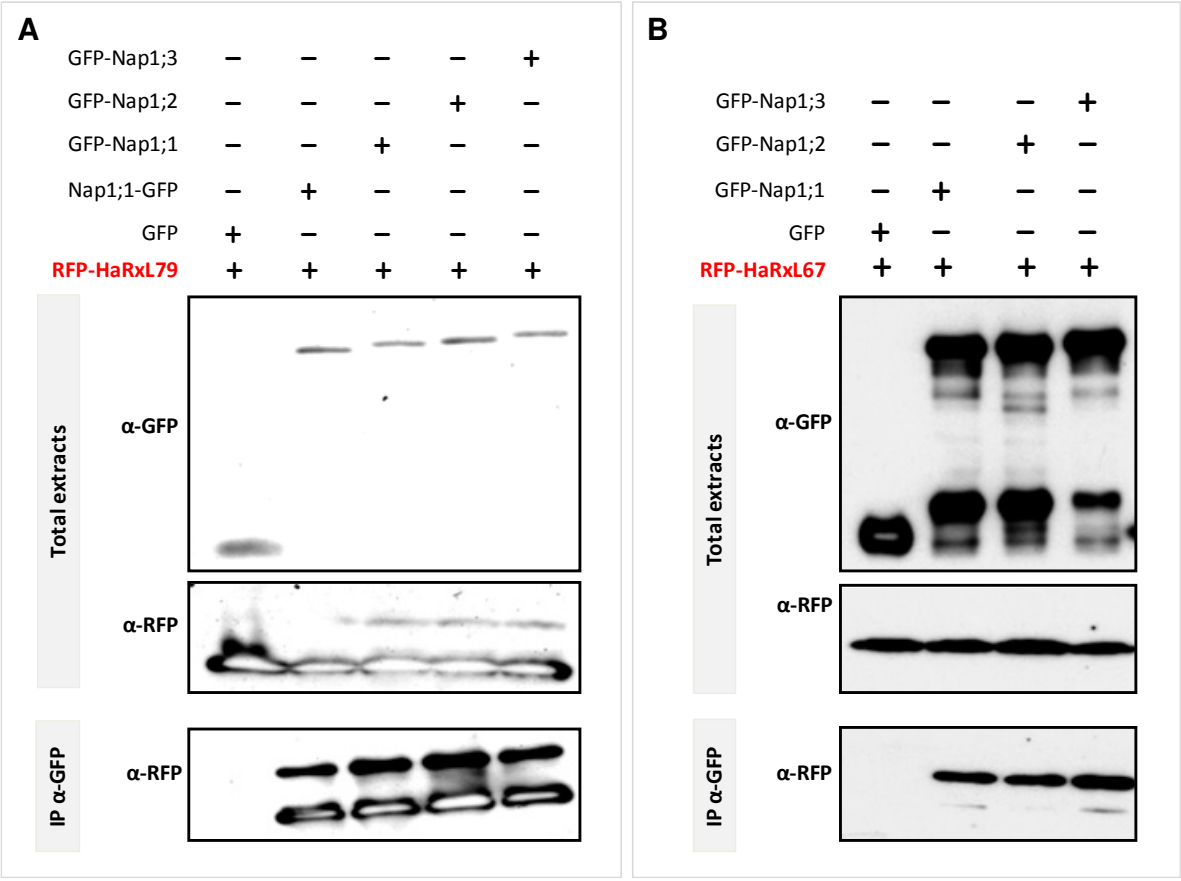

Figure 5.2. HaRxL79 and HaRxL67 co-immunoprecipitate with AtNAP1s.

GFP-tagged AtNAP1s and RFP-tagged HaRxL79 (**A**) or HaRxL67 (**B**) were transiently co-expressed *in N. benthamiana* for two days. Total proteins extracts were subjected to GFP-immunoprecipitation (IP). Western-blots of the total or immunoprecipitated extracts are shown as indicated on the left of each blot.

I next wanted to determine in which plant subcellular compartment the interaction between HaRxL79 and HaRxL67 and AtNAP1s took place. To do this I used fluorescent-tagged AtNAP1s and HaRxLs in order to observe their subcellular localisations by confocal microscopy. When transiently expressed in *N. benthamiana*, GFP-tagged AtNAP1s are cytoplasmic (**Figure 5.3B**) as reported by Galichet and Gruissem (2006) and Liu et al. (2009). Additionally, GFP-tagged HaRxL79 is nuclear-cytoplasmic at two days post-infiltration as described in **Chapter 4**. RFP-HaRxL67 is vacuolar as described in **Chapter 4** (Caillaud et al. 2012).

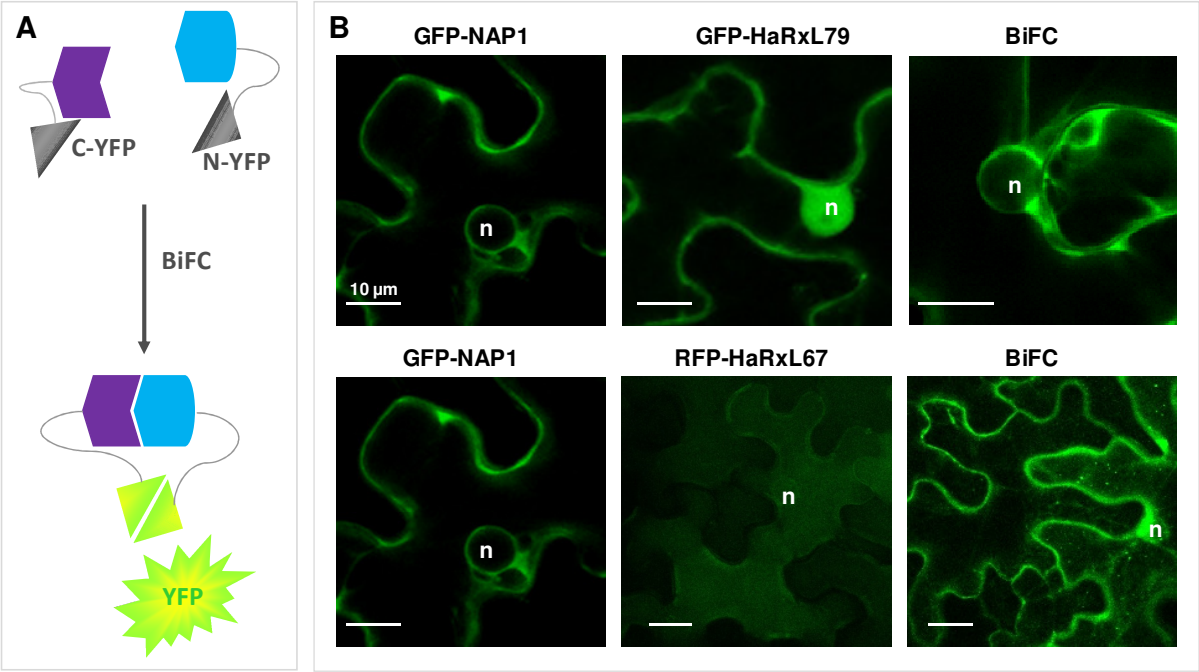

Figure 5.3. HaRxL79 and HaRxL67 interact with AtNAP1s in the plant cytoplasm.

A, Schematic representation of the bi-molecular fluorescence complementation (BiFC) assay. **B**, Plant subcellular localisation of transiently expressed GFP- or RFP-tagged proteins (left and middle panels), and BiFC (right panel) for NAP1s and HaRxL79 (top) and NAP1s and HaRxL67 (bottom). The same results were obtained for all three AtNAP1s, therefore defined as NAP1. Scale bar: 10 µm. n: nucleus.

In order to determine in which plant subcellular compartment the interaction between AtNAP1s and HaRxL79 or HaRxL67 occurs, I used a bi-fluorescence complementation (BiFC) assay (Caillaud et al. 2009), based on the transient co-expression of AtNAP1s and HaRxLs each tagged with complementary halves of YFP (**Figure 5.3A**). When two proteins tagged as such interact, a yellow fluorescence is observed as a functional YFP is reconstituted (**Figure 5.3A**).

Using the BiFC assay, HaRxL79 and AtNAP1s were observed to interact in the plant cytoplasm (**Figure 5.3B**). HaRxL67 and AtNAP1s were also shown to interact in the plant cytoplasm but also in vesicle-like bodies as observed by the dotty pattern (**Figure 5.3B**). This result might suggest that these two *Hpa* effectors can interact with histone chaperones in different ways.

In conclusion, I showed here that two *Hpa* effector candidates, HaRxL79 and HaRxL67, interact with AtNAP1s *in planta*. As a minimum of two HaRxLs have now been shown to interact with AtNAP1s, it seems likely that AtNAP1s may play an important role during *Hpa* infection. This inference is examined further in the next section.

5.2.2. AtNAP1s are required for susceptibility to *Hpa*

In order to better understand the role of the AtNAP1s during *Hpa* infection, I next tested *Hpa* susceptibility in Arabidopsis NAP1s loss of function mutants. In this experiment, I measured *Hpa* hyphal growth and sporulation during compatible and incompatible interactions in *Atnap1s* mutants in comparison with Col-0 plants. I used two Col-0 KO mutants described by Liu et al. (2009). The first KO mutant, named *m123-1*, is a *nap1;1 nap1;2 nap1;3* triple KO mutant. The second mutant, named *m123-2*, is a partial *nap1;1 nap1;2 nap1;3* triple KO mutant. In the *m123-2* KO mutant, a truncated AtNAP1;3 (AtNAP1;3T) protein is still produced (Liu et al. 2009). I also assessed the effect of AtNAP1s over-expression (OE) during infection. In this experiment, I used three OE mutants expressing under the constitutive promoter 35S, YFP-tagged *AtNap1;1*, *AtNap1;2* or *AtNap1;3* (Liu et al. 2009). I first analysed the phenotype of these mutants during plant development. At the macroscopic level, all these mutants did not exhibit any drastic developmental alterations in comparison with Col-0, even if five week-old *m123-1* and *m123-2* mutants appeared slightly smaller than Col-0 (not shown). I next assessed the phenotype of these mutants during *Hpa* infection (**Figure 5.4**).

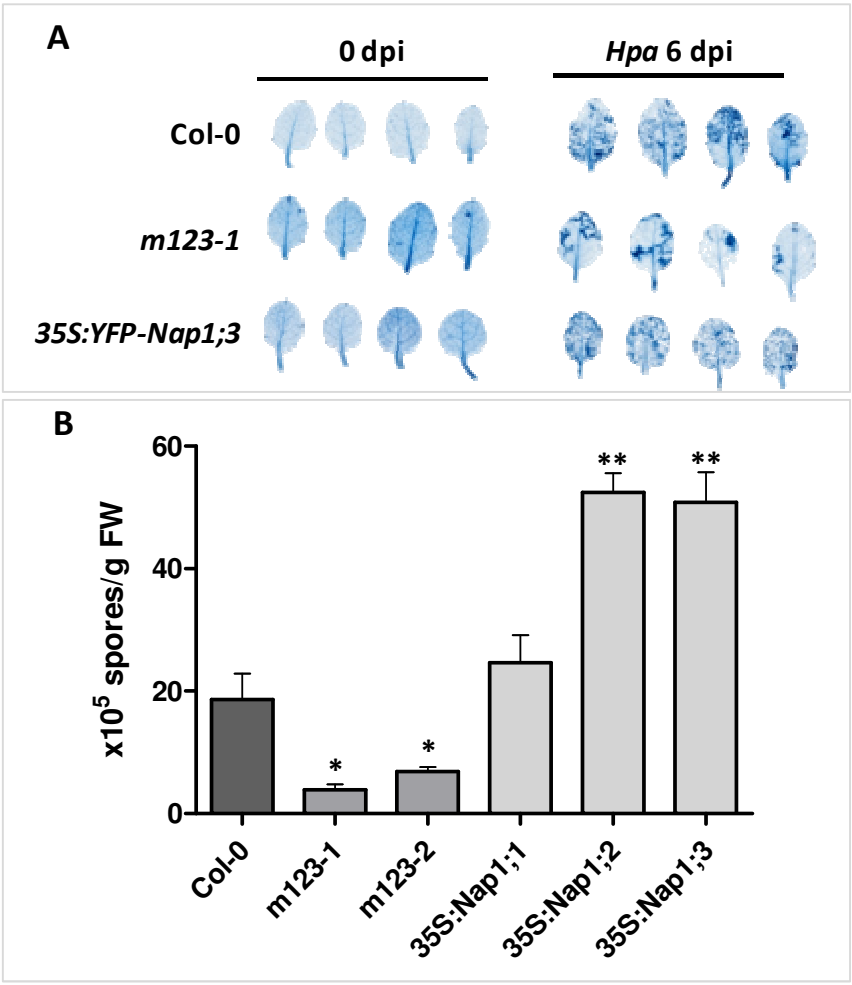

Figure 5.4. *nap1s* mutants show altered susceptibility to *Hpa* Waco9.
Three-week-old Arabidopsis plants were sprayed with 5 × 10^4 conidiospores/mL. **A**, Trypan blue staining was performed on mock-treated (0 days post-infection) or infected plants (6 dpi). **B**, Asexual sporulation count at 7 dpi. Error bars represent the standard error of the mean. Asterisks represent the significance of individual unpaired t-tests comparing the given column with the Col-0 control (one: $p<0.05$, two: $p<0.001$). It should be noted that using a one-way ANOVA with Bonferroni post-hoc comparison tests, *m123-1* and *m123-2* were not found significantly different from Col-0, but individual t-tests show a difference for these two conditions, suggesting a trend.

During compatible interaction, *Hpa* hyphal growth was examined with light microscopy after trypan blue staining (**Figure 5.4A**). Hyphal growth of *Hpa* Waco9 on *m123-1* was significantly reduced compared to Col-0 as shown in **Figure 5.4A**. Conversely *Hpa* Waco9 hyphal growth was increased in the OE mutant *AtNap1;3* (**Figure 5.4A**). The hyphal growth phenotypes were correlated with asexual sporulation, as both KO mutants (*m123-1* and *m123-2*) were more resistant to *Hpa* Waco9 whereas the three OE mutants were more susceptible compared to Col-0 (**Figure 5.4B**). Even if results were variable, KO mutants were

always observed to be more resistant to *Hpa* Waco9 compared to Col-0, whereas OE mutants were always more susceptible than Col-0 (**Figure 5.4B**). Trypan blue staining of *Hpa*-infected tissues allowed me to check for the occurrence of plant cell death at the infection sites. Occasional plant cell death was observed in *m123-1* and *m123-2* KO mutants as in wild type suggesting that the reduced hyphal growth in the KO mutants could not be explained solely by cell death-mediated resistance.

Arabidopsis Col-0 is resistant to *Hpa* Emoy2 due to *RPP4* (van der Biezen et al. 2002). However as *AtNap1s* OE mutants are more susceptible to *Hpa* Waco9, I tested whether they would also be more susceptible to the incompatible *Hpa* isolate Emoy2. In order to assess *Hpa* growth during incompatible interaction, I measured oospore production arising from sexual reproduction on OE mutants after infection with *Hpa* Emoy2 in comparison with Col-0. I observed no difference in the OE mutants compared to Col-0 (data not shown).

I next tested whether AtNAP1s subcellular localisation was altered in the presence of *Hpa* haustoria in the cell by confocal microscopy in infected tissues. As in non infected cells, YFP-AtNAP1s were observed in the cytoplasm of haustoria-infected cells (**Figure 5.5**).

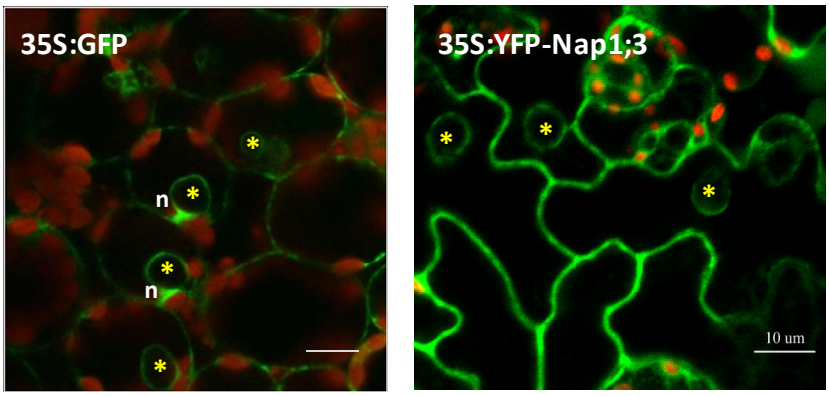

Figure 5.5. YFP-tagged AtNAP1s subcellular localisation during *Hpa* infection.
Three-week-old Arabidopsis plants were sprayed with 5 × 10^4 conidiospores/mL. AtNAP1s subcellular localisation was observed by confocal microscopy. *Hpa* haustoria are indicated by a star (*). n: nucleus. Scale bar: 10 µm.

5.2.3. *nap1s* mutants do not show altered defence responses

As *Atnap1s* KO mutants showed an altered susceptibility to *Hpa*, it became interesting to examine the plant defence responses induced during *Hpa* infection in the absence of *AtNap1s* expression. According to expression data generated in the laboratory, *AtNap1s* genes are not differentially regulated upon *Hpa* infection (Fabro, Ishaque and Jones, The Sainsbury laboratory, unpublished). Additionally, I did not observe any constitutive cell death activation on the *Atnap1s* KO mutants that could prevent *Hpa* growth (**Figure 5.4**). I then checked whether defence responses were constitutively activated during *Hpa* infection of the *nap1s* KO mutants. In order to test if the loss of *AtNap1s* led to a constitutive activation of plant defences, I performed RT-PCR and quantitative RT-PCR (q-RT-PCR) on *Atnap1s* mutants over a time course of *Hpa* infection (0, 2, 4 and 6dpi) on three defence marker genes: *PR1*, *PAD4* and *PDF1.2*. These genes were selected because they are respectively markers of the induction of salicylic acid and jasmonate/ethylene defence pathways (Glazebrook 2005). Preliminary results indicated that the defence marker genes induction was similar in the *Atnap1s* KO mutants and Col-0, again suggesting that no alteration in the defence response pathway occurs in the *Atnap1s* mutants upon *Hpa* infection (see poster in Appendix).

In addition, I tested whether the *Atnap1s* mutants were impaired in other defence responses involved in PTI like the ROS production induced by the perception of flg22 (**Figure 5.6**). However, no difference in terms of ROS burst production was observed in the *nap1s* mutants compared to Col-0 (**Figure 5.6**).

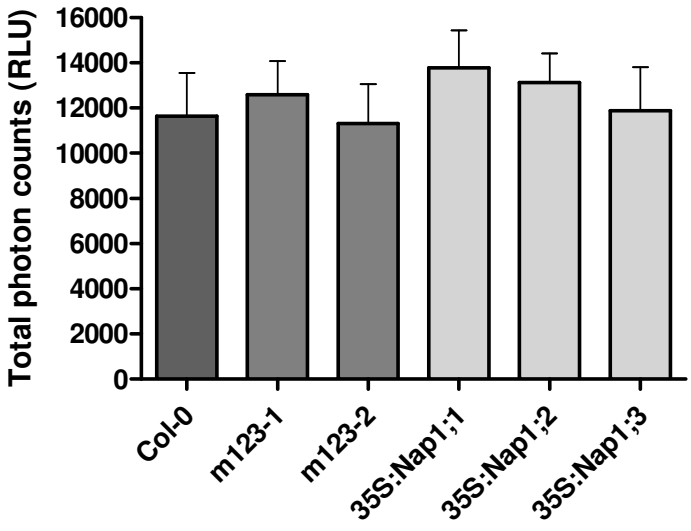

Figure 5.6. flg22-induced ROS burst on *Atnap1s* mutants.
The ROS burst was induced by addition of 100 nM flg22 and followed over time. The ROS burst was measured by the total photon counts emitted during the burst. This experiment was repeated three times. No statistically significant difference was found between the samples, either using a one-way ANOVA with Bonferroni post-hoc comparison test, or using individual unpaired t-tests comparing each condition with the Col-0 control.

Overall, these results indicated that the *Atnap1s* mutants were not altered in their common defence responses during *Hpa* infection but that nonetheless, *AtNap1s* loss caused an increased susceptibility to *Hpa*. These observations suggest that *AtNap1s* are good susceptibility factor candidates in the Arabidopsis/*Hpa* interaction.

5.2.4. *AtNap1s* loss also confers increased resistance to a necrotrophic pathogen

As *Nap1s* seem functionally conserved in eukaryotes (Galichet and Gruissem 2006; Park and Luger 2006), it would be interesting to know if they could act as susceptibility factors for other types of pathogens. To test whether *AtNap1s* are specifically involved in the susceptibility to biotrophic pathogens, I infected the *Atnap1s* mutants with three other types of pathogens, the hemi-biotrophic bacterium *Pst* DC3000, the hemi-biotrophic oomycete *Phytophthora parasitica* and the necrotrophic fungus *Botrytis cinerea* (**Figure 5.7**).

I first tested the susceptibility of the *Atnap1s* mutants towards the bacterial pathogen *Pst* DC3000. Five week-old *Atnap1s* leaves were syringe-infiltrated with 5×10^5 cfu/mL *Pst* DC3000, and bacterial titres were measured at three days post-infiltration. *Atnap1s* mutants did not show altered susceptibility to *Pst* DC3000 (**Figure 5.7A**). I then decided to test *Atnap1s* mutants with another hemi-biotrophic pathogen, the oomycete *P. parasitica* which can infect Arabidopsis roots and then spread to the aerial parts of the plant (Attard et al. 2010). This *P. parasitica* infection experiment was performed by collaborators in France (Dr. Agnès Attard, Sophia-Antipolis, Nice). *Atnap1s* mutants were grown *in vitro* for 30 days and single plants roots were infected with 500 *P. parasitica* zoospores. Disease symptoms were measured over time and scored according to a published disease index (Attard et al. 2010). *Atnap1s* mutants did not show altered resistance to *P. parasitica* (**Figure 5.7B**). Because *Atnap1s* mutants did not show altered susceptibility to infection with hemi-biotrophic pathogens, I tested the mutants for susceptibility to the necrotrophic fungus *B. cinerea*. Five week-old *Atnap1s* mutants leaves were inoculated with *B. cinerea* spores droplets, and lesion symptoms were scored three days post-inoculation. Interestingly, both KO mutants *m123-1*

and *m123-2* were more resistant to *B. cinerea*, while the OE mutants were not much different from Col-0 (**Figure 5.7C**).

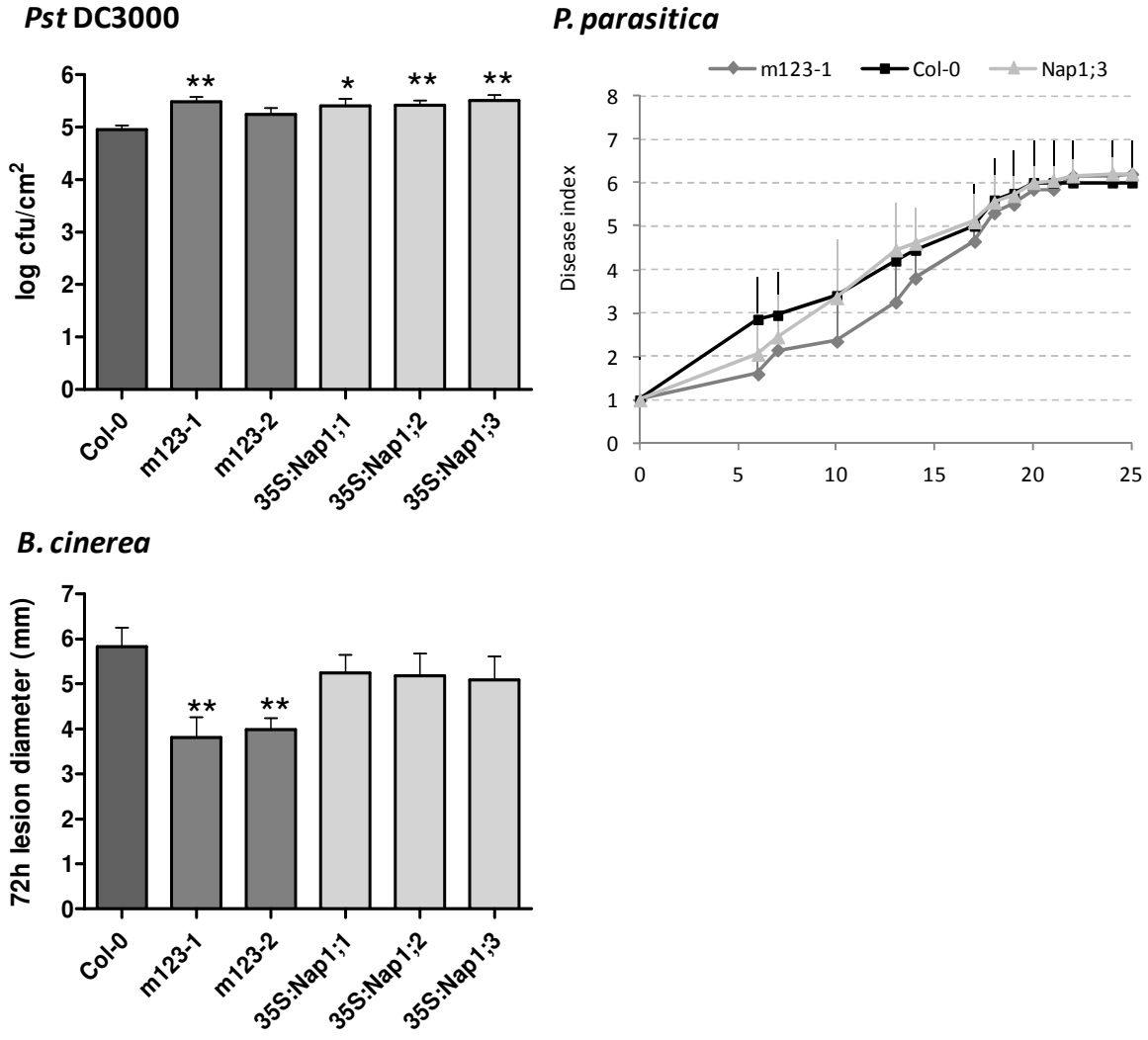

Figure 5.7. *Atnap1s* mutants susceptibility to hemi-biotrophic and necrotrophic pathogens.

A, Five week-old Arabidopsis *Atnap1s* mutants leaves were syringe-infiltrated with 5×10^5 cfu/mL *Pst* DC3000, and bacterial populations were measured at 3 dpi. Asterisks represent the significance of individual unpaired t-tests comparing the given column with the Col-0 control (one: $p<0.05$, two: $p<0.001$). However as bacterial growth differences varied and did not exceed 0.5 log in two biological replicates, *Atnap1s* mutants are considered not different from Col-0. **B**, Arabidopsis *Atnap1s* mutants roots were infected with 500 zoospores of *P. parasitica* and disease symptoms were measured up to 25 dpi. **C**, Five week-old Arabidopsis *Atnap1s* mutants leaves were inoculated with 2.5×10^5 spores/mL of *B. cinerea* and lesion symptoms were measured at 3 dpi. These experiments were repeated twice with similar results. Asterisks represent the significance of individual unpaired t-tests comparing the given column with the Col-0 control ($p<0.001$). It should be noted that using a one-way ANOVA with Bonferroni post-hoc comparison tests, m123-2 was not found significantly different from Col-0 (m123-1 was, $p<0.05$), but individual t-tests show a difference between this condition and the control ($p<0.001$).

It is surprising to find that the KO mutants show altered susceptibility to *B. cinerea* (and not the other hemi-biotrophic pathogens tested) while the OE mutants did not have a phenotype. As biotrophic and necrotrophic pathogens induce different defence responses, this result suggests that AtNAP1s manipulation by putative pathogen effectors may be a common feature of several plant pathogens. It would therefore be worth assessing if *AtNap1s* are important to other Arabidopsis biotrophic and necrotrophic pathogens in order to determine whether *AtNap1s* are specifically involved in the susceptibility to *Hpa* or if *AtNap1s* are also involved in the susceptibility of pathogens with distinct lifestyles and ecological behaviours, as the results presented here seem to show.

5.3. Conclusion and perpectives

In this chapter, I showed that two *Hpa* effector candidates, HaRxL79 and HaRxL67, interact with AtNAP1s *in planta*. In addition, the *Atnap1s* mutants (knock-out and over-expression mutants) display altered susceptibility to *Hpa*. Interestingly, the loss of *AtNap1s* caused an increase of resistance, while *AtNap1s* over-expression led to an increased susceptibility to *Hpa*. In addition, my results indicate that general defence responses (gene induction, ROS production) were not altered in *Atnap1s* mutants. Taken together, these data strongly suggest that *AtNap1s* act as susceptibility factors during *Hpa* infection of Arabidopsis, possibly upon the action of HaRxL79 and HaRxL67. Indeed, it appears plausible that HaRxL79 and HaRxL67 are secreted in the plant cytoplasm during infection and target specifically the AtNAP1s in order to promote susceptibility.

The possibility that histone chaperones are susceptibility factors is unprecedented and is a novel major finding of this thesis. The susceptibility factors described so far are mostly involved in amino-acid metabolism and cell wall integrity (Vogel et al. 2002; Nishimura et al. 2003; Vogel et al. 2004; van Damme et al. 2008; Quentin et al. 2009; van Damme et al. 2009; Stuttmann et al. 2011). More recently, two bHLH transcription factors were identified to contribute to plant susceptibility to the root nematode *Heterodera schachtii* (Jin et al. 2011), suggesting that not only the host metabolism and integrity matter for susceptibility but also the manipulation of gene expression. Although the precise mechanisms by which AtNAP1s manipulation leads to susceptibility need to be identified, this study provides a preliminary and valuable insight on the subject.

Different approaches could be used in the future to investigate this. We could first determine if HaRxL79 and HaRxL67 have a biochemical activity on AtNAP1s that could "modify" them. One strategy, currently pursued in our laboratory, is to use mass-spectrometry (MS) which could help to identify AtNAP1s modifications (like phosphorylations) by HaRxL79/67 either in a transient heterologous system or in *Hpa* infected tissues. For instance, full-length YFP-tagged AtNAP1s are currently produced in good enough quantities in the plant cell to be subjected to MS. I have already established that a good coverage of AtNAP1s peptides is obtained by MS (data not shown).

Another alternative to identify AtNAP1s function during *Hpa* infection could be to look for modifications in their described histone chaperone function. AtNAP1s histone chaperone function was never assessed, but because *AtNap1;1* can complement the yeast *nap1* mutant, and because AtNAP1s interact with each other and with H2A (Galichet and Gruissem 2006, Liu et al. 2009), it was supposed that AtNAP1s are true H2A and H2B chaperones. Assuming that this point is true, it is possible that HaRxL79/67 act on the H2A/H2B incorporation into nucleosomes. With the help of Dr. Vardis Ntoukakis (The Sainsbury Laboratory), I conceived an experiment based on a fluorescence recovery after photobleaching (FRAP) assay (**Figure 5.8**).

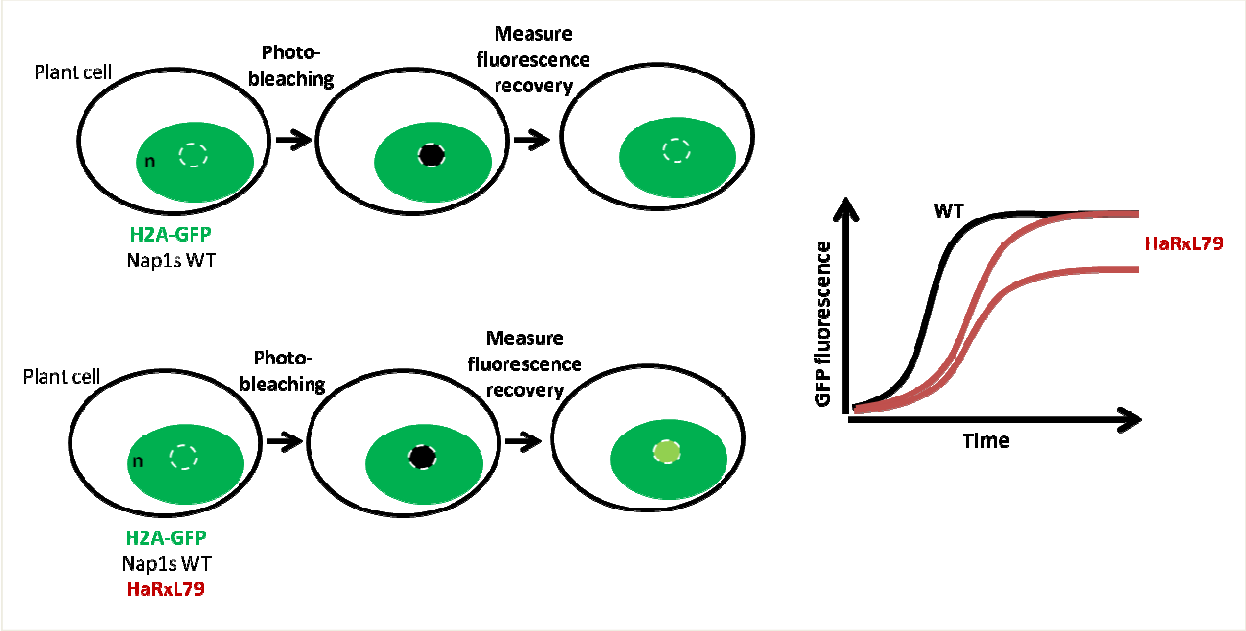

Figure 5.8. Schematic representation of the FRAP assay established to determine HaRxL79 role on H2A incorporation into nucleosomes.

A small area in the nucleus producing H2A-GFP protein is photobleached. The fluorescence recovery of the photobleached area is measured over time in the presence or absence of HaRxL79. The hypothesis to test is that the fluorescence recovery of H2A-GFP is impaired (delayed or reduced, as shown in red on the graph) in the presence of HaRxL79.

The idea is to perform FRAP on a transgenic line expressing both tagged H2A and HaRxL79. FRAP on an H2A-GFP line was developed in Dr. Peter Shaw's laboratory at the John Innes Centre and allows measuring the speed of *de novo* nucleosome assembly after photobleaching. This [H2A-GFP, Dex:HA-HaRxL79] line would be used to determine if when photobleaching the H2A-GFP signal in a small area in the nucleus, the presence of HaRxL79 impairs *de novo* nucleosome assembly (**Figure 5.8**). F1 progenies derived from a cross between an Arabidopsis transgenic line constitutively expressing GFP-tagged H2A (Dr. Peter Shaw laboratory, John Innes Centre, unpublished) and a Dex:HA-HaRxL79 line (HA-tagged HaRxL79 line) were recently obtained.

Even if the prospect of identifying a new family of susceptibility factors is exciting, it is nonetheless puzzling that two *Hpa* effector candidates, HaRxL79 and HaRxL67, with such different *in planta* subcellular localisations, both interact with AtNAP1s. As for now, we do not know if HaRxL79 and HaRxL67 target AtNAP1s similarly or in different specific ways or if there are part of a bigger complex. It is plausible that AtNAP1s are plant proteins with a central role in response to pathogens, in the same way as RIN4 is the target of several bacterial effectors and gets cleaved or phosphorylated which leads to subsequent defence signalling (Mackey et al. 2002; Axtell et al. 2003; Axtell and Staskawicz 2003; Mackey et al. 2003; Kim et al. 2005). In any case, results of this chapter imply that AtNAP1s are important for *Hpa* growth on Arabidopsis.

6. General discussion

Elucidating how pathogens suppress host immunity and promote disease is a major objective in the plant-microbe interaction research field. In this thesis I focused my work on investigating the role of downy mildew effectors in host resistance and susceptibility. The "effectoromics" project running in the laboratory and in which I took part was meant to identify key virulence factors and study their function in an effort to understand how *Hpa* colonises its host. The *Hpa*/Arabidopsis model to understand plant susceptibility and resistance may enable translation of this knowledge to more economically important Brassicaceae crops.

How to define effectors?

Effector genes are genes with an extended phenotype as defined by Richard Dawkins as they are produced by the pathogen but have an effect in the plant host cells (Dawkins 1999). Effectors are versatile molecules that promote plant susceptibility but can be recognised by plant resistance genes. Because *Hpa* cannot be genetically manipulated, we cannot generate knock-out mutants in effector candidate genes that would allow us to define their role in plant susceptibility. It is easier to identify effectors that have an avirulence phenotype *in planta*, because they are recognised by plant resistance genes and trigger macroscopic cell death.

The dominant class of intracellular effectors described in oomycete plant pathogens is the RxLR effector family, as initially four oomycete effectors recognised *in planta* were identified to carry an N-terminal RxLR motif (Allen et al. 2004; Shan et al. 2004; Armstrong et al. 2005; Rehmany et al. 2005). One hundred and thirty four RxLR effector candidates (HaRxLs) have been predicted in the *Hpa* Emoy2 reference genome (Baxter et al. 2010), and more than the 30 or so T3E are deployed by the bacterial pathogen *P. syringae* (Lindeberg et

al. 2006). Even this number of predicted HaRxLs is smaller than the 400 RxLR effectors predicted in *P. infestans* (Haas et al. 2009); depending on how many of these candidates are functional, this raises the question of effector redundancy. Effector redundancy has been observed in the bacterium *P. syringae*, for example AvrPto and AvrPtoB, and HopM1, AvrE and HopR1 (Lin and Martin 2005; Badel et al. 2006; Kvitko et al. 2009; Munkvold et al. 2009). So in *Hpa*, with a bigger genome, and for which more effectors have been predicted, there may be extensive effector redundancy. Further, as shown by Fabro et al. (2011) not every effector may be functional in every Arabidopsis accession.

Conceivably, *Hpa* effector expression is temporally and/or spatially regulated, as shown in other pathosystems. Bacterial pathogens like *Salmonella* produce and then secrete effectors in a temporal manner in order to fine-tune host manipulation processes (Schlumberger and Hardt 2006). The maize pathogen *U. maydis* has been shown to produce different sets of effectors in different organs during its 14 day life cycle (Skibbe et al. 2010).

The assumption of HaRxLs translocation is based on the observation that avirulent RxLR effectors such as ATR1, ATR13, Avr3a and RxLR-like effectors such as ATR5, are recognised by cytoplasmic resistance genes. It is important to keep in mind that we have no direct proof that oomycete plant pathogens can translocate hundreds of RxLR effectors into their host cells. The only direct proof of RxLR effector translocation into host cells comes from the immunolocalisation experiments done in fish cells for a *S. parasitica* RxLR effector (van West et al. 2010). Therefore HaRxLs are presumed to be translocated into plant cells. But what about all the HaRxLs for which no recognition has been observed? How can one be sure that they are translocated into the plant cells and are not playing some other role, such as a structural role at the EHMx? Notably, some *Albugo* RxLR proteins might even be structural components of the haustorium (Dr. A. Kemen and Dr. E. Kemen, The Sainsbury laboratory, unpublished). Despite assuming HaRxLs translocation into plant cells, we decided to go

forward and characterise HaRxLs function *in planta* using different methods. Indeed, if we can identify HaRxLs functions in the plant, it would bring evidence that effectors are translocated.

The particular case of avirulent effectors

ATR13 is interesting because it confers both avirulence and virulence activity to *Hpa* and *Pst* DC3000 (Sohn et al. 2007; Rentel et al. 2008). Sohn et al. (2007) made the puzzling observation that when delivered alone by *Pst* DC3000, $ATR13^{Emco5}$ is recognised in the Arabidopsis accession Ws-0, despite the fact that *Hpa* Emco5 can complete its life cycle on Ws-0. $ATR13^{Emco5}$ recognition triggers a weak HR and is sufficient to restrict bacterial growth (Sohn et al. 2007). I therefore investigated $ATR13^{Emco5}$ recognition in Ws-0.

I showed in **Chapter 3** that in accession Ws-0, $RPP13^{Ws}$ is not involved in $ATR13^{Emco5}$ recognition, contrary to what was expected. I also demonstrated that $ATR13^{Emco5}$ recognition is due to a novel single dominant resistance gene, *RHA13*, and presented several attempts to map its precise genomic location. I did not identify *RHA13* locus because of the $ATR13^{Emco5}$ weak phenotype complicating the mapping procedure. However it is exciting to have identified an additional resistance source to ATR13 that is *RPP13*-independent.

Additional resistance sources to various *ATR13* alleles have been already reported, and map to different loci (Hall et al. 2009): (a) the accession UKID8 is resistant to *Hpa* Hind2 and $ATR13^{Hind2}$ is recognised in UKID8 by a single dominant gene other than $RPP13^{UKID8}$; (b) the accessions UKID44 and UKID71 are susceptible to *Hpa* Maks9, but $ATR13^{Maks9}$ is recognised in these accessions by a single dominant gene other than $RPP13^{UKID44}$ or $RPP13^{UKID71}$ (Hall et al. 2009). Interestingly, Hall et al. (2009) mapped the resistance gene recognising $ATR13^{Maks9}$ to chromosome 1 in UKID44 and UKID71 (and not chromosome 4 as in my work), suggesting that Arabidopsis may have evolved various receptors and systems

to recognise this particular effector. It is worth noting that RPP13 can also recognise other (unknown) effector(s) than ATR13 (Hall et al. 2009).

I have not explained the paradox that despite *Hpa* Emco5 growth and reproduction on Ws-0, ATR13^{Emco5} is recognised in this accession, and I could not discriminate between the two following hypotheses: either *Hpa* Emco5 can suppress the ATR13^{Emco5}-triggered HR in Ws-0, possibly through the action of additional effectors jointly secreted with ATR13^{Emco5}, or the recognition of ATR13^{Emco5} in Ws-0 could be too weak to result in full resistance to *Hpa* Emco5, allowing the pathogen to overcome this weaker form of resistance.

The avirulence phenotype of ATR13 has been extensively investigated in the last decade. However, little is known about the function of this "model" *Hpa* effector. ATR13 contributes to *Hpa* virulence on Arabidopsis (as shown by Sohn et al. 2007 and Rentel et al. 2008) and converging evidence seem to pinpoint that this particular effector is of unusual importance for the pathogen and consequently for the plant immune system. Although the precise virulence function of ATR13 is unknown, a recently published large-scale Y2H assay (Mukhtar et al. 2011) revealed Arabidopsis proteins that interact with ATR13 and that are therefore putative virulence targets, which may provide good starting points for future characterisation studies. Additionally, some but not all alleles of *ATR13* encode proteins that are located in the nucleolus (Leonelli et al. 2011).

Virulence and avirulence functions are often physically distinct on the effector protein. This is the case for the bacterial effector AvrRpt2, in which mutations abolishing its avirulence activity, preserved its virulence activity, because of the reduced degradation of RIN4 (Lim and Kunkel 2004). This is also the case for *P. infestans* Avr3a, as the PIP binding positively charged patch of Avr3a is not involved in R3a-mediated recognition, but is required for suppression of INF1-induced cell death and CMPG1 accumulation (Yaeno et al. 2011).

How to characterise effector functions?

Hpa cannot be genetically manipulated, therefore we had to develop assays and use heterologous systems to assess HaRxL functions. Several screens were developed in our laboratory. Two screens, led by Dr. Fabro and Dr. Badel, were based on using the *Pst* DC3000 EDV system to assess the HaRxL effects on bacterial virulence and bacterial fitness *in planta*, respectively (Sohn et al. 2007; Fabro et al. 2011; Badel et al. *in preparation*). Another screen based on the subcellular localisation of the HaRxLs *in planta* was led by Dr. Caillaud (Caillaud et al. 2012). The last screen was led by collaborators and aimed to identify HaRxL plant targets (Mukhtar et al. 2011). HaRxL heterologous expression systems were used in this thesis work as it is often the method of choice for recalcitrant organisms. Yet, these results should be handled with caution since expression levels as well as post-translational modifications occurring in the native organism are known to influence protein folding, biochemical properties and subcellular localisation (Stulemeijer and Joosten 2008).

One approach to understand in which plant biological pathway the effector takes part is to identify its plant interacting proteins. This aspect was investigated using Y2H assay. The identification of HaRxL putative plant targets by Y2H helped our understanding of HaRxL possible mode of actions. However, the identification of HaRxL plant interactors by Y2H assay should also be handled with caution since false positives can occur. *Hpa* and Arabidopsis proteins can be auto-activated in yeast, which makes it more difficult to find specific binding partners that will enhance reporter gene expression as it is already activated. This is the case for HaRxL62 which activates the yeast reporter gene without a binding partner. This is also the case for the plant CSN5 protein which was identified to interact with multiple HaRxLs and *P. syringae* T3E (Nordgard et al. 2001; Mukhtar et al. 2011).

What have we learnt looking for effector functions?

Despite some drawbacks existing in our assays to test HaRxL functions, the four screens described above led to the identification of interesting HaRxLs and to their initial characterisation. Altogether we showed that HaRxLs localise to different plant subcellular compartments (Caillaud et al. 2012), and can alter plant susceptibility to pathogens (Fabro et al. 2011, Caillaud et al. 2012).

The first screen (HaRxL-EDV screen) identified 64 HaRxLs that confer enhanced or decreased virulence of *Pst* DC3000 on at least one Arabidopsis accession (Fabro et al. 2011). Most of the HaRxLs identified confer increased *Pst* DC3000 virulence on a subset of Arabidopsis accessions, suggesting that these HaRxLs may promote *Hpa* growth in Arabidopsis. Only few HaRxLs conferred reduced *Pst* DC3000 virulence but none triggered macroscopic HR symptoms characteristic of avirulent effectors. In a similar screen meant to identify avirulence factors, (Goritschnig et al. 2012) screened 18 HaRxLs versus 83 Arabidopsis accessions to identify a single new avirulent effector ATR39, highlighting the fact that avirulence is rare. Interestingly, we observed that HaRxLs performed differently in different Arabidopsis accessions, suggesting that the effector repertoire might be different from one host plant to another. This hypothesis correlates well with the observation that *Hpa* virulence varies from one accession to another (Nemri et al. 2010). Fabro et al. (2011) also observed that increased bacterial virulence conferred by certain HaRxLs was linked to the suppression of PTI responses. Notably, HaRxLs were expressed in a non-host plant (turnip) in order to test if they were active. HaRxLs that confer increased bacterial virulence in Arabidopsis, mostly confer increased bacterial virulence in turnip too, but some did not. This suggests that only some HaRxLs plant targets are conserved between Arabidopsis and turnip, but also that turnip may be a non-host for *Hpa* because some HaRxLs are not functional or recognised in turnip.

The second screen was based on the subcellular localisation of 49 HaRxLs, transiently expressed in *N. benthamiana* (Caillaud et al. 2012). This screen identified that HaRxLs target predominantly the plant nucleus and membranes. Notably, this screen identified HaRxL17 as a tonoplast-associated effector conferring increased virulence to compatible and incompatible *Hpa* isolates. Caillaud et al. (2012) reported HaRxL17 localisation at the EHM in infected tissues (Caillaud et al. 2012, Caillaud et al. in press). This important result supports the idea that the EHM may be a tonoplast-derived membrane as suggested by Chou (Chou 1970) and is well correlated with the unusual vacuolar dynamics observed in *Hpa*-infected cells (Caillaud et al. 2012). Given how little we know about the *Hpa*/Arabidopsis interface, HaRxL17 can be exploited to further investigate the composition and function of the EHM during haustorium ontogenesis (Caillaud et al. in press). In parallel, another group showed that the *P. infestans* RxLR effector Avrblb2 focally accumulates around haustoria in infected tissues (Bozkurt et al. 2011), but they could not pinpoint its localisation to the EHM as did Caillaud et al. (2012).

Sixty six percent of the HaRxLs tested localised to the plant nucleus, among which 33% localised strictly to the nucleus and 21% localised strictly to the nucleolus (Caillaud et al. 2012). Conceivably, these nucleus/nucleolus localised HaRxLs hijack plant nuclear processes like transcription in order to promote susceptibility. Increasing evidence suggests that many pathogen effectors target the plant nucleus. This is the case for several bacterial effectors (Tasset et al. 2010), *P. infestans* CRNs effector proteins (Schornack et al. 2010), *Glomus intraradices* SP7 (Kloppholz et al. 2011), and for several cyst nematodes effectors (Tytgat et al. 2005; Jones et al. 2009). In the laboratory, nuclear-localised HaRxLs are of particular interest and the characterisation of their function is being analysed by expression profiling in transgenic Arabidopsis expressing HaRxLs (developed by Dr. Rallapalli in the laboratory). The analysis of expression changes at the Arabidopsis genome-scale could reveal plant

processes in which HaRxLs are involved. Arabidopsis transgenic lines expressing nuclear-localised effector genes are used for this type of analysis, conducted by Dr. Asai in the laboratory.

The combined approach of several screens was very successful in identifying *bona fide* *Hpa* effectors from the initial RxLR effector candidates list (Baxter et al. 2010). If the reader compares the **Table 1.2** presented in **Chapter 1** summarising what we know about oomycete effectors translocated into the host cells, with the **Table 4.1** presented in **Chapter 4**, summarising the data we generated in our laboratory for these last four years, it becomes clear that the approaches undertaken were fruitful and constitute the basis for a new area which will focus on the effector's biology itself. Follow up work on several *Hpa* effectors is currently underway in the laboratory.

What have we learnt about the role of HaRxL79 during infection?

Particularly, from the HaRxLs subcellular localisation screen, I identified one HaRxL with a peculiar localisation to plant microtubules (**Chapter 4**). HaRxL79-GFP co-localised with the microtubule marker MAP4-RFP, and more importantly showed a dotty pattern on the microtubules, suggesting that HaRxL79 could be associated with kinesin(s). Very interestingly, by Y2H assay, HaRxL79 was shown to interact with two putative microtubules associated proteins, a kinesin and a kinesin light chain protein (**Chapter 4**, Mukhtar et al. 2011). Why would HaRxL79 associate with kinesins? Conceivably HaRxL79 can either interfere with microtubule trafficking or hijack microtubules to target a specific plant subcellular compartment. However, HaRxL79 mode of action seems different from HopZ1a, the only plant pathogen effector (from *P. syringae*) that was reported to target microtubules. HopZ1a acetylates tubulin oligomers and degrades microtubules structure (Dr. David Guttman, Toronto University, oral conference communication). The prospect of having

identified an effector that targets plant microtubules is really exciting as little is known about microtubules role in *Hpa*-infected cells, even if it appears clear that cytoskeleton dynamics is altered in infected cells (Takemoto et al. 2003; Caillaud et al. 2012; personal communication from Dr. Mickael Quentin, INRA Nice-Sophia-Antipolis).

I showed that *HaRxL79* belongs to a gene family in *Hpa* Emoy2 in which paralogs share a conserved N-terminus but exhibit very divergent C-termini. Interestingly three HaRxL79 paralogs localise to three different plant subcellular compartments, suggesting that the C-terminal part of HaRxL79 paralogs direct them to specific plant subcellular compartments and is responsible for the effector's function. *HaRxL79* gene family is present but extremely diversified in all *Hpa* isolates tested and seems absent from the closely related *Phytophthora spp*., suggesting that this gene family is likely under high evolution pressure and has a crucial role during *Hpa* infection, and possibly in *Hpa* biotrophy.

From the Y2H assay performed by collaborators, HaRxL79 was shown to interact with two histone chaperones, AtNAP1;1 and AtNAP1;2 (Mukhtar et al. 2011). I confirmed that HaRxL79 interacts with AtNAP1;1, AtNAP1;2 and AtNAP1;3 (referred as AtNAP1s) *in planta*. Interestingly, collaborators in Germany showed HaRxL67, another HaRxL, to interact with AtNAP1s in Arabidopsis (Dr. Fraiture and Dr. Brunner, personnal communication). Because AtNAP1s are targeted by HaRxLs, I investigated *AtNap1s* function during *Hpa* infection. *Atnap1s* mutants displayed altered susceptibility to *Hpa*. Interestingly, the loss of *AtNap1s* caused an increase of resistance, while *AtNap1s* over-expression led to an increased susceptibility to *Hpa*. In addition, my results indicated that the general defence responses were not altered in *Atnap1s* mutants. Taken together, these data strongly suggest that *AtNap1s* act as susceptibility factors during *Hpa* infection, possibly upon the action of HaRxL79 and HaRxL67. Indeed, it appears plausible that HaRxL79 and HaRxL67 are

secreted in the plant cytoplasm during infection and target specifically the AtNAP1s in order to promote susceptibility.

The possibility that histone chaperones are susceptibility factors is a novel major finding of this thesis. The susceptibility factors described so far are mostly involved in amino-acid metabolism and cell wall integrity (Vogel et al. 2002; Nishimura et al. 2003; Vogel et al. 2004; van Damme et al. 2007; van Damme et al. 2009; Quentin et al. 2009; Stuttmann et al. 2011). Although the precise mechanisms by which AtNAP1s manipulation leads to susceptibility need to be identified, this study provides a preliminary yet valuable insight on the subject.

Even if the prospect of identifying a new family of susceptibility factors is exciting, it is nonetheless puzzling that two *Hpa* effector candidates, HaRxL79 and HaRxL67, with such different subcellular localisations *in planta*, both interact with AtNAP1s. As for now, we do not know if HaRxL79 and HaRxL67 target AtNAP1s similarly or in different specific ways or if there are part of a bigger complex. It is conceivable that AtNAP1s are plant proteins with a central role in response to pathogens, in the same way as RIN4 is the target of several bacterial effectors and gets cleaved or phosphorylated which leads to subsequent defence signalling (Mackey et al. 2002; Axtell et al. 2003; Axtell and Staskawicz 2003; Mackey et al. 2003; Kim et al. 2005).

Concluding remarks

This thesis work attempted to elucidate some of the molecular mechanisms involved in the Arabidopsis/*Hpa* interaction. We definitely learned a lot in four years. To describe in two sentences the highlights of my thesis work, I would say that: I contributed to the identification of various HaRxLs phenotypes *in planta* (Fabro et al. 2011; Caillaud et al. 2012; Caillaud et al. in press; Badel et al. *in preparation*). In addition, I identified in Arabidopsis a good susceptibility factor candidate, the *AtNap1s* gene family that is targeted by at least two *Hpa* effectors.

Several major questions, recently reviewed by Hok and colleagues (Hok et al. 2010), are still unanswered:

a) how and when HaRxLs are delivered into plant cells?

b) what are the plant targets of effectors?

c) what are the mechanisms by which effectors hijack plant proteins?

d) what is the role of the plant targets in the absence of the pathogen?

By answering to these questions and particularly by understanding how effectors manipulate their hosts in order to promote susceptibility, we will gain knowledge on how to help crops resist plant pathogens.

References

Aarts, N., et al. (1998). "Different requirements for EDS1 and NDR1 by disease resistance genes define at least two R gene-mediated signaling pathways in Arabidopsis." Proc Natl Acad Sci U S A **95**(17): 10306-11.

Alfano, J. R. and A. Collmer (2004). "Type III secretion system effector proteins: double agents in bacterial disease and plant defense." Annu Rev Phytopathol **42**: 385-414.

Allen, R. L., et al. (2004). "Host-parasite coevolutionary conflict between Arabidopsis and downy mildew." Science **306**(5703): 1957-60.

Allen, R. L., et al. (2008). "Natural variation reveals key amino acids in a downy mildew effector that alters recognition specificity by an Arabidopsis resistance gene." Mol Plant Pathol **9**(4): 511-23.

Angelov, D., et al. (2006). "Nucleolin is a histone chaperone with FACT-like activity and assists remodeling of nucleosomes." Embo J **25**(8): 1669-79.

Arabidopsis Interactome Mapping, C. (2011). "Evidence for Network Evolution in an Arabidopsis Interactome Map." Science **333**(6042): 601-607.

Armstrong, M. R., et al. (2005). "An ancestral oomycete locus contains late blight avirulence gene Avr3a, encoding a protein that is recognized in the host cytoplasm." Proc Natl Acad Sci U S A **102**(21): 7766-71.

Attard, A., et al. (2010). "The immediate activation of defense responses in Arabidopsis roots is not sufficient to prevent Phytophthora parasitica infection." New Phytol **187**(2): 449-60.

Austin, M. J., et al. (2002). "Regulatory role of SGT1 in early R gene-mediated plant defenses." Science **295**(5562): 2077-80.

Axtell, M. J., et al. (2003). "Genetic and molecular evidence that the Pseudomonas syringae type III effector protein AvrRpt2 is a cysteine protease." Mol Microbiol **49**(6): 1537-46.

Axtell, M. J. and B. J. Staskawicz (2003). "Initiation of RPS2-specified disease resistance in Arabidopsis is coupled to the AvrRpt2-directed elimination of RIN4." Cell **112**(3): 369-77.

Badel, J. L., et al. (2006). "A Pseudomonas syringae pv. tomato avrE1/hopM1 mutant is severely reduced in growth and lesion formation in tomato." Mol Plant Microbe Interact **19**(2): 99-111.

Bailey, K., et al. (2010). "Molecular cloning of ATR5(Emoy2) from Hyaloperonospora arabidopsidis, an avirulence determinant that triggers RPP5-mediated defense in Arabidopsis." Mol Plant Microbe Interact **24**(7): 827-38.

Bailey, K., et al. (2011). "Molecular cloning of ATR5(Emoy2) from Hyaloperonospora arabidopsidis, an avirulence determinant that triggers RPP5-mediated defense in Arabidopsis." Mol Plant Microbe Interact **24**(7): 827-38.

Ballvora, A., et al. (2002). "The R1 gene for potato resistance to late blight (Phytophthora infestans) belongs to the leucine zipper/NBS/LRR class of plant resistance genes." Plant J **30**(3): 361-71.

Baxter, L., et al. (2010). "Signatures of adaptation to obligate biotrophy in the Hyaloperonospora arabidopsidis genome." Science **330**(6010): 1549-51.

Beakes, G. W., et al. (2011). "The evolutionary phylogeny of the oomycete "fungi"." Protoplasma.

Bentley, G. A., et al. (1984). "The crystal structure of the nucleosome core particle by contrast variation." Basic Life Sci **27**: 105-17.
Bhattacharjee, S., et al. (2006). "The malarial host-targeting signal is conserved in the Irish potato famine pathogen." PLoS Pathog **2**(5): e50.
Bisgrove, S. R., et al. (1994). "A disease resistance gene in Arabidopsis with specificity for two different pathogen avirulence genes." Plant Cell **6**(7): 927-33.
Bittner-Eddy, P., et al. (1999). "Genetic and physical mapping of the RPP13 locus, in Arabidopsis, responsible for specific recognition of several Peronospora parasitica (downy mildew) isolates." Mol Plant Microbe Interact **12**(9): 792-802.
Bittner-Eddy, P. D., et al. (2003). "Use of suppression subtractive hybridization to identify downy mildew genes expressed during infection of Arabidopsis thaliana." Mol Plant Pathol **4**(6): 501-7.
Bittner-Eddy, P. D. and J. L. Beynon (2001). "The Arabidopsis downy mildew resistance gene, RPP13-Nd, functions independently of NDR1 and EDS1 and does not require the accumulation of salicylic acid." Mol Plant Microbe Interact **14**(3): 416-21.
Bittner-Eddy, P. D., et al. (2000). "RPP13 is a simple locus in Arabidopsis thaliana for alleles that specify downy mildew resistance to different avirulence determinants in Peronospora parasitica." Plant J **21**(2): 177-88.
Block, A. and J. R. Alfano (2011). "Plant targets for Pseudomonas syringae type III effectors: virulence targets or guarded decoys?" Curr Opin Microbiol **14**(1): 39-46.
Blume, B., et al. (2000). "Receptor-mediated increase in cytoplasmic free calcium required for activation of pathogen defense in parsley." Plant Cell **12**(8): 1425-1440.
Bos, J. I. B., et al. (2010). "Phytophthora infestans effector AVR3a is essential for virulence and manipulates plant immunity by stabilizing host E3 ligase CMPG1." Proceedings of the National Academy of Sciences of the United States of America **107**(21): 9909-9914.
Botella, M. A., et al. (1998). "Three genes of the arabidopsis RPP1 complex resistance locus recognize distinct Peronospora parasitica avirulence determinants." Plant Cell **10**(11): 1847-1860.
Boutemy, L. S., et al. (2011). "Structures of Phytophthora RXLR effector proteins: a conserved but adaptable fold underpins functional diversity." J Biol Chem **286**(41): 35834-42.
Bouwmeester, K., et al. (2011). "The Lectin Receptor Kinase LecRK-I.9 Is a Novel Phytophthora Resistance Component and a Potential Host Target for a RXLR Effector." Plos Pathogens **7**(3).
Bozkurt, T. O., et al. (2011). "Phytophthora infestans effector AVRblb2 prevents secretion of a plant immune protease at the haustorial interface." Proc Natl Acad Sci U S A **108**(51): 20832-7.
Bozkurt, T. O., et al. (in press). "Phytophthora infestans effector AVRblb2 prevents secretion of a plant immune protease at the haustorial interface." Proc Natl Acad Sci U S A.
Brunner, F., et al. (2002). "Pep-13, a plant defense-inducing pathogen-associated pattern from Phytophthora transglutaminases." Embo Journal **21**(24): 6681-6688.
Cabral, A., et al. (2011). "Identification of Hyaloperonospora arabidopsidis transcript sequences expressed during infection reveals isolate-specific effectors." PLoS One **6**(5): e19328.
Caillaud, M.-C., et al. (2012). "Subcellular localization of the Hpa RxLR effector repertoire identifies a tonoplast-associated protein HaRxL17 that confers enhanced plant susceptibility." The Plant Journal **69**(2): 252-265.
Caillaud, M., et al. (in press). "Characterization of the membrane-associated HaRxL17 Hpa effector candidate." Plant Signalling and Behavior.

Caillaud, M. C., et al. (2008). "Cytoskeleton reorganization, a key process in root-knot nematode-induced giant cell ontogenesis." Plant Signal Behav **3**(10): 816-8.
Caillaud, M. C., et al. (2009). "Spindle assembly checkpoint protein dynamics reveal conserved and unsuspected roles in plant cell division." PLoS One **4**(8): e6757.
Cao, H., et al. (1997). "The Arabidopsis NPR1 gene that controls systemic acquired resistance encodes a novel protein containing ankyrin repeats." Cell **88**(1): 57-63.
Cao, J., et al. (2011). "Whole-genome sequencing of multiple Arabidopsis thaliana populations." Nat Genet **43**(10): 956-63.
Century, K. S., et al. (1995). "NDR1, a locus of Arabidopsis thaliana that is required for disease resistance to both a bacterial and a fungal pathogen." Proc Natl Acad Sci U S A **92**(14): 6597-601.
Century, K. S., et al. (1997). "NDR1, a pathogen-induced component required for Arabidopsis disease resistance." Science **278**(5345): 1963-5.
Champouret, N., et al. (2009). "Phytophthora infestans isolates lacking class I ipiO variants are virulent on Rpi-blb1 potato." Mol Plant Microbe Interact **22**(12): 1535-45.
Chaparro-Garcia, A., et al. (2011). "The receptor-like kinase SERK3/BAK1 is required for basal resistance against the late blight pathogen phytophthora infestans in Nicotiana benthamiana." PLoS One **6**(1): e16608.
Chevreux, B., et al. (1999). "Genome Sequence Assembly Using Trace Signals and Additional Sequence Information." German Conference on Bioinformatics, from citeulike-article-id:8949626
http://citeseerx.ist.psu.edu/viewdoc/summary?doi=10.1.1.23.7465
Chinchilla, D., et al. (2007). "A flagellin-induced complex of the receptor FLS2 and BAK1 initiates plant defence." Nature **448**(7152): 497-500.
Chisholm, S. T., et al. (2006). "Host-microbe interactions: shaping the evolution of the plant immune response." Cell **124**(4): 803-14.
Chou, C. K. (1970). "An Electron-Microscope Study of Host Penetration and Early Stages of Haustorium Formation of Peronospora parasitica (Fr.) Tul. on Cabbage Cotyledons." Ann. Bot. **34**: 189-204.
Chou, S., et al. (2011). "Hyaloperonospora arabidopsidis ATR1 effector is a repeat protein with distributed recognition surfaces." Proc Natl Acad Sci U S A **108**(32): 13323-8.
Clapier, C. R. and B. R. Cairns (2009). "The biology of chromatin remodeling complexes." Annu Rev Biochem **78**: 273-304.
Clough, S. J. and A. F. Bent (1998). "Floral dip: a simplified method for Agrobacterium-mediated transformation of Arabidopsis thaliana." Plant J **16**(6): 735-43.
Coates, M. E. and J. L. Beynon (2010). "Hyaloperonospora Arabidopsidis as a pathogen model." Annu Rev Phytopathol **48**: 329-45.
Consonni, C., et al. (2006). "Conserved requirement for a plant host cell protein in powdery mildew pathogenesis." Nat Genet **38**(6): 716-20.
Cunnac, S., et al. (2009). "Pseudomonas syringae type III secretion system effectors: repertoires in search of functions." Curr Opin Microbiol **12**(1): 53-60.
Daganzo, S. M., et al. (2003). "Structure and function of the conserved core of histone deposition protein Asf1." Curr Biol **13**(24): 2148-58.
Dangl, J. L. and J. D. Jones (2001). "Plant pathogens and integrated defence responses to infection." Nature **411**(6839): 826-33.
Davis, E. L. and M. G. Mitchum (2005). "Nematodes. Sophisticated parasites of legumes." Plant Physiol **137**(4): 1182-8.
Dawkins, R. (1999). The extended phenotype: the long reach of the gene. Oxford, Oxford University Press.

de Bary, H. A. (1863). "Recherches sur le developpement de quelques champignons parasites." Ann Sci Nat Part Bot **20**: 5–148.
de Jonge, R., et al. (2011). "How filamentous pathogens co-opt plants: the ins and outs of fungal effectors." Curr Opin Plant Biol **14**(4): 400-6.
de Koning-Ward, T. F., et al. (2009). "A newly discovered protein export machine in malaria parasites." Nature **459**(7249): 945-9.
DebRoy, S., et al. (2004). "A family of conserved bacterial effectors inhibits salicylic acid-mediated basal immunity and promotes disease necrosis in plants." Proc Natl Acad Sci U S A **101**(26): 9927-32.
Djamei, A., et al. (2011). "Metabolic priming by a secreted fungal effector." Nature **478**(7369): 395-+.
Dodds, P. N., et al. (2006). "Direct protein interaction underlies gene-for-gene specificity and coevolution of the flax resistance genes and flax rust avirulence genes." Proc Natl Acad Sci U S A **103**(23): 8888-93.
Dong, S., et al. (2011). "Phytophthora sojae Avirulence Effector Avr3b is a Secreted NADH and ADP-ribose Pyrophosphorylase that Modulates Plant Immunity." PLoS Pathog **7**(11): e1002353.
Dong, S. M., et al. (2011). "Sequence Variants of the Phytophthora sojae RXLR Effector Avr3a/5 Are Differentially Recognized by Rps3a and Rps5 in Soybean." Plos One **6**(7).
Donofrio, N. M. and T. P. Delaney (2001). "Abnormal callose response phenotype and hypersusceptibility to Peronospora parasitica in defense-compromised Arabidopsis nim1-1 and salicylate hydroxylase-expressing plants." Molecular Plant-Microbe Interactions **14**(4): 439-450.
Dou, D., et al. (2010). "Different domains of Phytophthora sojae effector Avr4/6 are recognized by soybean resistance genes Rps4 and Rps6." Mol Plant Microbe Interact **23**(4): 425-35.
Dou, D., et al. (2008). "Conserved C-terminal motifs required for avirulence and suppression of cell death by Phytophthora sojae effector Avr1b." Plant Cell **20**(4): 1118-33.
Dou, D., et al. (2008). "RXLR-mediated entry of Phytophthora sojae effector Avr1b into soybean cells does not require pathogen-encoded machinery." Plant Cell **20**(7): 1930-47.
Eitas, T. K., et al. (2008). "Arabidopsis TAO1 is a TIR-NB-LRR protein that contributes to disease resistance induced by the Pseudomonas syringae effector AvrB." Proc Natl Acad Sci U S A **105**(17): 6475-80.
Ellis, J., et al. (2006). "The problem of how fungal and oomycete avirulence proteins enter plant cells." Trends Plant Sci **11**(2): 61-3.
Enright, A. J., et al. (2002). "An efficient algorithm for large-scale detection of protein families." Nucleic Acids Res **30**(7): 1575-84.
Espinosa, A. and J. R. Alfano (2004). "Disabling surveillance: bacterial type III secretion system effectors that suppress innate immunity." Cellular Microbiology **6**(11): 1027-1040.
Eulgem, T., et al. (2004). "Gene expression signatures from three genetically separable resistance gene signaling pathways for downy mildew resistance." Plant Physiology **135**(2): 1129-1144.
Fabro, G., et al. (2011). "Multiple Candidate Effectors from the Oomycete Pathogen Hyaloperonospora arabidopsidis Suppress Host Plant Immunity." PLoS Pathog **7**(11): e1002348.

Falk, A., et al. (1999). "EDS1, an essential component of R gene-mediated disease resistance in Arabidopsis has homology to eukaryotic lipases." Proc Natl Acad Sci U S A **96**(6): 3292-7.
Fellbrich, G., et al. (2002). "NPP1, a Phytophthora-associated trigger of plant defense in parsley and Arabidopsis." Plant Journal **32**(3): 375-390.
Feys, B. J., et al. (2001). "Direct interaction between the Arabidopsis disease resistance signaling proteins, EDS1 and PAD4." Embo J **20**(19): 5400-11.
Feys, B. J., et al. (2005). "Arabidopsis SENESCENCE-ASSOCIATED GENE101 stabilizes and signals within an ENHANCED DISEASE SUSCEPTIBILITY1 complex in plant innate immunity." Plant Cell **17**(9): 2601-13.
Flor, H. H. (1971). "Current Status of Gene-for-Gene Concept." Annual Review of Phytopathology **9**: 275-&.
Frye, C. A. and R. W. Innes (1998). "An Arabidopsis mutant with enhanced resistance to powdery mildew." Plant Cell **10**(6): 947-56.
Fuchs, J., et al. (2006). "Chromosomal histone modification patterns--from conservation to diversity." Trends Plant Sci **11**(4): 199-208.
Galan, J. E. and H. Wolf-Watz (2006). "Protein delivery into eukaryotic cells by type III secretion machines." Nature **444**(7119): 567-73.
Galichet, A. and W. Gruissem (2006). "Developmentally controlled farnesylation modulates AtNAP1;1 function in cell proliferation and cell expansion during Arabidopsis leaf development." Plant Physiol **142**(4): 1412-26.
Gan, P. H., et al. (2010). "Lipid binding activities of flax rust AvrM and AvrL567 effectors." Plant Signal Behav **5**(10): 1272-5.
Gao, H., et al. (2005). "Two classes of highly similar coiled coil-nucleotide binding-leucine rich repeat genes isolated from the Rps1-k locus encode Phytophthora resistance in soybean." Mol Plant Microbe Interact **18**(10): 1035-45.
Garcia, A. V., et al. (2010). "Balanced nuclear and cytoplasmic activities of EDS1 are required for a complete plant innate immune response." PLoS Pathog **6**: e1000970.
Gaulin, E., et al. (2006). "Cellulose binding domains of a Phytophthora cell wall protein are novel pathogen-associated molecular patterns." Plant Cell **18**(7): 1766-77.
Gherbi, H., et al. (2008). "SymRK defines a common genetic basis for plant root endosymbioses with arbuscular mycorrhiza fungi, rhizobia, and Frankiabacteria." Proc Natl Acad Sci U S A **105**(12): 4928-32.
Gilroy, E. M., et al. (2011). "Presence/absence, differential expression and sequence polymorphisms between PiAVR2 and PiAVR2-like in Phytophthora infestans determine virulence on R2 plants." New Phytologist **191**(3): 763-776.
Glazebrook, J. (2005). "Contrasting mechanisms of defense against biotrophic and necrotrophic pathogens." Annual Review of Phytopathology **43**: 205-227.
Glazebrook, J., et al. (1996). "Isolation of Arabidopsis mutants with enhanced disease susceptibility by direct screening." Genetics **143**(2): 973-82.
Glazebrook, J., et al. (1997). "Phytoalexin-deficient mutants of Arabidopsis reveal that PAD4 encodes a regulatory factor and that four PAD genes contribute to downy mildew resistance." Genetics **146**(1): 381-92.
Goritschnig, S., et al. (2012). "Computational prediction and molecular characterization of an oomycete effector and the cognate Arabidopsis resistance gene." PLoS Genet **8**(2): e1002502.
Gouget, A., et al. (2006). "Lectin receptor kinases participate in protein-protein interactions to mediate plasma membrane-cell wall adhesions in Arabidopsis." Plant Physiol **140**(1): 81-90.

Grouffaud, S., et al. (2008). "Plasmodium falciparum and Hyaloperonospora parasitica effector translocation motifs are functional in Phytophthora infestans." Microbiology **154**(Pt 12): 3743-51.
Gu, B., et al. (2011). "Rust Secreted Protein Ps87 Is Conserved in Diverse Fungal Pathogens and Contains a RXLR-like Motif Sufficient for Translocation into Plant Cells." PLoS One **6**(11): e27217.
Gurlebeck, D., et al. (2006). "Type III effector proteins from the plant pathogen Xanthomonas and their role in the interaction with the host plant." J Plant Physiol **163**(3): 233-55.
Haas, B. J., et al. (2009). "Genome sequence and analysis of the Irish potato famine pathogen Phytophthora infestans." Nature **461**(7262): 393-8.
Hahlbrock, K., et al. (1995). "Oligopeptide Elicitor-Mediated Defense Gene Activation in Cultured Parsley Cells." Proceedings of the National Academy of Sciences of the United States of America **92**(10): 4150-4157.
Hahn, M. and K. Mendgen (1992). "Isolation by Cona Binding of Haustoria from Different Rust Fungi and Comparison of Their Surface Qualities." Protoplasma **170**(3-4): 95-103.
Hahn, M., et al. (1997). "A putative amino acid transporter is specifically expressed in haustoria of the rust fungus Uromyces fabae." Molecular Plant-Microbe Interactions **10**(4): 438-445.
Haldar, K., et al. (2006). "Common infection strategies of pathogenic eukaryotes." Nat Rev Microbiol **4**(12): 922-31.
Hall, S. A., et al. (2009). "Maintenance of genetic variation in plants and pathogens involves complex networks of gene-for-gene interactions." Mol Plant Pathol **10**(4): 449-57.
Halterman, D. A., et al. (2010). "Competition between Phytophthora infestans effectors leads to increased aggressiveness on plants containing broad-spectrum late blight resistance." PLoS One **5**(5): e10536.
Hammond-Kosack, K. E. and J. D. Jones (1996). "Resistance gene-dependent plant defense responses." Plant Cell **8**(10): 1773-91.
Harder, D. E. and J. Chong (1991). Rust haustoria. Electron microscopy of plant pathogens. K. Mendgen and D. E. Lesemann. Berlin, Springer 235–250.
Harder, D. E. and K. Mendgen (1982). "Filipin-Sterol Complexes in Bean Rust-Fungal and Oat Crown Rust-Fungal Plant Interactions - Freeze-Etch Electron-Microscopy." Protoplasma **112**(1-2): 46-54.
Hardham, A. R., et al. (2008). "Rapid and dynamic subcellular reorganization following mechanical stimulation of Arabidopsis epidermal cells mimics responses to fungal and oomycete attack." Bmc Plant Biology **8**.
Harries, P. A., et al. (2010). "Intracellular transport of viruses and their components: utilizing the cytoskeleton and membrane highways." Mol Plant Microbe Interact **23**(11): 1381-93.
Hauck, P., et al. (2003). "A Pseudomonas syringae type III effector suppresses cell wall-based extracellular defense in susceptible Arabidopsis plants." Proc Natl Acad Sci U S A **100**(14): 8577-82.
Haverkort, A. J., et al. (2008). "Societal Costs of Late Blight in Potato and Prospects of Durable Resistance Through Cisgenic Modification." Potato Research **51**: 47-57.
Heese, A., et al. (2007). "The receptor-like kinase SERK3/BAK1 is a central regulator of innate immunity in plants." Proc Natl Acad Sci U S A **104**(29): 12217-22.
Hok, S., et al. (2010). "Getting the most from the host: how pathogens force plants to cooperate in disease." Mol Plant Microbe Interact **23**(10): 1253-9.

Holub, E. B. (2001). "The arms race is ancient history in Arabidopsis, the wildflower." Nat Rev Genet **2**(7): 516-27.
Holub, E. B. (2007). "Natural variation in innate immunity of a pioneer species." Curr Opin Plant Biol **10**(4): 415-24.
Holub, E. B. (2008). "Natural history of Arabidopsis thaliana and oomycete symbioses." European Journal of Plant Pathology **122**(1): 91-109.
Holub, E. B. and J. L. Beynon, Eds. (1997). Symbiology of mouse-ear cress (*Arabidopsis thaliana*) and oomycetes. Advances in botanical research, Academic press.
Holub, E. B., et al. (1994). "Phenotypic and Genotypic Characterization of Interactions between Isolates of Peronospora-Parasitica and Accessions of Arabidopsis-Thaliana." Molecular Plant-Microbe Interactions **7**(2): 223-239.
Hruz, T., et al. (2008). "Genevestigator v3: a reference expression database for the meta-analysis of transcriptomes." Adv Bioinformatics **2008**: 420747.
Huang, S., et al. (2005). "Comparative genomics enabled the isolation of the R3a late blight resistance gene in potato." Plant J **42**(2): 251-61.
Huitema, E., et al. (2011). "A straightforward protocol for electro-transformation of Phytophthora capsici zoospores." Methods Mol Biol **712**: 129-35.
Innes, R. W., et al. (1993). "Molecular Analysis of Avirulence Gene Avrrpt2 and Identification of a Putative Regulatory Sequence Common to All Known Pseudomonas-Syringae Avirulence Genes." Journal of Bacteriology **175**(15): 4859-4869.
Itoh, R., et al. (2001). "Kinesin-related proteins with a mitochondrial targeting signal." Plant Physiol **127**(3): 724-6.
Jacobs, A. K., et al. (2003). "An Arabidopsis Callose Synthase, GSL5, Is Required for Wound and Papillary Callose Formation." Plant Cell **15**(11): 2503-13.
Jacobs, K. A., et al. (1997). "A genetic selection for isolating cDNAs encoding secreted proteins." Gene **198**(1-2): 289-296.
Jiang, R. H. Y., et al. (2008). "RXLR effector reservoir in two Phytophthora species is dominated by a single rapidly evolving superfamily with more than 700 members." Proceedings of the National Academy of Sciences of the United States of America **105**(12): 4874-4879.
Jin, J., et al. (2011). "The Arabidopsis bHLH25 and bHLH27 transcription factors contribute to susceptibility to the cyst nematode Heterodera schachtii." Plant J **65**(2): 319-28.
Jirage, D., et al. (1999). "Arabidopsis thaliana PAD4 encodes a lipase-like gene that is important for salicylic acid signaling." Proc Natl Acad Sci U S A **96**(23): 13583-8.
Jones, J. D. and J. L. Dangl (2006). "The plant immune system." Nature **444**(7117): 323-9.
Jones, J. T., et al. (2009). "Identification and functional characterization of effectors in expressed sequence tags from various life cycle stages of the potato cyst nematode Globodera pallida." Mol Plant Pathol **10**(6): 815-28.
Kadota, Y. and K. Shirasu (2011). "The HSP90 complex of plants." Biochim Biophys Acta.
Kale, S. D., et al. (2010). "External lipid PI3P mediates entry of eukaryotic pathogen effectors into plant and animal host cells." Cell **142**(2): 284-95.
Kamoun, S. (2006). "A catalogue of the effector secretome of plant pathogenic oomycetes." Annu Rev Phytopathol **44**: 41-60.
Kamoun, S. (2007). "Groovy times: filamentous pathogen effectors revealed." Current Opinion in Plant Biology **10**(4): 358-365.
Kamoun, S. (2009). The Secretome of Plant-Associated Fungi and Oomycetes. The Mycota V. H. Deising. Berlin heidelberg, Springer-Verlag.
Kamper, J., et al. (2006). "Insights from the genome of the biotrophic fungal plant pathogen Ustilago maydis." Nature **444**(7115): 97-101.

Kanneganti, T. D., et al. (2006). "Synergistic interactions of the plant cell death pathways induced by Phytophthora infestans Nep1-like protein PiNPP1.1 and INF1 elicitin." Molecular Plant-Microbe Interactions **19**(8): 854-863.
Karimi, M., et al. (2002). "GATEWAY vectors for Agrobacterium-mediated plant transformation." Trends Plant Sci **7**(5): 193-5.
Kay, S. and U. Bonas (2009). "How Xanthomonas type III effectors manipulate the host plant." Curr Opin Microbiol **12**(1): 37-43.
Kaya, H., et al. (2001). "FASCIATA genes for chromatin assembly factor-1 in arabidopsis maintain the cellular organization of apical meristems." Cell **104**(1): 131-42.
Kelley, B. S., et al. (2010). "A secreted effector protein (SNE1) from Phytophthora infestans is a broadly acting suppressor of programmed cell death." Plant J **62**(3): 357-66.
Kemen, E., et al. (2011). "Gene gain and loss during evolution of obligate parasitism in the white rust pathogen of Arabidopsis thaliana." PLoS Biol **9**(7): e1001094.
Kemen, E., et al. (2005). "Identification of a protein from rust fungi transferred from haustoria into infected plant cells." Mol Plant Microbe Interact **18**(11): 1130-9.
Kemen, E., et al. (2011). Immunolocalization of Pathogen Effectors
Plant Immunity, Humana Press. **712:** 211-225.
Keppler, L. D., et al. (1989). "Active Oxygen Production during a Bacteria-Induced Hypersensitive Reaction in Tobacco Suspension Cells." Phytopathology **79**(9): 974-978.
Khang, C. H., et al. (2010). "Translocation of Magnaporthe oryzae effectors into rice cells and their subsequent cell-to-cell movement." Plant Cell **22**(4): 1388-403.
Kim, A. J. and S. A. Endow (2000). "A kinesin family tree." J Cell Sci **113 Pt 21**: 3681-2.
Kim, M. C., et al. (2002). "Calmodulin interacts with MLO protein to regulate defence against mildew in barley." Nature **416**(6879): 447-51.
Kim, M. G., et al. (2005). "Two Pseudomonas syringae type III effectors inhibit RIN4-regulated basal defense in Arabidopsis." Cell **121**(5): 749-59.
Kloppholz, S., et al. (2011). "A secreted fungal effector of Glomus intraradices promotes symbiotic biotrophy." Curr Biol **21**(14): 1204-9.
Knepper, C., et al. (2011). "Arabidopsis NDR1 is an integrin-like protein with a role in fluid loss and plasma membrane-cell wall adhesion." Plant Physiol **156**(1): 286-300.
Koch, E. and A. Slusarenko (1990). "Arabidopsis is susceptible to infection by a downy mildew fungus." Plant Cell **2**(5): 437-45.
Koh, S., et al. (2005). "Arabidopsis thaliana subcellular responses to compatible Erysiphe cichoracearum infections." Plant Journal **44**(3): 516-529.
Kruger, J., et al. (2002). "A tomato cysteine protease required for Cf-2-dependent disease resistance and suppression of autonecrosis." Science **296**(5568): 744-7.
Kvitko, B. H., et al. (2009). "Deletions in the repertoire of Pseudomonas syringae pv. tomato DC3000 type III secretion effector genes reveal functional overlap among effectors." PLoS Pathog **5**(4): e1000388.
Lamb, C. and R. A. Dixon (1997). "The Oxidative Burst in Plant Disease Resistance." Annu Rev Plant Physiol Plant Mol Biol **48**: 251-275.
Lee, M. C., et al. (2004). "Bi-directional protein transport between the ER and Golgi." Annu Rev Cell Dev Biol **20**: 87-123.
Leonelli, L., et al. (2011). "Structural Elucidation and Functional Characterization of the Hyaloperonospora arabidopsidis Effector Protein ATR13." PLoS Pathog **7**(12): e1002428.
Leonelli, L., et al. (in press). "Structural elucidation and functional characterization of the Hyaloperonospora arabidopsidis effector protein ATR13." PLoS Pathog.

Levesque, C. A., et al. (2010). "Genome sequence of the necrotrophic plant pathogen Pythium ultimum reveals original pathogenicity mechanisms and effector repertoire." Genome Biol **11**(7): R73.
Li, H. and S. Luan (2010). "AtFKBP53 is a histone chaperone required for repression of ribosomal RNA gene expression in Arabidopsis." Cell Res **20**(3): 357-66.
Li, H., et al. (2008). "Mapping short DNA sequencing reads and calling variants using mapping quality scores." Genome Res **18**(11): 1851-8.
Lim, M. T. and B. N. Kunkel (2004). "Mutations in the Pseudomonas syringae avrRpt2 gene that dissociate its virulence and avirulence activities lead to decreased efficiency in AvrRpt2-induced disappearance of RIN4." Mol Plant Microbe Interact **17**(3): 313-21.
Lim, M. T. and B. N. Kunkel (2004). "The Pseudomonas syringae type III effector AvrRpt2 promotes virulence independently of RIN4, a predicted virulence target in Arabidopsis thaliana." Plant J **40**(5): 790-8.
Lin, N. C. and G. B. Martin (2005). "An avrPto/avrPtoB mutant of Pseudomonas syringae pv. tomato DC3000 does not elicit Pto-mediated resistance and is less virulent on tomato." Mol Plant Microbe Interact **18**(1): 43-51.
Lindeberg, M., et al. (2006). "Closing the circle on the discovery of genes encoding Hrp regulon members and type III secretion system effectors in the genomes of three model Pseudomonas syringae strains." Mol Plant Microbe Interact **19**(11): 1151-8.
Links, M. G., et al. (2011). "De novo sequence assembly of Albugo candida reveals a small genome relative to other biotrophic oomycetes." BMC Genomics **12**: 503.
Liu, T., et al. (2011). "Two host cytoplasmic effectors are required for pathogenesis of Phytophthora sojae by suppression of host defenses." Plant Physiol **155**(1): 490-501.
Liu, Z., et al. (2005). "Patterns of diversifying selection in the phytotoxin-like scr74 gene family of Phytophthora infestans." Mol Biol Evol **22**(3): 659-72.
Liu, Z., et al. (2009). "Molecular and reverse genetic characterization of NUCLEOSOME ASSEMBLY PROTEIN1 (NAP1) genes unravels their function in transcription and nucleotide excision repair in Arabidopsis thaliana." Plant J **59**(1): 27-38.
Liu, Z. Q., et al. (2009). "A truncated Arabidopsis NUCLEOSOME ASSEMBLY PROTEIN 1, AtNAP1;3T, alters plant growth responses to abscisic acid and salt in the Atnap1;3-2 mutant." Mol Plant **2**(4): 688-99.
Lloyd, C. and J. Chan (2004). "Microtubules and the shape of plants to come." Nat Rev Mol Cell Biol **5**(1): 13-22.
Lokossou, A. A., et al. (2009). "Exploiting knowledge of R/Avr genes to rapidly clone a new LZ-NBS-LRR family of late blight resistance genes from potato linkage group IV." Mol Plant Microbe Interact **22**(6): 630-41.
Luger, K., et al. (1997). "Crystal structure of the nucleosome core particle at 2.8 A resolution." Nature **389**(6648): 251-60.
Ma, K. W., et al. (2011). "Chromatin configuration as a battlefield in plant-bacteria interactions." Plant Physiol **157**(2): 535-43.
Mackey, D., et al. (2003). "Arabidopsis RIN4 is a target of the type III virulence effector AvrRpt2 and modulates RPS2-mediated resistance." Cell **112**(3): 379-89.
Mackey, D., et al. (2002). "RIN4 interacts with Pseudomonas syringae type III effector molecules and is required for RPM1-mediated resistance in Arabidopsis." Cell **108**(6): 743-54.
Manning, V. A. and L. M. Ciuffetti (2005). "Localization of Ptr ToxA Produced by Pyrenophora tritici-repentis Reveals Protein Import into Wheat Mesophyll Cells." Plant Cell **17**(11): 3203-12.
Mathur, J. and N. H. Chua (2000). "Microtubule stabilization leads to growth reorientation in Arabidopsis trichomes." Plant Cell **12**(4): 465-77.

Mauch-Mani, B. and A. J. Slusarenko (1993). "Arabidopsis as a model host for studying plant-pathogen interactions." Trends Microbiol **1**(7): 265-70.
McDowell, J. M., et al. (2000). "Downy mildew (Peronospora parasitica) resistance genes in Arabidopsis vary in functional requirements for NDR1, EDS1, NPR1 and salicylic acid accumulation." Plant J **22**(6): 523-9.
McDowell, J. M., et al. (1998). "Intragenic recombination and diversifying selection contribute to the evolution of downy mildew resistance at the RPP8 locus of arabidopsis." Plant Cell **10**(11): 1861-1874.
McHale, L., et al. (2006). "Plant NBS-LRR proteins: adaptable guards." Genome Biol **7**(4): 212.
Mendgen, K. and M. Hahn (2002). "Plant infection and the establishment of fungal biotrophy." Trends Plant Sci **7**(8): 352-6.
Meyer, D., et al. (2009). "Extracellular transport and integration of plant secretory proteins into pathogen-induced cell wall compartments." Plant J **57**(6): 986-99.
Meyers, B. C., et al. (2003). "Genome-wide analysis of NBS-LRR-encoding genes in Arabidopsis." Plant Cell **15**(4): 809-34.
Micali, C. O., et al. (2011). "Biogenesis of a specialized plant-fungal interface during host cell internalization of Golovinomyces orontii haustoria." Cellular Microbiology **13**(2): 210-226.
Mims, C. W., et al. (2004). "Ultrastructure of the host-pathogen interface in Arabidopsis thaliana leaves infected by the downy mildew Hyaloperonospora parasitica (vol 82, pg 1001, 2004)." Canadian Journal of Botany-Revue Canadienne De Botanique **82**(10): 1545-1545.
Morgan, W. and S. Kamoun (2007). "RXLR effectors of plant pathogenic oomycetes." Curr Opin Microbiol **10**(4): 332-8.
Mukhtar, M. S., et al. (2011). "Independently evolved virulence effectors converge onto hubs in a plant immune system network." Science **333**(6042): 596-601.
Munkvold, K. R., et al. (2009). "Pseudomonas syringae pv. tomato DC3000 type III effector HopAA1-1 functions redundantly with chlorosis-promoting factor PSPTO4723 to produce bacterial speck lesions in host tomato." Mol Plant Microbe Interact **22**(11): 1341-55.
Muskett, P. R., et al. (2002). "Arabidopsis RAR1 exerts rate-limiting control of R gene-mediated defenses against multiple pathogens." Plant Cell **14**(5): 979-92.
Nawrath, C. and J. P. Metraux (1999). "Salicylic acid induction-deficient mutants of Arabidopsis express PR-2 and PR-5 and accumulate high levels of camalexin after pathogen inoculation." Plant Cell **11**(8): 1393-404.
Nemri, A., et al. (2010). "Genome-wide survey of Arabidopsis natural variation in downy mildew resistance using combined association and linkage mapping." Proc Natl Acad Sci U S A **107**(22): 10302-7.
Nemri, A., et al. (2007). "Marker development for the genetic study of natural variation in Arabidopsis thaliana." Bioinformatics **23**(22): 3108-9.
Nirmala, J., et al. (2011). "Concerted action of two avirulent spore effectors activates Reaction to Puccinia graminis 1 (Rpg1)-mediated cereal stem rust resistance." Proc Natl Acad Sci U S A **108**(35): 14676-81.
Nishimura, M. T., et al. (2003). "Loss of a callose synthase results in salicylic acid-dependent disease resistance." Science **301**(5635): 969-72.
Nordgard, O., et al. (2001). "JAB1/CSN5 interacts with the GAL4 DNA binding domain: a note of caution about two-hybrid interactions." Biochimie **83**(10): 969-71.

Nurnberger, T., et al. (1994). "High-Affinity Binding of a Fungal Oligopeptide Elicitor to Parsley Plasma-Membranes Triggers Multiple Defense Responses." Cell **78**(3): 449-460.
Oh, S. K., et al. (2009). "In planta expression screens of Phytophthora infestans RXLR effectors reveal diverse phenotypes, including activation of the Solanum bulbocastanum disease resistance protein Rpi-blb2." Plant Cell **21**(9): 2928-47.
Ossowski, S., et al. (2008). "Sequencing of natural strains of Arabidopsis thaliana with short reads." Genome Res **18**(12): 2024-33.
Palade, G. (1975). "Intracellular aspects of the process of protein synthesis." Science **189**(4206): 867.
Park, Y. J. and K. Luger (2006). "Structure and function of nucleosome assembly proteins." Biochem Cell Biol **84**(4): 549-58.
Parker, J. E., et al. (1997). "The Arabidopsis downy mildew resistance gene RPP5 shares similarity to the toll and interleukin-1 receptors with N and L6." Plant Cell **9**(6): 879-894.
Parker, J. E., et al. (1996). "Characterization of eds1, a mutation in Arabidopsis suppressing resistance to Peronospora parasitica specified by several different RPP genes." Plant Cell **8**(11): 2033-46.
Parker, J. E., et al. (1993). "Phenotypic Characterization and Molecular Mapping of the Arabidopsis-Thaliana Locus Rpp5, Determining Disease Resistance to Peronospora-Parasitica." Plant Journal **4**(5): 821-831.
Pemberton, C. L. and G. P. C. Salmond (2004). "The Nep1-like proteins - a growing family of microbial elicitors of plant necrosis." Molecular Plant Pathology **5**(4): 353-359.
Perfect, S. E. and J. R. Green (2001). "Infection structures of biotrophic and hemibiotrophic fungal plant pathogens." Mol Plant Pathol **2**(2): 101-8.
Plett, J. M., et al. (2011). "A secreted effector protein of Laccaria bicolor is required for symbiosis development." Curr Biol **21**(14): 1197-203.
Poueymiro, M. and S. Genin (2009). "Secreted proteins from Ralstonia solanacearum: a hundred tricks to kill a plant." Curr Opin Microbiol **12**(1): 44-52.
Quentin, M., et al. (2009). "Imbalanced lignin biosynthesis promotes the sexual reproduction of homothallic oomycete pathogens." PLoS Pathog **5**(1): e1000264.
Qutob, D., et al. (2002). "Expression of a Phytophthora sojae necrosis-inducing protein occurs during transition from biotrophy to necrotrophy." Plant Journal **32**(3): 361-373.
Qutob, D., et al. (2009). "Copy number variation and transcriptional polymorphisms of Phytophthora sojae RXLR effector genes Avr1a and Avr3a." PLoS One **4**(4): e5066.
Raffaele, S., et al. (2010). "Analyses of genome architecture and gene expression reveal novel candidate virulence factors in the secretome of Phytophthora infestans." BMC Genomics **11**: 637.
Rafiqi, M., et al. (2010). "Internalization of flax rust avirulence proteins into flax and tobacco cells can occur in the absence of the pathogen." Plant Cell **22**(6): 2017-32.
Reader, J. (2009). Potato: A History of the Propitious Esculent, Yale Univ. Press.
Rehmany, A. P., et al. (2005). "Differential recognition of highly divergent downy mildew avirulence gene alleles by RPP1 resistance genes from two Arabidopsis lines." Plant Cell **17**(6): 1839-50.
Rehmany, A. P., et al. (2000). "A comparison of Peronospora parasitica (Downy mildew) isolates from Arabidopsis thaliana and Brassica oleracea using amplified fragment length polymorphism and internal transcribed spacer 1 sequence analyses." Fungal Genet Biol **30**(2): 95-103.

Reiss, K., et al. (2011). "Structural and phylogenetic analyses of the GP42 transglutaminase from Phytophthora sojae reveal an evolutionary relationship between oomycetes and marine Vibrio bacteria." J Biol Chem.

Rentel, M. C., et al. (2008). "Recognition of the Hyaloperonospora parasitica effector ATR13 triggers resistance against oomycete, bacterial, and viral pathogens." Proc Natl Acad Sci U S A **105**(3): 1091-6.

Richmond, T. J., et al. (1984). "Structure of the nucleosome core particle at 7 A resolution." Nature **311**(5986): 532-7.

Rietz, S., et al. (2011). "Different roles of Enhanced Disease Susceptibility1 (EDS1) bound to and dissociated from Phytoalexin Deficient4 (PAD4) in Arabidopsis immunity." New Phytol **191**(1): 107-19.

Roberts, A. M., et al. (1993). "Molecular Differentiation in the Extrahaustorial Membrane of Pea Powdery Mildew Haustoria at Early and Late Stages of Development." Physiological and Molecular Plant Pathology **43**(2): 147-160.

Rooney, H. C., et al. (2005). "Cladosporium Avr2 inhibits tomato Rcr3 protease required for Cf-2-dependent disease resistance." Science **308**(5729): 1783-6.

Rose, J. K. C., et al. (2002). "Molecular cloning and characterization of glucanase inhibitor proteins: Coevolution of a counterdefense mechanism by plant pathogens." Plant Cell **14**(6): 1329-1345.

Rose, L. E., et al. (2004). "The maintenance of extreme amino acid diversity at the disease resistance gene, RPP13, in Arabidopsis thaliana." Genetics **166**(3): 1517-1527.

Roux, M., et al. (2011). "The arabidopsis leucine-rich repeat receptor-like kinases BAK1/SERK3 and BKK1/SERK4 are required for innate immunity to Hemibiotrophic and Biotrophic pathogens." Plant Cell **23**(6): 2440-55.

Ryals, J., et al. (1997). "The Arabidopsis NIM1 protein shows homology to the mammalian transcription factor inhibitor I kappa B." Plant Cell **9**(3): 425-39.

Sacks, W., et al. (1995). "Molecular Characterization of Nucleotide-Sequences Encoding the Extracellular Glycoprotein Elicitor from Phytophthora-Megasperma." Molecular & General Genetics **246**(1): 45-55.

Sandhu, D., et al. (2004). "Deletion of a disease resistance nucleotide-binding-site leucine-rich- repeat-like sequence is associated with the loss of the Phytophthora resistance gene Rps4 in soybean." Genetics **168**(4): 2157-67.

Sarin, S., et al. (2008). "Caenorhabditis elegans mutant allele identification by whole-genome sequencing." Nat Methods **5**(10): 865-7.

Sarma, G. N., et al. (2005). "Structure of Ptr ToxA: an RGD-containing host-selective toxin from Pyrenophora tritici-repentis." Plant Cell **17**(11): 3190-202.

Schatz, G. and B. Dobberstein (1996). "Common principles of protein translocation across membranes." Science **271**(5255): 1519-26.

Schlumberger, M. C. and W. D. Hardt (2006). "Salmonella type III secretion effectors: pulling the host cell's strings." Curr Opin Microbiol **9**(1): 46-54.

Schmelzer, E. (2002). "Cell polarization, a crucial process in fungal defence." Trends Plant Sci **7**(9): 411-5.

Schneeberger, K., et al. (2009). "SHOREmap: simultaneous mapping and mutation identification by deep sequencing." Nat Methods **6**(8): 550-1.

Schneeberger, K., et al. (2011). "Reference-guided assembly of four diverse Arabidopsis thaliana genomes." Proc Natl Acad Sci U S A **108**(25): 10249-54.

Schornack, S., et al. (2009). "Ten things to know about oomycete effectors." Molecular Plant Pathology **10**(6): 795-803.

Schornack, S., et al. (2010). "Ancient class of translocated oomycete effectors targets the host nucleus." Proceedings of the National Academy of Sciences of the United States of America **107**(40): 17421-17426.
Segonzac, C., et al. (2011). "Hierarchy and roles of pathogen-associated molecular pattern-induced responses in Nicotiana benthamiana." Plant Physiol **156**(2): 687-99.
Senchou, V., et al. (2004). "High affinity recognition of a Phytophthora protein by Arabidopsis via an RGD motif." Cell Mol Life Sci **61**(4): 502-9.
Shan, W., et al. (2004). "The Avr1b locus of Phytophthora sojae encodes an elicitor and a regulator required for avirulence on soybean plants carrying resistance gene Rps1b." Mol Plant Microbe Interact **17**(4): 394-403.
Sinapidou, E., et al. (2004). "Two TIR : NB : LRR genes are required to specify resistance to Peronospora parasitica isolate Cala2 in Arabidopsis." Plant Journal **38**(6): 898-909.
Singh, R. P., et al. (2011). "The emergence of Ug99 races of the stem rust fungus is a threat to world wheat production." Annu Rev Phytopathol **49**: 465-81.
Skibbe, D. S., et al. (2010). "Maize tumors caused by Ustilago maydis require organ-specific genes in host and pathogen." Science **328**(5974): 89-92.
Skou, J. P., et al. (1984). "Comparative Studies on Callose Formation in Powdery Mildew Compatible and Incompatible Barley." Phytopathologische Zeitschrift-Journal of Phytopathology **109**(2): 147-168.
Slusarenko, A. J. and N. L. Schlaich (2003). "Downy mildew of Arabidopsis thaliana caused by Hyaloperonospora parasitica (formerly Peronospora parasitica)." Mol Plant Pathol **4**(3): 159-70.
Smertenko, A. and V. E. Franklin-Tong (2011). "Organisation and regulation of the cytoskeleton in plant programmed cell death." Cell Death Differ **18**(8): 1263-70.
Sohn, J., et al. (2000). "High level activation of vitamin B1 biosynthesis genes in haustoria of the rust fungus Uromyces fabae." Molecular Plant-Microbe Interactions **13**(6): 629-636.
Sohn, K. H., et al. (2007). "The downy mildew effector proteins ATR1 and ATR13 promote disease susceptibility in Arabidopsis thaliana." Plant Cell **19**(12): 4077-90.
Sohn, K. H., et al. (2009). "The Pseudomonas syringae effector protein, AvrRPS4, requires in planta processing and the KRVY domain to function." Plant J **57**(6): 1079-91.
Soylu, E. M. and S. Soylu (2003). "Light and electron microscopy of the compatible interaction between Arabidopsis and the downy mildew pathogen Peronospora parasitica." Journal of Phytopathology-Phytopathologische Zeitschrift **151**(6): 300-306.
Stassen, J. H. M. and G. Van den Ackerveken (2011). "How do oomycete effectors interfere with plant life?" Current Opinion in Plant Biology **14**(4): 407-414.
Stavrinides, J., et al. (2006). "Terminal reassortment drives the quantum evolution of type III effectors in bacterial pathogens." PLoS Pathog **2**(10): e104.
Stefanato, F. L., et al. (2009). "The ABC transporter BcatrB from Botrytis cinerea exports camalexin and is a virulence factor on Arabidopsis thaliana." Plant J **58**(3): 499-510.
Stracke, S., et al. (2002). "A plant receptor-like kinase required for both bacterial and fungal symbiosis." Nature **417**(6892): 959-62.
Struck, C., et al. (2002). "Characterization of a developmentally regulated amino acid transporter (AAT1p) of the rust fungus Uromyces fabae." Molecular Plant Pathology **3**(1): 23-30.
Struck, C., et al. (1996). "Plasma membrane H+-ATPase activity in spores, germ tubes, and haustoria of the rust fungus Uromyces viciae-fabae." Fungal Genetics and Biology **20**(1): 30-35.

Struck, C., et al. (2004). "The Uromyces fabae UfAAT3 gene encodes a general amino acid permease that prefers uptake of in planta scarce amino acids." Molecular Plant Pathology **5**(3): 183-189.
Struck, C., et al. (1998). "The plasma membrane H+-ATPase from the biotrophic rust fungus Uromyces fabae: Molecular characterization of the gene (PMA1) and functional expression of the enzyme in yeast." Molecular Plant-Microbe Interactions **11**(6): 458-465.
Stulemeijer, I. J. and M. H. Joosten (2008). "Post-translational modification of host proteins in pathogen-triggered defence signalling in plants." Mol Plant Pathol **9**(4): 545-60.
Stuttmann, J., et al. (2011). "Perturbation of Arabidopsis Amino Acid Metabolism Causes Incompatibility with the Adapted Biotrophic Pathogen Hyaloperonospora arabidopsidis." Plant Cell **23**(7): 2788-803.
Sugio, A., et al. (2011). "Phytoplasma protein effector SAP11 enhances insect vector reproduction by manipulating plant development and defense hormone biosynthesis." Proc Natl Acad Sci U S A **108**(48): E1254-63.
Swiderski, M. R., et al. (2009). "The TIR domain of TIR-NB-LRR resistance proteins is a signaling domain involved in cell death induction." Mol Plant Microbe Interact **22**(2): 157-65.
Takahashi, A., et al. (2003). "HSP90 interacts with RAR1 and SGT1 and is essential for RPS2-mediated disease resistance in Arabidopsis." Proc Natl Acad Sci U S A **100**(20): 11777-82.
Takemoto, D., et al. (2003). "GFP-tagging of cell components reveals the dynamics of subcellular re-organization in response to infection of Arabidopsis by oomycete pathogens." Plant Journal **33**(4): 775-792.
Taneva, S. G., et al. (2009). "A mechanism for histone chaperoning activity of nucleoplasmin: thermodynamic and structural models." J Mol Biol **393**(2): 448-63.
Tasset, C., et al. (2010). "Autoacetylation of the Ralstonia solanacearum effector PopP2 targets a lysine residue essential for RRS1-R-mediated immunity in Arabidopsis." PLoS Pathog **6**(11): e1001202.
Thines, M. and S. Kamoun (2010). "Oomycete-plant coevolution: recent advances and future prospects." Current Opinion in Plant Biology **13**(4): 427-433.
Thistlethwaite, P., et al. (1986). "Photophysics of the Aniline Blue Fluorophore - a Fluorescent-Probe Showing Specificity toward (1-]3)-Beta-D-Glucans." Journal of Physical Chemistry **90**(21): 5058-5063.
Thomas, W. J., et al. (2009). "Recombineering and stable integration of the Pseudomonas syringae pv. syringae 61 hrp/hrc cluster into the genome of the soil bacterium Pseudomonas fluorescens Pf0-1." Plant J **60**(5): 919-28.
Tian, M. Y., et al. (2005). "A second kazal-like protease inhibitor from Phytophthora infestans inhibits and interacts with the apoplastic pathogenesis-related protease P69B of tomato." Plant Physiology **138**(3): 1785-1793.
Tian, M. Y., et al. (2004). "A Kazal-like extracellular serine protease inhibitor from Phytophthora infestans targets the tomato pathogenesis-related protease P69B." Journal of Biological Chemistry **279**(25): 26370-26377.
Tian, M. Y., et al. (2011). "454 Genome Sequencing of Pseudoperonospora cubensis Reveals Effector Proteins with a QXLR Translocation Motif." Molecular Plant-Microbe Interactions **24**(5): 543-553.
Tian, M. Y., et al. (2007). "A Phytophthora infestans cystatin-like protein targets a novel tomato papain-like apoplastic protease." Plant Physiology **143**(1): 364-377.
Tor, M., et al. (2002). "Arabidopsis SGT1b is required for defense signaling conferred by several downy mildew resistance genes." Plant Cell **14**(5): 993-1003.

Torres, M. A., et al. (2002). "Arabidopsis gp91(phox) homologues AtrbohD and AtrbohF are required for accumulation of reactive oxygen intermediates in the plant defense response." Proceedings of the National Academy of Sciences of the United States of America **99**(1): 517-522.
Torto, T. A., et al. (2003). "EST mining and functional expression assays identify extracellular effector proteins from the plant pathogen Phytophthora." Genome Research **13**(7): 1675-1685.
Tyler, B. M. (2002). "Molecular basis of recognition between phytophthora pathogens and their hosts." Annu Rev Phytopathol **40**: 137-67.
Tyler, B. M., et al. (2006). "Phytophthora genome sequences uncover evolutionary origins and mechanisms of pathogenesis." Science **313**(5791): 1261-1266.
Tytgat, T., et al. (2005). "An SXP/RAL-2 protein produced by the subventral pharyngeal glands in the plant parasitic root-knot nematode Meloidogyne incognita." Parasitol Res **95**(1): 50-4.
Van Damme, D., et al. (2004). "In vivo dynamics and differential microtubule-binding activities of MAP65 proteins." Plant Physiol **136**(4): 3956-67.
van Damme, M., et al. (2005). "Identification of arabidopsis loci required for susceptibility to the downy mildew pathogen Hyaloperonospora parasitica." Mol Plant Microbe Interact **18**(6): 583-92.
van Damme, M., et al. (2008). "Arabidopsis DMR6 encodes a putative 2OG-Fe(II) oxygenase that is defense-associated but required for susceptibility to downy mildew." Plant J **54**(5): 785-93.
van Damme, M., et al. (2009). "Downy mildew resistance in Arabidopsis by mutation of HOMOSERINE KINASE." Plant Cell **21**(7): 2179-89.
van der Biezen, E. A., et al. (2002). "Arabidopsis RPP4 is a member of the RPP5 multigene family of TIR-NB-LRR genes and confers downy mildew resistance through multiple signalling components." Plant J **29**(4): 439-51.
van der Biezen, E. A. and J. D. G. Jones (1998). "Plant disease-resistance proteins and the gene-for-gene concept." Trends in Biochemical Sciences **23**(12): 454-456.
van Poppel, P. M., et al. (2008). "The Phytophthora infestans avirulence gene Avr4 encodes an RXLR-dEER effector." Mol Plant Microbe Interact **21**(11): 1460-70.
van West, P., et al. (2010). "The putative RxLR effector protein SpHtp1 from the fish pathogenic oomycete Saprolegnia parasitica is translocated into fish cells." Fems Microbiology Letters **310**(2): 127-137.
van West, P., et al. (1998). "The ipiO gene of Phytophthora infestans is highly expressed in invading hyphae during infection." Fungal Genet Biol **23**(2): 126-38.
Vleeshouwers, V. G., et al. (2011). "Understanding and exploiting late blight resistance in the age of effectors." Annu Rev Phytopathol **49**: 507-31.
Vleeshouwers, V. G., et al. (2008). "Effector genomics accelerates discovery and functional profiling of potato disease resistance and phytophthora infestans avirulence genes." PLoS One **3**(8): e2875.
Vlot, A. C., et al. (2009). "Salicylic Acid, a multifaceted hormone to combat disease." Annu Rev Phytopathol **47**: 177-206.
Voegele, R. T. and K. W. Mendgen (2011). "Nutrient uptake in rust fungi: how sweet is parasitic life?" Euphytica **179**(1): 41-55.
Voegele, R. T., et al. (2001). "The role of haustoria in sugar supply during infection of broad bean by the rust fungus Uromyces fabae." Proc Natl Acad Sci U S A **98**(14): 8133-8.
Voegele, R. T., et al. (2006). "Cloning and characterization of a novel invertase from the obligate biotroph Uromyces fabae and analysis of expression patterns of host and

pathogen invertases in the course of infection." Molecular Plant-Microbe Interactions **19**(6): 625-634.
Vogel, J. and S. Somerville (2000). "Isolation and characterization of powdery mildew-resistant Arabidopsis mutants." Proc Natl Acad Sci U S A **97**(4): 1897-902.
Vogel, J. P., et al. (2002). "PMR6, a pectate lyase-like gene required for powdery mildew susceptibility in Arabidopsis." Plant Cell **14**(9): 2095-106.
Vogel, J. P., et al. (2004). "Mutations in PMR5 result in powdery mildew resistance and altered cell wall composition." Plant J **40**(6): 968-78.
Wang, W., et al. (2009). "Specific targeting of the Arabidopsis resistance protein RPW8.2 to the interfacial membrane encasing the fungal Haustorium renders broad-spectrum resistance to powdery mildew." Plant Cell **21**(9): 2898-913.
Wang, Y., et al. (2010). "A Pseudomonas syringae ADP-ribosyltransferase inhibits Arabidopsis mitogen-activated protein kinase kinases." Plant Cell **22**(6): 2033-44.
Whisson, S. C., et al. (2007). "A translocation signal for delivery of oomycete effector proteins into host plant cells." Nature **450**(7166): 115-8.
Wiermer, M., et al. (2005). "Plant immunity: the EDS1 regulatory node." Curr Opin Plant Biol **8**(4): 383-9.
Wildermuth, M. C., et al. (2001). "Isochorismate synthase is required to synthesize salicylic acid for plant defence." Nature **414**(6863): 562-5.
Will, T. and A. J. van Bel (2006). "Physical and chemical interactions between aphids and plants." J Exp Bot **57**(4): 729-37.
Wilson, C. and C. Tisdell (2001). "Why farmers continue to use pesticides despite environmental, health and sustainability costs." Ecological Economics **39**(3): 449-462.
Wilton, M., et al. (2010). "The type III effector HopF2Pto targets Arabidopsis RIN4 protein to promote Pseudomonas syringae virulence." Proc Natl Acad Sci U S A **107**(5): 2349-54.
Win, J., et al. (2007). "Adaptive evolution has targeted the C-terminal domain of the RXLR effectors of plant pathogenic oomycetes." Plant Cell **19**(8): 2349-69.
Wolter, M., et al. (1993). "The mlo resistance alleles to powdery mildew infection in barley trigger a developmentally controlled defence mimic phenotype." Mol Gen Genet **239**(1-2): 122-8.
Wu, S., et al. (2011). "Bacterial effector HopF2 suppresses arabidopsis innate immunity at the plasma membrane." Mol Plant Microbe Interact **24**(5): 585-93.
Yaeno, T., et al. (2011). "Phosphatidylinositol monophosphate-binding interface in the oomycete RXLR effector AVR3a is required for its stability in host cells to modulate plant immunity." Proc Natl Acad Sci U S A **108**(35): 14682-7.
Zeng, L., et al. (2012). "A tomato LysM receptor-like kinase promotes immunity and its kinase activity is inhibited by AvrPtoB." Plant J **69**(1): 92-103.
Zhu, S., et al. (2011). "SAG101 Forms a Ternary Complex with EDS1 and PAD4 and Is Required for Resistance Signaling against Turnip Crinkle Virus." PLoS Pathog **7**(11): e1002318.
Zhu, Y., et al. (2006). "Arabidopsis NRP1 and NRP2 encode histone chaperones and are required for maintaining postembryonic root growth." Plant Cell **18**(11): 2879-92.
Zipfel, C., et al. (2004). "Bacterial disease resistance in Arabidopsis through flagellin perception." Nature **428**(6984): 764-7.

Appendix

- Media recipes
- List of primers used in this thesis
- MAFFT alignment of *Hpa* HaRxL79 paralogs nucleotide sequences
- Details on Illumina sequence reads used for the comparative genomics section in **Chapter 4**
- Publications associated with this work:

Fabro, G., Steinbrenner, J., Coates, M., Ishaque, N., Baxter, L., Studholme, D.J., Korner, E., Allen, R.L., **Piquerez, S.J.M**, Rougon-Cardoso, A., Greenshields, D., Lei, R., Badel, J.L., Caillaud, M.C., Sohn, K.H., Van den Ackerveken, G., Parker, J.E., Beynon, J., and Jones, J.D.G. (2011). **Multiple Candidate Effectors from the Oomycete Pathogen Hyaloperonospora arabidopsidis Suppress Host Plant Immunity.** PLoS Pathogens 7(11): e1002348.

Caillaud, M.C., **Piquerez, S.J.M**, Fabro, G., Steinbrenner, J., Ishaque, N., Beynon, J., and Jones, J.D. (2012). **Subcellular localization of the Hpa RxLR effector repertoire identifies a tonoplast-associated protein HaRxL17 that confers enhanced plant susceptibility.** The Plant Journal 69(2):252-265.

Caillaud, M.C., **Piquerez, S.J.M**, and Jones, J.D.G. (2012). **Characterization of the membrane-associated HaRxL17 Hpa effector candidate.** Plant Signaling & Behavior 7(1):145-149.